NASA CONTRACTOR REPORT

NASA CR-898

STUDY AND ANALYSIS OF SATELLITE POWER SYSTEMS CONFIGURATIONS FOR MAXIMUM UTILIZATION OF POWER

Prepared by
TRW SYSTEMS
Redondo Beach, Calif.
for Goddard Space Flight Center

NATIONAL AERONAUTICS AND SPACE ADMINISTRATION • WASHINGTON, D. C. • OCTOBER 1967

NASA CR-898

STUDY AND ANALYSIS OF SATELLITE POWER SYSTEMS CONFIGURATIONS FOR MAXIMUM UTILIZATION OF POWER

Issued by Originator as Report No. 04898-6001-R000

Prepared under Contract No. NAS 5-9178 by
TRW SYSTEMS
Redondo Beach, Calif.

for Goddard Space Flight Center

NATIONAL AERONAUTICS AND SPACE ADMINISTRATION

For sale by the Clearinghouse for Federal Scientific and Technical Information
Springfield, Virginia 22151 – CFSTI price $3.00

ITENTS

CONTENTS (Continued)

CONTENTS (Continued)

ILLUSTRATIONS

ILLUSTRATIONS (Continued)

ILLUSTRATIONS (Continued)

ILLUSTRATIONS (Continued)

ILLUSTRATIONS (Continued)

TABLES

TABLES (Continued)

GLOSSARY

Å	angstroms
a, b, k	constants for the particular type of conditioning equipment and operating voltage
ac	alternating current
ACS	Attitude Control System
ADCS	Attitude Determination and Control System
AgCd	silver cadmium
AgZn	silver zinc
AM	amplitude modulated
AMO	air mass zero
amp	ampere
Amp-hr	ampere hour
AMU	atomic mass unit
AOSO	Advanced Orbiting Solar Observatory
ARC	Ames Research Center
A to D	analog-to-digital
AU	astronomical unit
bev	billion electron volts
C	rated ampere-hour capacity per hour
C_d	discharge capacity at end-of-life, ampere-hours
C_e	battery ampere-hour capacity at end-of-life
C'_e	maximum available capacity at end-of-life under optimum conditions, ampere-hours
C/15	current rate required to transfer that fraction (1/15) of the battery rated ampere-hours in 1-hr
cm	centimeters
COMSAT	communications satellite
cps	cycles per second
C_r	manufacturer's rated capacity, ampere-hours
ct	center tapped
dc	direct current

dc-dc	direct current to direct current
deg	degrees
DOD	depth of discharge
e	2.71828
ECF	efficiency correction factor
e/cm^2	electrons per square centimeter
E_{in}	input voltage
EMC	electromagnetic compatibility
emf	electromotive force
EMI	electromagnetic interference
EOGO	Equatorial Orbiting Geophysical Observatory
EPSOM	Electrical Power System Optimization Method
ES	energy storage
ev	electron volts
f	switching frequency
freq mult	frequency multiplier
FSK	frequency-shift-keyed
ft^2	square feet
gc	gigacycle
GRCSW	Graduate Research Center of the South West
GSFC	Goddard Space Flight Center
H	efficiency
hr	hour
I	current
i_c	charge current density, $= \frac{I_c}{C_e} hr^{-1}$
i_d	discharge current density, $= \frac{I_d}{C_e} hr^{-1}$
I_c	charge rate, amperes
I_d	discharge rate, amperes
IMP	Interplanetary Monitoring Platform

GLOSSARY (Continued)

I_o	RTG current at maximum power out
I_{sc}	short circuit current
I-V	current-voltage
kc	kilocycles
kev	thousand-electron volts
lb	pounds
lb/cu in	pounds per cubic inch
LC	inductive-capacitive
ma	milliamperes
mc	megacycle
mev	million electron volts
min	minutes
MIT	Massachusetts Institute of Technology
mo	months
msec	milliseconds
mv	millivolts
mw	milliwatts
NiCd	nickel cadmium
nmi	nautical miles
nsec	nanosecond (10^{-9} seconds)
OAO	Orbiting Astronomical Observatory
OECF	overall efficiency correction factor
OGO	Orbiting Geophysical Observatory
OPEP	Orbital Plane Experiment Package
OSO	Orbiting Solar Observatory
PCM	pulse code modulated
pwr amp	power amplifier
P	power
P_A	maximum power received by element P_A under optimum mission conditions
PbTe	lead telluride
POGO	Polar Orbiting Geophysical Observatory

p-p	peak to peak
Pu-238	The radioisotope No. 238 of Plutonium
PWI	pulsewidth inverter
PWM	pulsewidth modulated
rf	radio frequency
R_L	load resistance
RMS	root mean squared
RSWI	regulated squarewave inverter
RTG	radioisotope thermoelectric generator
sec	seconds
SiGe	silicon germanium
SNAP	Secondary Nuclear Auxiliary Power
t	sunlight time of the orbit
T	time of total switching period
T_c	cold junction temperature
T_h	hot junction temperature
T_j	junction temperature
t_{off}	time switch is OFF
t_{on}	time switch is ON
TR	transformer rectifier
TWT	traveling wave tube
UK-1	United Kingdom Satellite No. 1
UV	ultraviolet
v	volts
VA	volt-amperes
vac	volts alternating current
vdc	volts direct current
Vela	Nuclear Detection Satellite
VLF	very low frequency
V_o	RTG voltage at maximum power out
V_{oc}	open circuit voltage

GLOSSARY (Continued)

w	watts
w/ft^2	watts per square foot
wgt	weight
w-hr	watt hour
w/lb	watts per pound
yr	years
γ	gamma
Δ_i	percentage of total output power per output circuit
ΔV	incremental velocity
η	efficiency
η_A	efficiency of element P_A
$\eta_{a, b, c, \ldots m}$	efficiencies of output power conditioning equipments
η_B	watt-hour efficiency of energy storage
η_{PN}	efficiency of parallel energy source control
η_{SN}	efficiency of series energy source control
η_{P3}	efficiency of source shunt control
η_{S3}	efficiency of input line conditioner
η_{S4}	efficiency of output line conditioner
η_{S5}	efficiency of energy storage input control
η_{S6}	efficiency of energy storage output control
μsec	microsecond (10^{-6} seconds)
τ	total orbit time
φ	phase
Ω	ohms
$^\circ F$	degrees Fahrenheit
$^\circ C$	degrees centigrade

1. INTRODUCTION

1.1 GENERAL

This technical report covers work performed by TRW Systems under Contract NAS 5-9178, "Study and Analysis of Satellite Power Systems Configurations for Maximum Utilization of Power." The report covers the period 18 May 1965 through 18 July 1966. The study consists of seven major tasks:

Task I. A survey of the power requirements and characteristics of spaceborne equipment used in typical unmanned satellites.

Task II. A survey of typical spacecraft electrical power system designs.

Task III. Collection and presentation of parametric data on the individual assemblies constituting a power system (i.e., power control, energy storage, and power conditioning equipment).

Task IV. Analysis of three representative space missions, selected by Goddard Space Flight Center, with respect to their electrical power requirements and to the characteristics of photovoltaic power systems which could meet those requirements. Evaluation of various power system configurations with respect to efficiency, weight, reliability, and interface constraints.

Task V. Investigation of possible means of standardizing electrical power requirements and power characteristics for satellites as well as designs of power systems and their equipments.

Task VI. Investigation of the characteristics of alternate electrical power systems using radioisotope thermoelectric generators (RTG) rather than photovoltaic sources.

Task VII. Review of new design techniques, circuits, and components which could allow improvement in power-conditioning equipment efficiency, weight, and/or reliability. Provisions of updated parametric data to reflect the latest state-of-the-art in power-conditioning equipment designs.

The results of the first four tasks were used to establish an evaluation technique or method which would allow various proposed power system designs to be evaluated for optimization. Application of this technique was demonstrated on proposed designs for the three missions specified by Goddard Space Flight Center. Analysis of the power systems optimized for maximum utilization of power permitted recommendations for standardization of satellite power systems, requirements, characteristics, and equipments.

Primary consideration was given to the selection of circuit configurations which would result in the maximum utilization of available power. Percent regulation, ripple, and efficiency of a common bus system were analyzed and compared to a multiple bus system. Adequate power, reliability, weight, complexity, availability of equipment, and cost were all factors considered in recommended design configurations. Tradeoffs between various configurations were fully evaluated, and standardization and minimization of components was investigated. Several recommended power system configurations described by block diagrams, graphs, figures, and the analyses for various orbits, payloads, and life requirements were furnished at the conclusion of this study.

2. SUMMARY

2.1 BACKGROUND

The United States has successfully flown more than 350 functional spacecraft since the attempted launch of the first Vanguard back in 1957. Each of these vehicles has contained its own custom-designed electrical power systems, which have ranged from simple battery packs to relatively complex combinations of solar arrays, batteries, and nuclear power sources. This multiplicity of power system designs has been usually attributed to the need for designs responsive to the differences inherent n the following major factors:

- Mission requirements
- Orbits
- Vehicle design characteristics
- Attitude control method
- State-of-the-art in power system components.

In addition to the above factors, the variety of power system designs has also resulted from the personal preferences and intuitive decisions arising from the specific experience of the various spacecraft designers, and from the general lack of acceptable industry-wide power system standards.

Thus, after almost ten years of accumulated satellite design experience, certain key questions and objective answers to them have yet to be determined:

- Is the power system design of today better than yesterday's ?
- Is today's power system design being used to the maximum of its capability ?
- Is today's power system design the best that the state-of-the-art will allow ?

The reliability and adequacy of the design or configuration of the power system for most satellites can be ascertained from their flight performance. From the large number of satellites utilizing various power system configurations and multiple voltages, it becomes evident that in

many cases the maximum power available was not utilized. In all new designs and in existing systems where a considerable saving of power could be realized, designs should be considered which provide maximum utilization of available power.

This study program—Satellite Power Systems Configurations for Maximum Utilization of Power—was undertaken in an attempt to answer these questions and to establish an objective method for comparative evaluation of power system designs. A portion of the study was devoted to the development of an analytical method which would be specifically applicable to the evaluation of power system designs. The method used was identified as EPSOM (Electrical Power System Optimization Method). EPSOM is a technique for directly comparing two or more power system designs on the basis of any one optimization criterion. Proper use of state-of-the-art parametric data facilitates a methodical objective comparison among several candidate designs. The technique is based upon the logical step-by-step process which a power system designer normally uses for analysis and optimization. The process was reduced to mathematical equations which can be used to determine the relative maximum utilization of power for the power system designs under consideration.

2.2 PURPOSE AND SCOPE

The ultimate purpose of this study was to evaluate and analyze solar array power system configurations in order to identify those which would maximize the economical and reliable utilization of power. One objective of the study was to determine the state of the art of major power system components. Analysis of the electrical power requirements and characteristics was to be used for establishing recommendations for standardization of power system designs.

Another objective of the study was consideration of the use of radioisotope thermoelectric generators (RTGs) as a spacecraft primary electrical power source. The fact that an RTG constitutes a self-contained power plant while the solar array is dependent on the sun as an energy source prompted its study. The use of RTGs in space has been extremely limited because of a few undesirable characteristics. As these are gradually overcome by improved technology, the use of RTGs will probably increase for missions

which can benefit from their desirable features, i.e., applications which cannot or are difficult to satisfy with solar array - battery systems.

2.3 SUMMARY OF ANALYTICAL RESULTS

2.3.1 Model Missions

The analytical and optimization processes were applied to electrical power systems synthesized for the three model missions specified by NASA/GSFC. They are:

1) Earth-synchronous communications satellite

2) Sun-synchronous navigation or mapping satellite

3) Scientific satellite having an inclined (30 deg) elliptical orbit ranging from 200 to 180,000 nmi.

Synthesis of worthy power system configurations was supported by the study of load equipment characteristics and requirements, existing power system designs, and parametric performance data of power system equipment.

2.3.2 Equipment Characteristics and Requirements

Design specifications, schematics, test and performance data of the following five major subsystems were examined: communications, data handling, stabilization and control, experiments, and electrical power systems. Power requirements and characteristics for each of these subsystems were catalogued and analyzed for similarities, differences, and areas where uniformity and improvements could be introduced to enhance performance. Electrical requirements were related to the mission specifications and the functional performance parameters of each equipment.

Equipments comprising an electrical power system are identified as: energy sources, energy source controls, energy storage, energy storage controls, and load power conditioning equipments. Design and performance characteristics for each of these equipment types were studied and analyzed in depth. Performance parameters, e.g., efficiency, power level, frequency, and weight were inter-related and are presented in a manner suitable for optimization tradeoffs. State-of-the-art designs are investigated and evaluated for use in optimal power system configurations.

Photovoltaic energy sources have been the most commonly used type of unmanned satellite electrical power generator. Considerable research and development have been devoted to improving their state of the art, and optimal configurations have been defined by extensive study programs. It is not the purpose of this study to repeat or extend this area of technology, but only to report sufficient performance and parametric data to allow power system optimization tradeoffs.

The performance of any solar array design is controlled by three principal parameters

- Illumination (sun orientation)
- Temperature
- Radiation degradation as a function of time

A wide variation of performance factors can occur depending upon the mission, orbital parameters, vehicle configuration, orientation, and solar array design. Low solar array specific power ratios (w/lb) emphasize the extreme importance of attaining high efficiencies in the remainder of the power system in order to minimize total system weight.

The function of energy source control is to regulate the voltage and/or current delivered by the solar array. Source control is used only to protect the equipment connected to the bus since the solar array can safely sustain open or short circuit loads. Source controls may perform their function in a variety of ways depending upon the type of circuit employed. The more common circuit types can be classified as follows

- Series or shunt
- Dissipative or nondissipative
- Full regulating or limiting
- Switching or continuous

The choice of regulator type to be used for source control is dependent upon the solar array configuration, battery operating characteristics, voltage regulation requirements, and load variation.

Electrical power systems for spacecraft generally employ batteries selected from three main types. Silver-zinc primary (one shot) batteries are used mainly for short missions or on long missions to meet peak power

and emergency requirements when those vehicles have another source of continuous electrical power. The nickel-cadmium battery has been used in space systems for the longest period of time. Long cycle life is a predominant and controlling requirement for many satellite applications. The nickel-cadmium battery has demonstrated superior cycle life to date, but a steady improvement in the cycling performance of the lighter silver-cadmium battery is being realized.

Controls for energy storage equipment (batteries) commonly have two distinct functions: to regulate the energy input to the battery, and to control the energy out of the battery. Some power systems connect the battery directly to the solar array load bus and effectively use the energy source control as the battery charge control. The various types of regulator circuits used for energy source controls are also usable for battery control. In general, the controlled parameters during battery charging are current magnitude and voltage limit. Voltage regulation only is used for battery discharging. The choice of regulator type to be used for charge-discharge control is dependent upon the solar array and load bus voltages, and voltage regulation requirements.

Load power conditioning is used for accepting electrical power from a bus with specified characteristics and altering them to meet the individual requirements of the load equipment. These load requirements may include multiple dc voltages, voltage regulation, filtering, dc isolation, generation of ac voltages at one or more frequencies, and frequency regulation. The equipments which perform these functions are classified as regulators, converters, inverters, and transformer-rectifiers (TR units).

Most satellites require some part of the electrical load power to have closer voltage regulation than can be inherently supplied by the solar array battery combination. When this required regulation cannot be accomplished in the energy source or energy storage regulator, additional regulating circuits must be included. Here again, a choice can be made from each of the fundamental types of regulator circuits previously mentioned. When the regulators are designed as separate equipments, they can be either a central (ac or dc) line regulator or smaller distributed units. The specific configuration of equipments is usually dictated by the mission requirements, reliability, and other optimization and design criteria.

Sometimes it is advantageous to combine the regulating function within the inverting or converting equipment.

The regulated dc-to-dc converter was chosen as the investigation model because it is representative of, and contains all of the power conditioning functions found in a satellite electrical power system: regulating, inverting, transforming, rectifying and filtering. Selected circuit designs were parametrically analyzed to determine their optimum operating limits and tradeoff factors. Weight and efficiency as functions of output power and switching frequency were derived for each functional section of the circuits. Circuit efficiency and weights were reduced to frequency-dependent and frequency-independent components for convenient identification of frequency limitations resulting from circuit design and component selection. The final converter parametric data is the result of synthesizing the applicable groups of data derived for each functional section of the converter circuit.

Comparison of the data for the minimum weight converter shows an overall reduction in switching frequency and a change toward the higher efficiency converter designs to obtain the minimum weight systems. The maximum efficiency system requires the maximum efficiency converter designs with the accompanying increased converter weights.

The composite parametric curves for inverter designs were generated from design center values of existing equipment. The overall levels of efficiency are greater than for converters because rectification and output filter losses have been eliminated. Changes in weight and efficiency as a function of frequency and output power are very similar to those which occur in converter circuitry since the controlling elements are the input filter, semiconductors, and magnetic components. The mechanical hardware weights associated with a separately packaged inverter are comparable to those of a converter.

Performance factors for electrical cabling, power switching, under- and over-voltage protection, telemetry sensors, etc. are very difficult to generalize, since mission requirements usually control the design of these equipments rather than any one power system characteristic. Typical harness weight as a function of power system output power has ranged

between 2 and 7 w/lb. Use of higher distribution voltages would provide the same power handling capacity at a lower weight, by decreasing the wire size proportionately; or provide a higher efficiency by decreasing current density for the same wire size weight.

It appears that characteristics other than power consumption may dictate the selection of a switching device, but all other things being equal, solid-state switches would be used for low-power circuits, and relays for high-power circuits to obtain maximum power system efficiency.

2.4 CONCLUSIONS AND RECOMMENDATIONS

2.4.1 General

Generalized guidlines were established relative to the performance of power systems within the scope of the contemplated missions. In a specific example, (Mission I) the EPSOM evaluation method was applied to four proposed system configurations. The result was an improvement in the power system efficiency for the best configuration which was approximately 9 percent better than the poorest configuration, making the solar array 17.74 w smaller. This system improvement was attributable to a 16.5-w reduction in bus power resulting from the improved net efficiency of the power conditioning equipment. An additional 1.24 w was saved by not requiring the battery to deliver the 16.5 w during the orbital dark period.

2.4.2 Conclusions

The optimum power system design which will provide the maximum utilization of power is the system having maximum efficiency and which meets the performance requirements for all phases of the selected mission. This system may or may not have minimum weight, depending upon the choice of equipment, system configuration, and the operating constraints such as switching frequency, which are required to provide the maximum efficiency design. For most designs of the power conditioning equipment, maximum equipment efficiency is not synonymous with minimum equipment weight, as opposed to solar arrays where the most efficient array is also the lightest array.

Maximum efficiency power conditioning equipment designs are a necessary constituent of a maximum efficiency power system. The minimum weight power system typically contains power conditioning equipment whose design is a compromise between maximum efficiency and minimum weight equipment. The most favorable compromise, starting from the minimum weight power conditioning equipment, is reached by incrementally increasing the power conditioning equipment weight until the resultant power saving, (due to the higher efficiency) translated into battery and solar array weight reduction is just equal to the added incremental equipment weight.

Based upon the equipment performance characteristics, parametric data, and study results, the conclusions applicable to unmanned earth-orbiting satellites are summarized as follows:

1) Centralized (e.g., the use of a single regulator for the entire system) rather than distributed equipment usually results in higher efficiency and lower weight.

2) The minimum weight power system is a compromise between maximum efficiency and minimum weight power conditioning equipment.

3) The maximum efficiency solar array is also the minimum weight array and is necessary for the highest efficiency power system.

4) Higher distribution voltages (such as 50 vdc or 150 vac) provide the higher efficiency power systems.

5) The higher efficiency power systems usually result from configurations employing a central ac bus.

6) The power system having the least number of output voltages is the higher efficiency, lighter weight and more reliable system if two systems are compared having equal output power.

7) RTGs will probably be used in unmanned earth orbiters only for special purposes.

Most of the above conclusions appear to apply to a wide range of satellites and spacecraft in addition to those specific types investigated in this study. However, the special requirements of any mission must be taken into account in applying these study results. A considerable number of missions and spacecraft designs have special requirements which pre-empt,

to some degree, the optimization of the electrical power system. Power system studies should be broadened to include additional examination of the interfaces and interactions with other subsystems and the constraints they impose. A typical example is the requirement for full satellite operation in sunlight with or without the battery. Another common requirement specified by other subsystems, is the electrical isolation of their equipment. Optimization of the power system thus becomes a series of compromises involving the performance of the other subsystems.

In addition to restrictions placed on the uses of these study results by mission and spacecraft design constraints, necessary limitations on the scope and depth of this study have required that certain areas be given superficial treatment or be entirely excluded. Electromagnetic compatibility (EMC) is an exceedingly important aspect of any electric power system design. Further analysis of ac and dc distribution systems would clarify the applicability of certain types of circuits and system configurations, and increase the opportunities for power system optimization.

Reliability and cost were considered to a limited degree. Basic equipment designs used throughout this study can be made more reliable by exercising derating and redundancy techniques and accepting the associated penalties in system efficiency and/or weight. Tradeoff studies of weight, efficiency, and reliability for missions requiring lifetimes of 5 years and more deserve increased emphasis.

2.4.3 Recommendations

Although this study did not develop a conclusive technical justification for selecting specific standard voltages, it appears that a reduction to a single voltage for each of the several voltage ranges would be economical for new equipment designs without compromising performance.

The following voltages are recommended at this time as low-voltage dc standards, +50, ±28, ±15, ±10, and ±5.

Satellite designs using a relatively large amount of ac power require further investigation to optimize the choice of frequency for best utilization of satellite weight and maximum power system efficiency. Where the

using equipment requires a large amount of 400-cps power, it is recommended that 115-vac, 400-cps, two-phase, and 28-vac, 400-cps, single-phase power be established as standard. Satellite systems which do not have a definite 400-cps requirement should use a higher frequency, in the area of 2 kc, for best overall performance.

The third area for standardization is the circuit design and modularization of power conditioning equipments. Once standard voltages are established, power conditioning equipment can be optimized for efficiency, weight, and reliability. The use of standard modules of these circuits will reduce production costs and increase the built-in and proven reliability of power systems.

3. USER EQUIPMENT ELECTRICAL POWER CHARACTERISTICS

The study began with the accumulation of data covering the input power requirements and characteristics of spacecraft equipment and an analysis of the data to determine the reasons for those specific requirements. In each case, power characteristics required by the user equipments after conversion, inversion, or regulation, were determined. The collected data consisted of design specifications, schematic diagrams, and test data for five different spacecraft covering the missions indicated in Table 3-I. The spacecraft loads were divided into four major subsystem categories; communications, data handling, stabilization and control, and experiments.

3.1 COMMUNICATIONS EQUIPMENT

Tables 3-II through 3-IV summarize the communications equipment characteristics including input voltages, power, and design parameters which have a major influence on input power requirements. For purposes of analysis, the communications systems have been divided into their functional elements, transmitters, receivers, and decoders.

3.1.1 Transmitters

The transmitters listed in Table 3-II reflect the state-of-the-art designs. Although each application listed is unique, the study effort attempted to define general equipment categories and characteristics for purposes of comparison. Major factors in transmitter design which influence the input power requirements are rf output power, operating frequency, data rate, and bandwidth. Output power is a function of antenna gain and directionality, maximum range, and the ground station receiver characteristics. Operating frequency is restricted by available ground stations in many cases; however, improved performance results from operating in the 2- to 4-gc frequency range (S band) for telemetry data transmission. Communications satellites operate in the 4- to 8-gc range (C band). Transmitter power requirements increase with bandwidth, which is a direct function of the data transmission rate, type of modulation, and stability requirements. Typically, the phase-modulated transmitters investigated required bandwidths of two to five times the maximum data rate. Whereas the OGO data rate is relatively high, future requirements

Table 3-I. Spacecraft Designs Used for Analysis of Load Characteristics

I.	Orbiting Geophysical Observatory (OGO)	
	Payload	Approximately 20 scientific experiments
	Orientation	Three-axis attitude control
	Approximate power	250 w average
	Orbit:	
	EOGO	64 hr eccentric inclined
	POGO	104 min near circular polar
II.	Nuclear Detection Satellite (Vela)	
	Payload	Radiation detectors
	Orientation	Spin stablized
	Approximate power	80 w
	Orbit	108 hr circular inclined
III.	Pioneer	
	Payload	Scientific experiments
	Orientation	Spin stabilized with active orientation of spin axis normal to sun vector
	Approximate power	60 w
	Orbit	Not applicable, space probe to 1.2 or 0.8 AU
IV.	Able-V	
	Payload	Scientific experiments
	Orientation	Spin stabilized
	Approximate power	30 w
	Orbit	1400 to 2500 nmi circumlunar
V.	Communication Satellite (Comsat)	
	Payload	Communications repeater
	Orientation	Spin stabilized with active orientation of spin axis normal to orbital plane
	Approximate power	105 w
	Orbit	24 hr synchronous

Table 3-II. Transmitter Characteristics

Type	Antenna Gain	Output Power (w)	Output Frequencies (mc)	Maximum Data Rate/Bandwidth	Maximum Range (nmi)	Required Voltages and Regulation	Input Power (w)	Usage
Transistor pwr amp plus varactor freq mult	High	4.0	400	128,000 bits/sec	90,000	23 vdc ±2% 70 vdc ±2%	23.0	OGO telemetry data
Transistor pwr amp plus varactor freq mult	High	0.5	400	64,000 bits/sec	90,000	20 vdc ±2%	5.0	OGO telemetry data
Transistor pwr amp	Low	10.0	136	-	90,000	23 vdc ±2%	27.0	OGO tracking beacon
Transistor pwr amp	Low	0.1	136	-	90,000	23 vdc ±2%	1.0	OGO tracking beacon
Transistor pwr amp plus varactor freq mult	Low	4.0	400	256 bits/sec	60,000	23 vdc ±2% 70 vdc ±2%	21.0	Vela data and transponder
Traveling wave tube	High	8.0	2292	8 bits/sec*	41.5×10^6	-940 vdc ±0.5% -545 vdc ±1% 8 vdc ±1% 5 vac ±2.5%	26.0	Pioneer data and transponder
Transistor pwr amp plus varactor freq mult	Low	0.05	2292	8 bits/sec*	3.5×10^6	-16 vdc ±2%	1.5	Pioneer data or TWT driver
Vacuum tube pwr amp	High	2.0	378	1 bit/sec*	240,000	-12 vdc ±5% -20 vdc ±5% 210 vdc ±5% 6 vdc ±5% 6.3 vac ±5%	7.0	Able V data and transponder
Traveling wave tube	High	4.0	4000	200 mc	8,000	1440 vdc ±0.5% 1340 vdc ±0.5% 650 vdc ±0.5% 355 vdc ±0.5% 3 vdc ±0.5%	14.0	COMSAT repeater and telemetry data
Traveling wave tube	-	0.1	4000	500 mc	-	620 vdc ±0.5% 570 vdc ±0.5% 355 vdc ±0.5% 3 vdc ±0.5%	2.0	COMSAT TWT driver
Electronically Despun Antenna	13.2 db	-	4000	3.7 to 4.2 gc	-	±10 vdc ±3% +6 vdc ±3% +3.2 vdc ±1%	7.4	COMSAT Antenna

*Higher data rate at reduced range

are predicted for telemetry data rates of 20×10^6 bits/sec, which will require bandwidths of 50 to 100 mc. As indicated for the COMSAT design, frequency-modulated commercial communications repeaters with bandwidths of 200 mc are required. As indicated in Table 3-II, increased range for eccentric orbits and space probes generally has required reduced data rates to compensate for the increased transmission losses and input power limitations.

A limiting factor in transmitter design has been the unavailability of transistors capable of operating at higher power and frequency. The relatively early Able V design employed vacuum tubes to achieve a 20-w output at approximately 400 mc. This approach is reflected in the required input voltages listed. The more recent OGO and Vela transmitters employ all solid-state components with transistor power amplifiers and varactor frequency multiplier stages to achieve the desired 400-mc output frequency. The 70-v input requirement for the designs was dictated by the ratings of available transistors at the higher rf output ratings. The use of the relatively inefficient output frequency multiplier was necessitated by state-of-the-art transistor frequency limitations for the 400-mc applications. The 20- to 23-v requirements represent a selection based on the availability of nominal 28-v power.

A system tradeoff between maximum transmitter power consumption and input power conditioning requirements is necessary to justify transmitter power limitations. Typical commercially available operational amplifiers have been used which operate directly from unregulated 28-v power sources to eliminate dc-dc conversion requirements. With this approach, transmitter input power requirements are specified in terms of transmitter efficiency and minimum rf output power without imposing the additional input power limitations at the higher input voltages. A major consideration in the "no converter" approach is the increased system reliability which results.

Although reasonable steady-state voltage ranges can be tolerated without transmitter performance degradation, power source noise or ripple magnitudes of greater than 8 percent may introduce modulation of the transmitter output. Most of the solid-state transmitter designs investigated utilize low (phase) modulation indices (high sensitivity to modulating voltage signals). In addition, the trend to higher data rates and corresponding

increased bandwidth increases the transmitter sensitivity to a wide spectrum of ripple frequencies. In general, solid-state transmitters are not damaged by transient or sustained undervoltage conditions and will resume normal operation upon recovery of the input voltage. The use of high-frequency transistors (100-mc range), however, has greatly increased the susceptibility of these units to damage from overvoltage transients. Typically, 60-v breakdown ratings are the best available and input voltage spikes of microsecond duration represent potentially damaging transients. Considerations of ripple, noise, and transients, in many cases, lead to the use of input voltage regulators as well as filters to protect the transmitter from damage or degraded performance, or both.

Predicted future applications for solid-state transmitters are restricted to rf power levels of 5 to 10 w maximum at frequencies in the 2-gc range based on the availability of improved transistors. The need for increased radiated power at these frequencies has led to the development of the traveling wave tube (TWT) power amplifiers. These devices require a variety of closely regulated dc input voltages with extremely low ripple and noise content. Steady-state voltage levels range up to approximately 1500 vdc at ±0.5 percent regulation. In addition, variations in TWT characteristics make it desirable to provide for limited voltage adjustments at the power supply to optimize the TWT input voltages and, as a result, the efficiency of each tube.

Sensitivity of phase-modulated TWT transmitters to input voltage fluctuations is greater than that for the solid-state designs. Ripple limits of ±0.05 percent rms are required for critical tube inputs (cathode to helix) over a typical frequency range of 20 cps to 1 mc. Correspondingly, stringent limitations are placed on overvoltage spikes. In addition, certain TWT designs are susceptible to damage from undervoltage conditions of durations greater than 100 msec. Besides its higher power and frequency capabilities in relation to solid-state transmitter designs, the TWT transmitter provides efficiencies of approximately 30 percent as indicated in Table 3-II. Best estimates for comparable solid-state designs indicate achievable efficiencies of 10 to 15 percent in the 5 w, 2-gc range.

3.1.2 Receivers

Receiver data are summarized in Table 3-III. The Able, Vela, and Pioneer receivers represent similar phase-lock designs with identical data rates and omnidirectional antennas. A basic advantage of this design is its ability to keep the receiver tuned to the incoming frequency and thereby minimize bandwidth and resultant power requirements by automatically compensating for component drift and doppler shift. This design permits coherent retransmission of the received signal at the transmitter frequency for purposes of determining range rate information.

Input voltage levels represent selections based on the particular components used but generally fall in the 10- to 15-vdc range. As in the case of transmitters, steady-state regulation requirements result from minimum output and maximum input limits. Commercial operational amplifiers are being used in some receiver development programs and require plus and minus 15-vdc inputs.

Input voltage ripple frequencies below 100 kc can produce false modulation of the receiver output in phase-lock systems; it is desirable, therefore, to limit bus voltage fluctuations to less than 1 percent. Undervoltage conditions present no problem in resumption of normal performance; overvoltage transient limits are set by normal component breakdown ratings.

The AM receiver used on OGO provided for a relatively high command data rate at a lower carrier frequency. However, the OGO design, is not

Table 3-III. Receiver Characteristics

Type	Antenna Gain	Receiver Frequency (mc)	Maximum Data Rate/Bandwidth	Maximum Range (nmi)	Required Voltages and Regulation	Input Power (w)	Usage
AM demodulator	Low	120	128 bits/sec	90,000	20 vdc ±2% 13 vdc ±2% 9 vdc ±2%	2.7	OGO command
Phase lock	Low	375	1 bit/sec	60,000	10 vdc ±2% 12 vdc ±2%	1.6	Vela transponder and command
Phase lock	Low	2115	1 bit/sec	18.6×10^6	12.8 vdc ±2% -12.8 vdc ±2%	1.2	Pioneer transponder and command
Phase lock	Low	400	1 bit/sec	240,000	18.5 vdc ±13.5%	1.8	Able V transponder and command
Tunnel diode amplifier	High	6000	200 mc	8,000	28 vdc ±3%	0.4	COMSAT repeater

considered typical of current spacecraft applications due to the more general use of phase or frequency modulation techniques for the ground-satellite communications link.

The use of tunnel diode amplifiers in spacecraft receivers has yielded improved designs of low noise and reduced power requirements. The COMSAT receiver design listed in Table 3-III cannot be compared directly with the command receivers shown for other spacecraft because of different functions and resultant configuration. The COMSAT design employs tunnel diode circuits to amplify the received wideband communications signals without converting to a lower intermediate frequency as is generally required. After amplification, the nominal 6-gc received signals are converted to the 4-gc transmit frequencies and further amplified in the two-stage TWT transmitter. Command signals are detected and decoded after amplification in the low-level-transmitter stage. The data listed in Table 3-III reflect only the tunnel diode amplifier with the 6- to 4-gc conversion stages and exclude the command signal detector and local oscillator and frequency multiplier required for frequency conversion of the communications signals. Although the receiver operates on 28 v, resistive dividers are utilized to provide the required 0.125-v level across the tunnel diode. Regulation and ripple requirements are stringent at ±0.5 percent and less than 0.5 percent peak-to-peak, respectively.

3.2 DATA HANDLING EQUIPMENT

Command and telemetry data processing equipment encompasses a wide variety of circuit elements and designs. Several unit designs are listed in Tables 3-IV and 3-V to illustrate the types of power requirements involved. In each case, specific criteria such as data rates, modulation techniques, signal characteristics, accuracy requirements, and operational constraints, have produced equipment designs which are unique to each application. The individual circuits within the units are common in many cases; a detailed evaluation of each, however, is necessarily beyond the scope of this study.

Two categories of circuits have been investigated as representative of data handling systems; low-level logic and analog-to-digital converter.

3.2.1 Logic Circuits

Normal operating voltages lie in the 6- to 10-v range with typical

Table 3-IV. Command Decoder Characteristics

Type	Data Rate	Required Voltages and Regulation	Input Power (w)	Usage
Digital FSK	128 bits/sec	18 vdc ± 2%, 8 vdc ± 2%	3.0	OGO
3-Tone sequence	1 tone/sec	18 vdc ± 2%, 27 vdc ± 2%	1.7	OGO
Digital on-off tone	1 bit/sec	12.2 vdc ± 3%	0.7	Vela
Digital FSK	1 bit/sec	16.7 vdc ± 2%	0.4	Pioneer
Digital on-off tone	1 bit/sec	18 vdc ± 15%	0.6	Able V

regulation requirements including ripple and noise of ±2 percent. Lower voltages increase susceptibility to data anomalies resulting from voltage fluctuations; higher voltages produce undesirable increased power consumption in low-impedance circuits.

A significant development in the design of data handling equipment is the increasing use of microelectronic (integrated circuit) techniques. The advantages of this approach include improved reliability and response time in addition to the more obvious reductions in equipment size and weight. Existing voltage breakdown capabilities of the microelectronic circuit elements limit the power supply voltage to 6 v. Usage in current development programs at TRW requires typical input voltages of 2 and 4 v. As previously indicated, voltage ripple, noise, and transients at the low steady-state levels must be minimized to prevent erroneous data indications.

Table 3-V. Data Handling Equipment Characteristics

Type	Capacity	Maximum Data Rate	Required Voltages and Regulation	Input Power (w)	Usage
Magnetic core data storage	30,464 bits	256 bits/sec	28 vdc ±5%, -6 vdc ±5%	0.4	Vela
Magnetic core data storage	15,232 bits	512 bits/sec	+16 vdc ±5%, -16 vdc ±5%	0.1	Pioneer
Digital (PCM) telemetry encoder	90 channels	256 bits/sec	16 vdc ±2%, 10 vdc ±2%, -6 vdc ±2%, -16 vdc ±2%	1.2	Vela
Digital (PCM) telemetry encoder and subcarrier modulator	120 channels	512 bits/sec	16 vdc ±3%, 10 vdc ±3%, -16 vdc ±3%, 9.9 vdc ±3%	3.0	Pioneer
Analog-digital converter	416 channels	64,000 bits/sec	16 vdc ±1%, -16 vdc ±1%, 9 vdc ±1%	1.1	OGO
Digital data handling, timing and sync, and experiment controls		64,000 bits/sec	16 vdc ±1%, 9 vdc ±1%, -6 vdc ±1%	11.7	OGO

Higher currents and faster rise times are characteristic of integrated circuits and combine with the stringent noise limitations to create difficult problems in the design of power conditioning equipment, regulators, and filters.

3.2.2 Analog-to-Digital Converter Circuits

Required input voltages are selected to be several times the full scale analog input signal level. For a typical 0- to 5-v analog system, the A to D converter is designed for ±16 v. Higher voltages again yield increased power requirements for the circuits which operate in a more nearly constant current mode. The major influencing factor on power consumption and allowable voltage variations is the required accuracy of the data conversion process. As a result, regulation requirements of ±1 percent are necessary in some cases, although ±2 to 3 percent has proven adequate in several existing designs.

3.3 STABILIZATION AND CONTROL EQUIPMENT

Detailed data have been collected and tabulated covering the attitude control system for the OGO spacecraft. The attitude control system employs both reaction wheels and gas jets for three-axis vehicle orientation. In addition, the system provides for sun orientation of two solar cell panels and for experiment-package orientation relative to the orbital plane. Earth horizon sensors and sun sensors, as well as gyro reference assemblies, provide error signals to the control electronics. Two-phase, 400-cps motors are employed for the reaction wheels and mechanical drives of the panels and experiment package. Solenoid valves are utilized for gas jet control. The stabilization and control system represents an average load of 85 w with peak demands of 120 w and requires a variety of dc and ac inputs to operate the various control elements.

The sun sensor, pneumatics, and electronic control assemblies used for spin-axis orientation of the Pioneer space probe were analyzed to define representative input power characteristics for these spacecraft components.

Tables 3-VI, 3-VII, and 3-VIII summarize the results of the electrical power requirements survey for typical stabilization and control equipment. Stabilization and control systems usually consist of sensors and reaction

devices, connected through a set of electronics which provide the required data processing and logic functions. Table 3-VI shows voltage, voltage regulation, frequency, frequency regulation, ripple, duty cycle, and average power for samples of the three types of sensors commonly used (inertial, optical, electromechanical transducers). Table 3-VII provides the same data for the standard types of reaction devices and Table 3-VIII shows the requirements for typical digital and analog signal processing and logic units.

A review of these tables indicates the great variety of power requirements imposed by stabilization and control equipment, not only with regard to voltage regulation, but for ripple and noise as well. Consultations were held with responsible design engineers to determine the reasons for this wide variety. It was found that, in most cases, a component or part was chosen because it was available and met the functional requirements of the attitude control system. Its particular power requirements were accepted without consideration as to whether the power system could be simplified by selection of another part or component which might also meet the functional requirements. The lack of standardization results in part, from a lack of attention to the matter; TRW believes that if the equipment were to be redesigned or modified, it would be possible to standardize on a smaller range of electrical power requirements.

3.4 EXPERIMENTS

The OGO and Pioneer spacecraft experiments accounted for a majority of the accumulated data on experiments. In both, the experiment package contained power conditioning provisions which operated from a loosely regulated dc power bus. Such an approach establishes a simple interface between the power system and the loads but appears to sacrifice overall power system efficiency and weight. Considerable difficulty has been experienced in ascertaining the power characteristics required by the experiments after regulation, conversion, etc. In the majority of cases, only nominal voltage levels and total power consumption are available. For OGO, the average total experiment load of approximately 50 w represents a significant portion of the total required spacecraft power.

Table 3-VI. Stabilization and Control Sensor Characteristics

Sensor Type	Attitude Control System – Type	Required Voltage and Regulation	Required Freq and Regulation (cps)	Ripple p - p	Duty Cycle	Average Power	Usage
I. Inertial							
Rate gyro	Active 3-axis control	26/18 vac + 20 vdc ±2% - 20 vdc ±2% + $28^{+5.5}_{-4.5}$ vdc	400 ±0.1% 2φ - - -	- 300 mv 300 mv 300 mv	100% until stabilized in orbit	6.0 w 0.46 w 0.17 w 0.30 w	OGO
Rate gyro	Spin stabilized with active orientation	+ 22^{+2}_{-3} vdc	-	200 mv	100% until normal orbit attained	4 w plus 8 w heaters	Vela
Position gyro	Active 3-axis control	+ $28^{+5.5}_{-4.5}$ vdc	-	300 mv	100% 60%	4.84 w 12.0 w heaters	OGO
Accelerom-eter	Spin stabilized probe	+ 45 vdc ±10% + 20 vdc ±10% - 20 vdc ±10%			Command	9 mw 160 mw 160 mw	Able V
II. Optical							
Earth detector	Active 3-axis control	+ 20 vdc ±1.5% - 20 vdc ±1.5%	- -	- -	100% 100%	4.35 w 4.35 w	OGO
Earth detector	Active spin stabili-zation	+ 22^{+2}_{-3} vdc	-	200 mv	100%	3.0 w	Vela
Earth detector	Active spin stabili-zation	+ 26.5 ±4.5 vdc	-	200 mv	100%	0.75 w	COMSAT
Sun detector	Active spin stabili-zation	+ 15 vdc ±1.5%	-	±2%	100%	Negligible	Pioneer
Sun detector	Active 3-axis stabili-zation	None	-	-	-	-	OGO
Sun detector	Active spin stabili-zation	None	-	-	-	-	COMSAT
III. Transducers							
Resolver	Shaft position	115 vac ±1.5%	2461 ±0.1%	-	100%	150 mw	OGO
Pressure transducer	Pneumatic press	+5 vdc ±1%	-	50 mv	100%	10 mw	OGO

Table 3-VII. Stabilization and Control Reaction Device Characteristics

Device Type	Operating Mode	Required Voltage and Regulation	Required Freq and Regulation (cps)	Ripple p - p (mv)	Duty Cycle	Average Power	Usage
I. Reaction Wheel							
Yaw motor	Stall or acceleration	125 ±10 vac 135 ±10 vac	400 ± 5% 400 ± 5%	- -	51% 51%	22.7 w	OGO
	Full speed	125 ±10 vac 135 ±10 vac	400 ± 5% 400 ± 5%	- -	46% 46%	8.1 w	
Pitch or roll	Stall or acceleration	125 ±10 vac 135 ±10 vac	400 ± 5% 400 ± 5%	- -	40% 40%	6.5 w	OGO
	Full speed	125 ±10 vac 135 ±10 vac	400 ± 5% 400 ± 5%	- -	57% 57%	3.6 w	
Yaw or roll	All modes	$+22^{+2}_{-3}$ vdc	-	200	100%	3.0 w	Vela
II. Solenoids							
Yaw, pitch, or roll	Acquisition mode	26^{+5}_{-4} vdc	-	200	100%	3.4 w	OGO
	Orbit mode	26^{+5}_{-4} vdc	-	200	0.02%	0.7 mw	
Radial or axial	Acquisition mode	26 ±4.5 vdc	-	400	Command	4.2 w (on)	COMSAT
	Orbit mode	26 ±4.5 vdc	-	400	Command	4.2 w (on)	
Yaw, pitch, or roll	All modes	22^{+2}_{-3} vdc	-	200	Command	12.5 w (on)	Vela
Roll	Spin-up	16 ±0.5 vdc	-	-	0.06%	1.0 mw	Pioneer
III. Thrusters							
Heaters	Despin	22^{+2}_{-3} vdc	-	200	Command	33.0 w	Vela
	ΔV	22^{+2}_{-3} vdc	-	200	Command	132.0 w	
IV. Motors							
Solar array or OPEP drive motors	De-energized	125/135 ±10 vac	400 ± 5%	-	90%	20 mw	OGO
	Accelerating	125/135 ±10 vac	400 ± 5%	-	3%	170 mw	
	Full speed	125/135 ±10 vac	400 ± 5%	-	7%	213 mw	

Table 3-VIII. Stabilization and Control Electronic Characteristics

Circuit Type	Function	Required Voltage and Regulation		Required Freq. and Regulation	Ripple p - p (mv)	Duty Cycle	Average Power	Usage
		vdc	±%					
I. Digital								
Electrical integration assembly	Input to ADCS*	+26.5 ±4.5		-	200	100%	100 mw	COMSAT
		+10	3	-	200	100%	200 mw	
		+6	3	-	200	100%	3 mw	
*Attitude determination and control system	Control ACS	+15	3	-	200	100%	150 mw	COMSAT
		-15	3	-	200	100%	150 mw	
		+6	3	-	200	100%	350 mw	
		-6	3	-	200	100%	350 mw	
Control electronics assembly	Control ACS	+22 $^{+2}_{-3}$		-	200	100%	14 w	Vela
Valve drivers	De-energized	+28 $^{+5.5}_{-4.5}$		-	400	99.98%	11 mw	OGO
	Energized	+28 $^{+5.5}_{-4.5}$		-	400	0.02%	0.7 mw	
Reference signal	Horizon scanner demodulator	±20	1.5	-	300	100%	40 mw	OGO
		±10	1.5	-	600	100%	40 mw	
		+28 $^{+5.5}_{-4.5}$		-	600	100%	40 mw	
Drive electronics	Solar array or OPEP drive	115 vac	2	2461 cps ±0.1%	-	100%	950 mw	OGO
		+20	1.5	-	300	100%	100 mw	
		+10	3	-	300	100%	60 mw	
		+28 $^{+5.5}_{-4.5}$		-	300	10%	1.4 w	
		28 vac	3	400 cps ±5%	-	10%	750 mw	
II. Analog								
Horizon scanner central electronics	Process horizon sensor signals	+20	1.5	-	300	100%	4.35 w	OGO
		-20	1.5	-	300	100%	4.35 w	
OPEP gyro electronics	Process gyro signals	+28 $^{+5.5}_{-4.5}$		-	400	100%	3.54 w	OGO
Inertial reference unit	Provide reference signals	+28 $^{+5.5}_{-4.5}$		-	400	Hot 4.84 w Cold 16.84 w	12 w	OGO
Signal conditioner	Signal conditioning	+10	0.2	-	50	5%	300 mw	Vela
Signal Conditioner	Telemetry signal	-20	1.5	-	50	100%	20 mw	OGO
		+20	1.5	-	50	100%	50 mw	
		+10	1.5	-	50	100%	30 mw	
Valve driver	Bias	-20	2	-	400	100%	340 mw	OGO
Yaw motor driver	Stall or accel.	125/135 ±10 vac		400 cps ±5%	-	51%	16.6 w	OGO
	full speed	125/135 ±10 vac		400 cps ±5%	-	46%	6.6 w	
Pitch or roll motor drive	Stall or accel.	125/135 ±10 vac		400 cps ±5%	-	40%	4.9 w	OGO
	full speed	125/135 ±10 vac		400 cps ±5%	-	57%	3.3 w	
Bi-stable mag-amp	De-energized	115 vac	2	2461 cps ±0.1%	-	50%	23 mw	OGO
	Energized	115 vac	2	2461 cps ±0.1%	-	50%	350 mw	

Table 3-IX lists 58 experiments which were reviewed for the study. They are classified in the table in nine basic functional categories covering the range of nearly all present or anticipated satellite experiments. It can be seen that in many cases within a functional category, experiments may differ only in the range of the parameters they measure.

The general practice applied to electrical power for scientific experiments has been to provide the experiments with the nominal spacecraft bus voltage, leaving any required conversion, inversion, or additional regulation to be performed within the experiment package. This practice simplifies the definition of interfaces and undoubtedly expedites the overall program, but at the cost of considerable waste of power. It is not unreasonable to estimate that half the power supplied to the experiments has been wasted in power conditioning equipment within the experiment package.

Table 3-X summarizes the electrical power requirements for each of the experiments listed. From the data shown here, it is clear that the variety of requirements is much greater than for any other subsystem. Not only is there a wide range, but in some cases, the requirements differ so slightly (for example, different experiments require 5, 6, 7, 8, 9, and 10 vdc, respectively) that it seems very probable that standardization would be possible.

Table 3-IX. Classification of Experiments

I.	Radio Frequency		
	1)	#5001 Radio Astronomy - 2.4 mc cosmic noise	OGO-C
	2)	#5002 VLF Propagation - 0.2 to 100 kc	OGO-C
	3)	Range and Range Rate 2270 mc	OGO-C
	4)	#PC-1.05 Radio Propagation - Stanford	Pioneer
	5)	#4917 VLF Noise and Propagation 0.2 to 100 kc	OGO-A
	6)	#4918 Radio Astronomy 2 to 4 mc	OGO-A
II.	Audio Frequency		
	1)	#5003 Whistlers and Audio Frequency Electromagnetic Waves 500 cps to 18 kc	OGO-C
III.	Magnetic Fields		
	1)	#5005 Low-Frequency Magnetic-Field Fluctuations	OGO-C
	2)	#5006 Rubidium Vapor Magnetometer-Magnetic Field Survey	OGO-C
	3)	#PC-1.02 Magnetometer - GSFC	Pioneer
	4)	Flux Gate Magnetometer	Able V
	5)	Spin Coil Magnetometer	Able V
	6)	#4910 Low-Frequency Magnetic-Field Variations 0.01 cps to 3 kc	OGO-A
	7)	#4911 Magnetic-Field Strength and Direction 3γ to 0.14 gauss	OGO-A
IV.	Plasma Measurements		
	1)	#PC-1.03 Plasma Probe - MIT	Pioneer
	2)	#PC-1.08 Plasma Probe - ARC	Pioneer
	3)	Plasma Probe	Able V
	4)	#4902 Plasma (Electronstatic Analyzer) 100 ev to 200 kev	OGO-A
	5)	#4903 Plasma (Faraday Cup) 100 ev to 10 kev	OGO-A

Table 3-IX. Classification of Experiments (Continued)

V.	Light Frequencies		
	1)	#5012 Airglow and Aurora Photometer	OGO-C
	2)	#5013 Lyman Alpha and U.V. Airglow 1216 to 1550Å	OGO-C
	3)	#5014 Ultraviolet Spectra of the Earth's Atmosphere 1100 to 3300Å	OGO-C
	4)	#5019 Ionosphere Composition and Solar U.V. Flux	OGO-C
	5)	#5020 Solar U.V. Emissions 170 to 1700Å	OGO-C
	6)	#4919 Geocoronal Lyman-Alpha Scattering (1216Å)	OGO-A
	7)	#4920 Gegenschein Photometry	OGO-A
VI.	Particle Radiation		
	1)	#5008 Low-Energy Proton - Alpha Telescope Protons 0.5 to 40 mev - Alpha 2 to 160 mev	OGO-C
	2)	#5009 Galactic and Solar Cosmic Rays 40 mev to 1 bev	OGO-C
	3)	#5010 Corpuscular Radiation - Electrons 40 kev and >120 kev	OGO-C
	4)	#5011 Low-Energy Trapped Radiation and Auroral Particles 10 to 100 kev electrons, 100 kev to 10 mev protons, 10 kev to 10 mev total flux	OGO-C
	5)	#5007 Cosmic Ray and Polar Region Ionization	OGO-C
	6)	#5017 Neutral Particle Measurements (density, temp)	OGO-C
	7)	#5021 Solar X-Ray Emissions 0.5 Å, 2 to 8Å,	OGO-C
	8)	#PC-1.04 Cosmic Ray - University Chicago	Pioneer
	9)	#PC-1.06 Cosmic Ray - GRCSW	Pioneer
	10)	Solid State Detector - Proton Flux 0.5 to 10 mev	Able V
	11)	Low-Energy Scintillometer - Electron and Proton	Able V
	12)	Ion Chamber and Geiger Counter	Able V

Table 3-IX. Classification of Experiments (Continued)

	13)	Cosmic Ray Telescope	Able V
	14)	Scintillation Spectrometer - Protons	Able V
	15)	#4901 Solar Protons 2 to 100 mev	OGO-A
	16)	#4904 Positron Search and Gamma Rays	OGO-A
	17)	#4905 Trapped Radiation (Scintillation Counter) Electrons and Protons	OGO-A
	18)	#4906 Isotopic Abundance and Galactic Cosmic Rays	OGO-A
	19)	#4907 Cosmic Ray Spectra and Fluxes 0.3 mev to 4 bev	OGO-A
	20)	#4908 Trapped Radiation (Geiger Counter) (electrons 40 kev to 2 bev)(protons 0.5 mev to 23 mev)	OGO-A
	21)	#4909 Trapped Radiation (Electron Spectrometer) 50 kev to 4 mev	OGO-A
	22)	#4912 Thermal Charged Particles - electrons and ions 0.2 ev to 1 kev	OGO-A
	23)	#4913 Thermal Charged Particles - ± ions low energy	OGO-A
	24)	#4914 Electron Density by RF Propagation - electron density	OGO-A
VII.	Mass		
	1)	#5015 Neutral and Ion Mass Spectrometer 1 to 50 AMU	OGO-C
	2)	#5016 Positive Ion Composition 1 to 45 AMU	OGO-C
	3)	#4915 Atmospheric Composition 1 to 45 AMU Positive Ions	OGO-A
VIII.	Meteorites		
	1)	#5018 Micrometeorites - spatial density and mass distribution 10^{-13} to 10^{-19} grams	OGO
	2)	#PC-1.07 Micrometeoroid Detector - ARC	Pioneer

Table 3-IX. Classification of Experiments (Continued)

3)	Micrometeorites	Able V
4)	#4916 Micron Dust Particles (mass, velocity, direction, intensity, time and spatial variations)	OGO-A
IX.	Biological or Mineral Detectors	
1)	Microbiological Detector	Surveyor

Table 3-X. Power Characteristics of Experiments

Experiment Identification	Required Voltage and Regulation		Ripple p - p	Duty Cycle	Average Power	Usage
	vdc	± %				
I. Stanford Radio Propagation	- 3		-	?	1.4 w	Pioneer
	+ 2.5		-	?		
	+ 5		-	?		
	+ 12		-	?		OGO
II. 5003 Whistlers and Audio Frequency Electromagnetic Waves - 500 cps to 18 kc						
III. Magnetometer (UCLA)	+ 6	0.1	0.1%	Command	168 mw	OGO
	+ 8	1	20 mv	Command	960 mw	
	- 8	1	20 mv	Command	120 mw	
	+ 20	0.1	0.1%	Command	800 mw	
	- 20	1	20 mv	Command	200 mw	
	+ 3	1	20 mv	Command	300 mw	
Spin Coil Magnetometer	+ 10	1	1%	100%	100 mw.	Able V
	- 16	1	1%	100%	120 mw	
	± 6	5	1 mv max	100%	?	
Flux Gate Magnetometer	+ 6	1	1%	100%	180 mw	Able V
	- 6	1	1%	100%	12 mw	
	+ 18	2	(Special)	0-5 sec	3.24 w	
	+ 18	2	(Battery)	0-5 sec	72 w	
IV. MIT Plasma Probe	± 6		?		Lo avg	Pioneer
	± 12		?		0.9 w	
	+ 10		?		Hi avg	
	- 25		?		2.1 w	
	- 30		?		Peak	
	+ 75		?		7.9 w	
ARC Plasma Probe	- 3		?	?		Pioneer
	± 6		?	?		
	+ 12		?	?	1.5 w	
	- 18		?	?		
	± 150		?	?		
	+ 165		?	?		
V. White Light Coronagraph (*3 kv varied on command with superimposed variable 1 kv)	± 10	0.1	0.1%	100%	10 w	AOSO
	± 3	0.1	0.1%	100%		
	+ 3000*		1%	30 w max		

Table 3-X. Power Characteristics of Experiments (Continued)

Experiment Identification	Required Voltage and Regulation		Ripple p - p	Duty Cycle	Average Power	Usage
	vdc	±%				
VI. Proton Spectrometer (UCLA)	+ 1250	0.1	0.1%	Command	250 mw	OGO
	- 20	1	20 mw	Command	90 mw	
	+ 3	1	20 mw	Command	177 mw	
	+ 7	1	20 mw	Command	1.3 w	
	- 7	1	20 mw	Command	262 mw	
	- 6	0.1	0.1%	Command	150 mw	
	+ 5.1	0.1	0.1%	Command	122 mw	
	- 3	1	20 mw	Command	118 mw	
GRCSW Cosmic Ray	+ 1200	0.1	0.1%		1.5 w	Pioneer
	+ 3.1	1	1%			
	+ 12	1	1%			
Cosmic Ray Telescope	+ 6	1	1%	100%	240 mw	Able V
Ion Chamber and Geiger Counter	+ 6	1	1%	100%	90 mw	Able V
Solid State Detector	+ 6	1	1%	100%	55 mw	Able V
	+ 6	1	1%	100%	1.6 mw	
Scintillation Spectrometer	+ 1200	0.1	0.1%	100%	100 mw	Able V
	+ 16	1	1%	100%	240 mw	
	- 16	1	1%	100%	20 mw	
	+ 10	1	1%	100%	12 mw	
	+ 6	1	1%	100%	15 mw	
	- 6	1	1%	100%	23 mw	
	+ 18 ±3		-	one 1/2	2.5 w	
	+ 18 ±3		-	sec pulse	54 w	
	+ 10 ±0.5		200 mv max	?	?	
	+ 3 ±0.5		200 mv max	?	?	
	+ 8 ±0.5		200 mv max	?	?	
Low Energy Scintillometer	+ 1200	0.1	0.1%	100%	100 mw	Able V
	+ 16	1	1%	100%	208 mw	
	+ 6	1	1%	100%	132 mw	
Cosmic Ray and Gamma Ray	+ 10	0.1	0.1%	100%	650 mw	OSO-C
	+ 1200	0.1	0.1%	100%	50 mw	
X-Ray Instrument	+ 10	0.1	0.1%	100%	450 mw	OSO-C
	+ 1200	0.1	0.1%	100%	50 mw	
Primary Electron Detector	+ 10	0.5	0.5%	100%	1 w	OGO-E
	+ 2.5	2	0.2%	100%		
	+ 1350	0.1	0.1%	100%		

Table 3-X. Power Characteristics of Experiments (Continued)

Experiment Identification	Required Voltage and Regulation		Ripple p - p	Duty Cycle	Average Power	Usage
	vdc	±%				
VIII. Micrometeorite	+6	1	1%	100%	72 mw	Able V
IX. Microbiological Detector	±10 +10	0.25 1	2% 2%	100% 1w on 2 sec	200 mw 2 mw	Surveyor

4. EXISTING POWER SYSTEM DESIGNS

A spacecraft electrical power system can be simply defined in terms of the characteristics of the power available on its main power bus. These are basically the following:

- Voltage
- Voltage regulation
- Average and peak power
- Ripple and noise

Table 4-I lists these characteristics for eight different satellites. The range of values shown probably cover the requirements for most future unmanned spacecraft. For this reason, a detailed examination of these eight systems may offer a basis for establishing power system standards. In addition, the proposed configurations used in EPSOM (Section 6) were derived from the study of these systems.

Figures 4-1 through 4-8 are block diagrams showing the electrical power system configuration of the eight satellites listed in Table 4-I. In each case the system consists of a solar cell array and batteries. In general, the same functions are performed by each system and thus the same basic equipments are found. The differences result, to a large extent, from the varying emphasis on one or another requirements, such as the very long lifetime required for COMSAT, the intermittent heavy load in Relay, the stress on off-the-shelf designs for Vela, the heavy loads and relatively complex equipment on EOGO and POGO, and so on.

Another major influence on electrical power system design is the planned orbit for the spacecraft. Table 4-II indicates the characteristics of the orbits for the satellites discussed. Orbit characteristics affect power system design by dicatating such important parameters as length and frequency of eclipses, integrated radiation flux and solar radiation angles of incidence. These parameters directly affect the battery size, cycling requirements, the oversizing of the solar array, and the types of power control required.

Table 4-I. Load Bus Power Characteristics

Unregulated Bus v	%	Load Bus Power (w)	Batteries: Number Cells	Batteries: Amp-Hr	Batteries: Type	Load Bus: Impedance (ohm)	Load Bus: Ripple (p-p)	Load Bus: Transients	Usage	Maximum Solar Array Power (w)
28	-25 +10	50	21 x 2	4.0	Ni-Cd	-	-	-	Tiros	90
28	+25 -10	50	22 x 2	4.0	Ni-Cd	-	20 mv	34 vdc peak for 0.5 sec	Relay	90
28	+20 -16	300	22 x 2	12.0	Ni-Cd	<0.5	0.3 v	≤50 vdc peak for <10 msec	EOGO	600
28	+20 -16	500	22 x 2	12.0	Ag-Cd	0.5 to 3	0.3 v	≤50 vdc peak for <10 msec	POGO	600
28	+18 -16	55	18	1.0	Ag-Zn	<13	150 mv	±2.25 v peak	Pioneer	81
22	+10 -15	75	16 x 2	6.0	Ni-Cd	<1.0	200 mv	±2.20 v peak	Vela	100
18	+28 -22	35	14 x 2	4.0	Ni-Cd (F type)	<0.4	0.5 v		Able V	40
28	+15 -15	105	20	6.0	Ni-Cd	<1.0	<5 mv 0 to 10 kc	≤50 vdc peak for <10 msec	COMSAT	161

Table 4-II. Orbital Characteristics

Program	Orbit Time	Predicted Life Time	Type – Inclination
COMSAT	24 hr	5 yr	Equatorial – Synchronous
EOGO	64 hr	1 yr	30 deg inclined
POGO	104 min	1 yr	Polar - 87 deg inclined
Pioneer	Probe	6 mo	Solar orbit, 1.2 or 0.8 AU
Relay	185.1 min	1 yr	48 deg inclined
Vela	108 hr	3 yr	31 deg inclined
Tiros	113.5 min	6 mo	Polar - 101 deg inclined
Able-V	12 hr	1 yr	1400 to 2500 nmi lunar orbiter

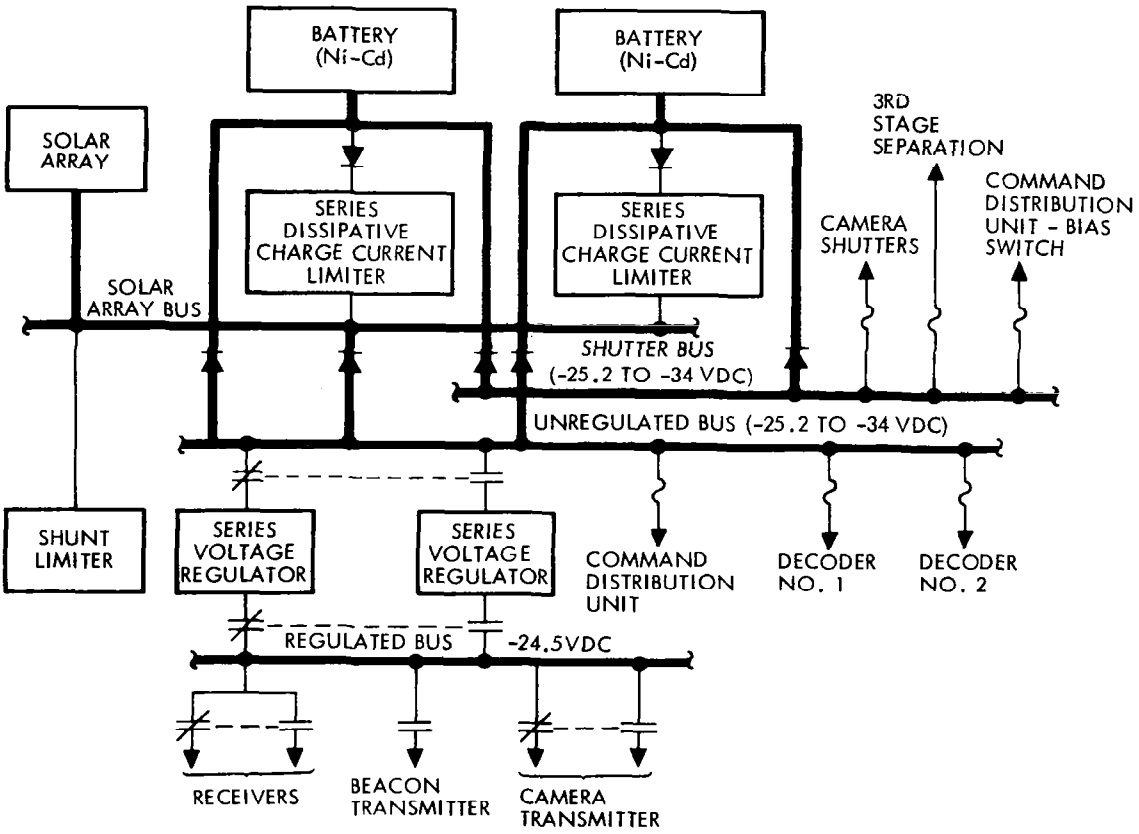

Figure 4-1. Tiros Electric Power Subsystem

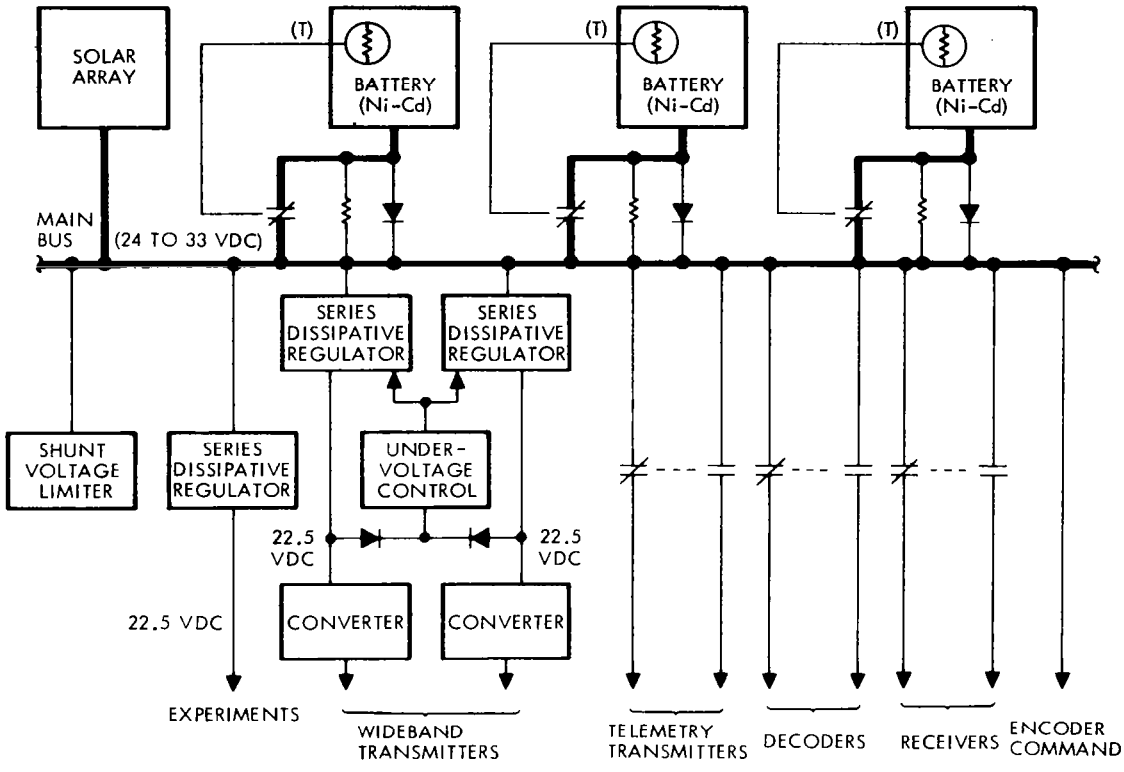

Figure 4-2. Relay Electric Power Subsystem

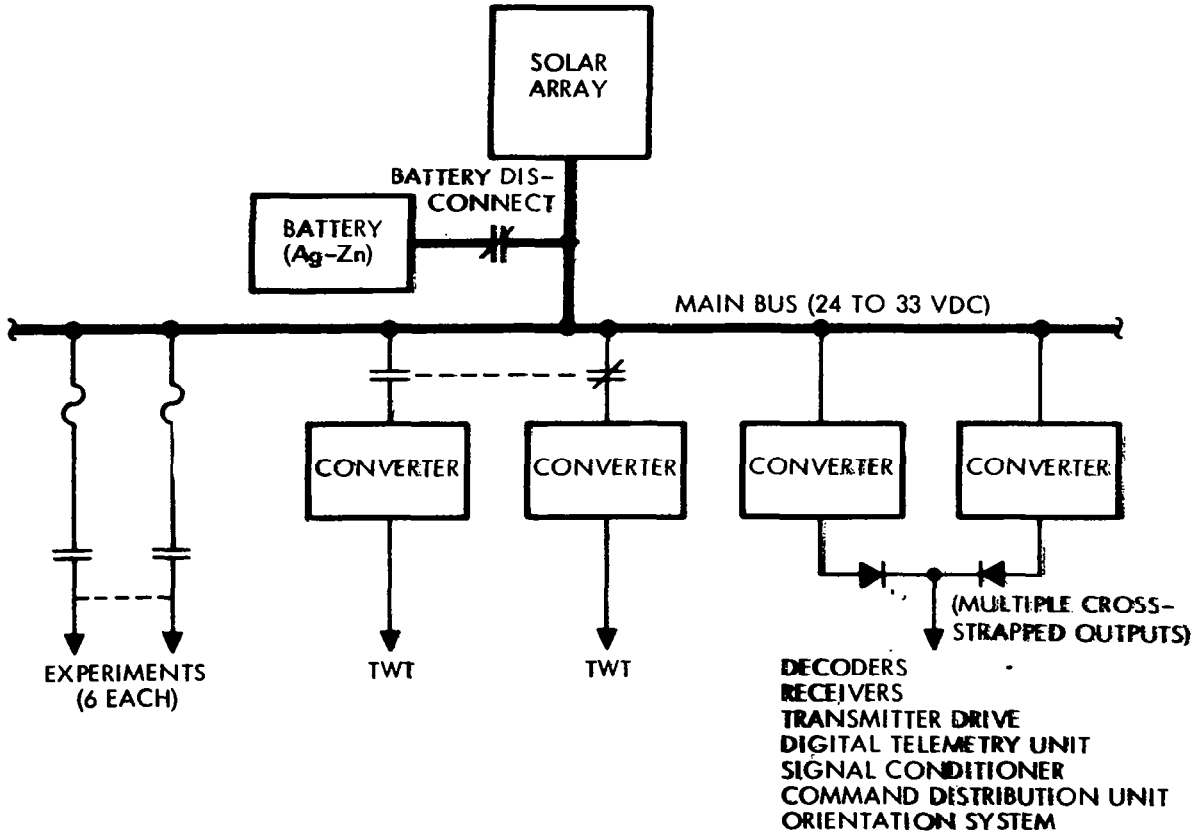

Figure 4-3. Pioneer Electric Power Subsystem

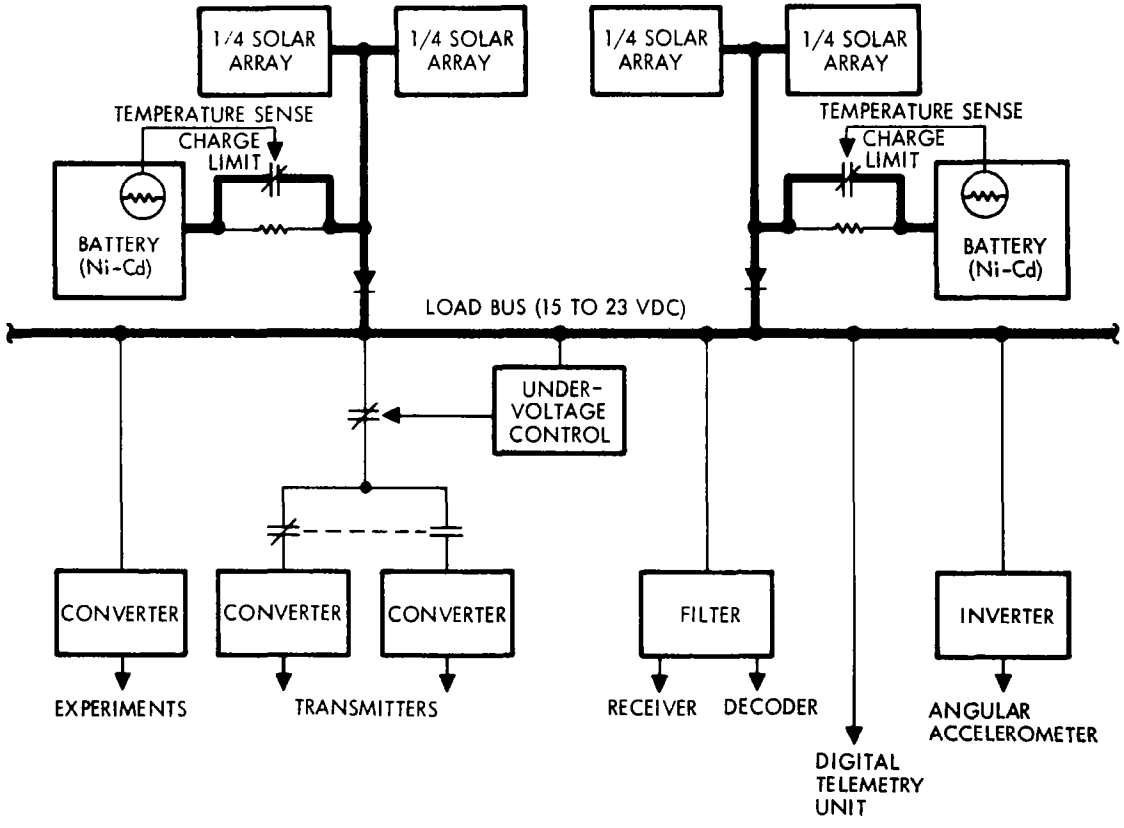

Figure 4-4. Able-V Electric Power Subsystem

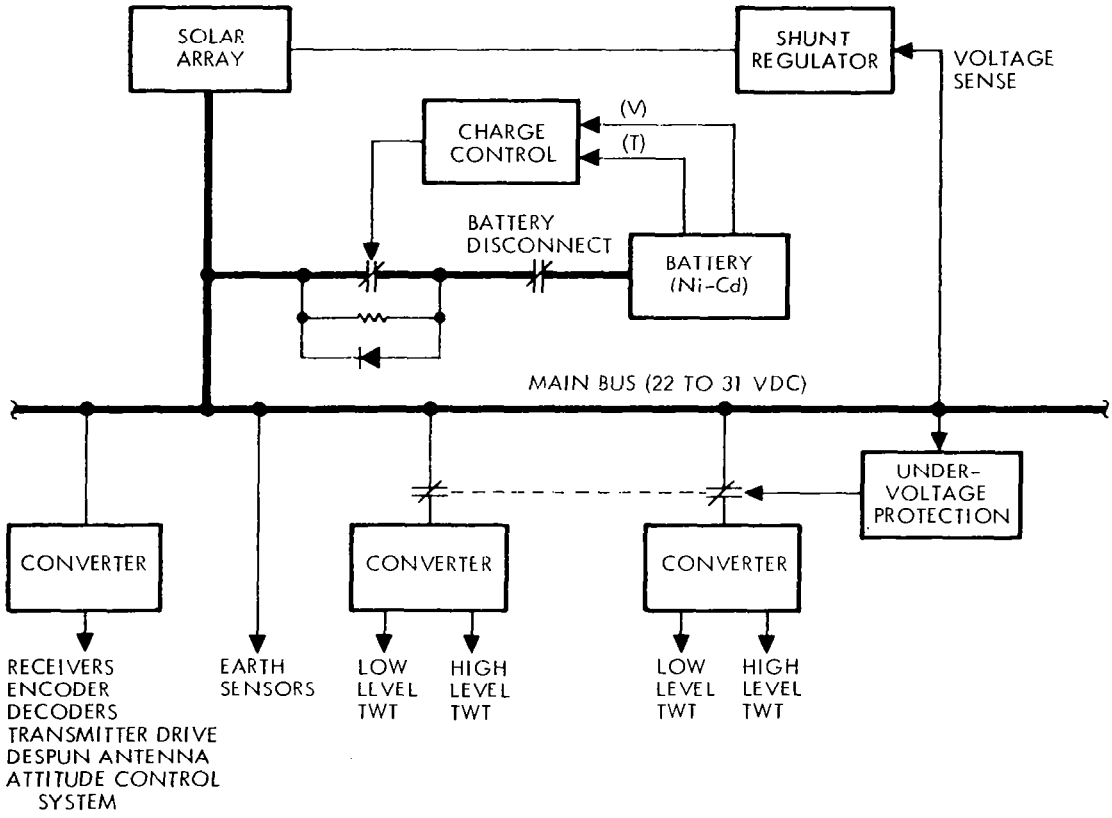

Figure 4-5. COMSAT Electric Power Subsystem

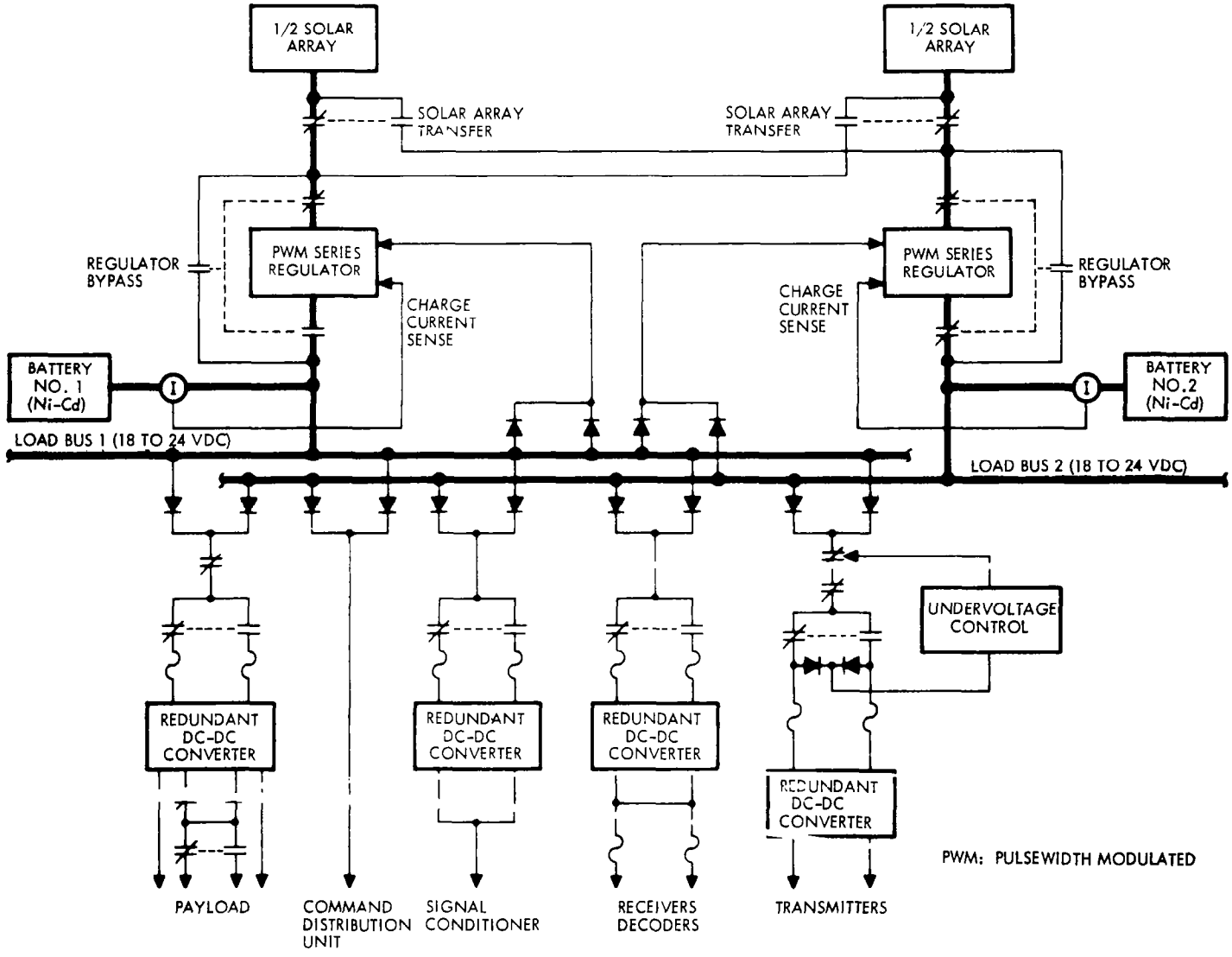

Figure 4-6. Vela Electric Power Subsystem

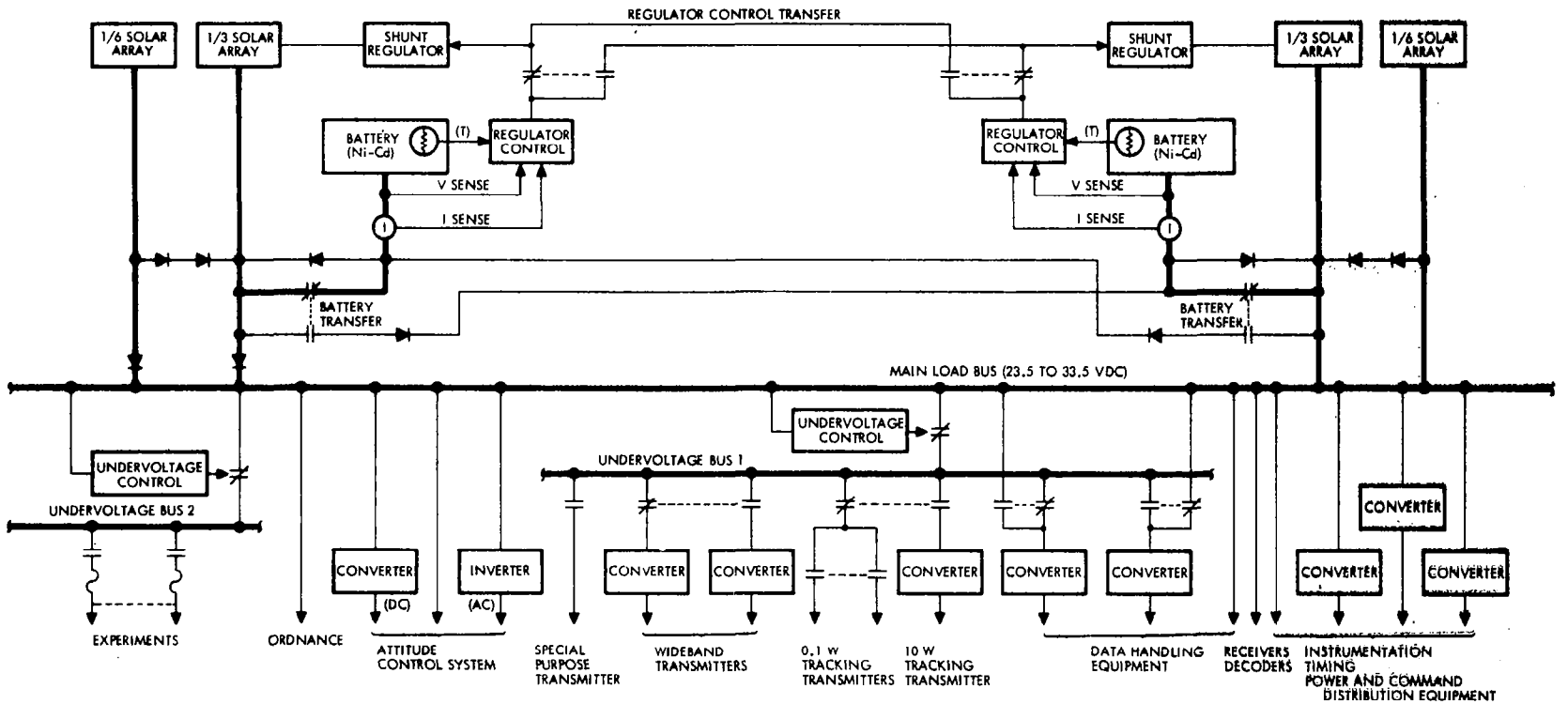

Figure 4-7. EOGO Electric Power Subsystem

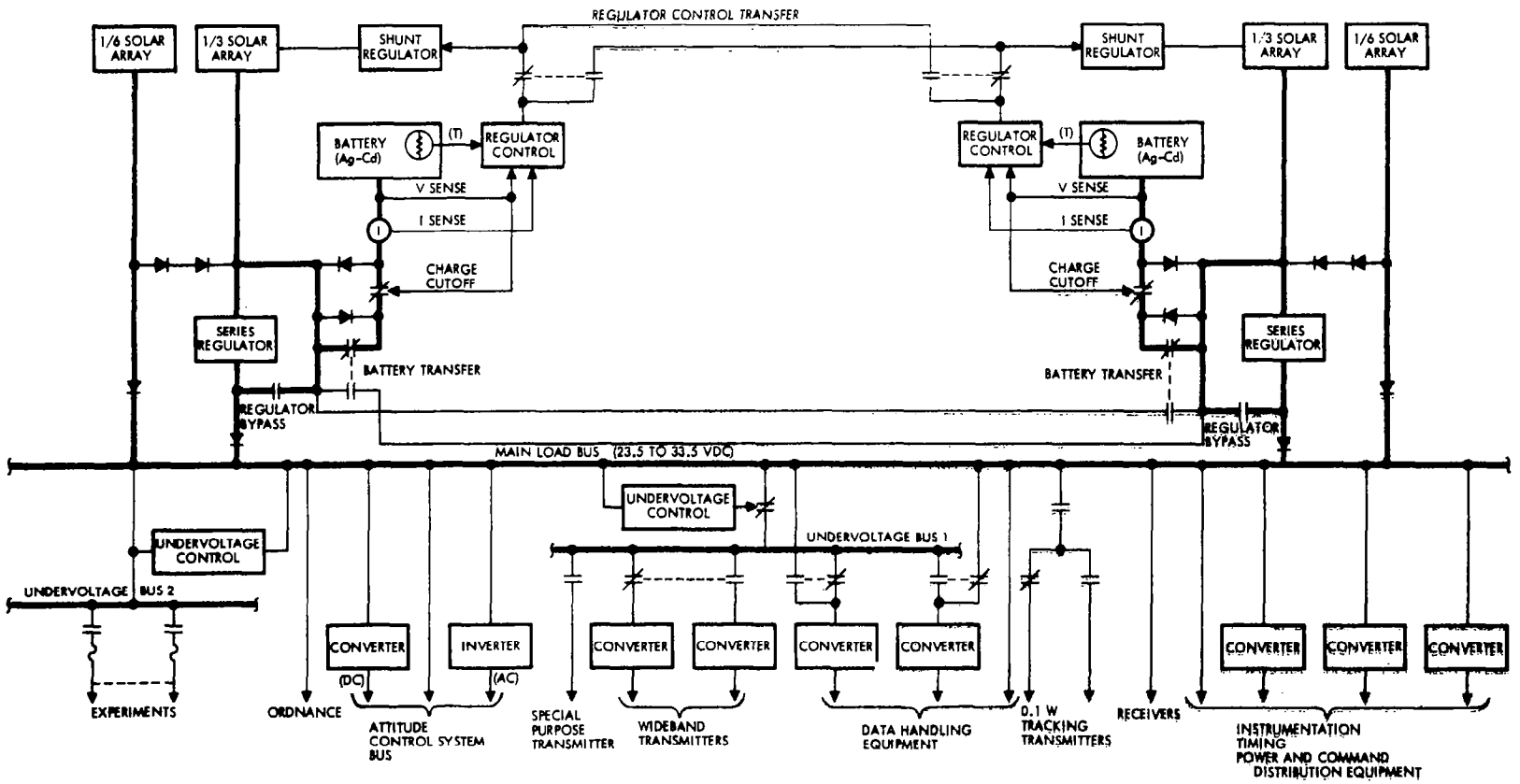

Figure 4-8. POGO Electric Power Subsystem

5. POWER SYSTEM EQUIPMENT CHARACTERISTICS AND PARAMETRIC DATA

5.1 GENERAL

Satellite electrical power systems can be subdivided into their functional equipments for the purpose of identifying efficiency, weight, reliability, performance characteristics, and interdependent tradeoff parameters. The following functional categories have been used throughout this study:

- Energy source – solar cell array, radioisotope thermoelectric generator (RTG)
- Energy source control – series or shunt regulators
- Energy storage – batteries, capacitors
- Energy storage control – charge and/or discharge regulators, relays
- Power conditioning equipment – regulators, converters, inverters, TR units
- Distribution equipment – harnesses, circuit protection, thermal blocks, power switches, under voltage protection, over voltage protection, isolation components

Although some satellite power systems may use these equipments in their simplest functional form, it is common to find several functions combined in a single piece of equipment. For example, a converter may combine the functions of a preregulator, inverter, and TR unit. In general, such a combination will save weight without sacrificing efficiency and reliability.

Succeeding sections describe each of the functional equipments listed above.

5.2 ENERGY SOURCE

Photovoltaic energy sources have been the most commonly used type of satellite electrical power generator. Considerable research and

development have been devoted to improving their state-of-the-art, and optimal configurations have been defined by extensive study programs. It is not the purpose of this study to repeat or extend this area of technology, but only to report sufficient performance and parametric data to allow power system optimization tradeoffs.

RTG energy sources are the second most common electrical power generators used in spacecraft. Because RTG's have a more limited application in earth orbiting satellites, photovoltaic sources have been given primary consideration in this study. Section 8 of this report presents a brief summary of the operating and performance characteristics of RTG's. It is believed that the substitution of an RTG energy source for the solar array in an optimized power system would have little effect on the maximum utilization of electrical power for the remainder of the system. Selection of an RTG in place of a solar array for a given satellite mission appears to be more dependent upon other criteria.

The performance of any solar array design is controlled by three principal parameters:

- Illumination (sun orientation)
- Temperature
- Radiation degradation as a function of time

The power output of a solar array is directly proportional to the cosine of the illumination incidence angle for angles less than approximately 50 deg. Power output declines slightly faster than the cosine for larger angles. The effect of temperature and radiation degradation is best described by the change in solar cell I-V characteristic. Figure 5-1 shows a typical set of solar cell characteristics for two temperatures and three levels of radiation flux.

Each of these three parameters varies as a function of time, satellite attitude and position, and mission profile. The exact design of a solar array is very complex; however, it should suffice to say that the size, weight, and minimum operating efficiency are usually determined

for the worst orbit operating condition. This condition is most often defined by the simultaneous occurrence of end-of-life radiation dosage, maximum array temperature, full load power, and the greatest angle of incidence. During all other operating periods, the solar array would have excess power available. This excess power must be accommodated through the use of temporary loads or by the energy source regulator.

Table 5-I summarizes a few characteristics of existing satellite photovoltaic power systems. A wide variation of performance factors can occur depending upon the mission, orbital parameters, vehicle configuration, orientation, and solar array design. Low solar array specific power ratios (w/lb) emphasize the extreme importance of attaining high efficiencies in the remainder of the power system in order to minimize total system weight.

5.3 ENERGY SOURCE CONTROL

The function of energy source control is to regulate the voltage and/or current delivered by the solar array. Source control is used only to protect the equipment connected to the bus since the solar array can safely sustain open or short circuits. The most common requirement is the prevention of high voltages when the array is cold (emergence from eclipse, for example), and/or when the bus load is very light. Some energy source control designs may also provide under voltage protection. Whenever the battery is connected directly to the solar array output during charge, the highest voltage permitted by the source control usually is established by the maximum safe battery voltage near the end of charge.

Source controls may perform their function in a variety of ways depending upon the type of circuit employed. The more common circuit types can be classified as follows:

- Series or shunt
- Dissipative or nondissipative
- Full regulating or limiting
- Switching or continuous
- Active or passive

Table 5-I. Spacecraft Photovoltaic Power System Characteristics

	Nimbus "B"	EGO	OSO	OAO	UK-1	Explorer XII	Explorer XIV	Relay	Tiros	IMP
Array[a]	0	0	0	No	No	No	No	No	No	No
Number of solar cells	11,000[b]	32,500	1,872	53,000	4,256	5,600	6,144	8,400	9,120	11,520
Cell mounting	Panels	Panels	Panels	Paddles	Paddles	Paddles	Paddles	Body	Body	Paddles
Weight of array (lb)	64	127	5.2	222	8.8	11.0	12.8	25.8	24.5	26.5
Weight of storage (lb)	113	74	30.7	177	14	6.3	6.3	28	40	6.7
Weight of power system (lb)	177	201	35.9	399	22.8	17.3	19.1	53.8	64.5	33.2
Maximum power developed (w)	410	560[f]	31[c]	772[d]	11.7	20.4	34.7	35	51[e]	74.3
Array (w/lb)	6.4	4.4	6.0	3.65	1.3	1.85	2.7	1.4	2.1	2.8
System (w/lb)	2.3	2.8	0.86	1.94	0.52	1.2	1.8	0.65	0.79	2.2
Array, area (ft^2)	43	78	4	187	11	15.3	15.3	17.6	17.7	28.7
Array (w/ft^2)	9.5	7.2	7.7	4.14	1.1	2.3	2.3	2.0	2.9	2.6
Array, efficiency (percent)	7.3	5.5	5.9	3.2	0.85	1.0	1.8	1.5	2.2	2.0

(a) "0" oriented; "No" not oriented

(b) 2 cm x 2 cm cells

(c) At 70°C

(d) Average power from cold to hot panel

(e) At 45 deg. inclination to sun

(f) At 60°C

Within these broad categories, many circuit configurations exist. Table 5-II summarizes the types of energy source control used in the eight satellite power systems studied. Regulator circuits which can be used as source controls are considered in more detail in the following paragraphs.

5.3.1 Series Dissipative Regulator

The series dissipative regulator requires that the input voltage be higher than the regulated output voltage. The amount of power dissipated by this circuit is a function of the input-output voltage difference and the load variations. Normally, a series dissipative regulator reaches maximum dissipation at maximum load and maximum voltage difference. However, when this type of regulator is used in conjunction with a solar array, maximum dissipation does not usually occur at maximum load. This is due to the rather unique power-voltage or power-current characteristic of the solar cell. In many cases, the circuit parameters are so selected that minimum dissipation occurs at full load. Figure 5-2 shows the variation in dissipation for a series dissipative regulator operating with a solar array. The dissipation is presented as a function of the solar array temperatures (equivalent to regulator input voltage) and at full load. As can be seen with an array temperature variation of 145°C, the dissipation is over 100 percent of the load and reduces efficiency to below 50 percent. Nevertheless, this relatively simple type of regulator has many advantages when used where the input voltage variation and consequent loss in efficiency are small. It has an excellent frequency response and very low output impedance. Because of its simplicity, it has a very high reliability rating.

5.3.2 Shunt Dissipative Regulator

The shunt dissipative regulator requires that the input voltage (solar array voltage) be at least equal to the desired bus voltage under the worst conditions. The advantage of partial shunt regulation over full shunt or series dissipative regulation is that dissipation is reduced by having part of the solar array continuously feeding the bus; the output of the remaining portion is regulated by the shunt which dissipates only as much power as

Table 5-II. Summary of Energy Source Control Types Studied

Usage	Battery Charge Control	Protection Feature	Battery Temperature Control	Regulator Limits	Type of Regulator
Able V	Trickle charge switch	Undervoltage bus	Thermal control to trickle charge (43°C)	±20%	None
Vela	Current limited	Undervoltage bus	--	±5%	Pulsewidth modulated series regulator
Pioneer	Floats on bus	ON-OFF battery switch (command)	--	Unregulated	None
Relay	Current limited	Undervoltage bus	Thermal control to trickle charge 26°C to 28°C		Full shunt voltage limiter and series regulator for selected loads
Tiros	Constant current to voltage limit		--		Full shunt voltage limiter and series regulator for selected loads
COMSAT	Voltage limited (individual cell monitoring)	Undervoltage bus	Thermal control to trickle charge	±0.4 v	Partial shunt voltage limiter
EOGO	Constant current to voltage limit	Undervoltage bus	Thermal control to trickle charge (35°C)	±5%	Partial shunt voltage limiter
POGO	Constant current to voltage limit	Undervoltage bus	Stop charging at (43°C)	±5%	Partial shunt voltage limiter

necessary to keep the combined voltage of the two portions below the specified value. The shunt is connected to a tap in the solar array in such a way that at maximum array voltage (minimum temperature), the shunt elements are driven into saturation and the array voltage is equal to the unshunted section voltage plus the saturated drop of the shunt elements. With this type of regulator maximum dissipation generally occurs at minimum load. Figures 5-3, 5-4, and 5-5 show dissipation of a partial shunt regulator as a function of minimum array temperature and minimum load for maximum array temperatures of 80, 60, and 40°C, respectively.

The variation of dissipation with load becomes much less pronounced for smaller array temperature variations, as does the amount of dissipation required. The effect of variation in maximum array temperature (and therefore in temperature range) can be seen by comparing Figures 5-3, 5-4, and 5-5. For example, the no-load curve of Figure 5-3 indicates 48 percent dissipation when the temperature varies from a minimum of -60°C to a maximum of 80°C. If the maximum array temperature is held to 60 or 40°C (for the same minimum temperature), the corresponding dissipation becomes 38 or 32 percent, respectively.

Figure 5-6 shows the relationship of shunt dissipation to electrical load on the system for a maximum array temperature of 80°C, and indicates that maximum dissipation usually occurs, as already noted, at minimum load for typical solar array temperature ranges. This characteristic illustrates an advantage of the partial shunt type of regulation, since it shows that losses are minimum when the load requirements approach the solar array power capability.

5.3.3 Pulsewidth Modulated Regulators

Pulsewidth modulated regulators utilize power transistors in a switching mode with controlled duty cycle to achieve the voltage regulation. They generally offer higher efficiencies than do dissipative regulators at the cost of a loss in frequency response and output impedance. Maximum efficiency is approached as the difference between input and output voltages becomes smaller, which makes them suitable for power control functions.

The input and output voltages of power regulators are designed to be nearly equal under worst operating conditions and normally do not reach a ratio as high as 2:1 at other times. The following paragraphs discuss the characteristics of the bucking, boost, and buck-boost pulsewidth modulating regulators.

A bucking regulator is used where the input voltage is always higher than the output voltage. The basic block diagram for this type of regulator is shown in Figure 5-7. The output voltage is related to the input voltage by the ratio t_{on}/T, where t_{on} is the ON time of the switch and T is the total drive period. Figure 5-8 shows typical series losses for a range of output currents under saturated conditions when losses are a function of output current only. Figure 5-9 indicates how efficiency varies with output power and with output voltage; these curves represent the losses which occur just prior to full saturation of the switching elements when OFF time is minimum and show that higher efficiencies are associated with higher output voltages. Variations in efficiency with changes in input voltage (assuming a constant output voltage) are shown in Figure 5-10 for two output voltages. The increase in losses as the voltage ratio increases results primarily from greater switching losses.

A boost regulator is used where the input voltage is always less than the output voltage. Figure 5-11 is a block diagram of a constant-frequency boost regulator of the pulsewidth modulated type. This case is the inverse of the bucking regulator. The ratio of output to input voltage is T to t_{off}, with T the total drive period and t_{off} the OFF time of the shunt switching element. Maximum efficiency of a boost regulator only occurs when the input voltage is slightly higher than the output voltage (not a normal operating mode for this type of regulator). The shunt element is open in this case, with all losses confined to the series elements. This condition can occur when the power available from the solar array is maximum (i.e., low temperature in sunlight). Figure 5-12 shows the losses of a boost regulator as a function of load current, and Figure 5-13 shows the efficiency as a function of output power for varying output voltages. The curves are taken for t_{off} almost equal to T; and, for lower

output voltages, the losses are greater. Figure 5-14 shows that for this type of regulator, as in the previous case, efficiency is greater when the input/output voltage ratio approaches unity.

A buck-boost regulator is used where output voltage is related to input voltage by the ratio t_{on}/t_{off}, which are, respectively, the ON and OFF times of the switch. When a 50-percent duty cycle for the switch occurs, the input and output voltages are equal. When t_{on} is greater than t_{off}, the circuit boosts the voltage; and, inversely, the circuit bucks (reduces) the voltage when t_{on} is less than t_{off}. Figure 5-15 illustrates a basic block circuit diagram of the buck-boost regulator. In this case also, efficiency is greatest when the voltage ratio is near unity, as shown in Figures 5-16 and 5-17, and varies with the chosen output voltage. As in the other cases, the higher output voltage shows the smaller losses. When the regulator is in the boosting mode, the saturated switch and series choke losses are predominant; while in the bucking mode, the switch losses predominate. Compared to the buck or the boost regulators, the major disadvantage of the buck-boost type is its lower efficiency (note the lower absolute values of efficiencies shown in Figure 5-17 for a given voltage ratio as compared to Figures 5-10 and 5-14).

5.4 ENERGY STORAGE

Electrical power systems for spacecraft generally employ batteries selected from three main types: silver-zinc, silver-cadmium, and nickel-cadmium. The state-of-the-art of the sealed secondary (rechargeable) silver-zinc battery is the least advanced for use in applications requiring long cycle life. Silver-zinc primary (oneshot) batteries are used mainly for short missions or on long missions to meet peak power and emergency requirements when those vehicles have another source of continuous electrical power.

The nickel-cadmium battery has been used in space systems for the longest period of time. However, the silver-cadmium battery is being used more for two reasons: It has a higher energy-per-unit-weight, and it is nonmagnetic. Conversely, the nickel-cadmium battery exhibits a residual magnetic field, even when not in use. The magnitude and

direction of this field vary as a function of the battery's previous history of charge and discharge. Long cycle life is a predominant and controlling requirement for many satellite applications. The nickel-cadmium battery has demonstrated superior cycle life to date, but a steady improvement in the cycling performance of the silver-cadmium battery is being realized.

5.4.1 Silver-Cadmium Batteries

Design data for silver-cadmium batteries are presented in Figures 5-18 through 5-27. Most of these data have been reduced to parametric form so that reasonable comparisons can be made with other battery types. Figure 5-18 presents cycle life data accumulated from various test programs as a function of temperature and depth of discharge. Many of the tests are incomplete and provide only limited design data. A "failure" is defined as a catastrophic occurrence such as an open or short condition in a cell, or the inability of the battery to supply the required depth-of-discharge in a given cycle. The cell capacity ratings as defined by Yardney are based on a C/15 charge rate and C/10 discharge rate at room temperature. In the following discussion of silver-cadmium batteries, the cell capacity ratings have been redefined so that battery capacities and rates will more realistically represent satellite applications where only the higher rates are used.

Figure 5-19 provides packaged battery weight per cell as a function of rated capacity. A packaging factor of 30 percent was used (based on the few existing designs). However, as larger batteries are manufactured and used, a factor as low as 20 percent appears reasonable. The curves of amp-hr efficiency versus temperature in Figure 5-20 apply to any state of charge within the operating life of the battery. The maximum achievable input capacity is a function of the charge rate and temperature as shown in Figure 5-21, in terms of the end-of-life rated capacity.

Output capacity varies with temperature, charge rate, and discharge rate. Figures 5-22 and 5-23 present the family of these curves in terms of C_e, the end-of-life capacity. The charge and discharge voltage curves as a function of rated capacity and at several temperatures appear on

Figures 5-24 and 5-25. The relationships of discharge rate and temperature on energy per unit-weight and w-hr efficiency are shown in Figures 5-26 and 5-27.

5.4.2 Nickel-Cadmium Batteries

Parametric design data are presented in Figures 5-28 through 5-40 for the nickel-cadmium batteries. Because this type of battery has a longer history, the data are more refined and lends itself to a systematic design approach. An example of a battery design is used to demonstrate the use of these curves. (See Appendix A.)

Figure 5-28 presents discharge data relating the maximum available capacity at end-of-life as a function of battery temperature and discharge current density. Best discharge performance and efficiency are attained at low currents and/or higher temperatures. Figures 5-29 through 5-33 relate the effects of temperature and charge current density on available capacity and amp-hr efficiency. The best conditions for obtaining high efficiencies and maximum capacity are to charge the battery at the cooler temperatures and higher current densities. During charge, the battery terminal voltage increases at cooler temperatures and higher charge rates and reduces the w-hr efficiency below that which might be predicted from the improved amp-hr efficiency. Optimum charge conditions occur in the region of $i_c = 0.3$ at $40^{\circ}F$, and $i_c = 0.5$ at $60^{\circ}F$. Significant improvements in power system performance and efficiency are possible if this type of operating information is used during the power system design stages.

Figure 5-34 presents accumulated test data from which cycle life can be predicted as a function of the depth-of-discharge (DOD). Cycle life versus depth-of-discharge data were extracted from NASA-SP 5004, "Space Batteries", after eliminating the effects of discharge at low temperatures. The per cell packaged battery weights shown in Figure 5-35 reflect the present state-of-the-art based upon extensive satellite flight experience.

The achievable capacity versus temperature data presented in Figure 5-36 shows the rather severe loss in capacity whenever high temperature

charging is necessary. The attempt to preserve some of the capacity by using higher charge current densities cause a further increase in temperature which in turn reduces the capacity. Adequate thermal design for the battery is very important if the system utilization of power is to be maximized.

Figures 5-37 through 5-40 show the effect of reconditioning* cycles on a nickel-cadmium battery. These treatments effectively restore the battery to nearly its original capacity after an extended period of cycling. If the period between reconditioning is set equal to or less than the original cycle life of the battery, mission life of the battery can be extended significantly. The available data have not established any limit to the number of times a nickel-cadmium battery can be reconditioned.

*Reconditioning of a nickel-cadmium battery is accomplished by discharging the battery (preferably individual cells) into a fixed resistance, approximately 2 ohms/cell, until the battery voltage is equivalent to 0.5 v/cell. Normal recharging is used. Caution is necessary during initial charge current surge so that the energy source bus voltage does not collapse.

5.5 ENERGY STORAGE CONTROL

Controls for energy storage equipment (batteries) commonly have two distinct functions: to regulate the energy input to the battery, and to control the energy out of the battery. Some power systems connect the battery directly to the solar array load bus and effectively use the energy source control as the battery charge control. The various types of regulator circuits previously discussed for energy source controls are also usable for battery control. The principal difference is that current regulation with voltage limiting are the controlled parameters for charging, and voltage for discharging. Many of the charge controls use auxiliary sensing, such as temperature and/or pressure for additional battery protection.

The choice of regulator type to be used for charge control is dependent upon the solar array and load bus voltages, and voltage regulation requirements. All batteries require a higher voltage for charging than they provide during discharge. If the solar array and load bus are common and the voltage regulation requirement is equal to or greater than the charge-discharge swing in battery voltage, the simplest form of energy storage control can be used. This is accomplished by directly connecting the battery to the bus through relay contacts, a diode, and a voltage dropping resistor. All other voltage and regulation conditions would require a step up or down in voltage accompanied by the necessary voltage or current regulator. When the nominal solar array load bus voltage is chosen equal to the battery discharge voltage, a boost type charge regulator is required. Alternately, the bus voltage may be chosen high enough to charge the battery directly. Then a boost type discharge regulator is required. When direct charging from the bus is chosen, relay contacts and a voltage dropping resistor are used to protect the battery from excessive voltage and current near the end of a charge period.

Control of the energy storage (battery) charge and discharge characteristics is a very complex function. As previously stated, the battery charge and discharge rates directly affect battery efficiency, operating performance, and life. The addition of energy storage regulation or control into the power system incorporates more equipment inefficiencies and reliability considerations. The idealistic approach is to use the

simplest circuit and nonpower dissipating components. An elementary design approach using relay contacts, voltage dropping resistor, and diode is practical for nickel-cadmium battery applications when the solar array is power limited, and the battery sets the bus potential during charge and discharge by being directly connected to the solar array load bus. Maximum charging current is made available to the battery by this technique, and the battery receives some of the excess power available from the cold solar array immediately after an eclipse period when recharging is required. During the final period of charge, the voltage dropping resistor is used to provide the reduced charge rate to prevent excessive battery temperatures and thermal problems. Concurrently, the array has heated and returns to its normal sunlight temperature and lower power level. The efficiency of this simple battery charge control approaches 100 percent.

Whenever energy storage is required for RTG systems, a similar direct control is desirable. The function of a battery in an RTG system is to supply peak or transient loads which seldom require a closely regulated discharge voltage. Usually, the RTG has a source regulator which is adequate for controlling battery charge.

5.6 POWER CONDITIONING EQUIPMENT

Power conditioning is the function of accepting electrical power from the bus with specified characteristics and altering them to meet the individual requirements of the load equipment. These load requirements may include multiple dc voltages, voltage regulation, generation of ac voltages and frequencies, and frequency regulation. The equipments which perform these functions are classified as regulators, converters, inverters, and transformer-rectifiers (TR units). In some cases, it is possible to combine one or more of these functions in the same equipment, such as a regulated inverter or converter.

5.6.1 Regulators

Most satellites require some part of the electrical load power to have closer voltage regulation than can be inherently supplied by the solar

array battery combination. When this required regulation cannot be accomplished in the energy source or energy storage regulator, additional regulating circuits must be included. Here again, a choice can be made from each of the fundamental types of regulator circuits previously mentioned. When the regulators are designed as separate equipments, they can be either a central (ac or dc) line regulator or smaller distributed units. The specific configuration of equipments is usually dictated by the mission requirements, reliability, and other optimization and design criteria.

Sometimes it is advantageous to combine the regulating function within the inverting or converting equipment. When separate preregulation in the inverter or converter circuit is necessary, a regulator circuit such as that shown in Figure 5-41 can be used. The input filter in this regulator design serves three purposes: to smooth out spikes and high-frequency transients with large peak values and small volt-second integrals; to eliminate input ripple having frequency components at or near the modulating frequency of the switching transistor which would produce low-frequency components by heterodyning; and to attenuate ac components produced by transistor switching. The switching transistor chops the dc output of the input filter in such a way as to deliver constant volt-second energy pulses to the integrator. The integrator portion of the circuit serves to smooth the pulsating dc. When the transistor is OFF, the diode conducts permitting continuous energy flow to the load from the integrator circuit. The inductor, along with its capacitor, becomes a means for storing sufficient electrical energy during the transistor ON period for delivery to the load during the OFF period to provide a regulated output voltage.

Figure 5-42 illustrates three simplified basic versions of inverter circuits, two with transformers and one without. The inverter can obtain its drive from the same source that produces the unmodulated drive for the preregulator. Addition of current feedback from collector to base of inverter transistor will reduce source drive power and improve efficiency. Inverter circuits and their parametric data are discussed further in Paragraph 5.6.3.

Converter circuits can take various forms. The transformer-rectifier circuits shown in Figure 5-43 can be combined with the inverter circuit shown in Figure 5-42 to form some of the more common types. When the load requirement is dc, the inverter output must be rectified and filtered. The circuits of Figure 5-43 show isolating transformers such as would be needed with those options shown as (a) and (c) of Figure 5-42. The secondary of each circuit in Figure 5-43 can be the transformer secondary of option (b) in Figure 5-42. Additional design data on converter circuits is presented in Paragraph 5.6.2.

There are times when the power conditioning circuits must provide better than normal ripple or regulation, or lower than average output impedance when subject to dynamic loading (pulsed loads). When this is necessary, active filtering (regulators) must be added to the outputs of the circuits shown in Figure 5-43. Dynamic loads on one or more outputs are pulsed demands for current which otherwise would produce significant output voltage transients on all output circuits. Normally, the preregulator circuit produces about 1 percent regulation to the inverter transformer secondaries for input line, dc load, and temperature variations combined. Figure 5-44(a) series regulator, or the shunt regulator, Figure 5-44(b), may be used as an active filter for any range of dynamic loads. The shunt regulator becomes more efficient than the series regulator at full load and when the load change is very small because the shunt element in the shunt regulator is required to carry only the amount of current equal to the change in load current. The series element in the series regulator always carries the load current.

5.6.2 Converters

The eight satellite electrical power systems investigated and reported in Section 4 contain a significant number of power conditioning equipments, largely converters. Table 5-III summarizes the pertinent electrical and performance data for these equipments. The wide range of characteristics exhibited corresponds to the extensive list of user equipment requirements reported in Section 3. It appears that the converter designs could be more efficient and lighter in weight if the quantity and variety of voltages were reduced. Standardization of user equipments and their electrical requirements should provide some degree of improvement.

Table 5-III. Summary of Converter and Inverter Characteristics

Usage	Input Voltage (vdc)	Input Regulation (%)	Output Voltage (vdc)	Output Current (ma)	Output Regulation (%)	Output Ripple (p - p)	Overload Protection	Switching Frequency	Transients	Output Power (w)	Efficiency (%)
Able V No. 2 Transmitter	18	+28	+210	30	±5	1%	Yes	1.6 to 2.2 kc	<10 msec	6.3	73
		-22	-20	3	±5	1%	Yes	1.6 to 2.2 kc		0.06	
			-12	130	±5	1%	Yes	1.6 to 2.2 kc		1.56	
			6.3 vac	750	±5			1.6 to 2.2 kc		4.7	
			+6.0	10	±5	1%	Yes	1.6 to 2.2 kc		0.06	
										12.68	
Able V No. 1 Payload	18	+28	+6.0	150	±0.3	1%	Yes	1.6 to 2.2 kc	<10 msec	0.9	67
		-22	-6.0	28	±0.3	1%	Yes	1.6 to 2.2 kc		0.2	
			+10	280	±0.3	1%	Yes	1.6 to 2.2 kc		2.8	
			+16	51	±0.3	1%	Yes	1.6 to 2.2 kc		0.8	
			-16	18	±0.3	1%	Yes	1.6 to 2.2 kc		0.3	
			6.0 vac	125						5.0	
Vela Payload	22.5	+10	+6.5	275	±3.0	10 mv	Yes	3.0 to 3.5 kc	<13%	13.8	64
		-15	-6.5	1840	±3.0	10 mv	Yes	3.0 to 3.5 kc	<13%		
Vela Transmitter	22.5	-20	+70	270	±2.0	350 mv	Yes	3.0 to 3.5 kc	<13%	21.9	70
		+10	+23	130	±2.0	160 mv	Yes	3.0 to 3.5 kc	<13%		
Vela Communications	22.5	-13	+16.2	20	±2.0	160 mv	Yes	3.0 to 3.5 kc	<13%	1.91	29
		+10	+10.0	140	±2.0	100 mv	Yes	3.0 to 3.5 kc	<13%		
			-6.2	15	±2.0	60 mv	Yes	3.0 to 3.5 kc	<13%		
			-16.2	6	±2.0	160 mv	Yes	3.0 to 3.5 kc	<13%		
			+28.0	15	±5.0	560 mv	Yes	3.0 to 3.5 kc	<13%	3.67	39
			+12.2	250	±3.0	130 mv	Yes	3.0 to 3.5 kc	<13%		
			+10.0	10	N.A.	100 mv	Yes	3.0 to 3.5 kc	<13%		
			-6.2	20	±5.0	120 mv	Yes	3.0 to 3.5 kc	<13%		
Pioneer Transmitter	28	+18	-940	2-10	±0.5	±0.1%	Yes	5.6 kc	±0.2	5.64	80
		-16	-545	32-40	±1.0	±1.0%	Yes		±0.2	19.62	
			+80	0.02-0.2	±1.0	±1.0%	Yes		±0.2	0.16	
			4.875 vac	300-400	±2.5		Yes		±0.2	1.68	
										27.10	

Table 5-III. Summary of Converter and Inverter Characteristics (Continued)

Usage	Input Voltage (vdc)	Input Regulation (%)	Output Voltage (vdc)	Output Current (ma)	Output Regulation (%)	Output Ripple (p-p)	Overload Protection	Switching Frequency	Transients	Output Power (w)	Efficiency (%)
Pioneer Equipment	28	+18 -16	+12.8 -12.4 +16.7 +16.0 +10.0 -16.0 +16.7 +12.8 -12.4 +15.0 15 vac 15 vac +10	10 76 22.2 54 246 134 22.2 10.0 76 No Load 1.66 1.66 60	±2.0 ±2.0 ±2.0 ±2.0 ±2.0 ±2.0 ±2.0 ±2.0 ±2.0 ±3.0	±2.0% ±2.0% ±2.0% ±2.0% ±2.0% ±2.0% ±2.0% ±2.0% ±2.0% ±2.0% ±2.0% ±2.0% ±2.0%	Yes Yes Yes Yes Yes Yes Yes Yes Yes Yes Yes Yes Yes	5.6 kc 5.6 kc 5.6 kc 5.6 kc 5.6 kc 5.6 kc 5.6 kc 5.6 kc 5.6 kc 5.6 kc 5.6 kc 5.6 kc 5.6 kc	±5.0 ±5.0 ±5.0 ±5.0 ±5.0 ±5.0 ±5.0 ±5.0 ±5.0 ±5.0 ±5.0 ±5.0 ±5.0	0.128 0.942 0.376 0.864 2.46 2.14 0.367 0.128 0.942 0.024 0.024 0.6 9.0	60
OGO No. 1 and 10	28	+20 -16	+70 +23	330 125	±2.0 ±2.0	±2.0% ±2.0%	Yes Yes	2461 cps 2461 cps	±5% ±5%	23.1 2.9 26.0	70
No. 2	28	+20 -16	+16 +9 +5 -6 -6	60 560 100 60 20	±1.0 ±1.0 ±1.0 ±1.0 ±1.0	±1.0% ±1.0% ±1.0% ±1.0% ±1.0%	Yes Yes Yes Yes Yes	2461 cps 2461 cps 2461 cps 2461 cps 2461 cps	±5% ±5% ±5% ±5% ±5%	1.0 5.0 0.5 0.36 0.12 6.98	44
No. 3 and 4	28	+20 -16	+70 +23	275 125	±2.0 ±2.0	±2.0% ±2.0%	Yes Yes	2461 cps 2461 cps	±5% ±5%	19.2 2.9 22.1	69
No. 5 and 6	28	+20 -16	+16 +9 -6 -16	300 789 280 10	1.0 1.0 1.0 1.0	1.0% 1.0% 1.0% 1.0%	Yes Yes Yes Yes	2461 cps 2461 cps 2461 cps 2461 cps	±5% ±5% ±5% ±5%	4.8 7.1 1.7 0.2 13.8	60

Table 5-III. Summary of Converter and Inverter Characteristics (Continued)

Usage	Input Voltage (vdc)	Input Regulation (%)	Output Voltage (vdc)	Output Current (ma)	Output Regulation (%)	Output Ripple (p-p)	Overload Protection	Switching Frequency	Transients	Output Power (w)	Efficiency (%)
No. 7 and 8	28	+20 -16	+16 +9 +6	20 107 20	2.0 2.0 2.0	2.0% 2.0% 2.0%	Yes Yes Yes	2461 cps 2461 cps 2461 cps	±5% ±5% ±5%	0.32 0.97 0.12 1.41	28
No. 9	28	+20 -16	+20 +10 -20 28 vac, ct	350 50 350 385	1.5 3.0 1.5 3.0	1.5% 3.0% 1.5% 3.0%	Yes Yes Yes Yes	2461 cps 2461 cps 2461 cps 2461 cps	±5% ±5% ±5% ±5%	7.0 0.5 7.0 10.8 25.3	75
ACS Inverter 350 V A 2 ϕ 400 cps	28	+20 -16	115 vac 18 vac 26 vac 125 vac 26 vac 135 vac 135 vac 125 vac 135 vac 135 vac	130 166 115 120 115 110 110 1240 1360 1360	2.0 2.0 * * * * * * * *	** ** ** ** ** ** ** ** ** **		400 cps	±5% ±5% ±5% ±5% ±5% ±5% ±5% ±5% ±5% ±5%	15 max 3 3 15 3 15 15 124 136 136 465	75
OGO Nongated Inverter	28	+20 -16	115 vac 18 vac 26 vac 125 vac 26 vac 135 vac 135 vac	130 167 115 1110 115 1110 1110	±2.0 ±2.0 * * * * *	** ** ** ** ** ** **		400 cps	±5%	15 3 3 139 3 151 151 465	80
COMSAT Equipment Converters	28	±15	+28 +15 +10 +6 -6 -15	77 165 208 411 218 165	±3.0 ±3.0 ±3.0 ±3.0 ±3.0 ±3.0		Yes	12 kc		2.15 2.47 2.08 2.46 1.3 2.47 12.99	73

* Varies proportionally with input

** No voltage spikes greater than 15% of the output

The weight of a typical converter is made up from three basic areas: electronic components, magnetic components, and mechanical hardware. Packaging densities vary from 0.030 to 0.050 lb/cu in. The allowable operating temperature directly affects weight since high power dissipation requires more structural mass to remove the heat and maintain the same temperature.

The inverter or converter transformer is probably the heaviest single part in the power conditioning equipment. The filter capacitors shown in Figures 5-41 and 5-43 are usually ceramic or tantalum types, with the tantalum type available in foil, solid, or wet versions. Selection of capacitors has a significant effect on weight since they are near the same weight range as transformers. Consideration must also be given to switching frequencies, because these capacitors tend to become inductive as frequencies approach the megacycle range. This makes it difficult to achieve low output impedance at high frequency, compensate a high-gain amplifier, or suppress high-frequency components for EMC (electromagnetic compatibility) reasons.

The inductors shown in Figure 5-41 and 5-43 are dc-current carrying types which make use of an air gap to store most of the energy while leaving the core with sufficient permeability to act as an inductance toward the ac components. In those cases where the inductors are shown as optional, they can be eliminated if the ac waveform is square or nearly square. They are always needed in applications with EMC or stringent ripple requirements. Caution must also be exercised with inductors at high frequencies, since they tend to become capacitive above one megacycle. Because inductors are in the same weight class as the filter capacitors, careful tradeoff consideration must be given to minimizing their combined weight.

Most high-reliability or high-temperature applications call for silicon rather than germanium semiconductors, even though the silicon semiconductor, when saturated, has a larger voltage drop (lower efficiency) than does the germanium type. When semiconductors are used in switching modes, there is the usual I-V forward conduction loss, and in addition, a storage carrier effect which causes the device to conduct into the next half cycle, after the complementary diode or transistor has turned ON.

This results in a short circuit for a brief period. These losses become very significant at the higher switching frequencies.

The converter parameters of most importance and which reflect maximum utilization of power are efficiency and weight. Both parameters are strongly related to switching frequency and output power level. Figure 5-45 shows the interrelationship of these four parameters based on existing hardware designs. The following observations can be made from the curves.

- Efficiency increases with power level because there are certain fixed losses in a converter, and these naturally become a smaller percentage of the total losses as power is increased. In addition, the variable losses increase at a slower rate than the power level and thus also become smaller in proportion.

- Higher switching frequencies result in considerable reduction of converter weight, but at the same time lower efficiency.

- High switching frequencies (100 to 200 kc) can be used at low power levels (up to 10 w), but should not be used at higher power levels because of the loss in efficiency associated with poor switching characteristics of presently available high power switching transistors and diodes.

As Figure 5-45 shows, there is a maximum efficiency attainable for any given power level. This is shown more simply in Figure 5-46 a curve of maximum efficiency versus power level for a typical preregulated 28-vdc converter. The efficiency increases with power level, but reaches a maximum at about 89 percent. This reflects the minimum attainable losses, which are attributable to losses in the power switches, rectifiers, and magnetic components, as well as to the fixed losses. Some increase in maximum efficiency may be attainable for low-power units by design innovations and in high-power units by incorporating regulation in the inversion stage.

Efficiency is affected, in part, by the magnitude and number of outputs. For single outputs other than 28 vdc, an efficiency correction factor (see Figure 5-47) must be applied to compensate for the change in rectification losses. At high voltage output, the efficiency correction

factor (ECF) is greater than unity because of the constant voltage drop across the rectifiers. For multiple outputs, the correction factor will also be utilized. A sample calculation will be instructive. The problem is to determine the efficiency of a 30-w converter with five dc outputs as follows:

+15 v at 5 w

-15 v at 5 w

+28 v at 10 w

+50 v at 8 w

+ 3 v at 2 w

The efficiency of a 30-w converter at 19-kc switching rate is 79 percent (see Figure 5-45). The corrected efficiency is obtained by determining an overall efficiency correction factor (OECF) taking into account the respective power outputs and the ECF's.

Output (vdc)	Efficiency Correction Factor (ECF)
+15	0.98
-15	0.98
+28	1.0
+50	1.01
+ 3	0.835

$$OECF = \frac{0.98(5) + 0.98(5) + 1.0(10) + 1.01(8) + 0.835(2)}{30}$$

$$OECF = 0.985$$

Corrected Efficiency = 79 percent (0.985) = 77.7 percent

Efficiency decreases near the extremes of the input voltage range when a converter designed to operate at a particular input voltage is connected to a variable bus. For a design nominal of 50 vdc input, converter efficiencies may increase approximately 2 percent reflecting the lower losses due to lower input current as compared to the 28-vdc design. Voltages significantly greater than 50-60v will compromise the collector voltage breakdown ratings for available power transistors.

These converter parametric data were derived using existing hardware designs as design centers. The design criteria, equations, and design center parameters used in the derivation are presented in Appendix B.

The converter parametric data presented in Figure 5-45 were subdivided so that the efficiency and weight performance of the individual sections (i. e., the inverter, and transformer-rectifier) could be identified separately. Parametric curves for these separate functions are presented in Paragraphs 5. 6. 3 and 5. 6. 4 and their derivations included in Appendix B.

During the past year, new methods and design techniques have been investigated by TRW Systems under its Independent Research program for improvement in performance, weight, efficiency, and/or reliability of power conditioning equipment. Some of these investigations were further examined in the laboratory to obtain circuit test data. Incorporation of these new techniques in some satellite hardware designs is now in process. In-depth analysis of these new techniques on this program for the purpose of improving the hardware-derived parametric data resulted in new information which is reported in Paragraph 5. 6. 5.

5. 6. 3 Inverters

The composite parametric curves for inverter designs (Figure 5-48) were generated from design centers as were the converter data. The overall levels of efficiency are greater than for converters because rectification and output filter losses have been eliminated. Changes in weight and efficiency as a function of frequency and output power are very similar to those which occur in converter circuitry since the controlling elements are the input filter, semiconductors, and magnetics. The mechanical hardware weights associated with a separately packaged inverter are comparable to those of a converter.

5. 6. 4 TR Units

The transformer-rectifier function of the converter can also be considered and used as a separate entity. Figure 5-49 presents the parametric relationships of efficiency, weight, frequency, and output power for TR designs. The design centers and equations for Figure 5-49 are included in Appendix B.

5.6.5 New Parametric Design Data

The new methods and design techniques investigated independently by TRW Systems were further examined during this program to determine the extent of their application to power conditioning equipment designs. Analysis of the circuit elements to determine the proper component for each circuit type as a function of the output power and operating frequency has permitted a more refined selection of circuit designs to improve efficiency, weight, and reliability. Selected circuit designs were parametrically analyzed to determine their optimum operating limits and tradeoff factors.

The regulated dc-to-dc converter was chosen as the investigation model because it is representative of and contains all of the power conditioning functions (regulating, inverting, transforming, and rectifying) found in a satellite electrical power system. A common converter requirement specification was selected to meet typical power conditioning requirements. Four basic regulated converter circuits were analyzed: 1) Regulated squarewave converter (RSWI) Figure 5-50; 2) Pulsewidth converter (PWI) Figure 5-51; 3) Energy storage converter (ES) Figure 5-52; 4) Push-pull energy storage converter (Push-Pull ES) Figure 5-53. Weight and efficiency as functions of output power and switching frequency were derived for each functional section of the circuits.

Circuit efficiencies and weights were reduced to frequency-dependent and independent components for convenient identification of frequency limitations resulting from circuit design and component selection. Baseline designs were established for each section of the circuit for a selected number of applicable power outputs. Expansion of the design data about each baseline design established crossover points. Data synthesis for the complete circuit resulted from selecting the more optimum values between the crossover points for each circuit section. The final converter parametric data is the result of synthesizing the applicable groups of data derived for each functional section of the converter circuit. This approach to data synthesis provided a more detailed derivation than reported in Paragraphs 5.6.1 through 5.6.4, which were based upon a statistical summary of data from actual equipments designed for spacecraft.

5.6.5.1 Performance Requirements

Performance requirements may be divided into primary and secondary categories. Primary requirements are those general requirements developed by all applications, and which usually determine the weight and efficiency of all power conditioning equipments. Secondary performance requirements are generated by specific applications which affect only the equipments so applied. It should be emphasized that secondary characteristics are of major importance to associated equipment, and may indirectly exert dominating influence on the power conditioning equipment weight and efficiency.

- Primary Performance Requirements

Primary performance requirements affecting equipment weight and efficiency are listed below in typical order of importance. Major effects are indicated qualitatively.

a) Output Power

Weight is approximately proportional to output power, with the major exception of the structure weight increase at low output power. Efficiency is proportional to power. The fixed power losses, determined by component operating point limitations, are an appreciable fraction of the output power for low wattage units.

b) Input Voltage Range

Input filter weight is a function of input voltage range. Efficiency is inversely proportional to input voltage range to an extent determined by RMS current.

c) Output Voltage

Weight increases when output voltage is increased to levels requiring special dielectric considerations. Efficiency decreases as output voltage is decreased and diode losses and transistor saturation losses become a larger percentage of the output voltage.

d) Thermal

Requirement for operation below -20°C reduces efficiency by increasing semiconductor voltage drive power. Requirement for operation above 75°C increases weight by controlling filter capacitor selection and structure gauge. Thermal requirements of conducted heat rejection may control structure configuration to increase weight.

- Secondary Performance Requirements

Secondary performance requirements affecting equipment weight and efficiency are collated below into subgroups having similar effects. Subgroups are listed in approximate order of importance and major effects are indicated qualitatively.

Reliability Requirements

Reliability requirements consist of those requirements selected for intra-equipment implementation versus implementation in other equipment or by a different system block diagram.

a) Redundancy

Channel redundancy doubles component weight and adds the weight of logic and transfer circuits. Part redundancy reduces efficiency by increasing saturation and drive losses.

b) Fault Isolation (or overload protection)

Load fault isolation adds the weight and losses of a control circuit as a minimum, and may add saturation losses if multiple loads are supplied by a single equipment.

Performance Requirements

The following requirements determine filter size and regulator switching frequency.

a) Audio Susceptibility

Magnitude of the specified modulation determines regulator range and gain similarly to input voltage range. Frequency range or band of the specified modulation may affect regulator switching frequency. Efficiency will be reduced and weight increased if damping resistors are required in series with filter capacitors.

b) Regulation Against Dynamic Load Variation

Regulation against step or high frequency load variation increases output filter size, and/or necessitates the addition of secondary regulators.

c) Close Tolerance Regulation

Requirement for regulation better than ±2 percent on units with multiple voltage outputs adds the dissipation and weight of secondary regulators.

Number of Outputs

A requirement for more than one output increases weight due to increased number of parts for each additional output, and may degrade efficiency by requiring added regulators in each output.

Conducted Interference

A requirement for minimal conducted interference increases weight by adding high frequency input and output filters, and added internal radiation shielding.

Special Requirements

a) Packaging Constraints

Occasionally an oversized package is specified for ease of maintainability or standardization reasons. While optimal for other applications, (e.g., data handling circuits or larger equipments), the oversized weight of a particular equipment may be undesirable.

b) Telemetry Conditioning

Efficiency is reduced with telemetry conditioning requirements, each of which typically requires 2 to 30 mw of conditioning power. Weight is increased by a small magnitude.

c) Synchronization

Weight is increased slightly, and efficiency is reduced by a small percentage except when EMC requirements require significant filtering and shielding due to the synchronization frequency distribution.

5.6.5.2 Model Converter Specification

The following model converter specification was established as typical for the primary and secondary requirements. Design techniques, component selection, and circuit configurations that will meet this specification are investigated to determine interactions and tradeoffs.

- Primary Requirements

Output power	1 to 200 w, parametrically variable
Input voltage range	28 vdc ±15 percent
Output voltage	28 vdc
Thermal	-20 to +50°C, mounting base

- Secondary Requirements

a) Reliability

Redundancy	None
Fault isolation	None

b) Performance

Output regulation	±3 percent
Load variation	50 to 100 percent of rated load
Audio susceptibility	3 v p-p from 30 cps to 150 kc
Regulation against dynamic load variation	Not required
Close tolerance regulation	Not required
Output ripple	±2 percent

c) Number of Outputs — 1

d) Conducted Interference — MIL-I-6181

e) Special Requirements — None

5.6.5.3 Converter Circuits

Regulated Squarewave Converter (RSWI)

The block diagram of the RSWI converter is shown in Figure 5-50, in a configuration convenient for weight and efficiency analysis. Simplified schematics are indicated in each block. All operating frequencies (noted in each block) are referenced to the squarewave switching frequency (f) of this circuit. A pulsewidth preregulator is included in the RSWI by a switch consisting of two transistors operating in push-pull into a nonsaturating power transformer. A saturating driver core provides drive and also determines the switching frequency (f). The squarewave output of the transformer is rectified and filtered to provide the necessary regulated dc voltage.

Advantages of the RSWI are:

- Minimum inverter design complexity
- Minimum output filter requirements
- Minimum voltage stress on switching transistors for higher reliability

Disadvantages of the RSWI are:

- Maximum overall design complexity due to the need for a separate preregulator
- Frequency-dependent inverter transistor switching losses, since one transistor turns on while the other transistor is still in storage time

Pulsewidth Converter (PWI)

The block diagram of the PWI converter is shown in Figure 5-51. The PWI circuit combines inversion and regulation functions in the pulsewidth inverter stage. Switching reference frequency (f) is determined by a separate oscillator transistor. Duty cycle of the inverter switch is controlled by an error amplifier to maintain a constant average rectified output voltage, independent of input voltage and load variations.

Advantages of the PWI are:

Regulation and inversion functions are combined in a single element.

Transistor switching load line is controlled so that storage time of the OFF transistor is over before the other transistor turns ON.

Disadvantages of the PWI are:

Transistor voltage rating must be at least twice maximum input voltage, in addition to any transient voltages which are not attenuated by the input filter.

Separate integrating inductors are required for each output as a result of the pulsewidth modulated waveform as opposed to the squarewave for the RSWI converter.

Energy Storage Converter (ES)

The block diagram of the ES converter is shown in Figure 5-52. When the transistor is ON, energy is stored in the transformer/inductor (air gapped transformer) through its primary winding, while load power is supplied from the integrating capacitor. The induced emf in the transformer/inductor secondary is blocked from producing an output current by the diode. When the transistor is switched OFF, the secondary emf reverses; and the stored energy is discharged through the secondary winding to supply load power and to recharge the output integrating capacitor. If the transistor ON time is set equal to T/2 at nominal input voltage and load, then the ON-OFF periods may be varied with input voltage and load variations to maintain constant output voltage.

Advantages of the ES are:

Inversion and regulation are performed by a single power transistor.

Voltage transformation and energy storage are accomplished by the same magnetics.

Load fault current rate of increase is limited by the transformer inductance, since energy is alternatively stored and discharged each half cycle.

Low part count.

Disadvantages of the ES are:

Transistor voltage rating must be at least twice maximum input voltage, in addition to low frequency transient voltages which are not attenuated by the input filter.

Output ripple is higher due to output capacitor supplying load power during ON time.

Push-Pull Energy Storage Converter (Push-Pull ES)

The block diagram of the (Push-Pull ES) converter is shown in Figure 5-53. The basic operation is the same as for the (ES) circuit except that transistors Q_1 and Q_2 alternate ON and OFF, providing power to the load on each half cycle. Assuming the same size components and switching frequency, the (Push-Pull ES) circuit can provide twice the power output of the (ES) circuit. The efficiency remains essentially the same for both circuits and the weight increase is approximately equal to the weight of the added (ES) circuit inverter/transformer/integrating inductor and rectifier. The input filter and integrating capacitor remain the same size because their operating frequency has now doubled. Thus, a significant improvement in weight per watt output is obtained.

Advantages of the Push-Pull ES are:

Inversion and regulation are performed by the same pair of transistors.

Voltage transformer and energy storage are accomplished by the same magnetics.

Load fault current rate of increase is limited by the transformer inductance, since energy is alternately stored and transferred each half cycle.

Low part count.

Transistor switching load line is controlled so that storage time of the OFF transistor is over before the other transistor turns ON.

Excellent attenuation of input ac voltages and noise.

Disadvantages of the Push-Pull ES are:

Transistor voltage rating must be at least twice maximum input voltage in addition to low frequency transient voltages which are not attenuated by the input filter.

Separate integrating capacitors are required for each output.

5.6.5.4 Circuit Analysis

The performance of a given circuit configuration will vary depending upon the choice of output power, switching frequency, load voltage, input voltage, output voltage regulation, ripple requirements, and component selection. In order to develop parametric data showing the relationship of efficiency and weight as functions of switching frequency and output power, a design center is used for each combination of selected frequency and output power covering the range of interest. The selected frequencies and output powers used in the analysis of all four circuits are: 0.4, 2, 6, 20, 60, and 200 kc; and 2, 6, 10, 20, 60, and 200 w.

The four converter circuits perform differently at any one design center, although similar sections of the different circuits may function in the same manner. Hence, each circuit is divided into its functional sections as shown in the block diagrams so that a single analysis can be made for those blocks having common circuit functions. For example, the LC input filter of each circuit contains the same generic type of components and is required to meet the same design criteria. However, the input filter designs for the RSWI and ES converter circuits having the same switching frequency are not the same size because the filters have different operating frequencies and may utilize a different type of inductor or capacitor. The choice of component type, such as tantalum or ceramic capacitor, varies with operating frequency and output power because of its power loss and weight tradeoffs.

The fundamental design equations, operating criteria, and performance analysis for each type of component, functional circuit section and converter circuit are presented in Appendix C. The choice of equations and coefficients for each functional circuit application permits the final

combining of weights and efficiencies for each converter circuit to reflect the more optimum selections of component type, component rating, and design configuration affecting the parameters to be held constant at each design center. The result is a set of parametric data for each circuit depicting the variation in performance as a function of the two main variables (switching frequency and output power) when the circuit design had been optimized for the secondary variables at each design center. The parametric data plots are straight line connections of the design centers at a constant switching frequency.

5.6.5.5 Efficiency Performance

The converter efficiency data for each of the four circuit designs are presented in Figures 5-54, 5-55, and 5-56 as a function of power output and switching frequency. The discontinuities occurring at the 10-w level for each frequency are caused by the change in semiconductor (transistors and diodes) ratings. At 10 w or less, devices rated at 1 amp are applicable. Above a 10-w output, devices with higher current ratings are required. Semiconductors rated at 10 amps were used for power levels between 10 and 200 w because their switching performance provided a more optimum efficiency without a significant weight increase. Available devices having ratings between 1 and 10 amps are not suitable for high performance switching applications. Consequently, their use in these circuits would have resulted in lower efficiencies. If intermediate rated, high performance switching semiconductors (such as a 5-amp device) were available, the magnitude of the discontinuity at 10 w would be reduced and another discontinuity would be introduced at a higher power level where the change would be made from the 5-amp to the 10-amp rating.

The two 20-kc curves shown in Figure 5-56 are a result of the changeover in filter capacitor type from tantalum to ceramic at the 20-kc switching frequency. Although the ceramic capacitors have a slightly higher weight, they provide a better circuit efficiency. The tradeoff between these two curves to select the minimum power system weight varies as the power system size and configuration change.

The apparent anomaly of the efficiency data between 2 and 10 w for the ES and Push-Pull ES converter, Figure 5-56, is caused by the change in type of inductor cores at 4 kc. As before, the 2-kc efficiency is lower than the 0.4 kc efficiency. The 6-kc data would normally be lower than the 2-kc data if the same components were used. The new core material used at 6 kc and 20 kc returned the efficiency to the 0.4-kc value. The 20-kc (high weight) efficiency data is better than the 20-kc (low weight) efficiency data because the capacitor type is changed from tantalum to ceramic at the 20-kc frequency.

The efficiency losses at high frequencies are directly attributable to the relatively poor switching characteristics of power semiconductors. Thus, the higher power electrical systems are limited to the lower switching frequencies. New semiconductors with improved switching characteristics or a new type of power switch is needed in order to realize the lower weight advantage of the high frequency designs.

5.6.5.6 Weight Performance

The complementary converter data showing equipment weights as a function of output power and switching frequency are presented in Figures 5-57, 5-58, 5-59, and 5-60. The discontinuities occurring at the 10-w level for each frequency are again caused by the change in semiconductors. The effect of the large efficiency difference at the higher frequencies compounds the weight penalities because of the increased power dissipation. Abnormal power dissipation is accommodated by an increase in equipment heat transfer area and its accompanying weight increase.

Converter equipment weights, represented on each of these figures by solid lines, consist of the total component weights plus the minimum container weight necessary to meet the mechanical environment specifications. The converter equipment weights (based on a cube-shaped container) necessary to satisfy the increased power dissipation are represented by the uniformly dashed lines. They intersect the solid lines at the power level where this thermal design begins to control the equipment container size. The cube shaped container is a poor configuration to take advantage of the usual satellite heat transfer methods, i.e., heat conduction through

the mounting base. Hence, the resulting equipment weights are excessive and establish an upper weight limit. Determination of the minimum converter weight, which will satisfy the heat dissipation requirements set by the equipment efficiency, is a complex function of the container configuration and heat transfer rates. Appendix D sets forth a simple graphical method for determining the optimum container configuration and weight for the stated heat transfer conditions. The nonuniformly dashed lines on Figures 5-57 through 5-60 represent these optimum (minimum) converter weights. Their intersection with the solid lines established the output power level and frequency at which the equipment size and weight exactly satisy both the mechanical and thermal limitations.

The "high weight" and "low weight" curves shown in Figure 5-56 for the 20-kc frequency have complementary "high efficiency" and "low efficiency" curves on Figures 5-59 and 5-60. The selection of the correct curves for use in power system designs may be ascertained for each power system configuration by the Comparative Analysis Method (see Section 6) to determine which one provides the minimum power system weight.

5.6.5.7 Analysis of Parametric Data and Conclusions

Converter Efficiency

Comparing the efficiency performance of the four converter circuits at equal power levels and switching frequency shows that the ES and Push-Pull ES converter type of circuits are better than the RSWI and PWI circuits. The PWI converter circuit is second best and shows from 5 to 15 percent better performance than the RSWI circuit. Considering only maximum efficiency of the converter designs, the selection of converter type and its switching frequency for given output power levels is shown in Table 5-IV.

Table 5-IV. Converter Characteristic for Maximum Efficiency Converters and Systems

Power (w)	Circuit (Type)	Frequency (kc)
≤10	ES and Push-Pull ES	20
>10	ES and Push-Pull ES	0.4

Comparison of this converter data with the previous hardware-based data presented in Section 5.6.2, Figure 5-45, reveals an efficiency improvement at the lower power levels. At the higher levels of power, the RSWI circuit provides a lower efficiency, while the other three circuits are equivalent or slightly better. The data of Figure 5-45 is predominantly based upon preregulated squarewave inverter type circuits very similar to the RSWI converter circuit. Thus, there is reasonably good agreement between the two sets of data. The efficiency improvements for the other three circuits bear out the predicted performance for the newer design methods.

Converter Weight

A general comparison of the weights represented by the solid lines for the four converter circuits, indicate the following order of performance from the lightest to the heaviest: Push-Pull ES, PWI, ES, and RSWI. A detailed analysis of the curves presented in Figures 5-57, 5-58, 5-59, and 5-60 show that at several values of output power and/or switching frequency crossover points occur when the equipment weight of one of the circuits is established by higher thermal dissipation.

Considering minimum weight converter designs only, Table 5-V provides the choice of circuit type and its operating frequency for various groups of output power. Although the PWI converter data shows a lower weight over the small range of output power between 13 and 25 w, the weight difference is only 0.15 to 0.20 lb. This small difference is completely offset by 17 percent better efficiency performance of the Push-Pull ES converter. Thus, the Push-Pull ES circuit provides the best efficiency and weight performance over the total power range.

Table V. Converter Characteristics for Minimum Weight Converters

Power (w)	Circuit (Type)	Frequency (kc)
≤10	Push-Pull ES	200
10 to 13	Push-Pull ES	20
13 to 25	PWI	60
25 to 200	Push-Pull ES	20

Power System Weight and Efficiency

The optimum power system design which will provide the maximum utilization of power is that system having maximum efficiency and meets the performance requirements for all phases of the selected mission. This maximum efficiency system may or may not have minimum weight, depending upon the choice of equipment, system configuration, and the operating constraints such as switching frequency, which are required to provide the maximum efficiency design. This becomes evident when the efficiency-weight tradeoff is considered for each of the four fundamental classes of equipment comprising the typical satellite power system. These four classes are:

- Power conditioning equipment – converter, inverter, TR-unit, regulator
- Energy source or storage control – regulator
- Energy storage – battery
- Energy source – solar array

For most designs of the power conditioning equipment, maximum equipment efficiency is not synonymous with minimum equipment weight. This is exemplified by the converter data presented in Tables 5-IV and 5-V. Maximum efficiency power conditioning equipment designs are a necessary constituent of a maximum efficiency power system. Because of the usual efficiency-weight tradeoff for the power conditioning equipment, the minimum weight power system would not utilize the maximum efficiency equipment. This is true unless the weight reduction in the battery and solar array, due to the power conditioning equipment efficiency improvement, completely offsets the accompanying increase in equipment weight necessary to obtain the maximum equipment efficiency. The minimum weight power system typically contains power conditioning equipment whose design is a compromise between maximum efficiency and minimum weight equipment. The most favorable compromise, starting from the minimum weight power conditioning equipment, is reached by incrementally increasing the power conditioning equipment weight until the resultant power saving, (due to the higher efficiency) translated into battery and solar array weight reduction is just equal to the added incremental equipment weight.

Energy source or energy storage controls follow the same tradeoff pattern as the power conditioning equipment. Many times, the efficiency-weight tradeoff for these controls results in a maximum efficiency regulator choice for a minimum weight system, because of the proportionately larger amount of power handled. Again, the maximum efficiency power system requires the maximum efficiency regulator design.

The battery is generally the heaviest type of equipment used in a power system when measured per watt-hour output, or translated to a per watt output basis for a given mission and system configuration. Because of this strong influence, selection of the optimum efficiency power conditioning equipment design varies as the energy output of the battery changes with mission conditions and system configuration. The minimum-weight power system normally requires the battery weight to be minimized. A maximum-efficiency power system design intuitively requires the best battery efficiency. Battery efficiency is a very complex function of ampere-hour capacity, depth of discharge, charge and discharge current densities, charge and discharge temperatures, and previous operating history. The tradeoff of battery weight (increasing amp-hour capacity) to improve its efficiency is difficult to relate for the general case. However, small improvements in efficiency are possible by increasing amp-hour capacity for some system designs. Generally, the weight penalty to gain a few percent improvement in efficiency is prohibitive for most applications. The minimum-weight-battery design is usually near enough to the maximum efficiency for the majority of designs.

The solar array efficiency-weight tradeoff is a function of the array physical configuration, operating temperatures, variation in insolation, basic solar cell efficiency and weight, impedance match to the system, and degradation rate. Assuming a constant set of operating conditions, and initial operation at the maximum power point, i.e., array impedance matched to system impedance, any change in array weight by increasing its size will lower the array efficiency and system efficiency. Alternately, if the initial operation is not at the maximum power point, a change in array size (weight) may increase or decrease the efficiencies. A maximum efficiency solar array design provides the minimum weight array.

Therefore, either the maximum efficiency system or the minimum weight system should use the maximum efficiency array design.

Assuming the following weight-tradeoff factors (Table 5-VI) for the power system equipment ahead of the power conditioning equipment, a tradeoff of converter weight is made to determine the converter operating parameters which provide the minimum weight system.

Table 5-VI. Power System Equipment Weight Tradeoff Factors

	Lb per w output		
	Min	Max	Typical
Solar Array	0.100	0.760	0.300
Battery	0.300	1.200	0.400
Regulator	0.030	0.160	0.050
Total	0.430	2.120	0.750

Using an optimistic 0.500-lb system weight factor for each watt change into the converter, Table 5-VII shows the converter operating characteristics which would result in the minimum weight system.

Table 5-VII. Converter Characteristics for Minimum Weight System

Power Output (w)	Circuit Type	Frequency (kc)	Weight (lb)	Efficiency (percent)
2	Push-Pull ES	20 kc (low wgt)	0.38	81.8
6	Push-Pull ES	20 kc (low wgt)	0.54	86.5
10	Push-Pull ES	20 kc (high wgt)	0.98	88.1
20	Push-Pull ES	6 kc	1.55	86.0
60	Push-Pull ES	6 kc	2.90	86.5
100	Push-Pull ES	6 kc	4.00	86.7
200	Push-Pull ES	6 kc	6.00	86.9

Using a 0.900-lb system weight factor instead of the 0.500 lb, changes only the 2- and 6-w designs of the Push-Pull ES circuit. The 20 kc (high weight) designs replace the 20 kc (low weight) designs and the respective weights and efficiencies become: 0.46 lb and 82.5 percent, 0.72 lb and 87.2 percent.

Comparing the data from these tables with Table 5-V data for the minimum weight converter shows an overall reduction in switching frequency and a change toward the higher efficiency converter designs in order to obtain the minimum weight systems. The maximum efficiency system requires the maximum efficiency converter designs with the accompanying increased converter weights. Unless the system weight tradeoff factor is very large, the maximum efficiency power system will not be the minimum weight power system. For maximum utilization of system power, the maximum efficiency design should be used.

5.7 POWER DISTRIBUTION EQUIPMENT CHARACTERISTICS

Power distribution equipment includes harnesses, circuit protection devices or fuses, terminal blocks, power switching, and under- or over-voltage protection and isolation diodes.

5.7.1 Harness

Voltage drop, weight, and wire gauge for the harnesses used on five of the considered programs are summarized in Table 5-VIII. Considerable standardization of component parts for harnesses had already been accomplished. Except for changing wire sizes to reduce power losses, very little contribution can be made in the harness area to the maximum utilization of power.

Figure 5-VIII. Harness Characteristics

Program	Voltage Drop		Weight (lb)	Wire Gauge
	Primary* Power	Secondary** Power		
OGO	<1.5 percent	<1.5 percent	110	20-28 AWG
Able	<50 mv	--	~15	20-28 AWG
VASP	<1200 mv	<80 mv	15	20-28 AWG
Pioneer	<250 mv	<50 mv	9.87	20-28 AWG
Vela	750 mv	60 mv	12	20-28 AWG

*Primary power losses are from primary sources to the users' equipment.

**Secondary power losses are from secondary sources to the users' equipment.

At present, these power losses are very minimal. Use of higher distribution voltages would allow the same dissipation at a lower weight, by decreasing the wire size proportionately, or less dissipation due to the lower current density for the same weight.

5.7.2 Circuit Protection

Circuit protection has been accomplished by the use of fuses in most vehicles to date. These devices operate in a linear mode as a function of I^2t. Other devices known as current limiters, which are nonlinear with I^2t have been used in special cases requiring only current limiting. Both devices are a source of system inefficiency but are required to protect the complete vehicle system from an equipment failure and maintain system reliability.

5.7.3 Power Switching

The use of relays for switching power or transferring power control functions has been the preferred design. Solid state switches have been proposed and used on two programs, Pioneer and 2029. All other programs

investigated have used relays. These devices each have advantages and disadvantages as summarized below.

Relays:

Advantages: Low power consumption; not susceptible to radiation damage; essentially unlimited current carrying capacity; well advanced in the state-of-the-art; and reasonably high reliability.

Disadvantages: Poor magnetic field properties; high volume; high weight; and subject to contact chatter causing interruptions and/or noise.

Solid-state switches:

Advantages: Light weight; very compact; no magnetic properties; no moving parts; and predicted high reliability.

Disadvantages: Subject to radiation damage; limited current carrying capacity; power consumption proportional to current carried; and relatively new in development.

For the purpose of this study, it appears that characteristics other than power consumption may dictate the selection of a switching device. All other things being equal, solid-state switches would be used for low power circuits, and relays for high power circuits in order to obtain maximum power system efficiency.

5.7.4 Voltage Protection

Under- and over-voltage protection have been accomplished by two methods in the spacecrafts surveyed. The Able V, Vela, and OGO vehicles have used unijunction transistors. The Pioneer, COMSAT, and 2029 program are using the differential amplifier method. The later method is superior to the former, but has only recently been fully developed. Its advantages are: lower power consumption, narrower hysteresis bandwidth, matrix logic outputs, better temperature range stability, and low dc voltage signals which can drive the power switching devices.

From a power efficiency point of view, the state-of-the-art in over- and/or under-voltage control is moving in the correct direction. At this time, no better choice is available.

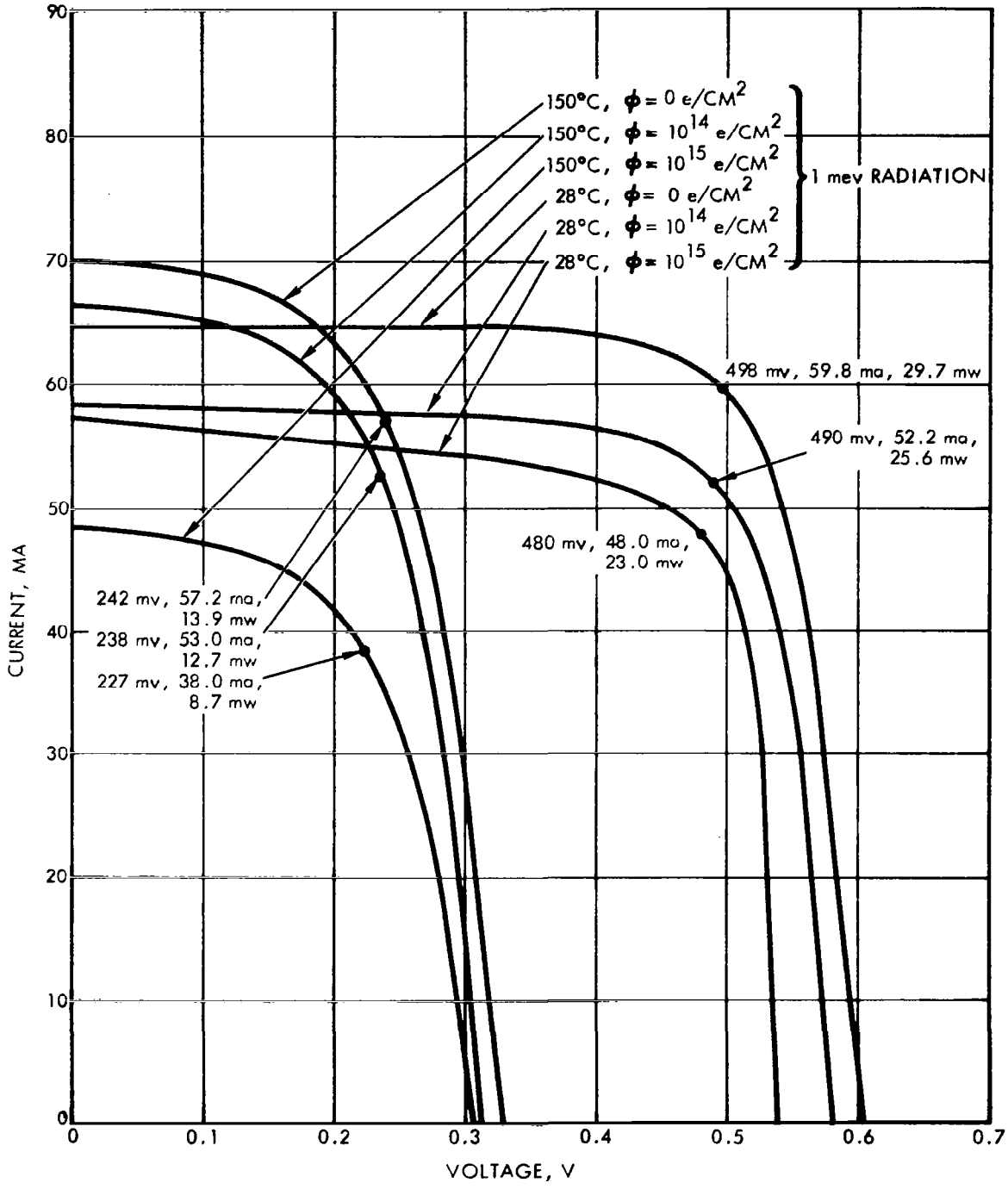

Figure 5-1. Solar Cell I-V Characteristics

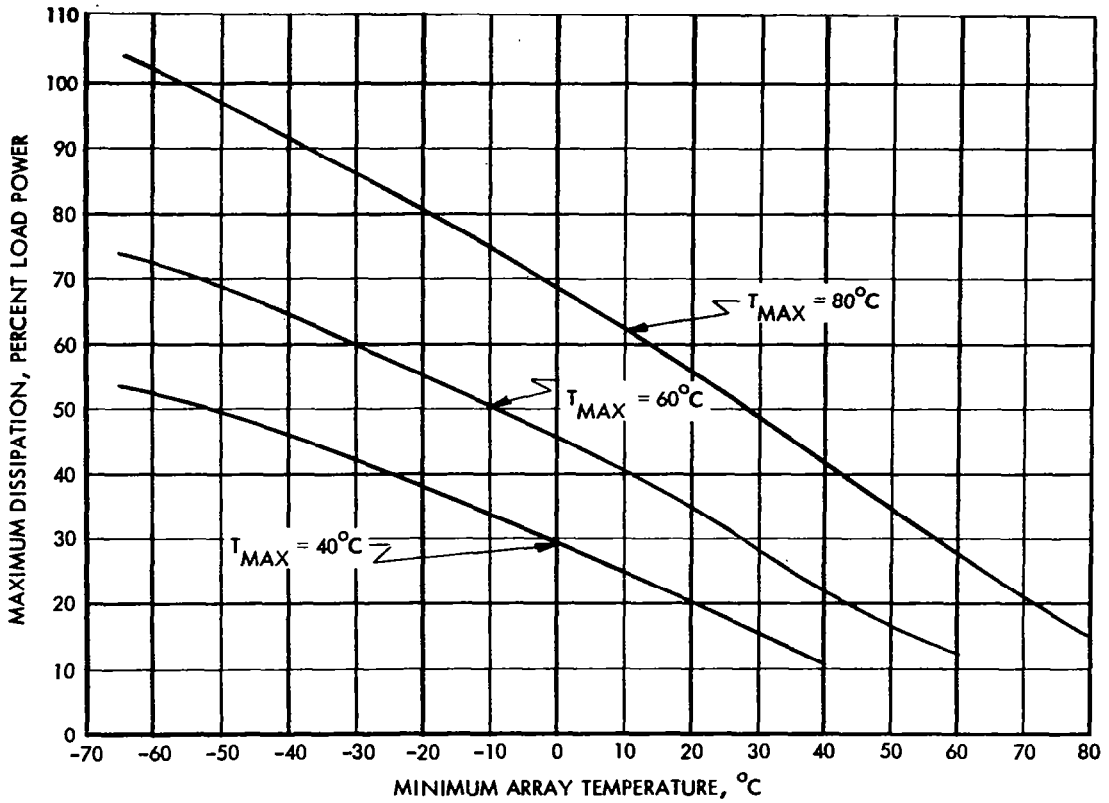

Figure 5-2. Series Dissipative Regulator, Maximum Load

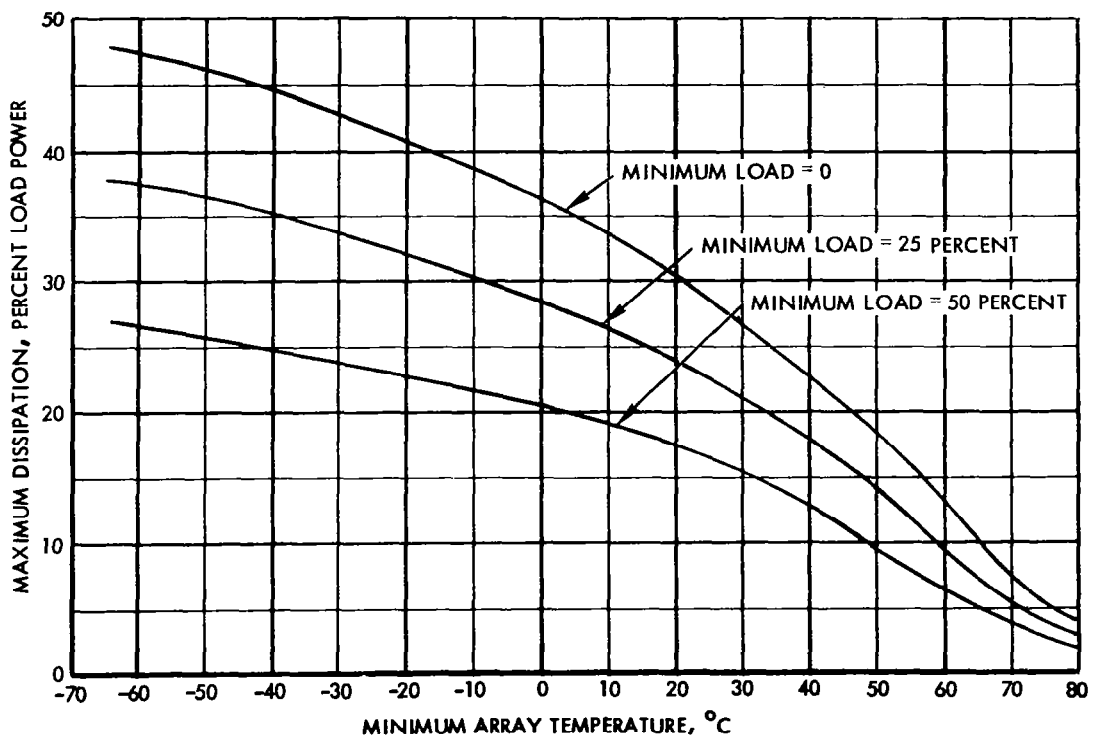

Figure 5-3. Partial Shunt Regulator, Maximum Array Temperature, 80°C

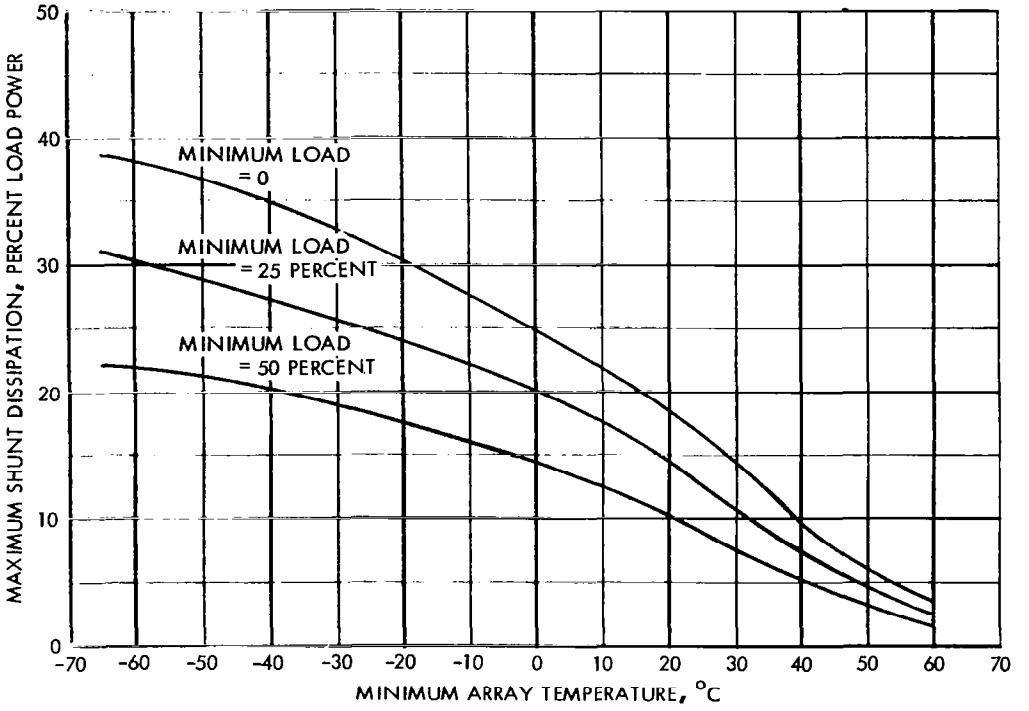

Figure 5-4. Partial Shunt Regulator, Maximum Array Temperature, 60°C

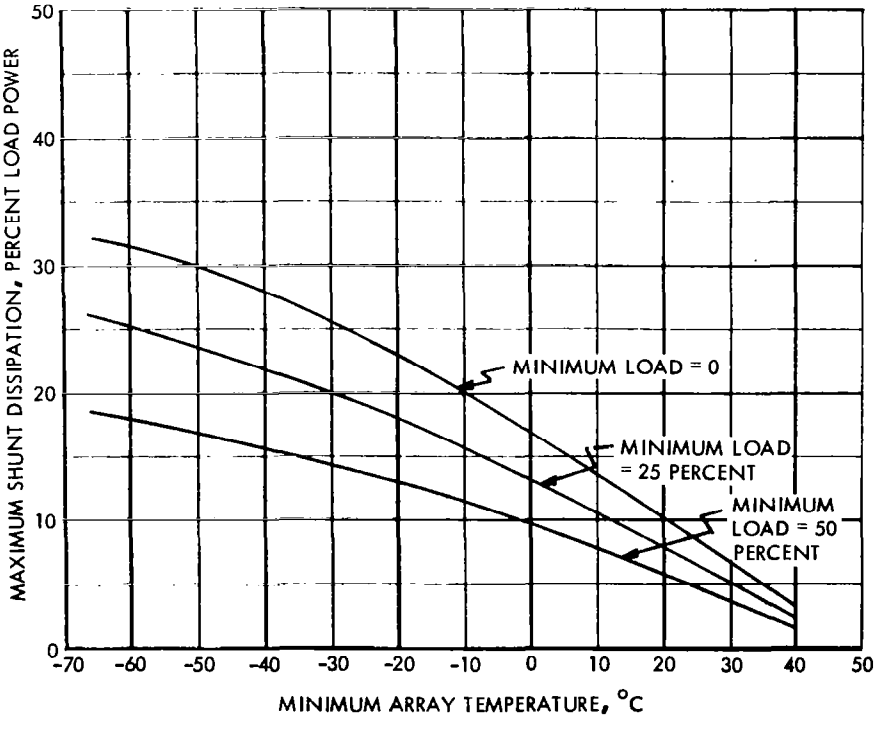

Figure 5-5. Partial Shunt Regulator, Maximum Array Temperature, 40°C

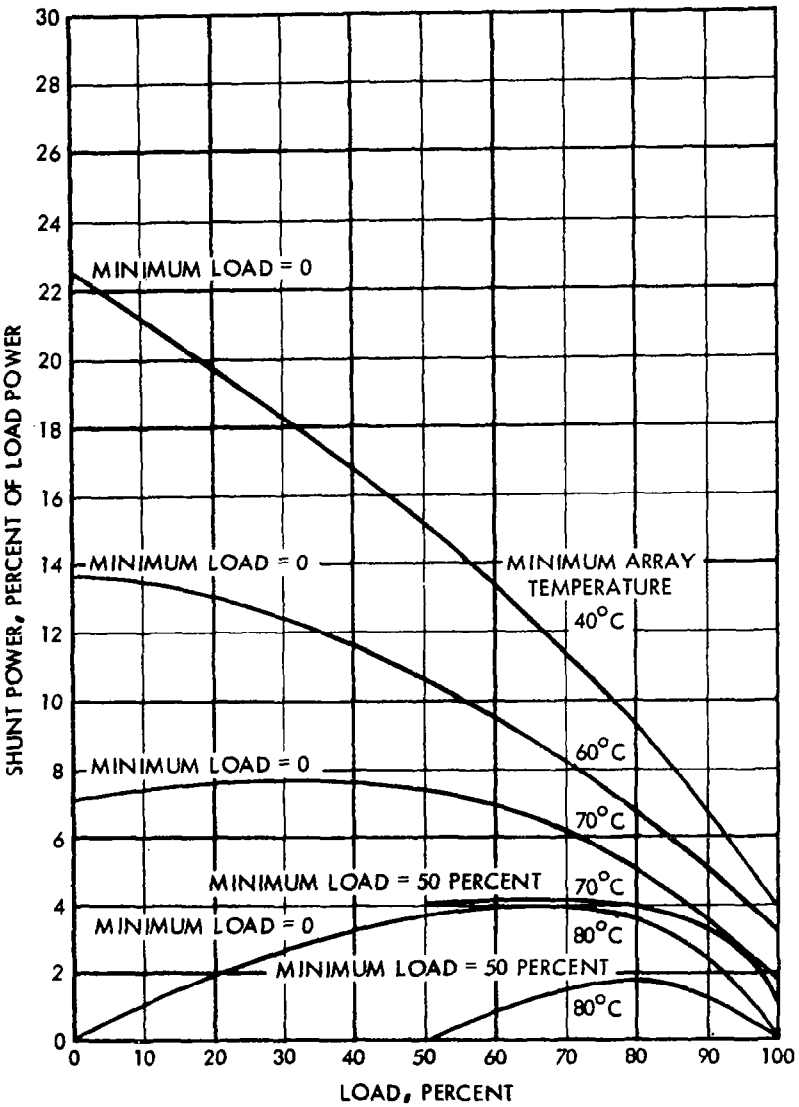

Figure 5-6. Partial Shunt Regulator, Maximum Array Temperature, 80°C

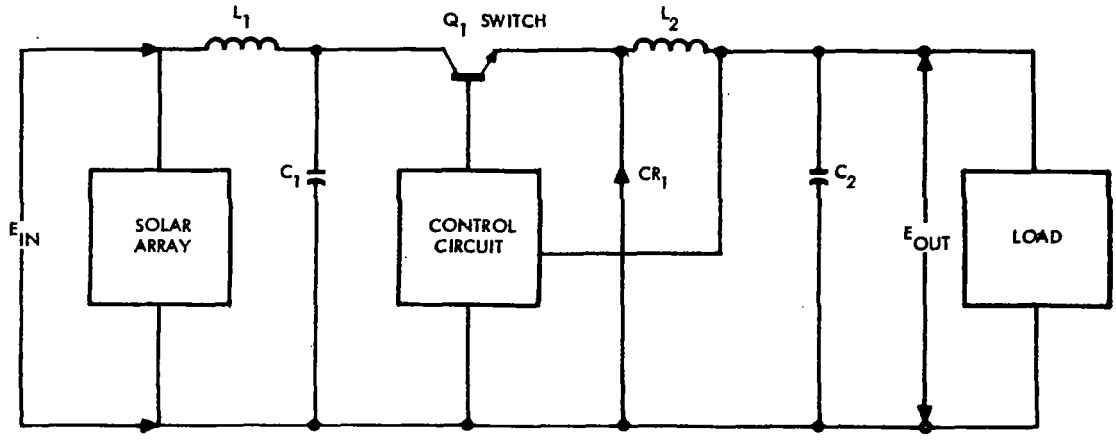

Figure 5-7. Pulsewidth Modulated Bucking Regulator Block Diagram

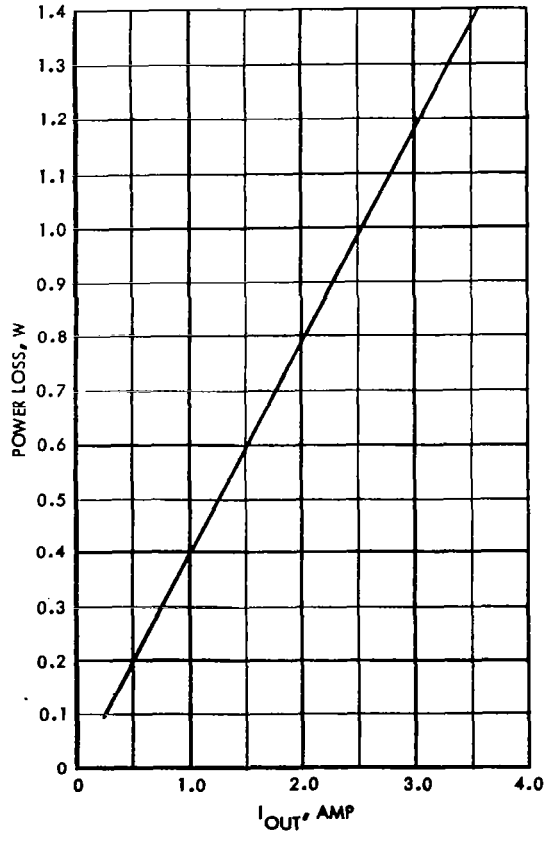

Figure 5-8. Pulsewidth Bucking Regulator, Saturated Conditions

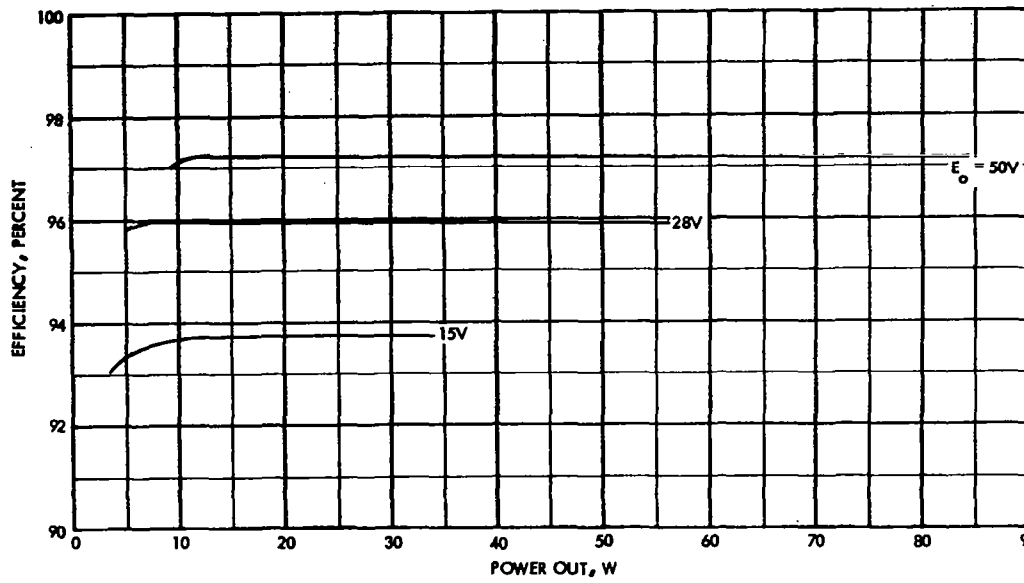

Figure 5-9. Pulsewidth Modulated Bucking Regulator, Power Loss Prior to Full Saturation

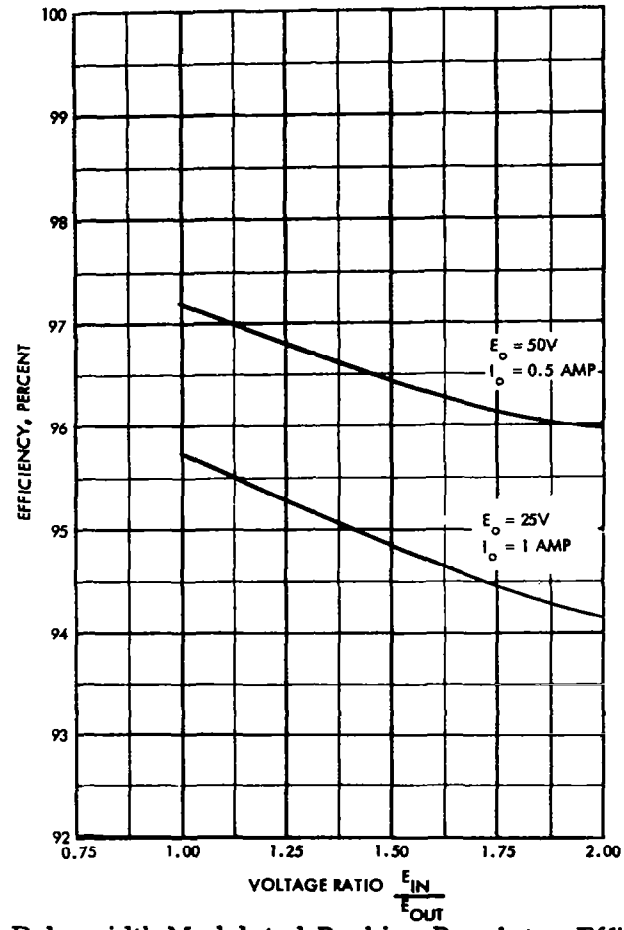

Figure 5-10. Pulsewidth Modulated Bucking Regulator Efficiency

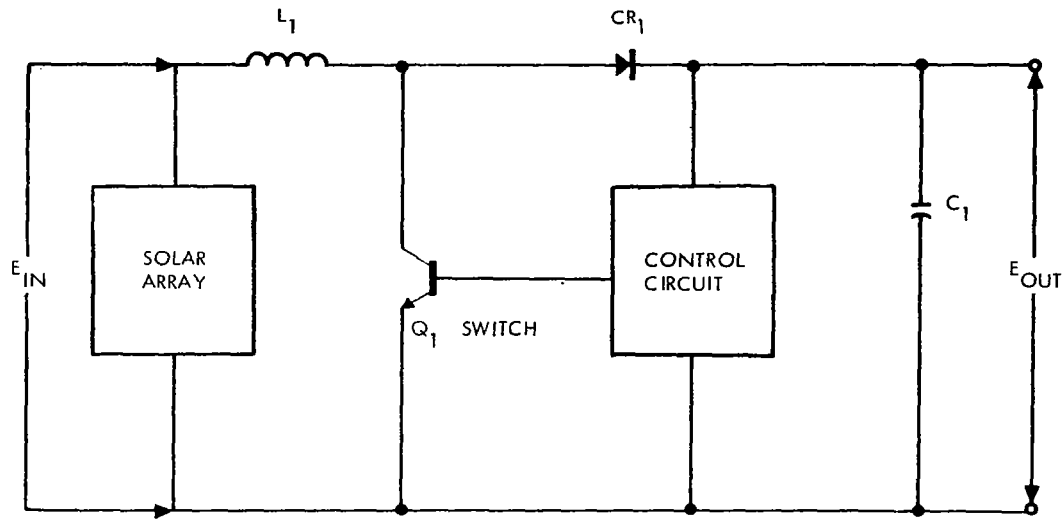

Figure 5-11. Pulsewidth Modulated Boost Regulator Block Diagram

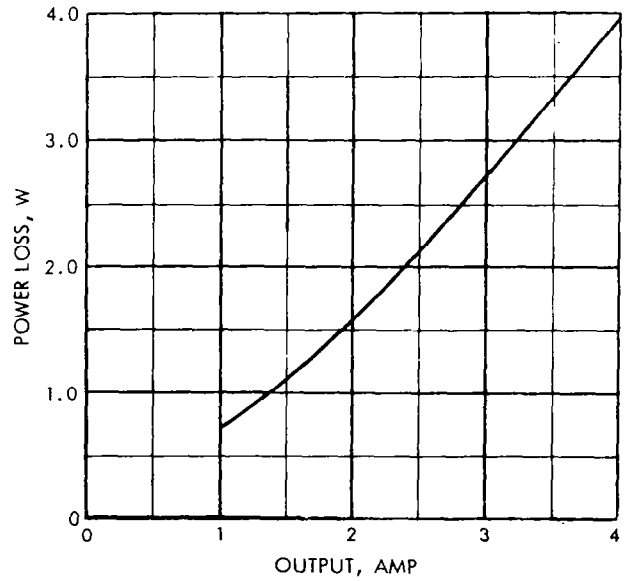

Figure 5-12. Pulsewidth Modulated Boost Regulator, Series Loss at the No Switching Point

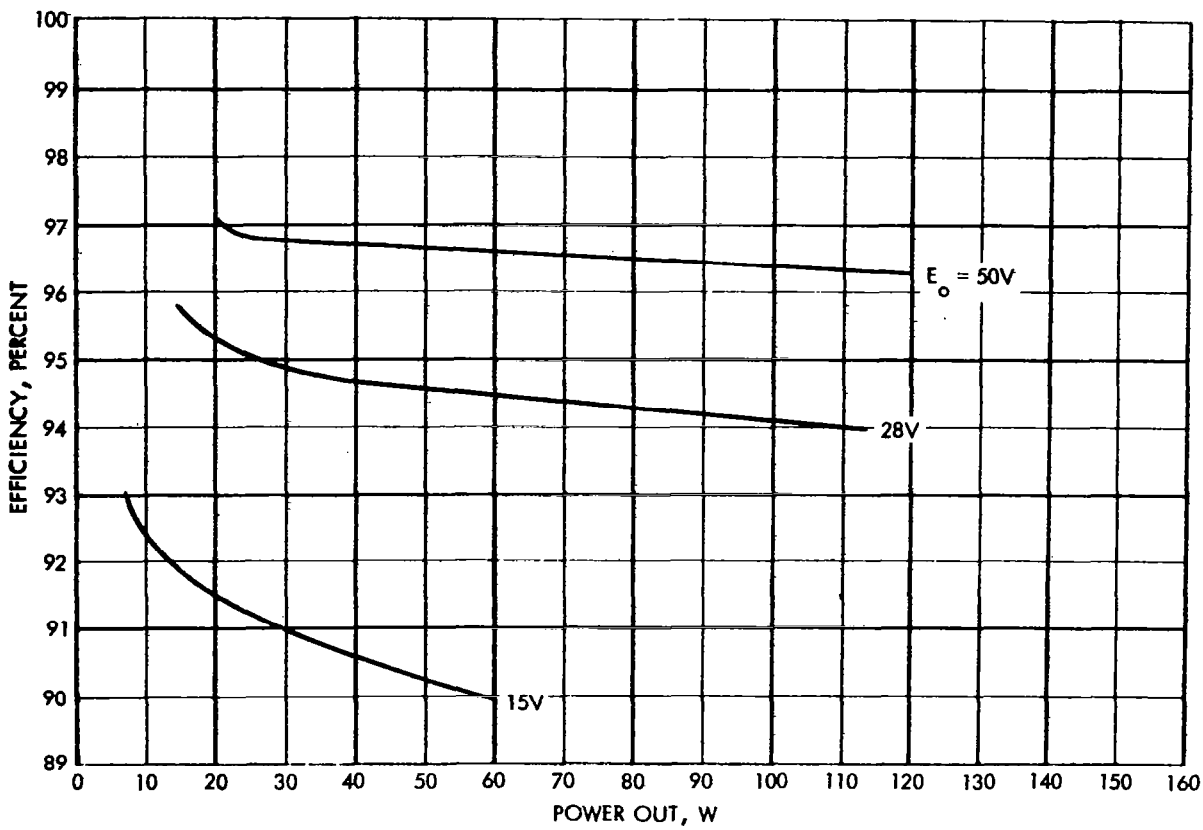

Figure 5-13. Pulsewidth Modulated Boost Regulator Efficiency, Shunt Element Open

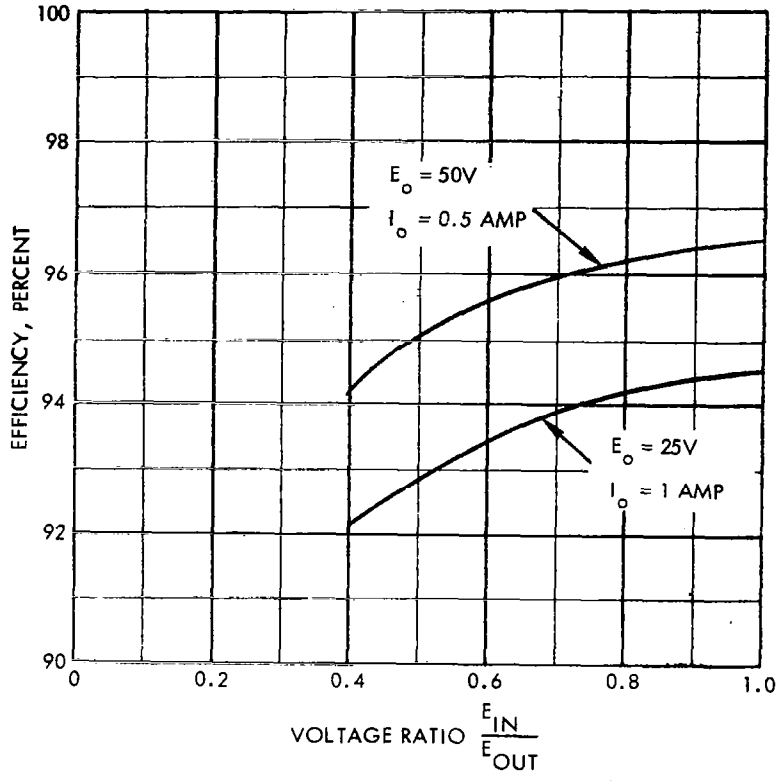

Figure 5-14. Pulsewidth Modulated Boost Regulator

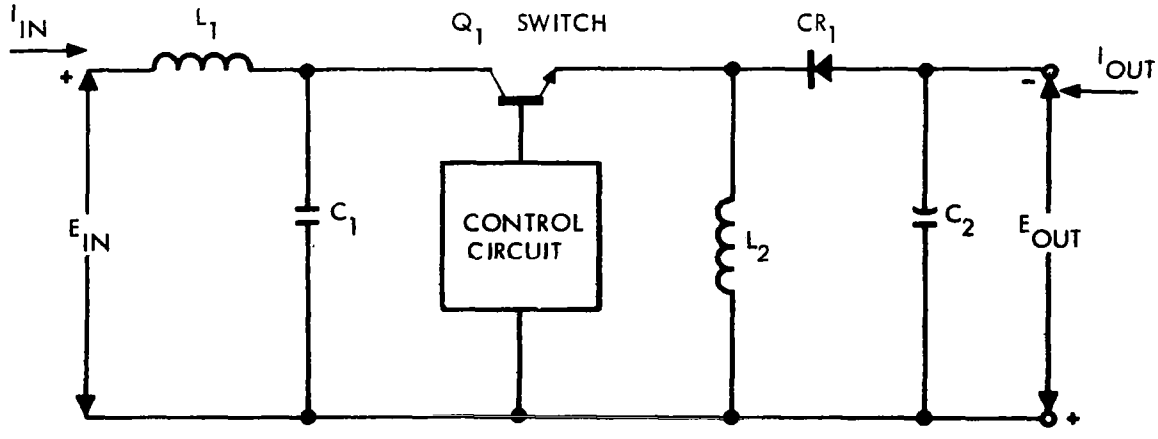

Figure 5-15. Pulsewidth Modulated Buck-Boost Regulator Block Diagram

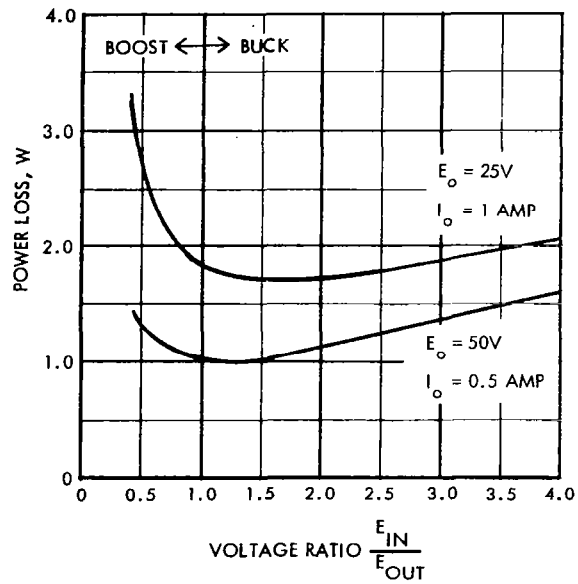

Figure 5-16. Pulsewidth Modulated Buck-Boost Regulator Power Loss

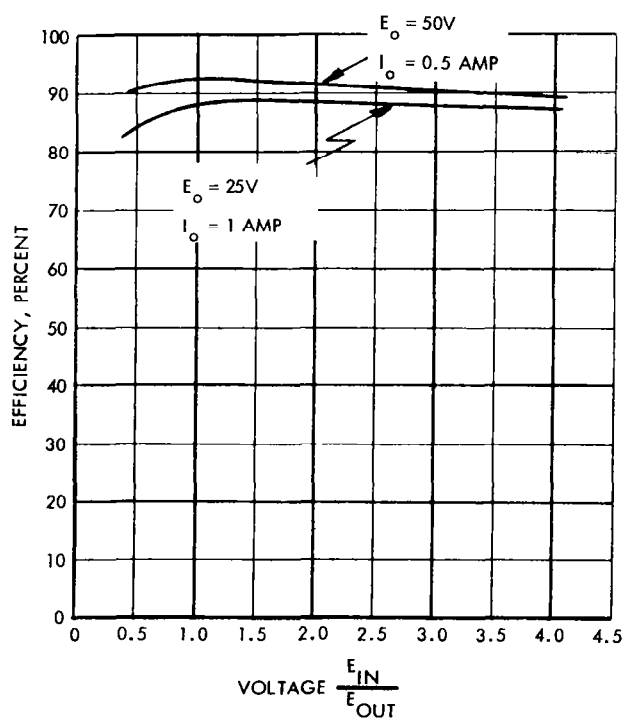

Figure 5-17. Pulsewidth Modulated Buck-Boost Regulator Efficiency

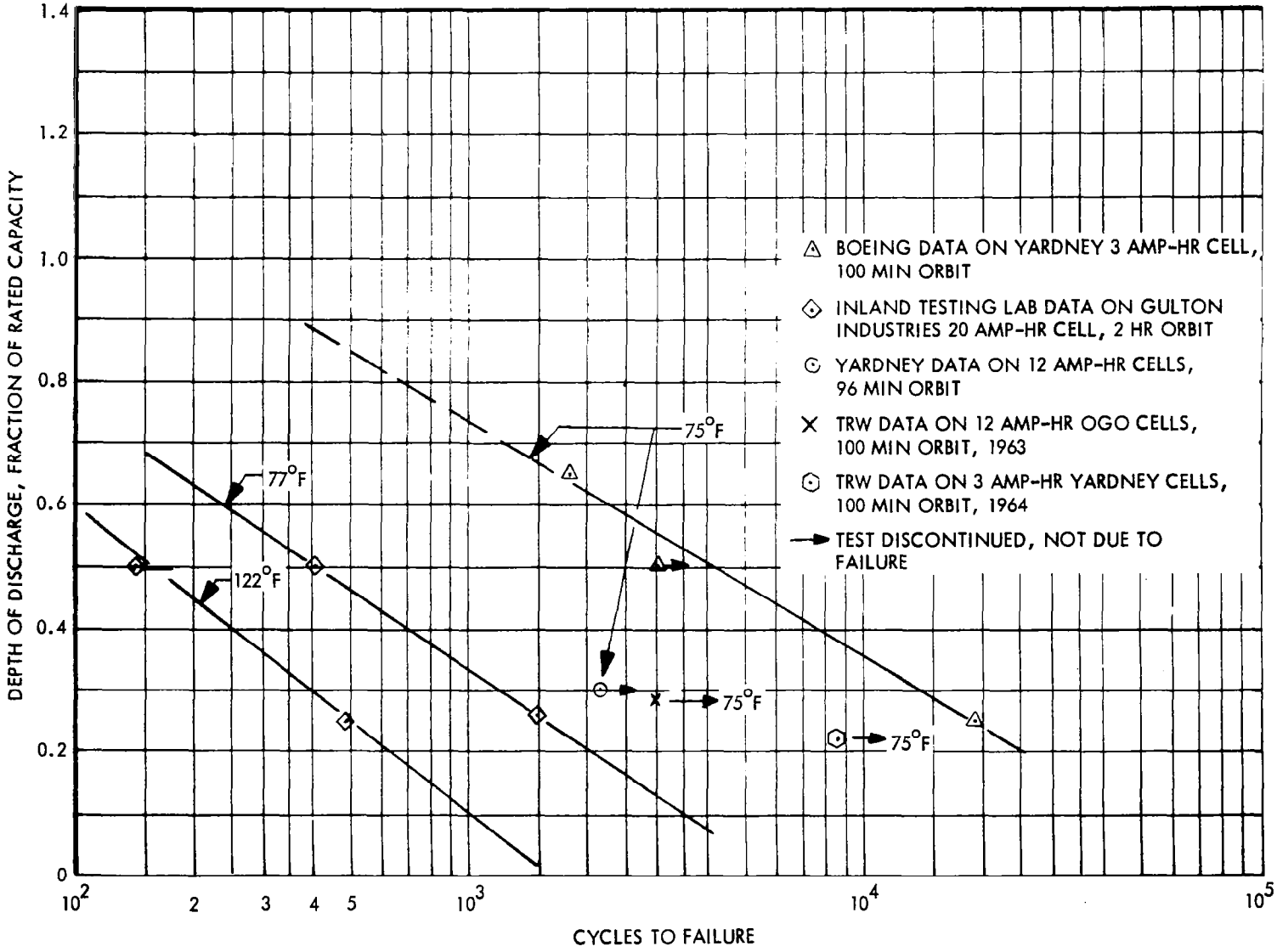

Figure 5-18. Observed Cycle Life of Silver-Cadmium Batteries

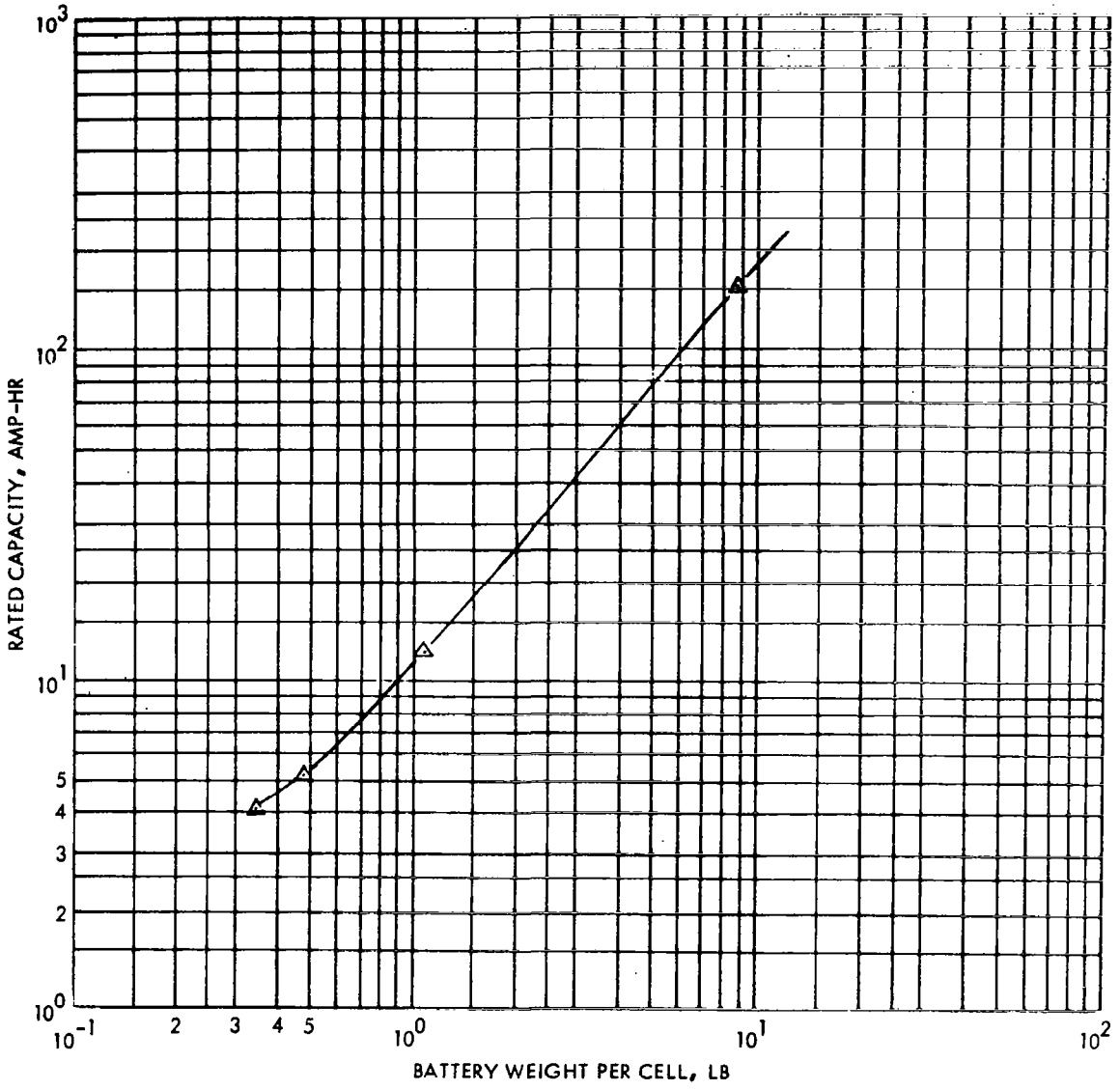

Figure 5-19. Silver-Cadmium Battery, Rated Capacity at 75°F Versus Battery Weight

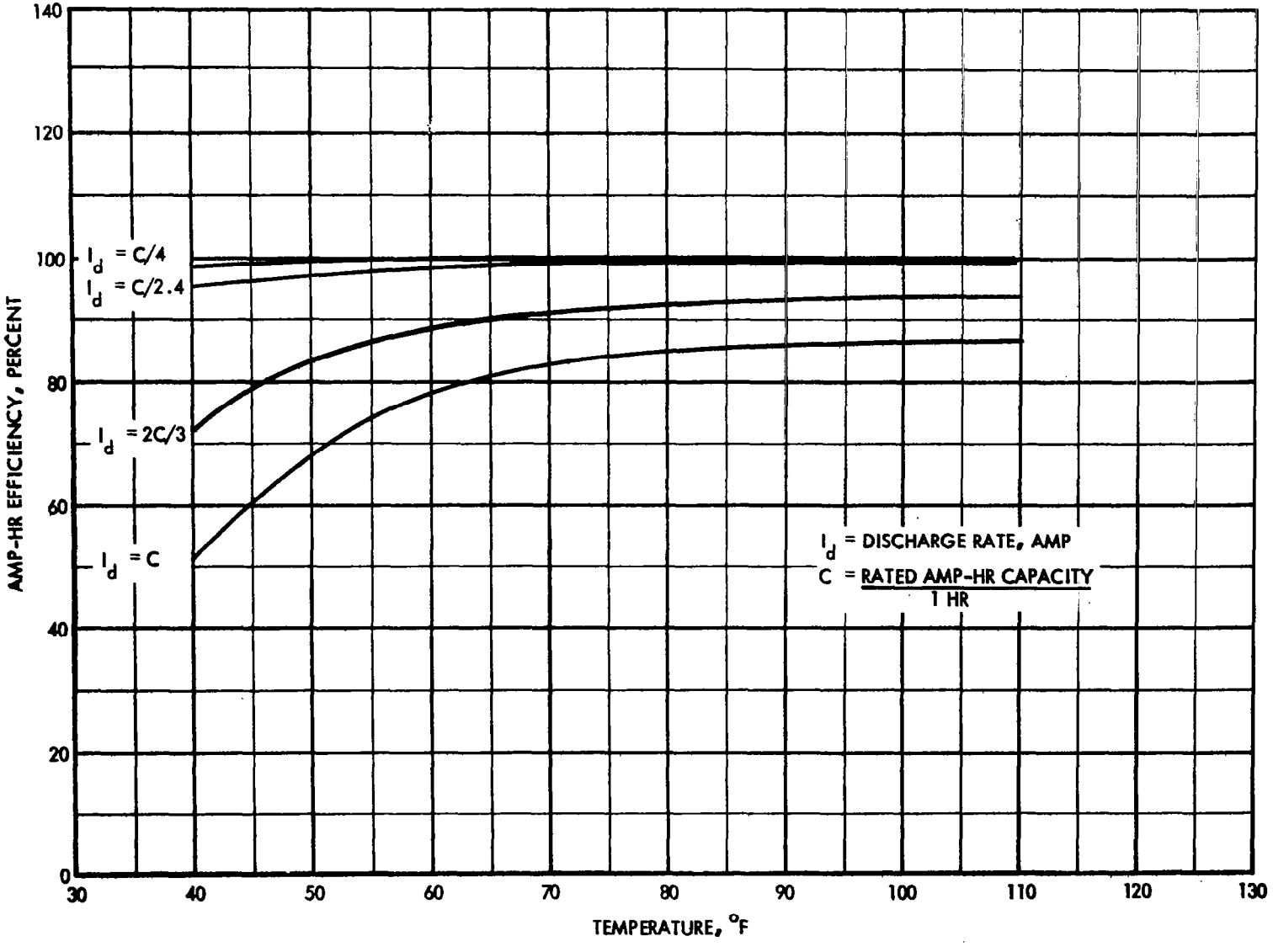

Figure 5-20. Silver-Cadmium Battery, Amp-Hr Efficiency Versus Temperature

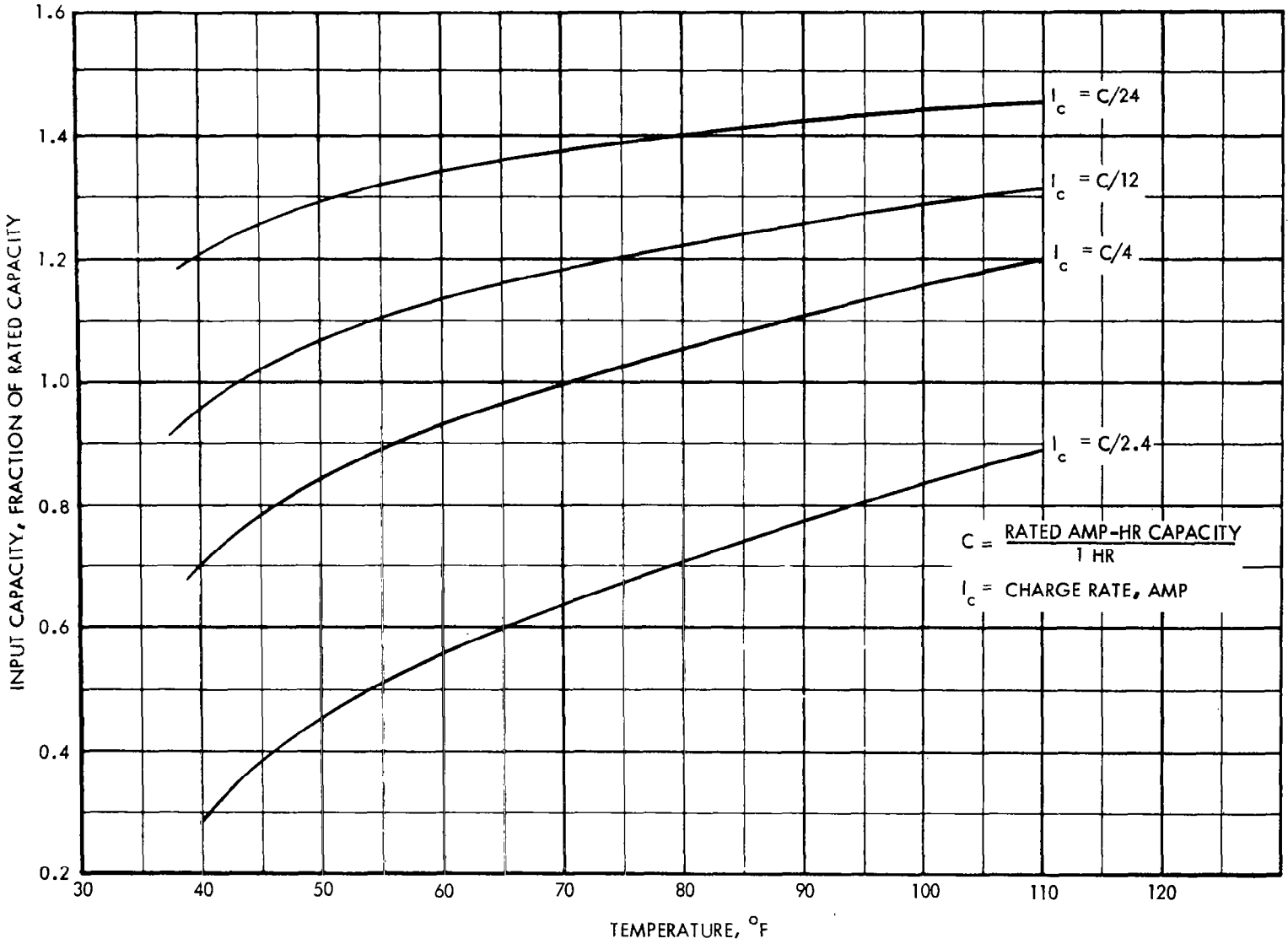

Figure 5-21. Silver-Cadmium Battery, Maximum Input Capacity Versus Temperature

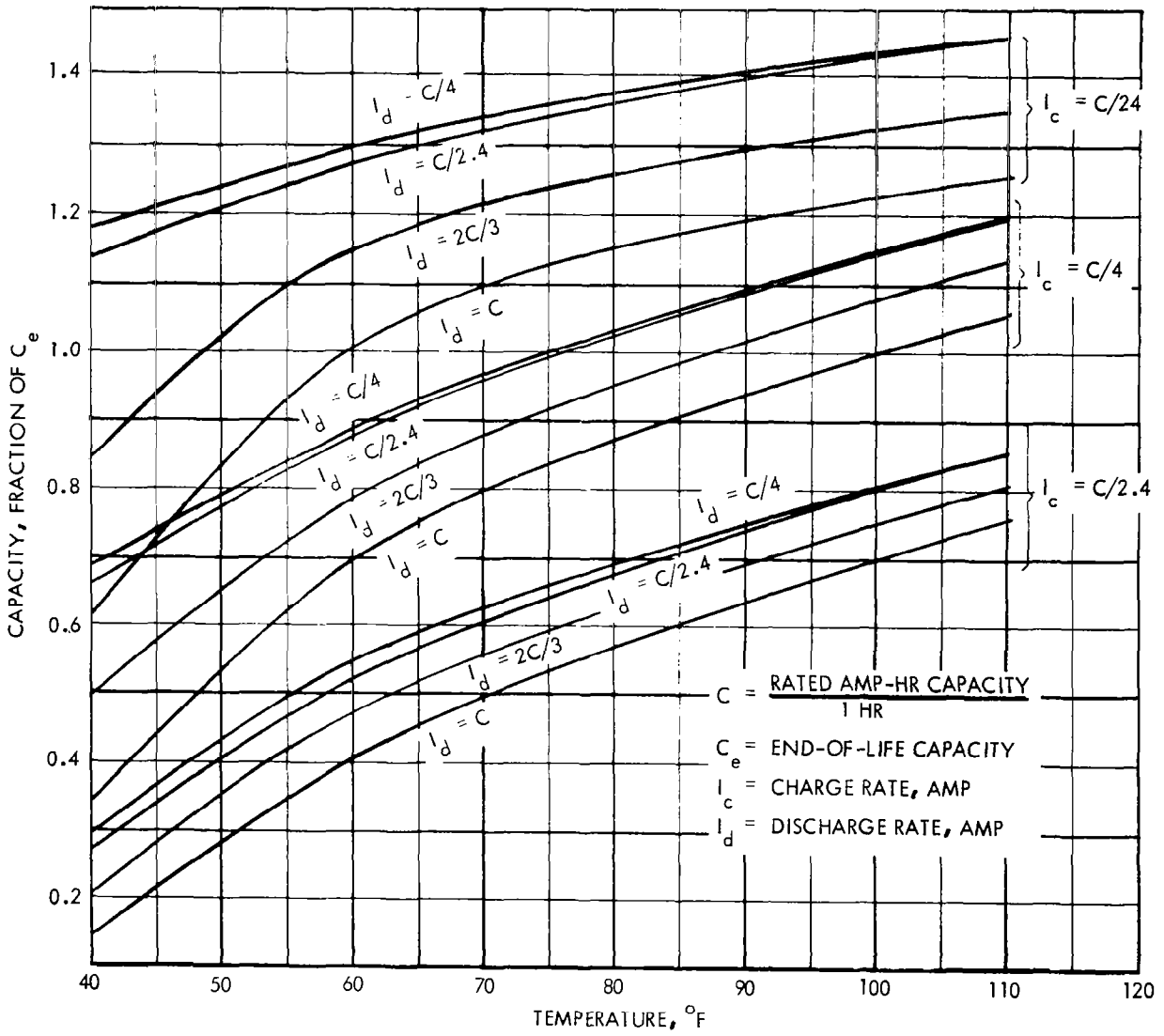

Figure 5-22. Silver-Cadmium Battery, Output Capacity Versus Temperature

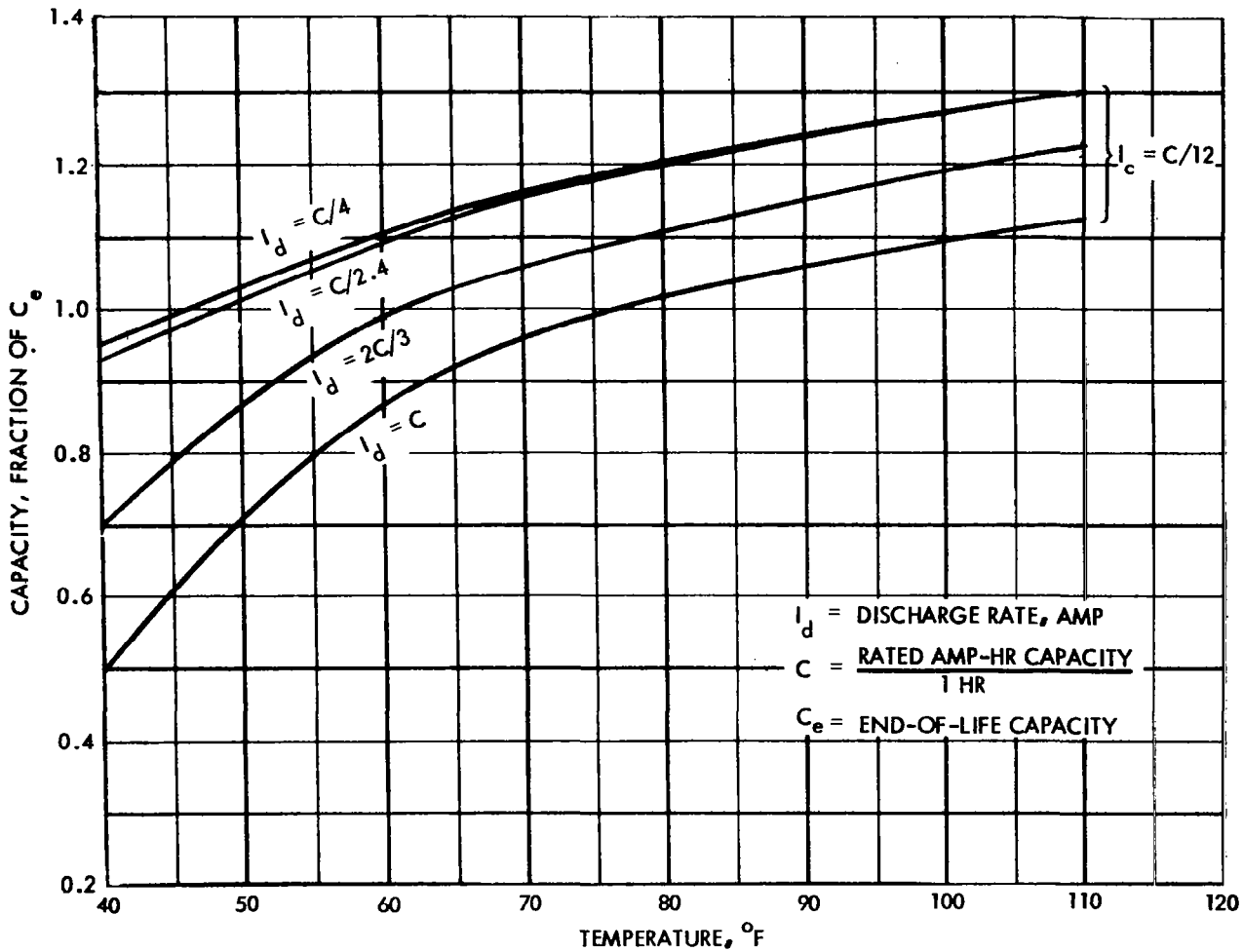

Figure 5-23. Silver – Cadmium Battery, Output Capacity Versus Temperature

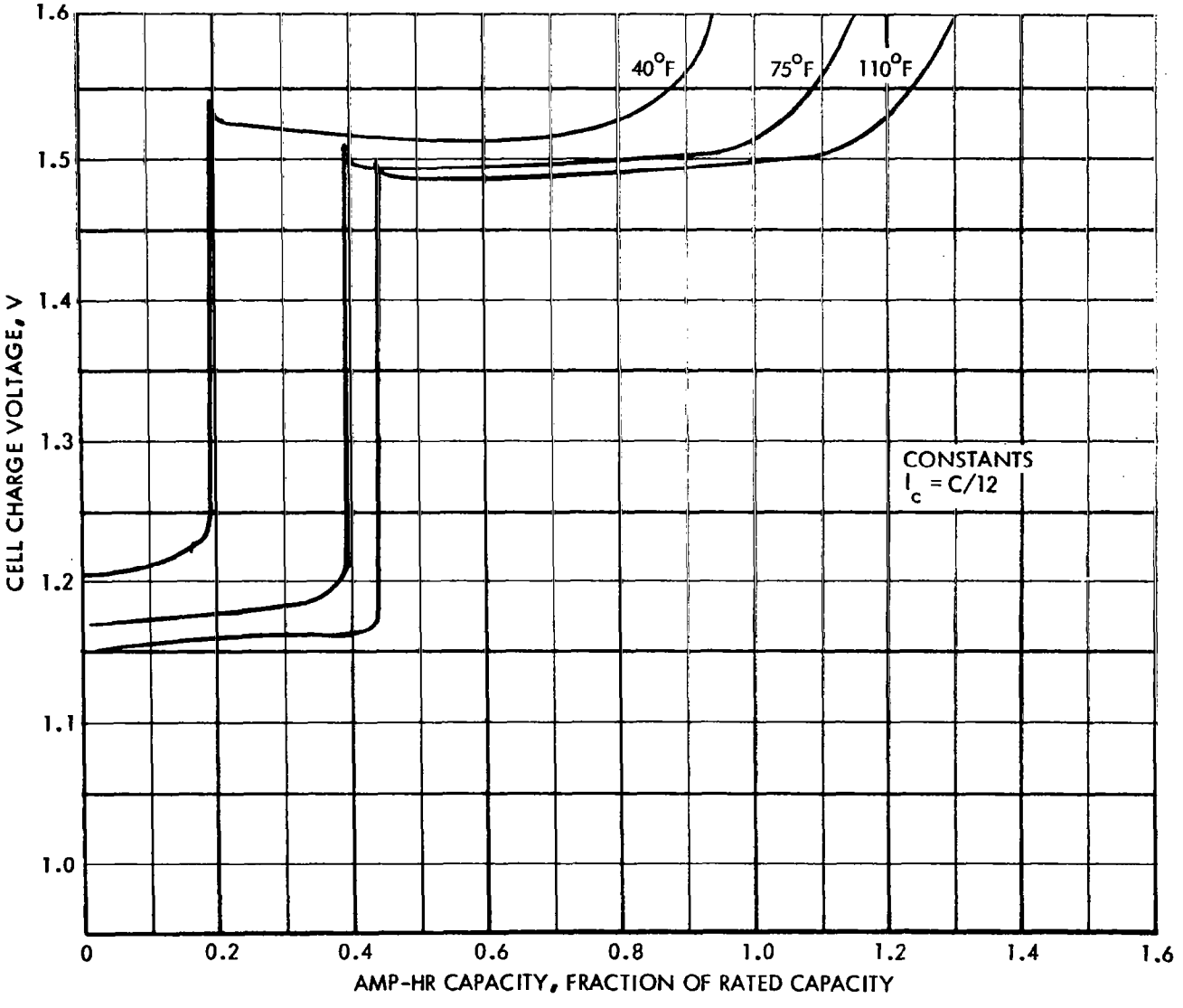

Figure 5-24. Silver – Cadmium Battery, Charge Voltage Versus Amp-Hr Capacity

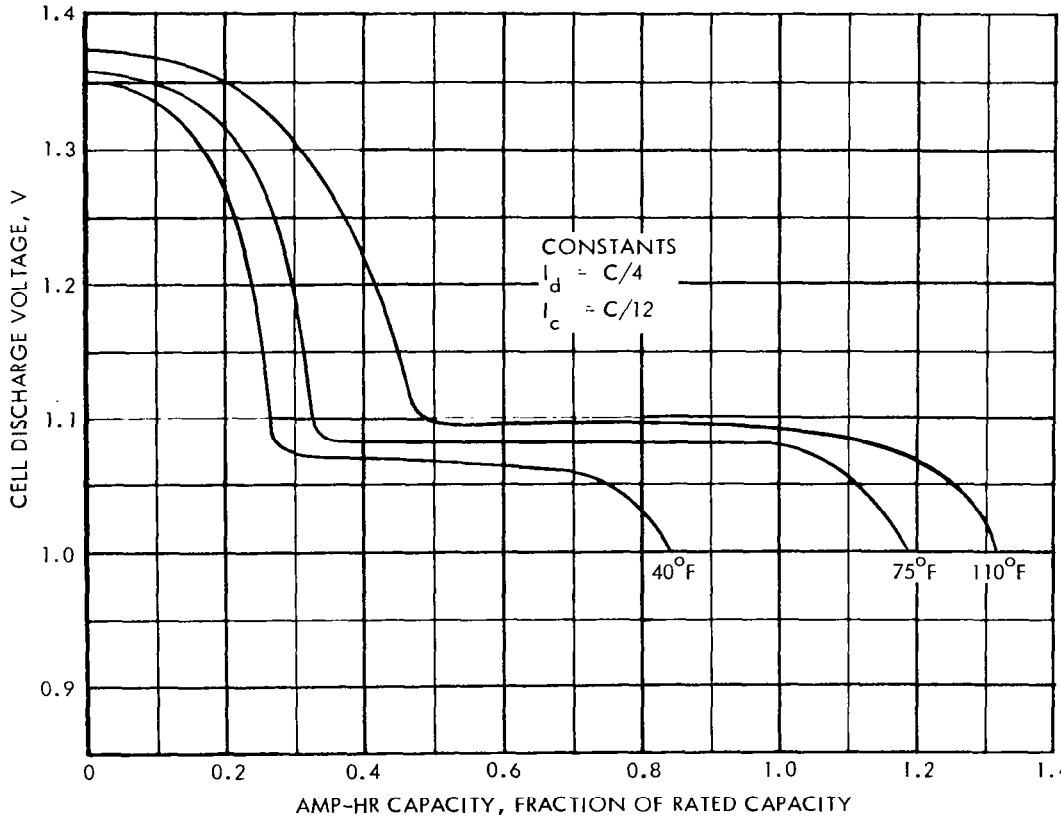

Figure 5-25. Silver – Cadmium Battery, Discharge Voltage Versus Amp-Hr Capacity

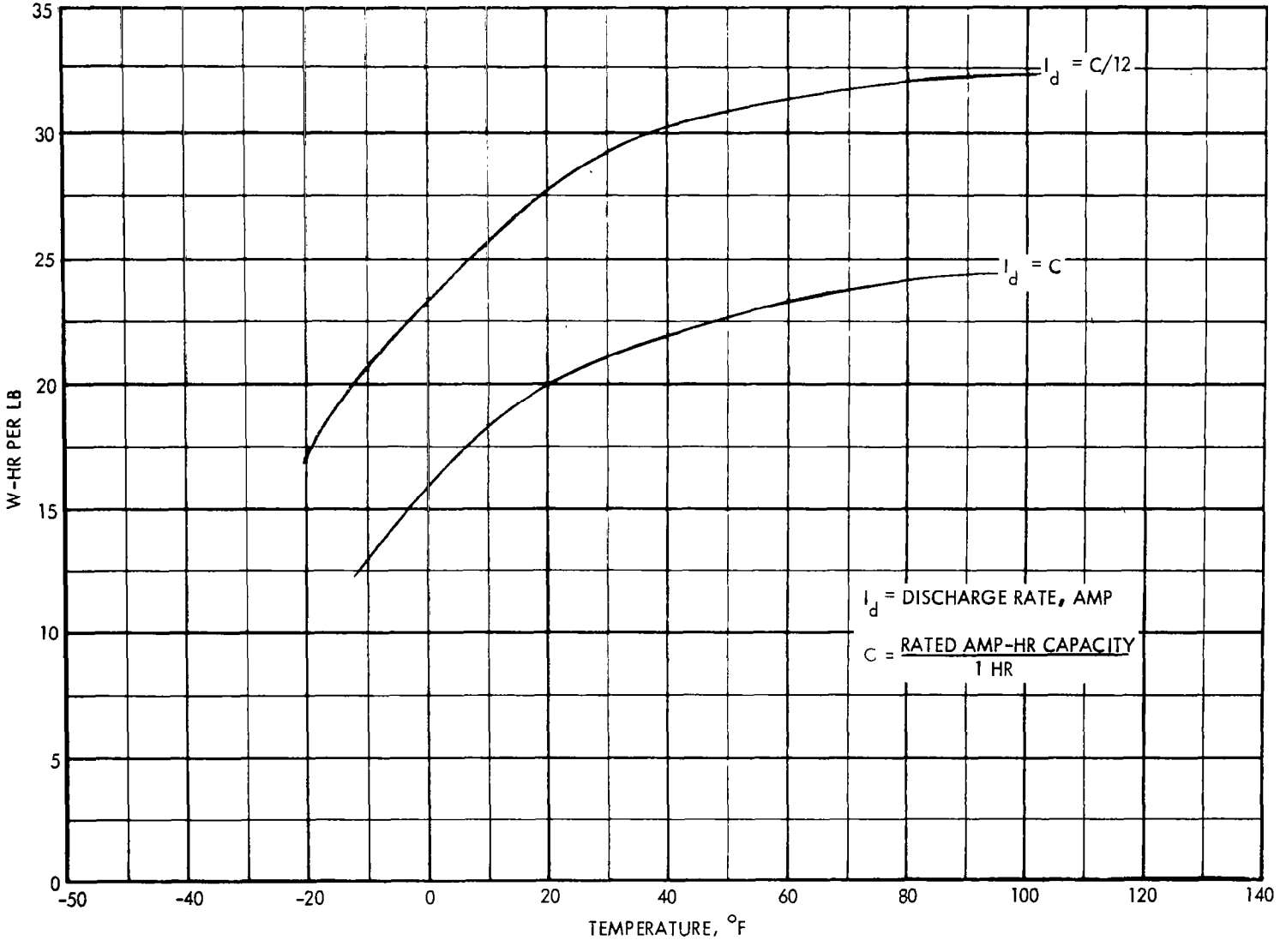

Figure 5-26. Silver – Cadmium Battery, Effect of Temperature on Energy per Unit-Weight

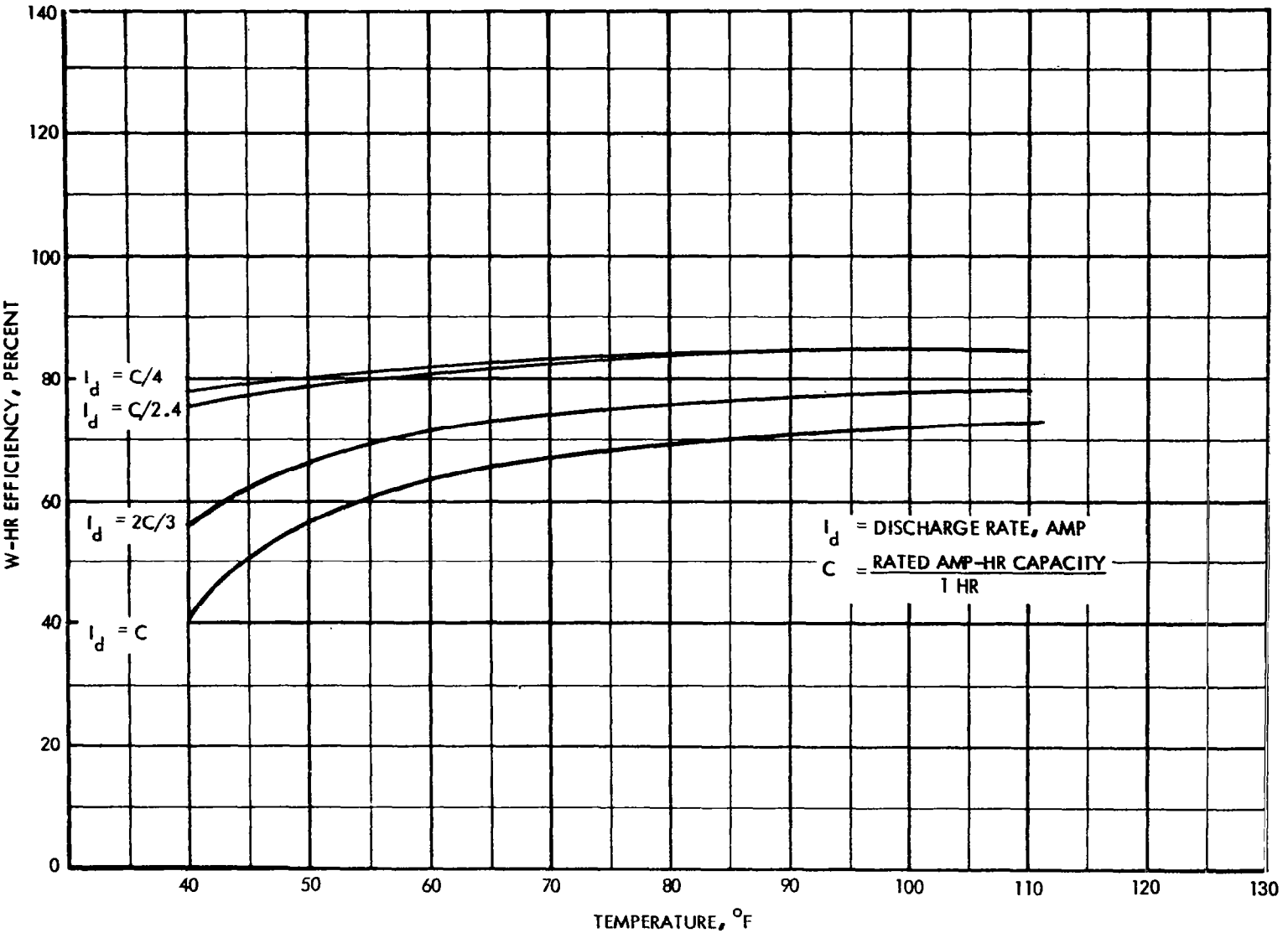

Figure 5-27. Silver – Cadmium Battery, Effect of Temperature on W-Hr Efficiency

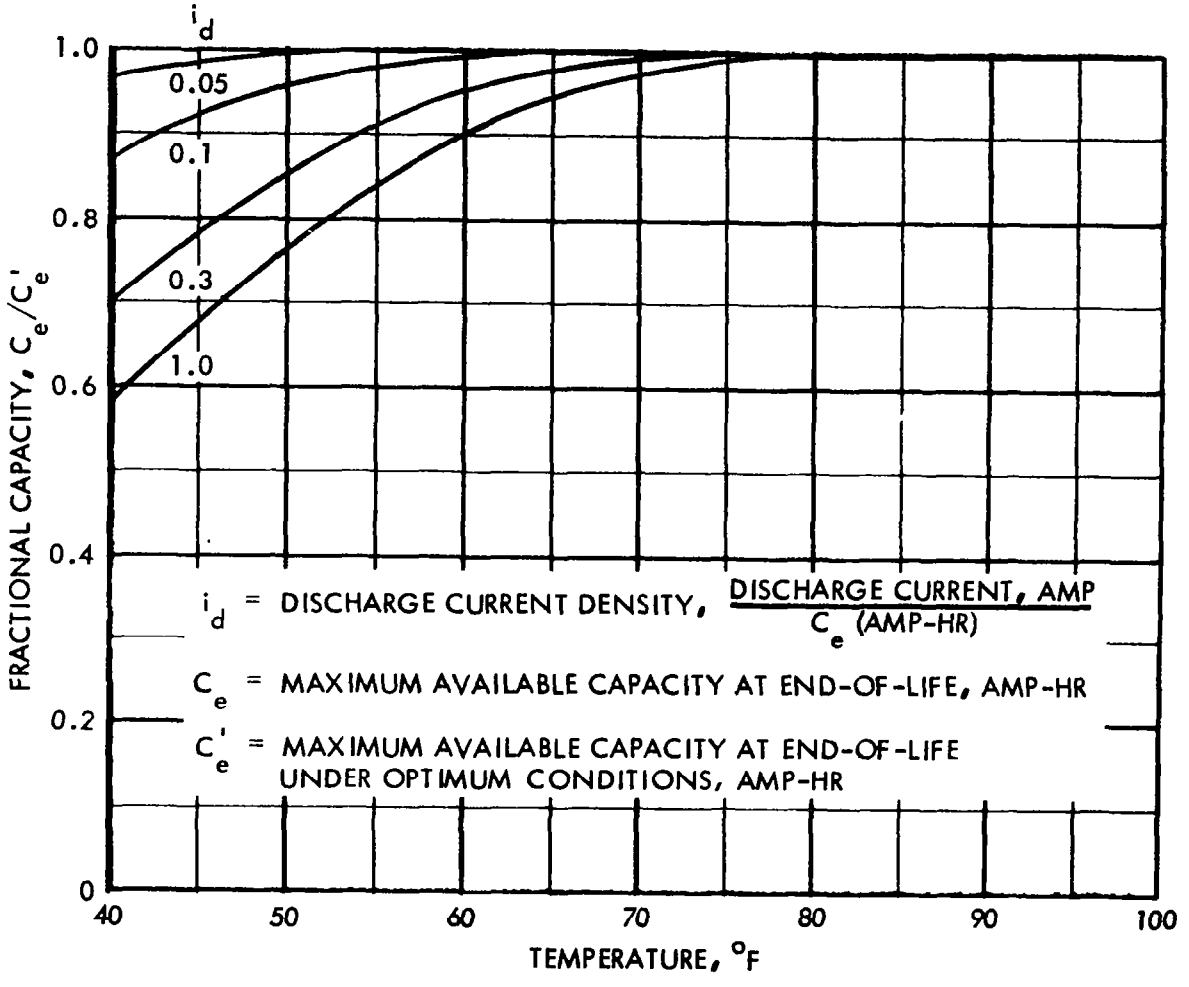

Figure 5-28. Nickel – Cadmium Battery, Discharge Design Data

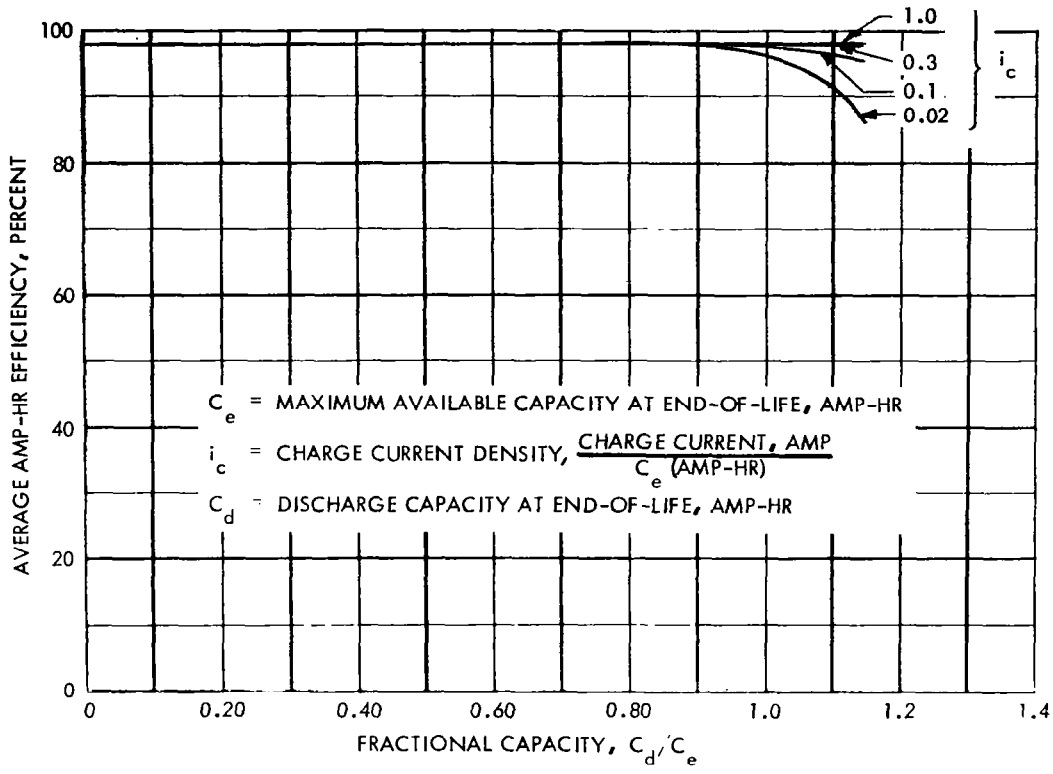

Figure 5-29. Nickel – Cadmium Battery, Amp-Hr Efficiency at 40°F

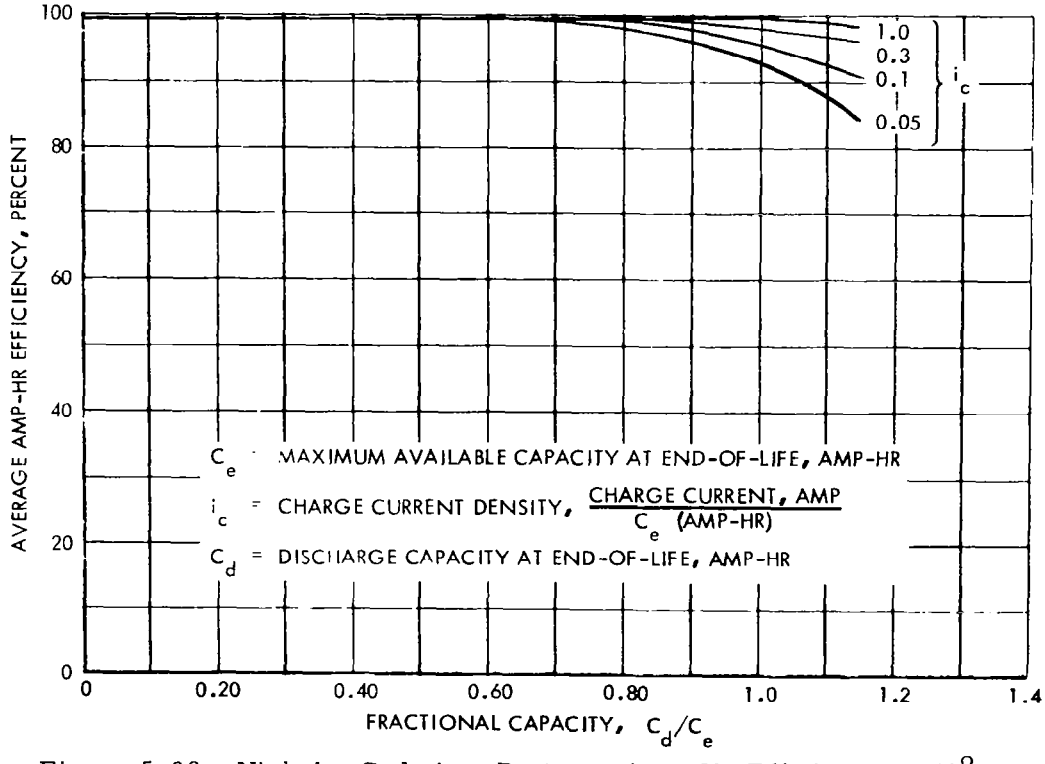

Figure 5-30. Nickel – Cadmium Battery, Amp-Hr Efficiency at 59°F

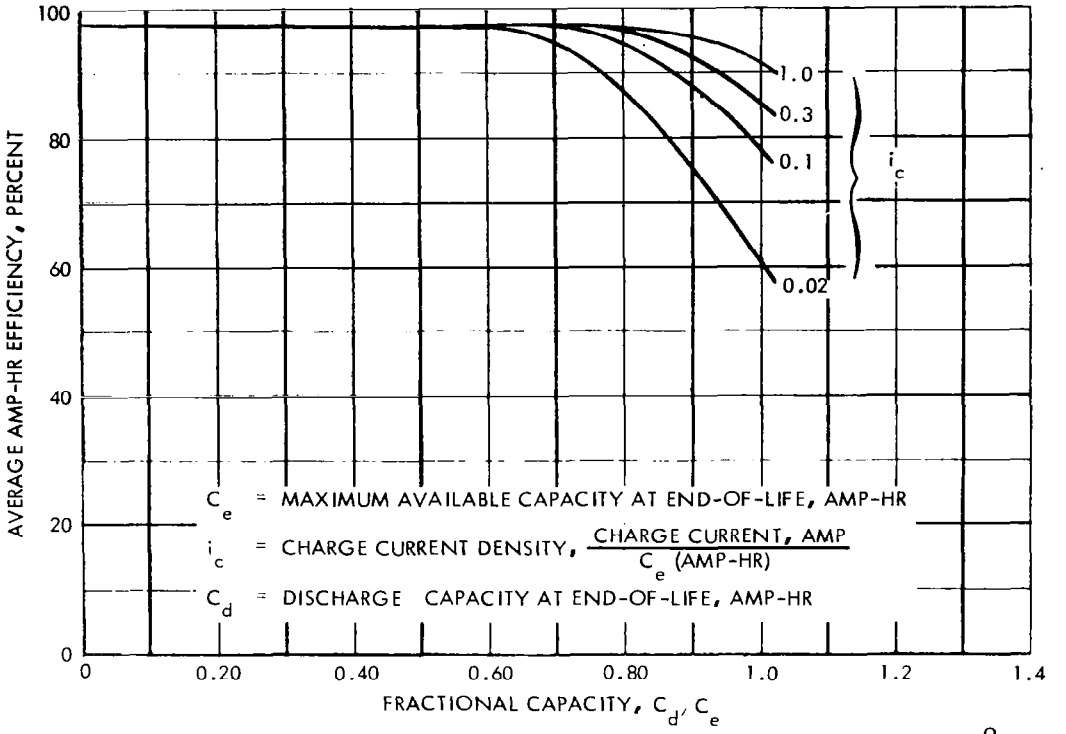

Figure 5-31. Nickel – Cadmium Battery, Amp-Hr Efficiency at 78°F

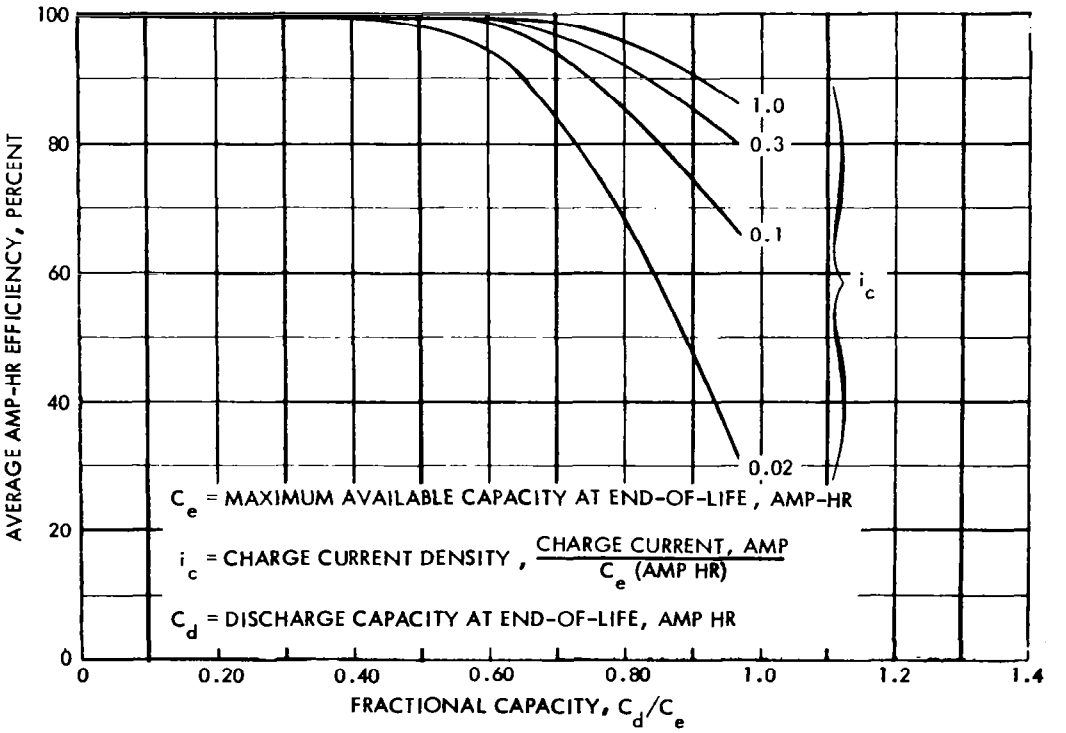

Figure 5-32. Nickel - Cadmium Battery, Amp-Hr Efficiency at 96°F

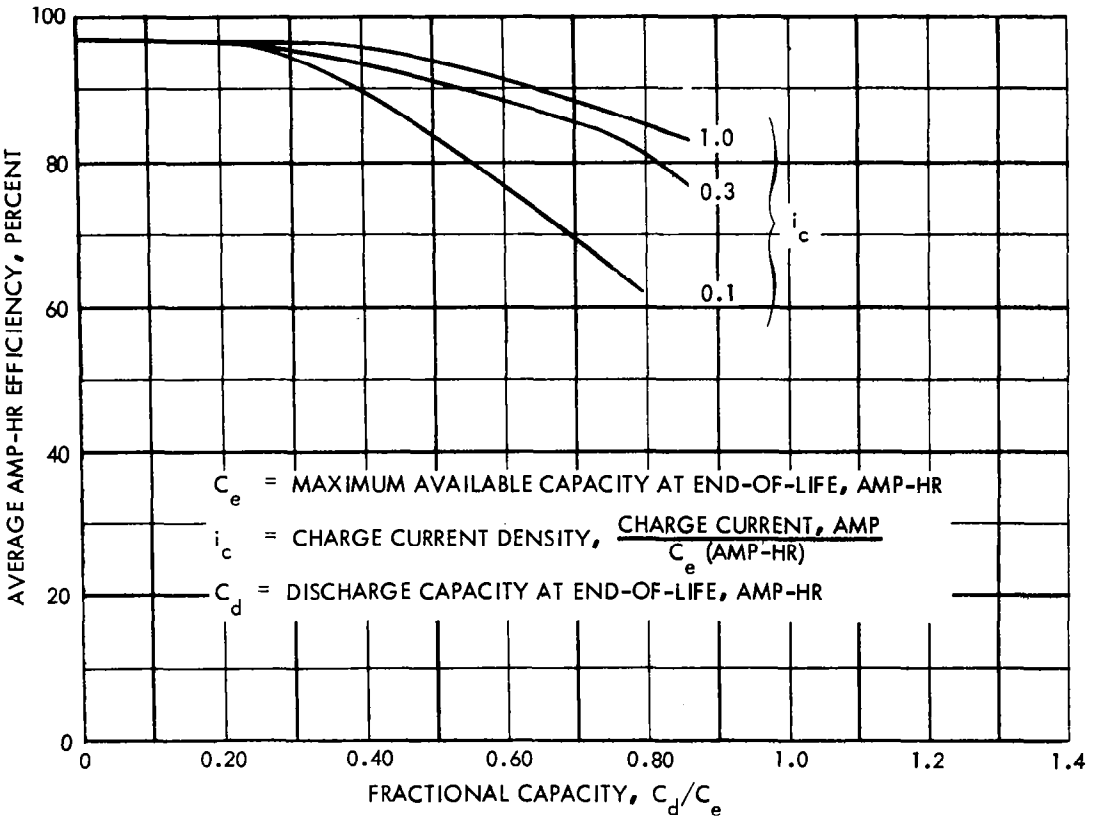

Figure 5-33. Nickel – Cadmium Battery, Amp-Hr Efficiency at 116°F

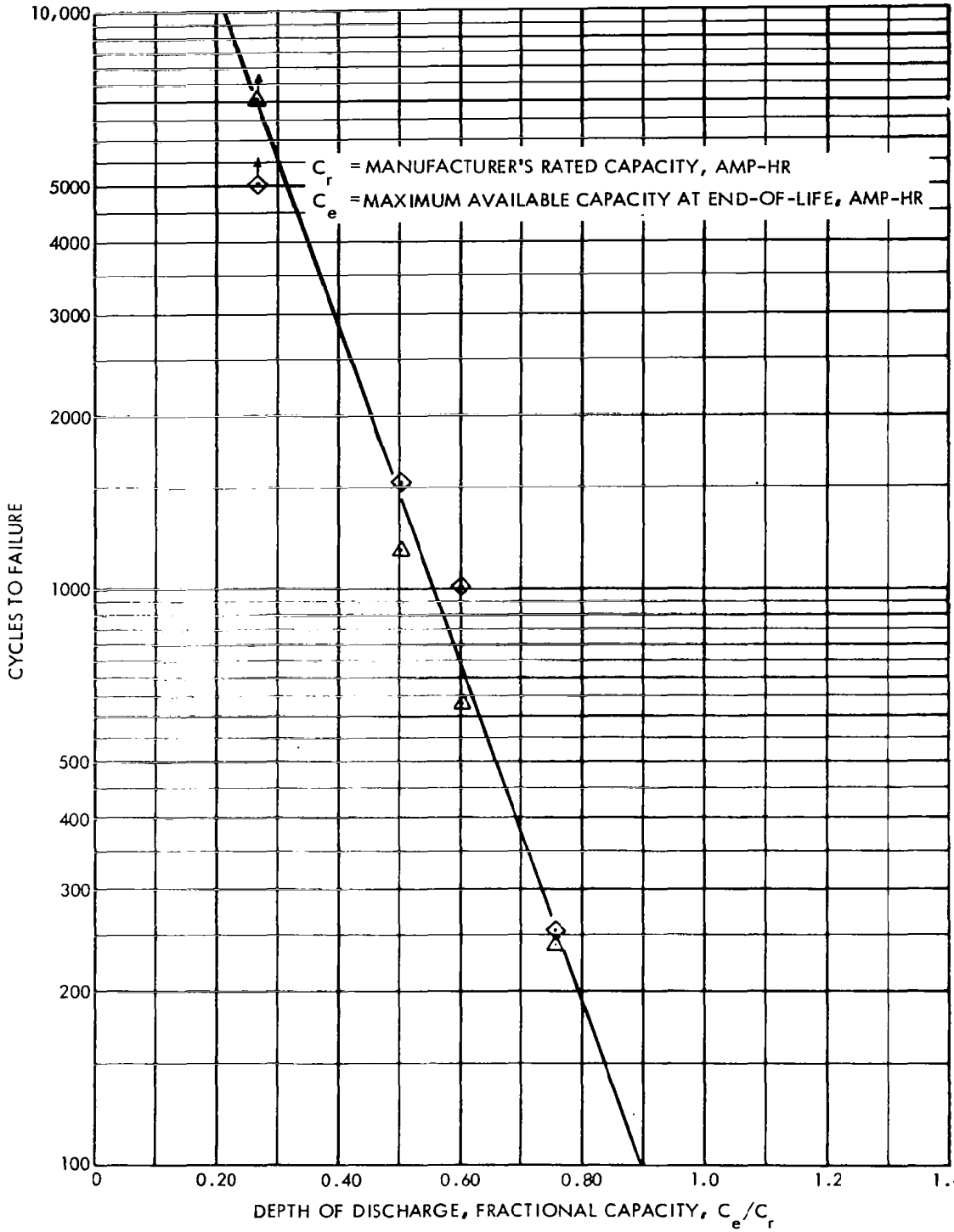

Figure 5-34. Nickel – Cadmium Battery, Cycle Life

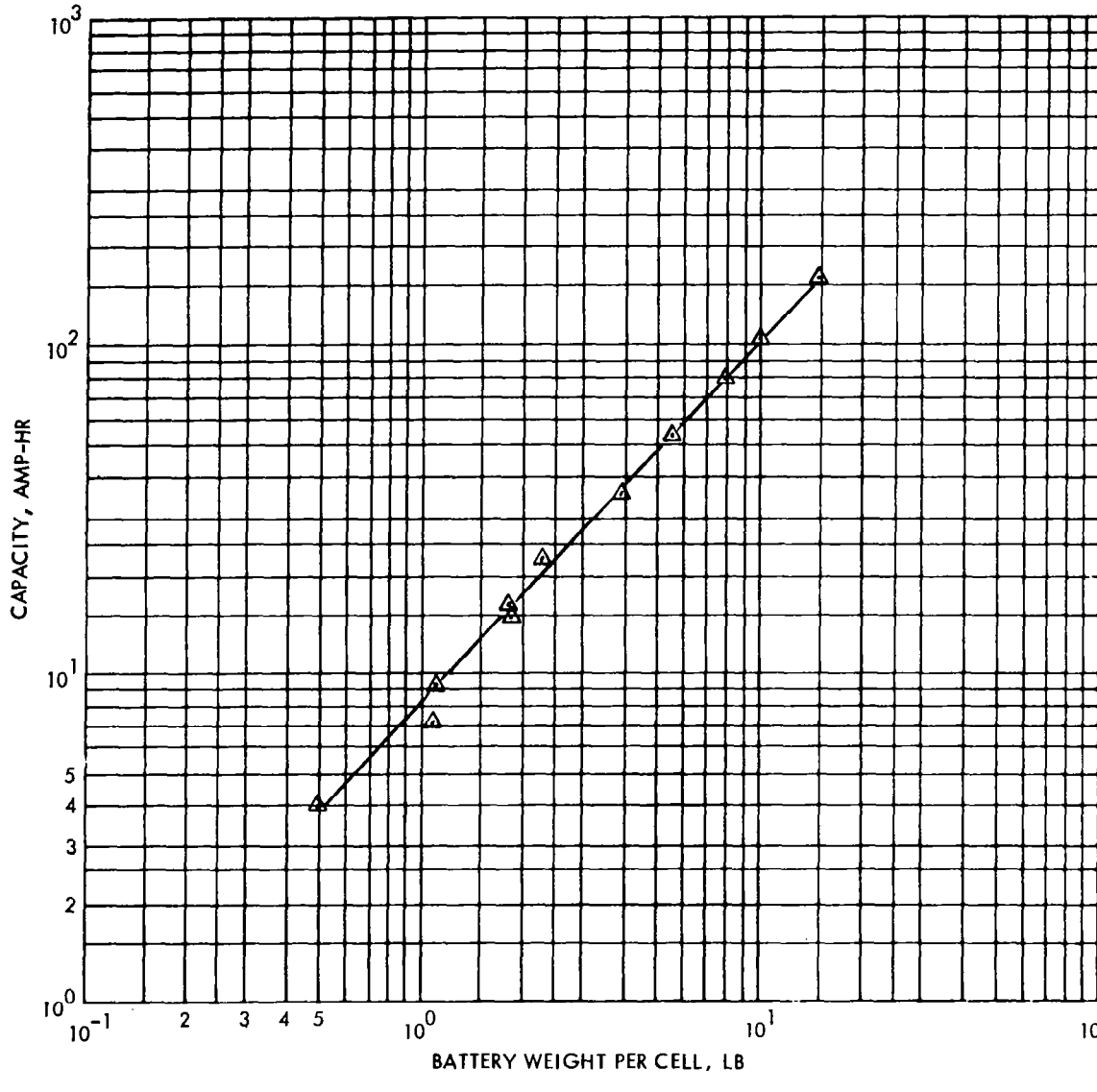

Figure 5-35. Nickel – Cadmium Battery, Amp-Hr Capacity Versus Battery Weight

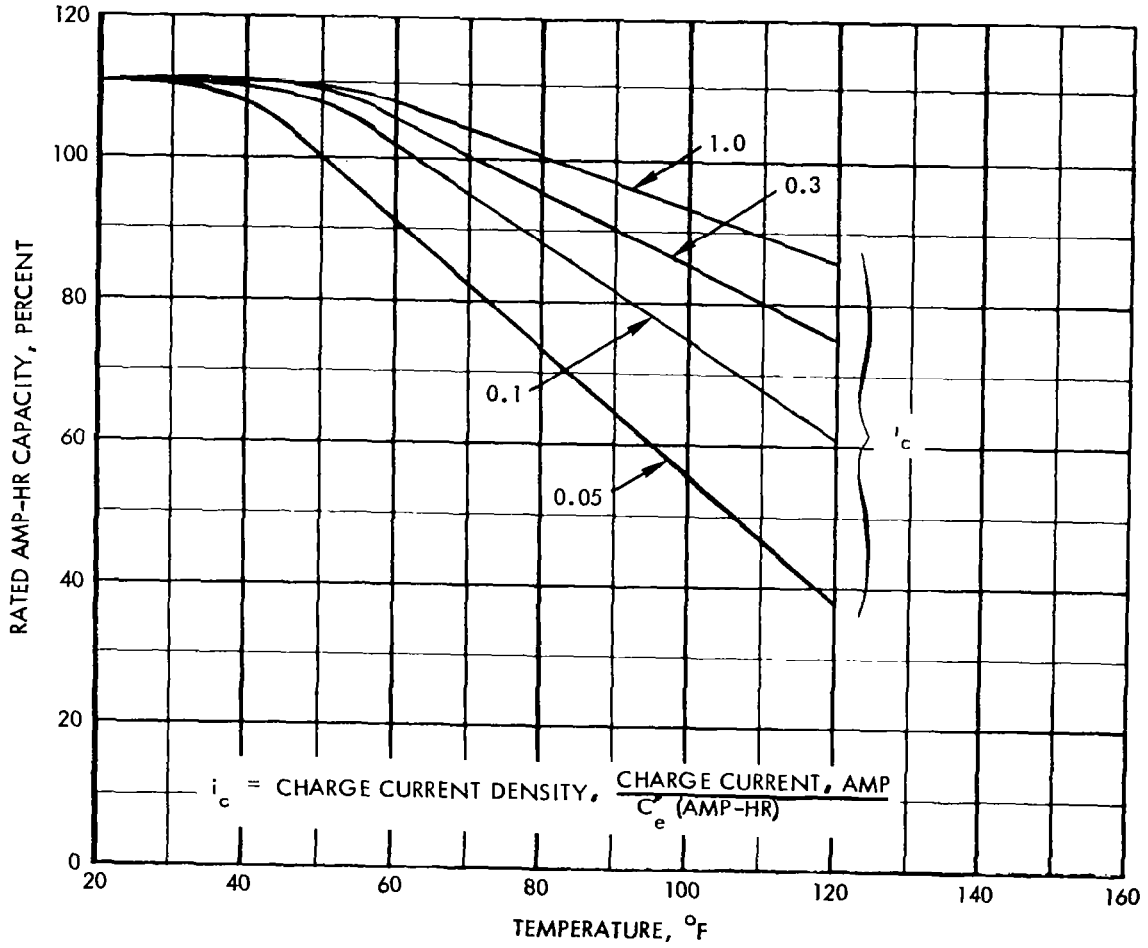

Figure 5-36. Nickel – Cadmium Battery, Maximum Achievable State of Charge Versus Temperature

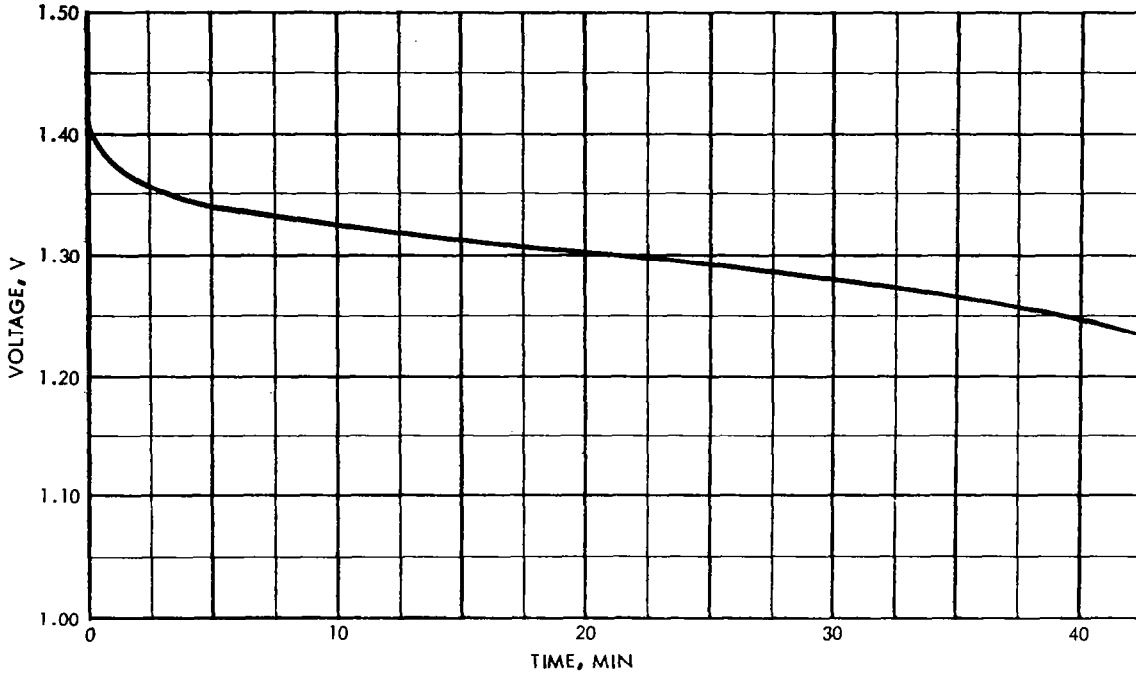

Figure 5-37. Nickel – Cadmium Battery, POGO Discharge Characteristic (250-w Discharge, 12-Amp-Hr Cell, 100°F, New Cell)

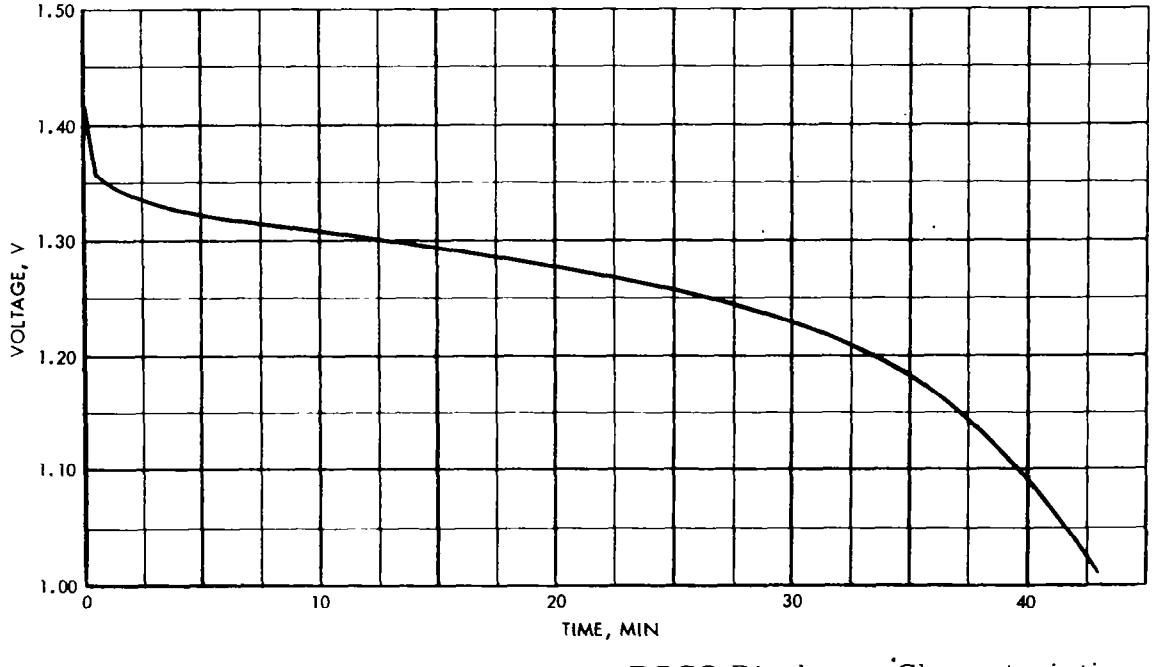

Figure 5-38. Nickel – Cadmium Battery, POGO Discharge Characteristic (250-w Discharge, 12 Amp-Hr Cell, 100°F, "Memorized" Cell)

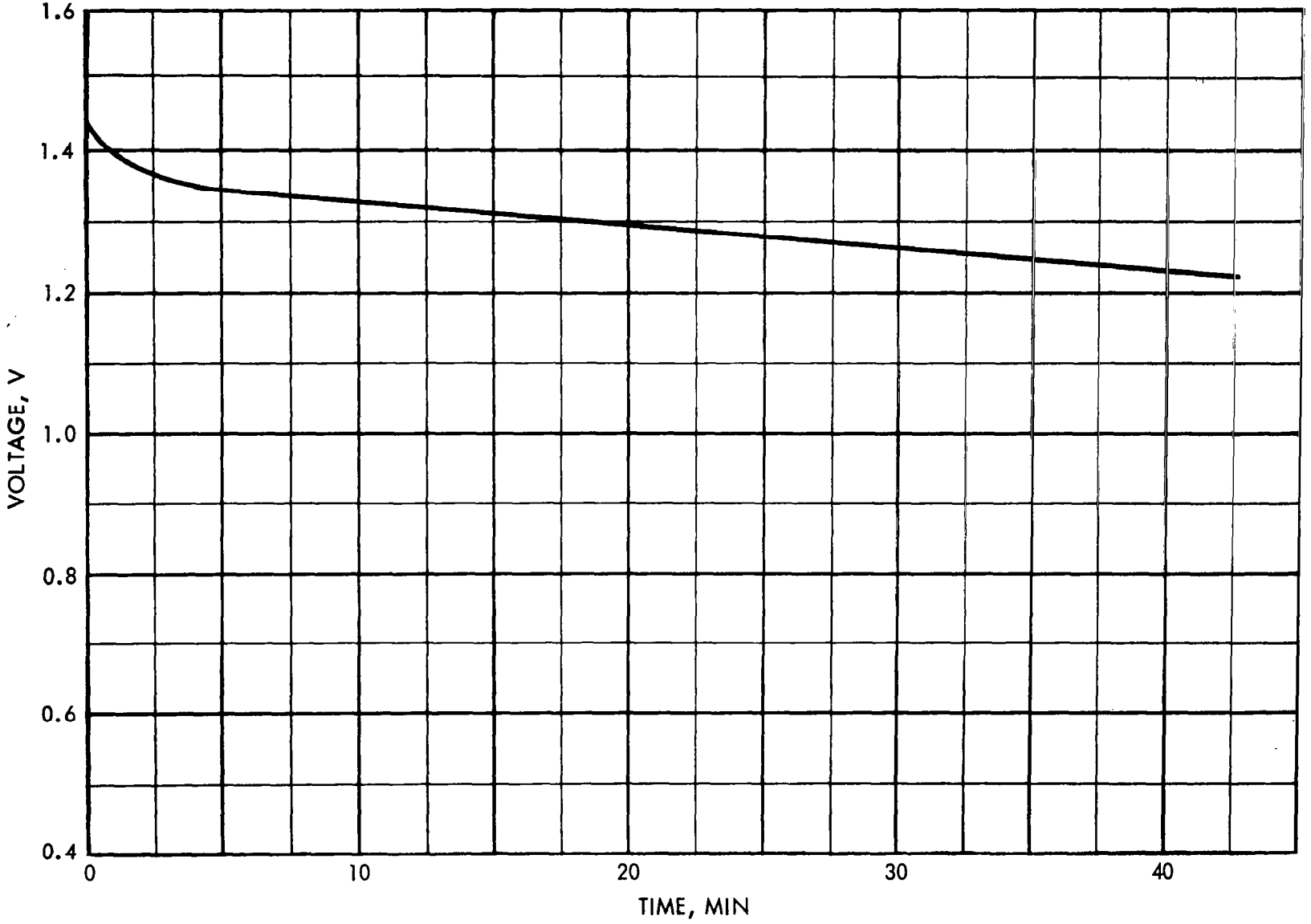

Figure 5-39. Nickel – Cadmium Battery, POGO Discharge Characteristic (7.9 Amp Discharge, 20 Amp-Hr Cell, 100°F, 27 % DOD Cycle No. 4502 (1/25/63), 26th Cycle After Reconditioning)

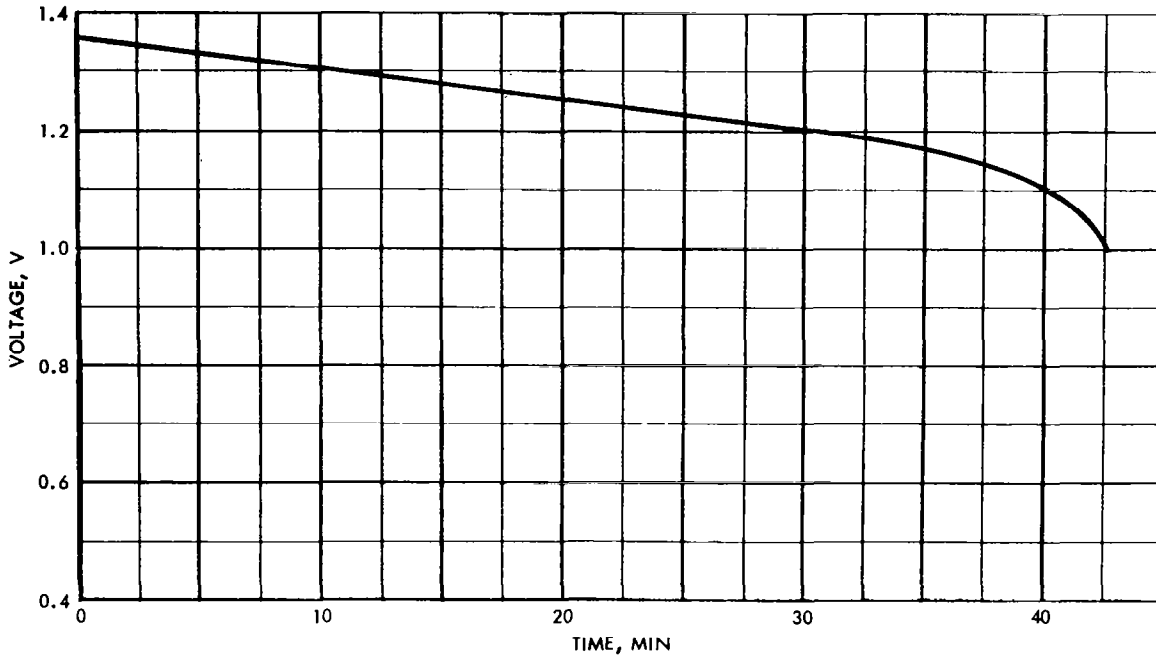

Figure 5-40. Nickel – Cadmium Battery, POGO Discharge Characteristic (7.9 Amp Discharge, 20 Amp-Hr Cell, 100°F, 27% DOD Cycle No. 5080 (3/7/63), 604th Cycle After Reconditioning

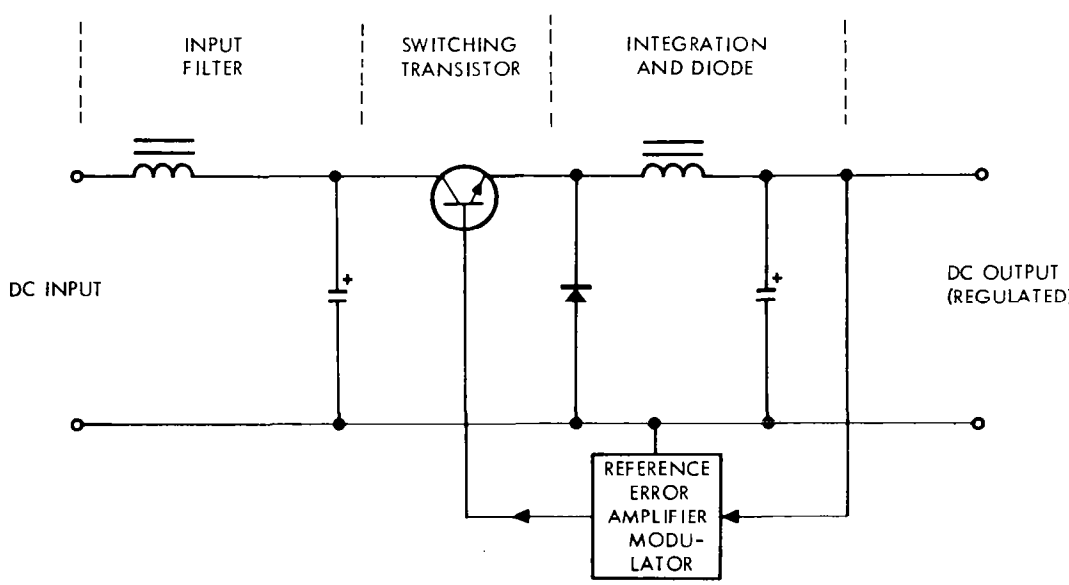

Figure 5-41. Typical Series Preregulator

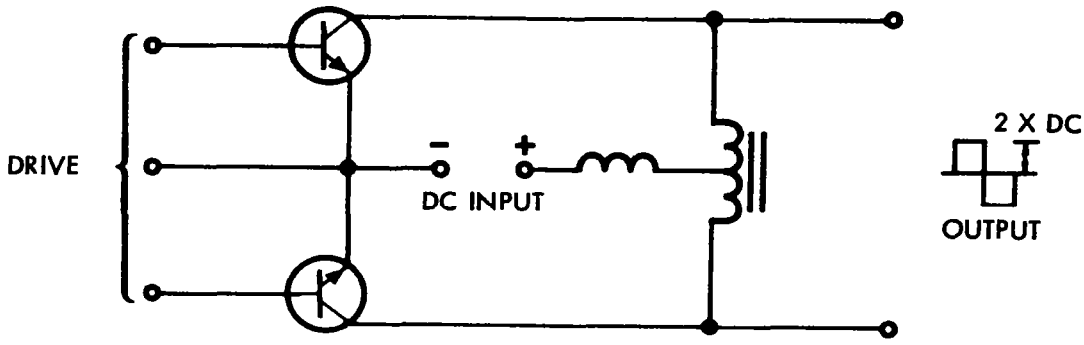

a) Chopper with Auto-Transformer

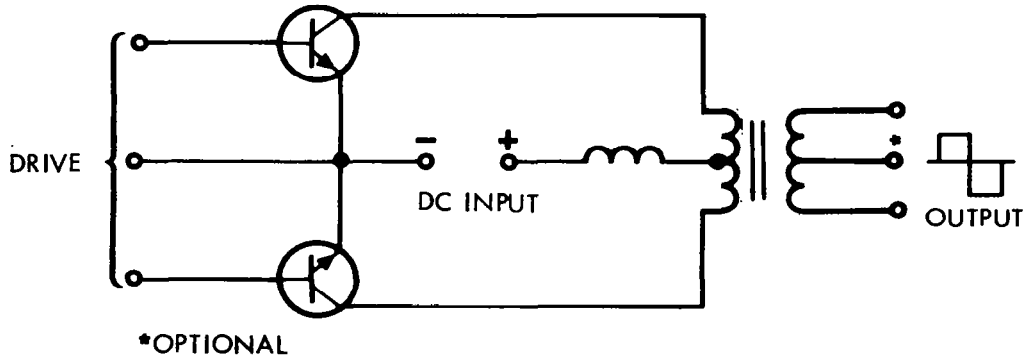

b) Chopper with Isolation Transformer

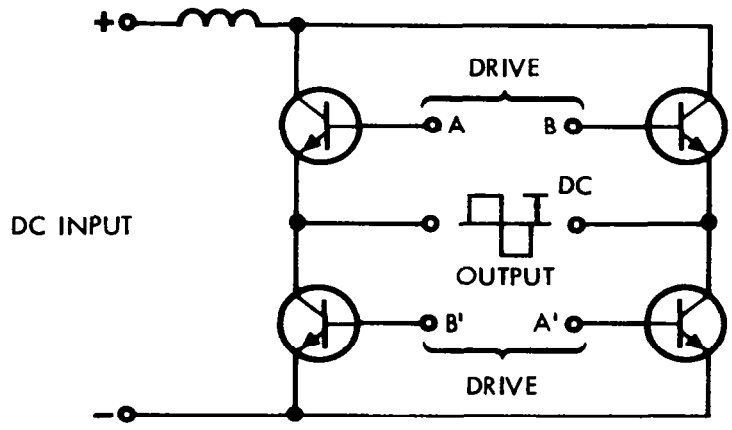

c) Bridge Chopper without Transformer

Figure 5-42. Types of Inverters

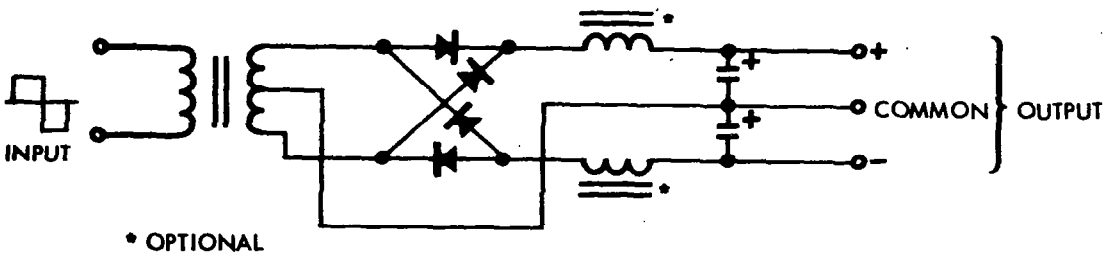

a) Equi-voltage, Duo-polarity Transformer Rectifier

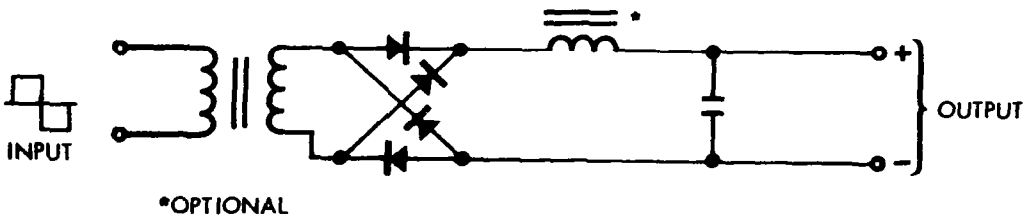

b) Bridge Circuit Transformer Rectifier

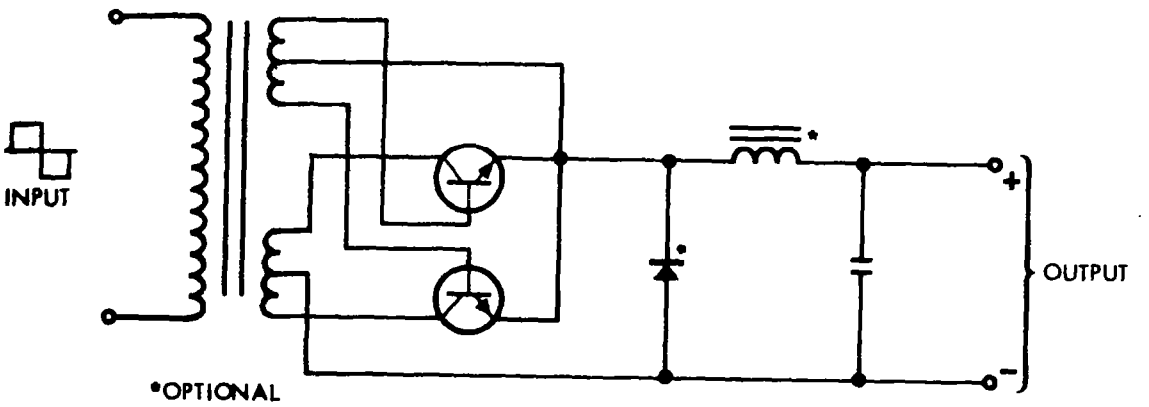

c) Synchronous Transformer Rectifier

Figure 5-43. Typical Transformer Rectifier Circuits

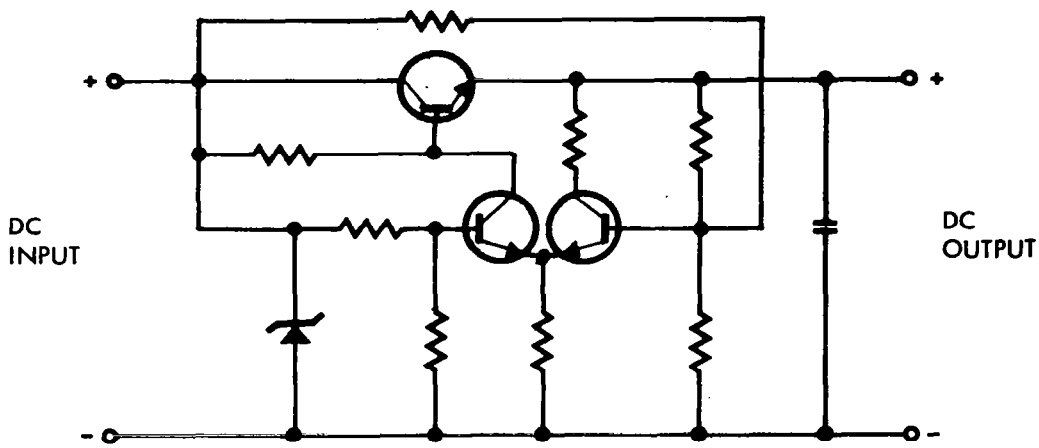

a) Typical Series Regulator

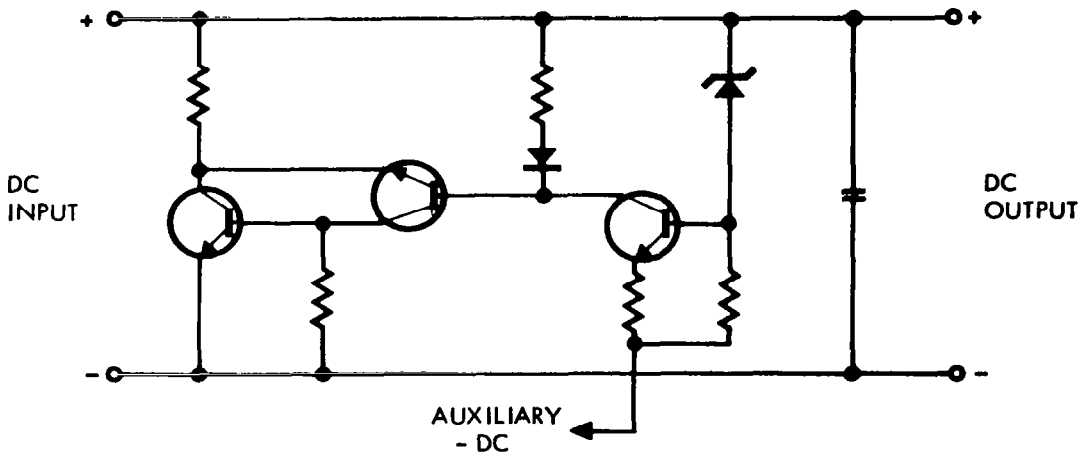

b) Typical Shunt Regulator

Figure 5-44. Active Filters

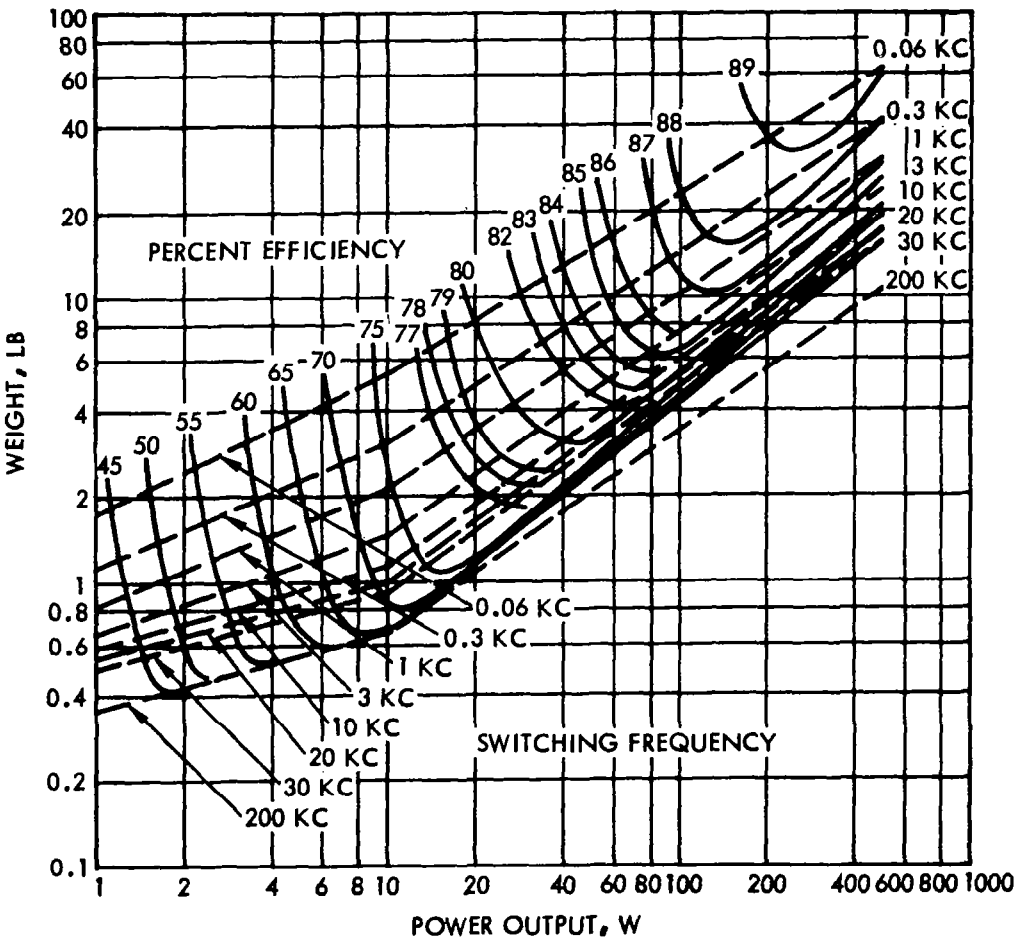

Figure 5-45. Parametric Data for DC-DC Converters

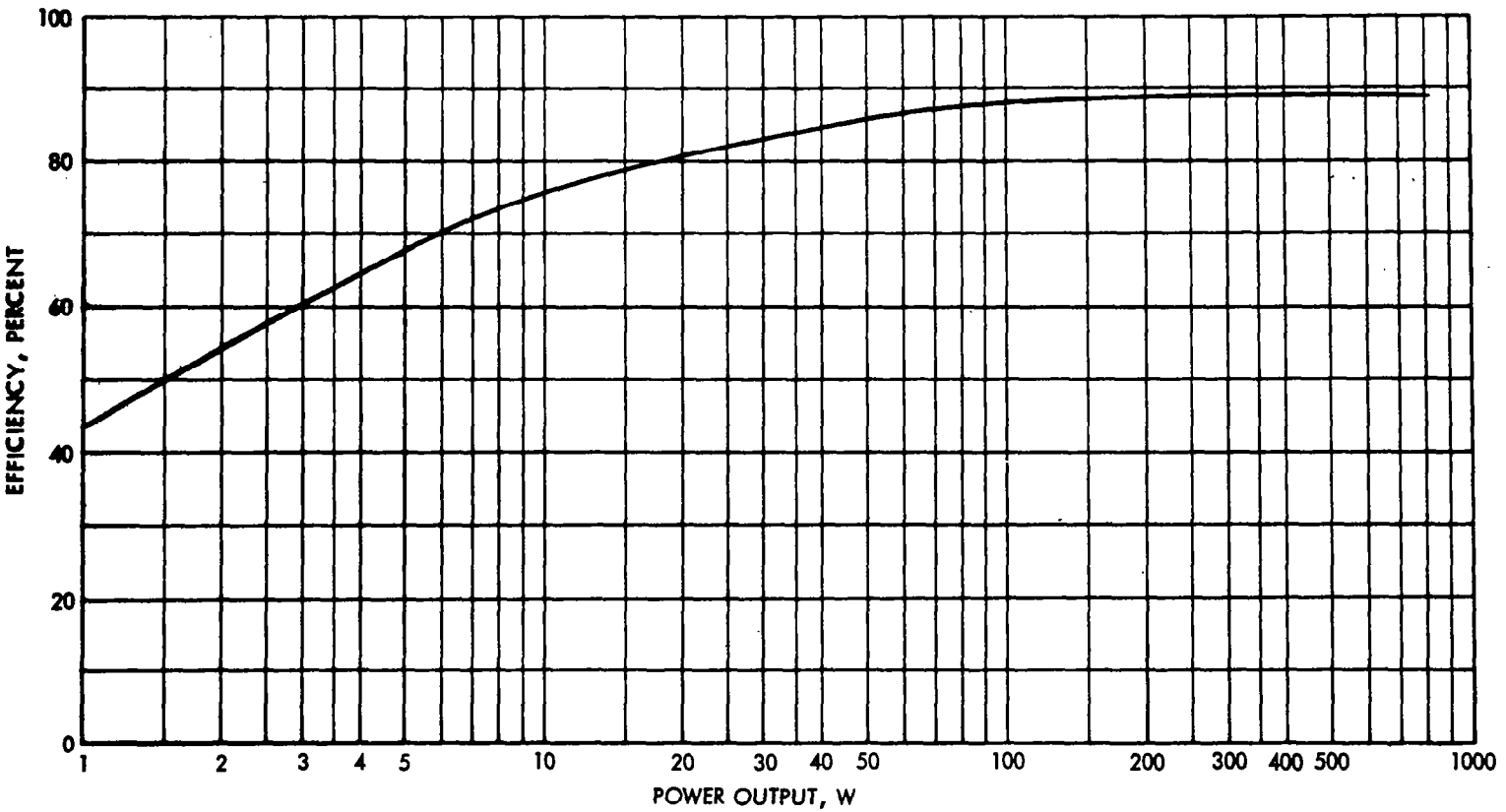

Figure 5-46. Maximum Efficiency Preregulated DC-DC Converters, 28 v Output

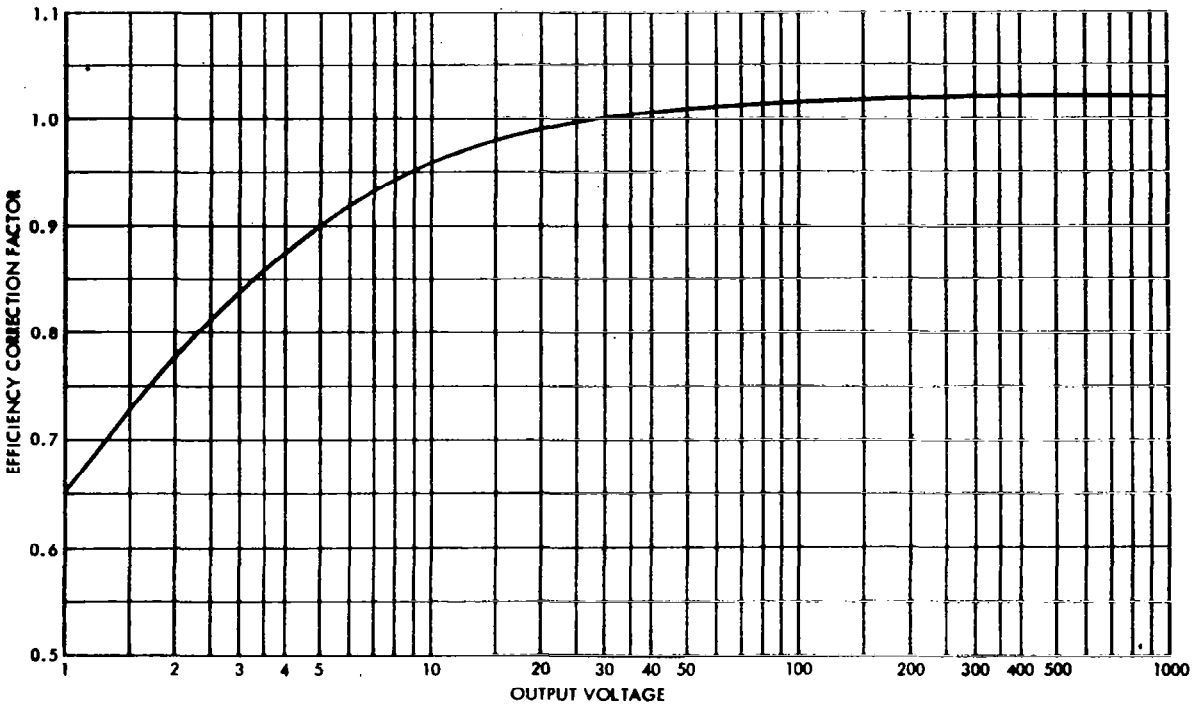

Figure 5-47. Efficiency Correction Factor for Non-28-v Output DC-DC Converters

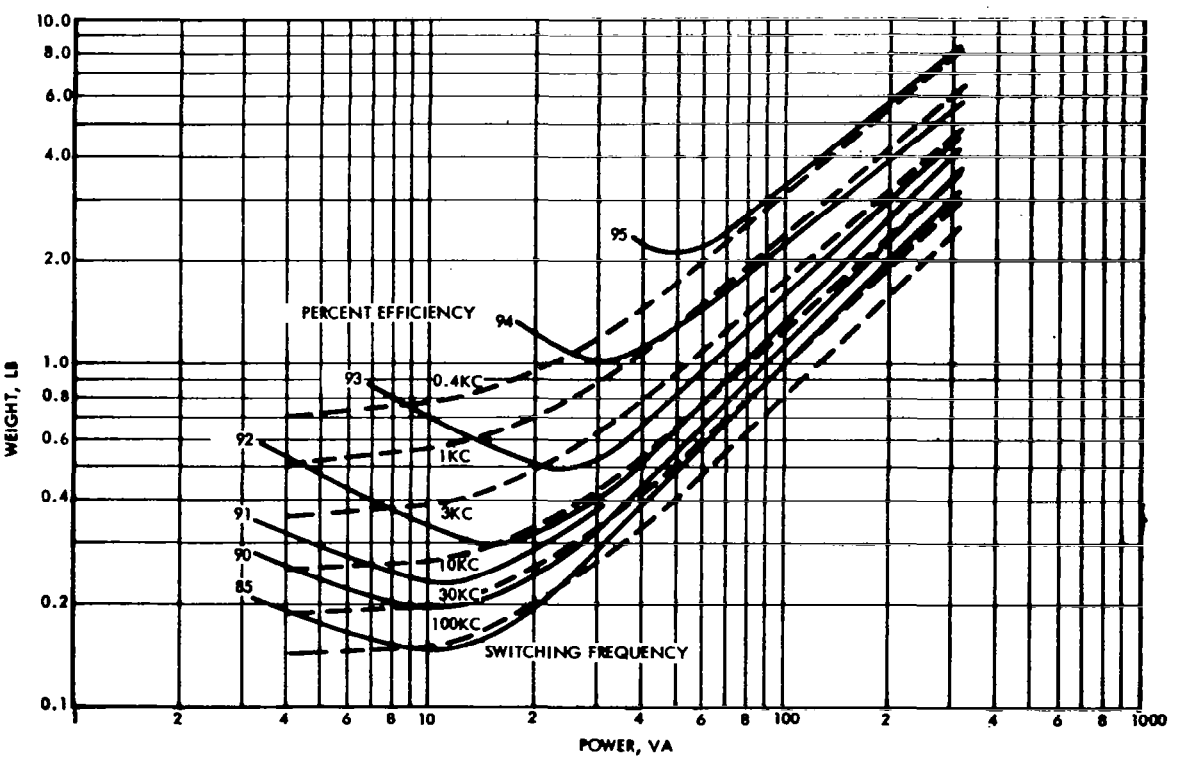

Figure 5-48. Inverters — Unregulated Squarewave Output

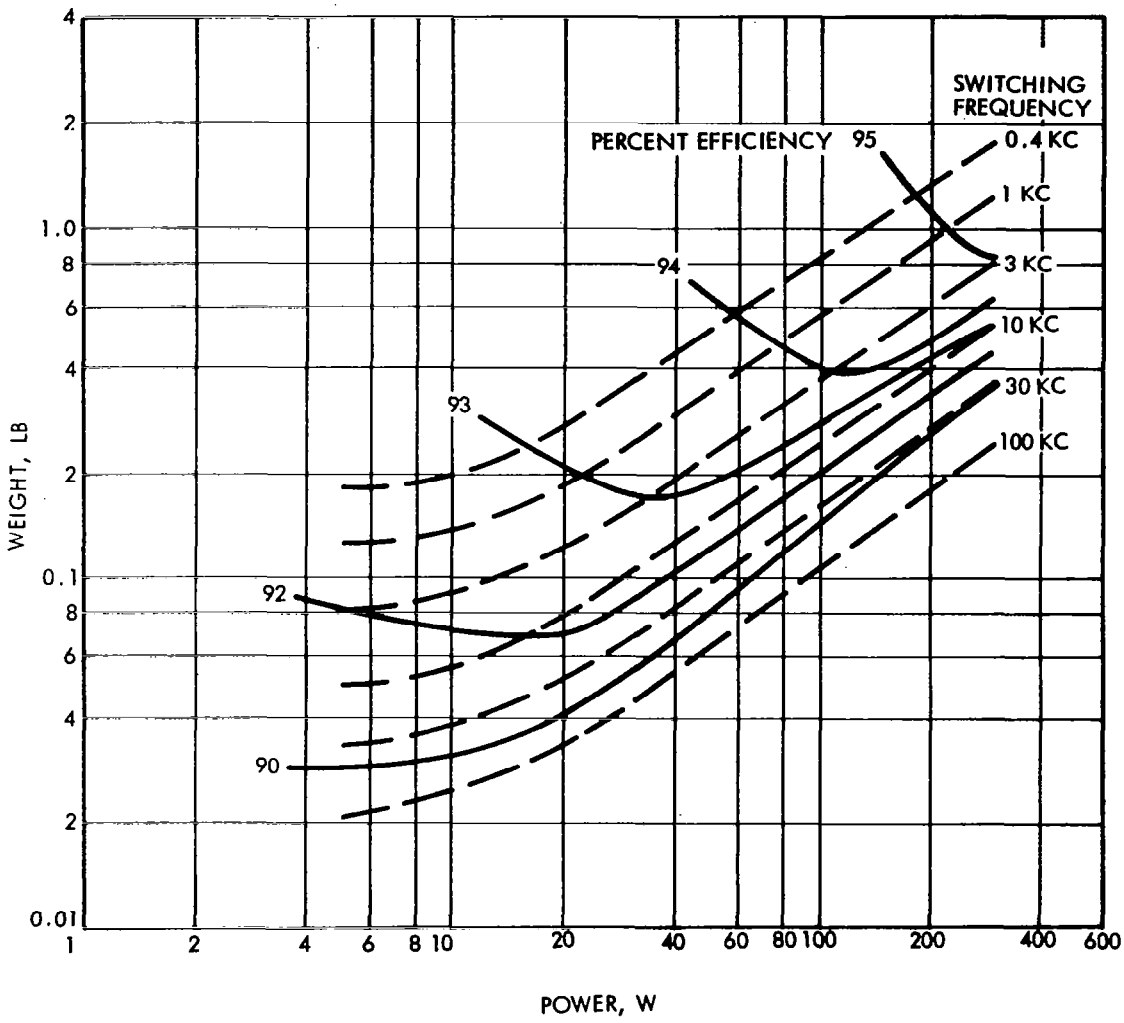

Figure 5-49. Data For TR Units

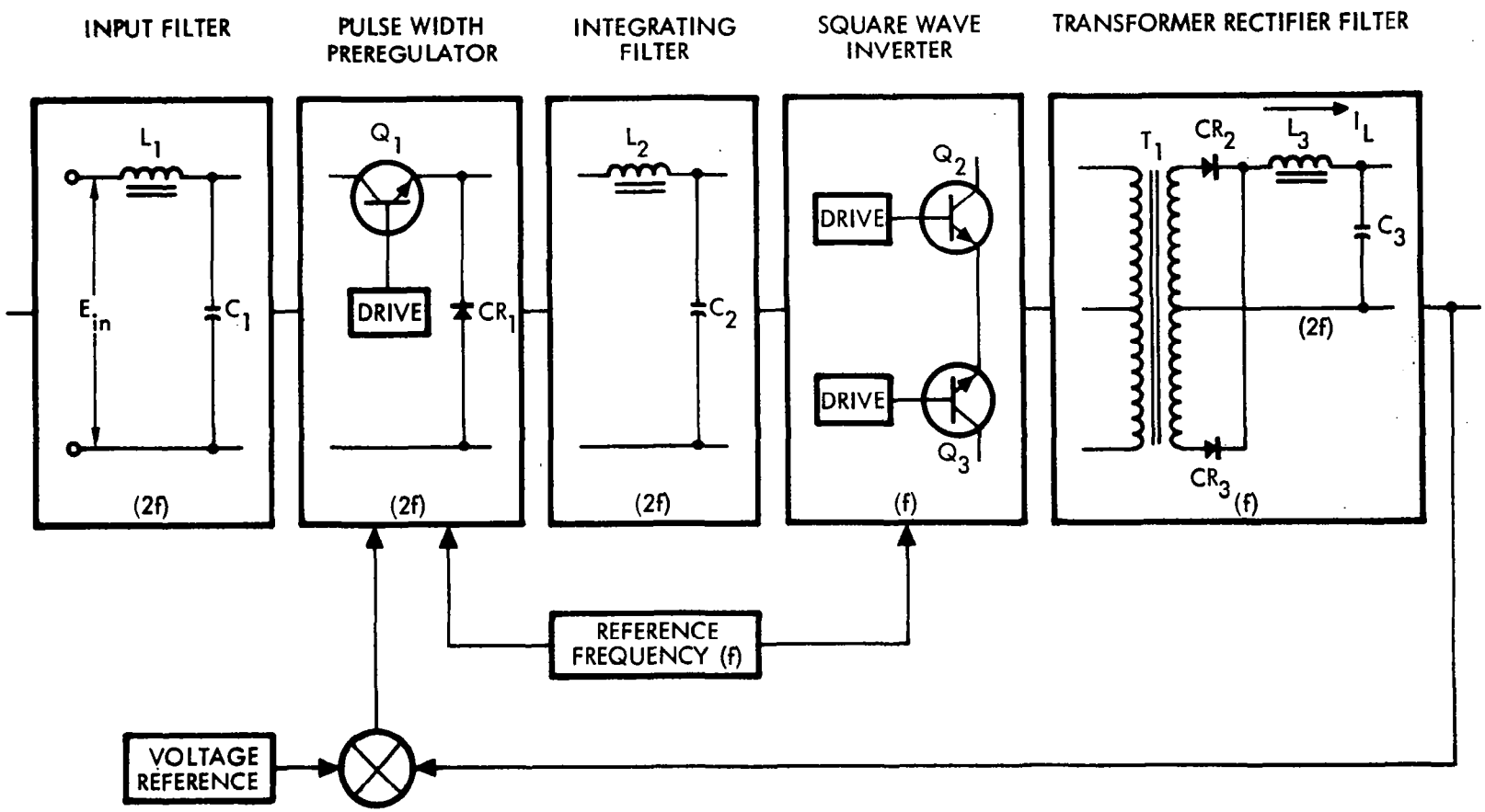

Figure 5-50. Block Diagram, RSWI Converter

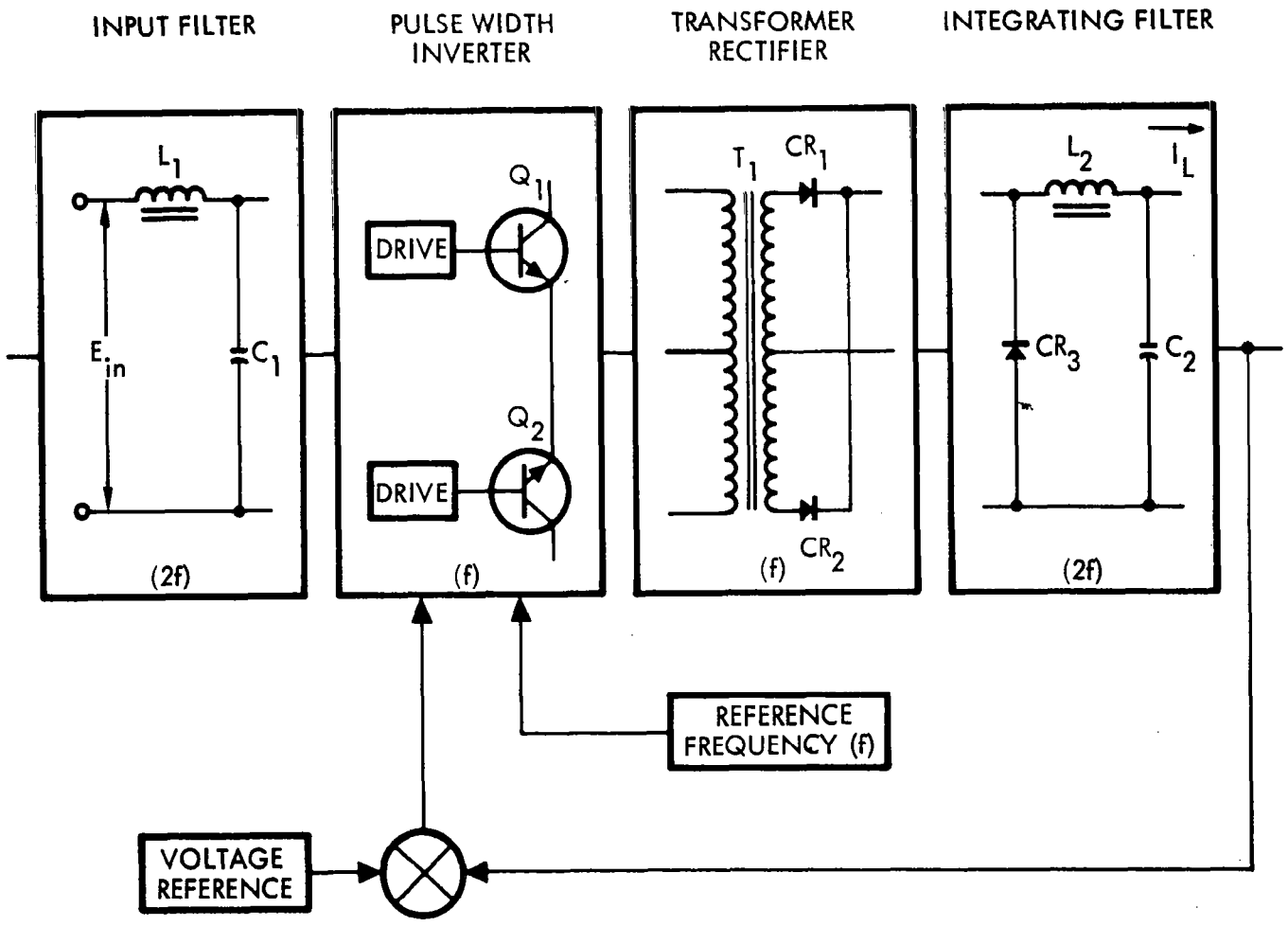

Figure 5-51. Block Diagram, PWI Converter

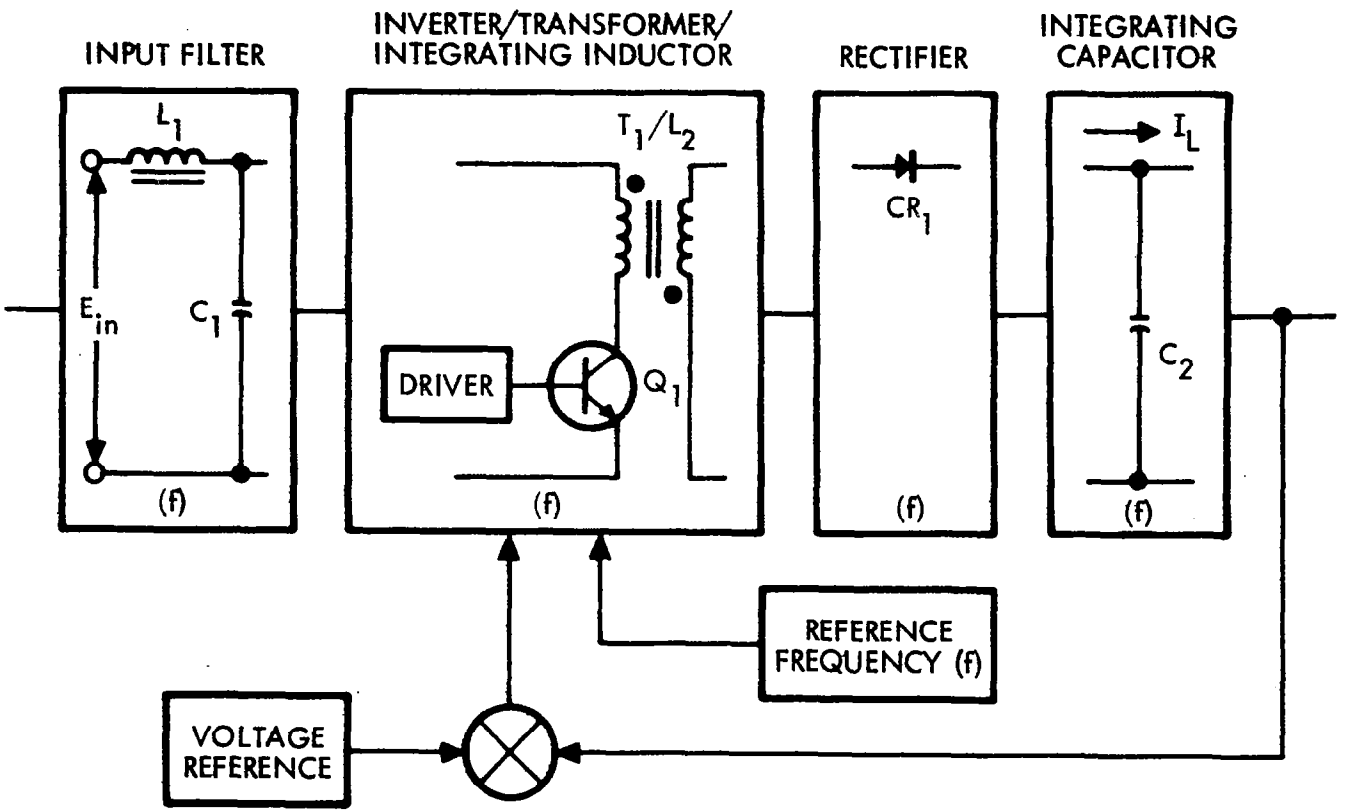

Figure 5-52. Block Diagram, ES Converter

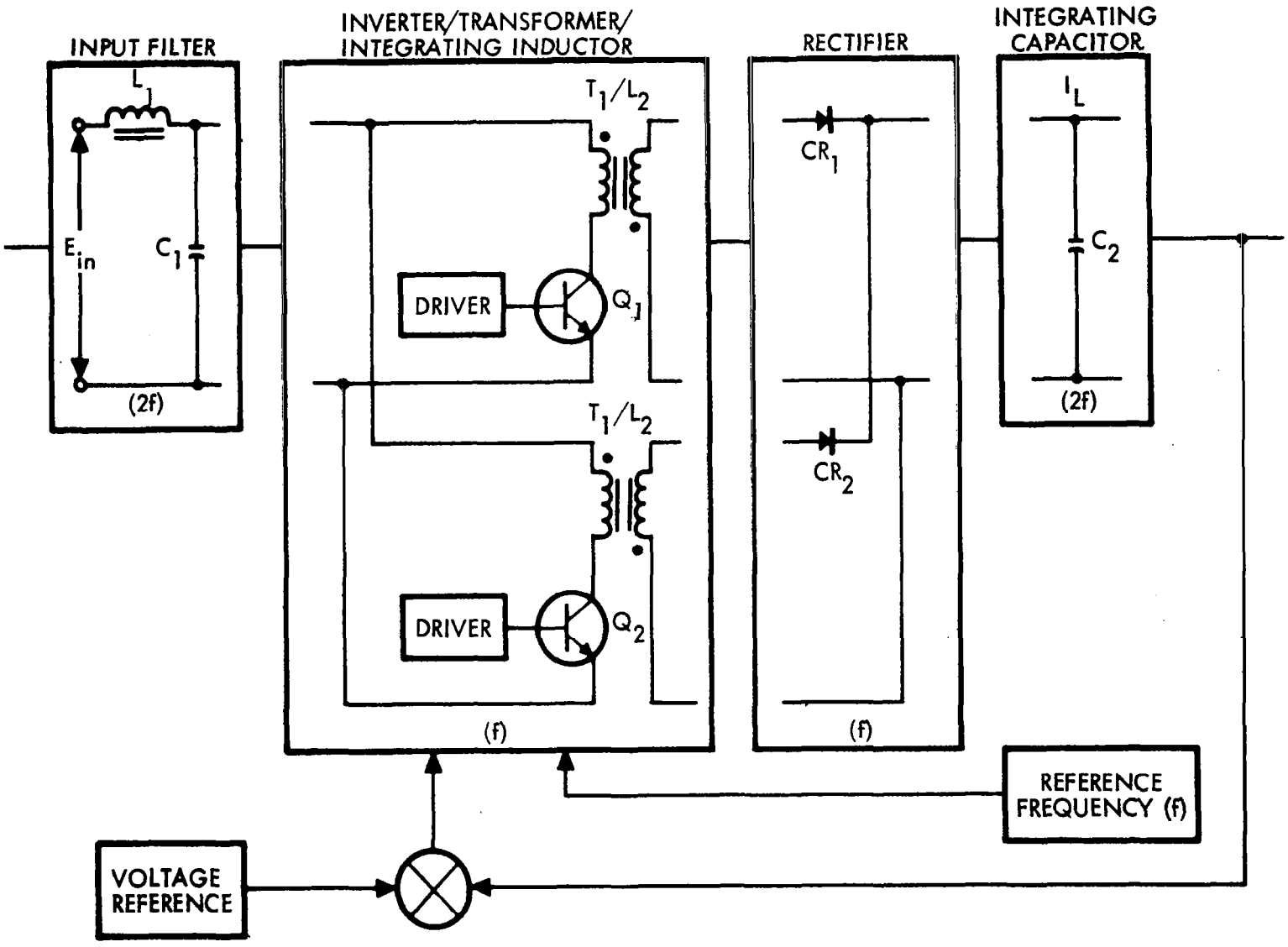

Figure 5-53. Block Diagram, ES Push-Pull Converter

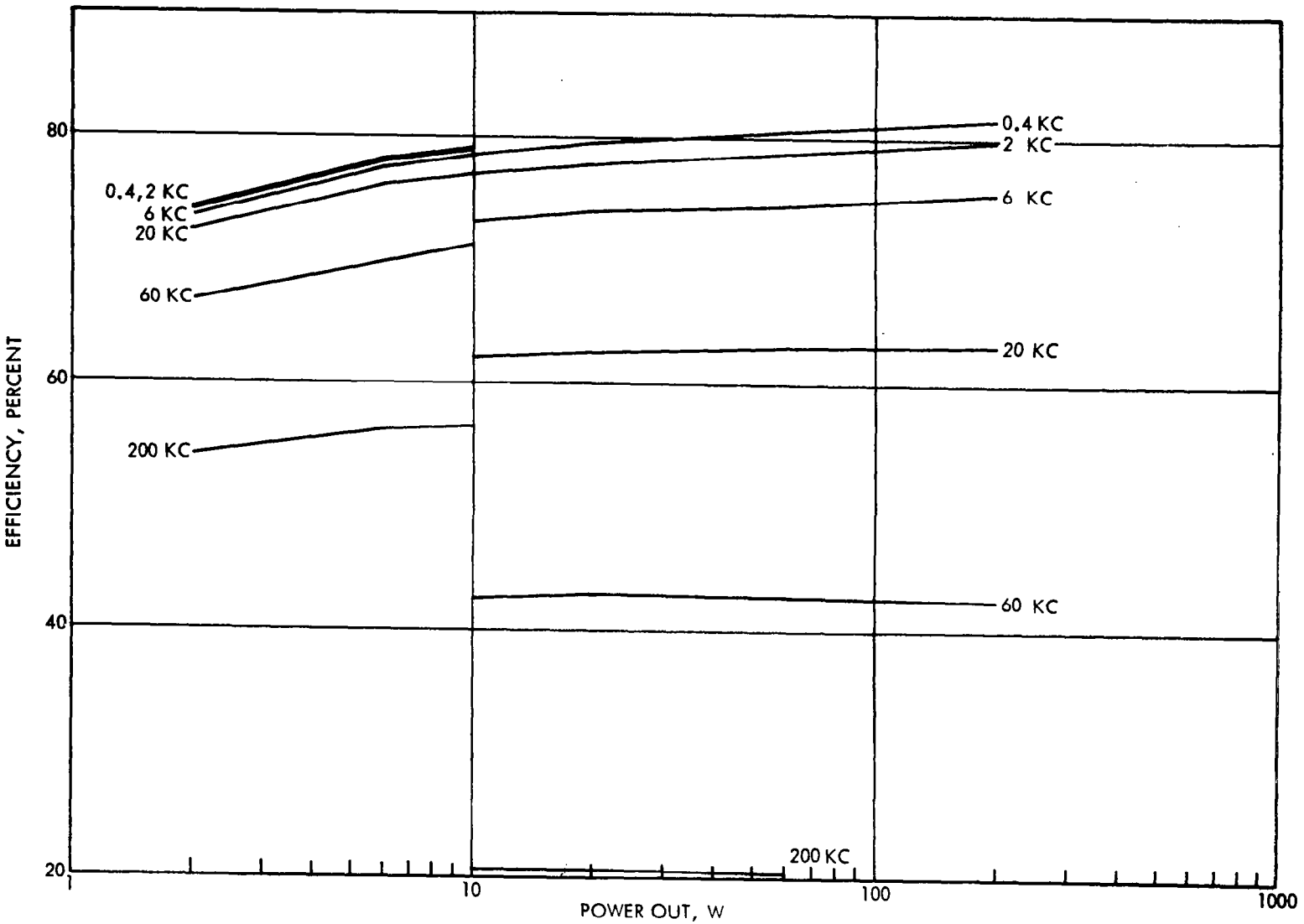

Figure 5-54. RSWI Converter, Efficiency Versus Power Output

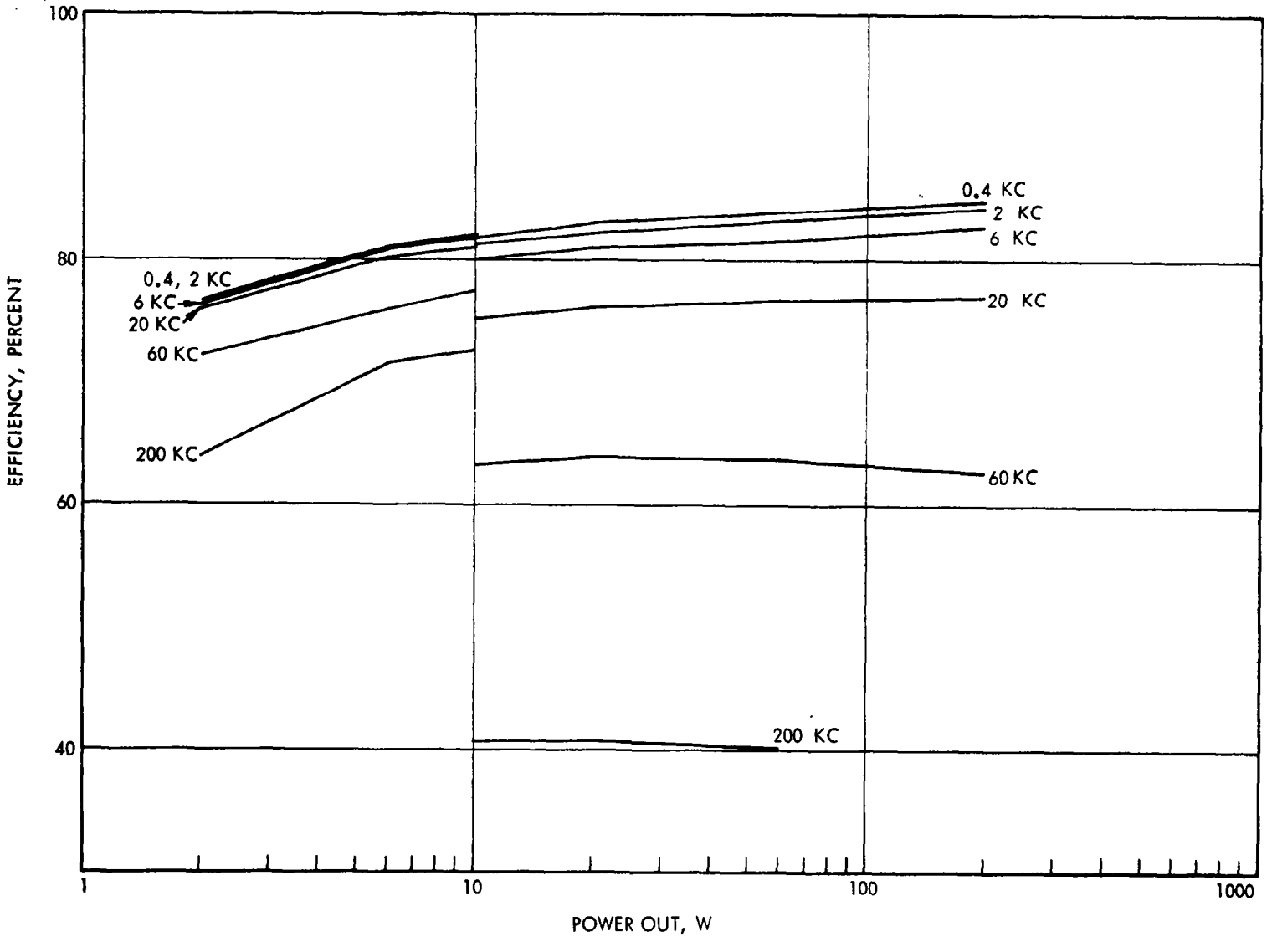

Figure 5-55. PWI Converter, Efficiency Versus Power Output

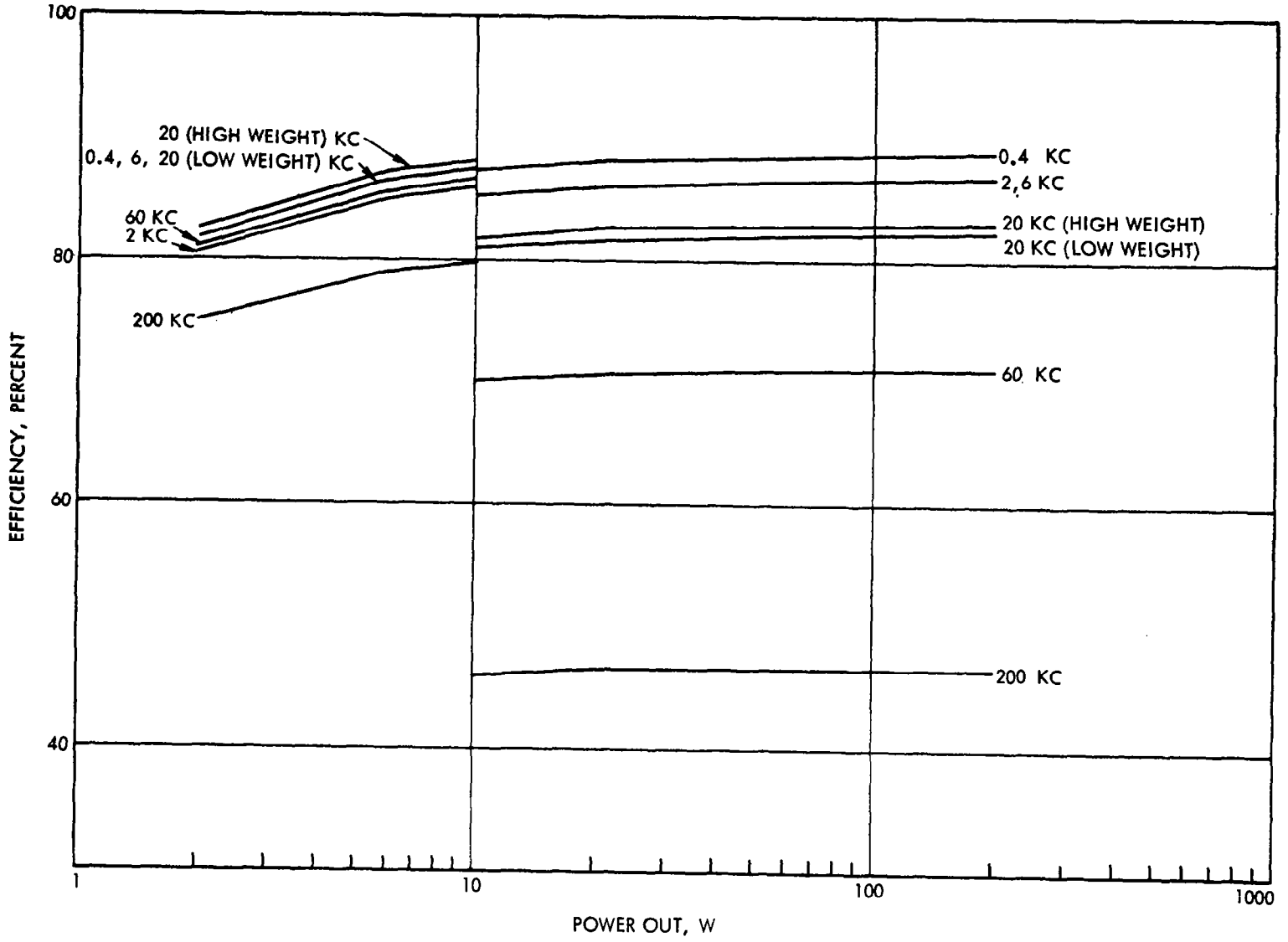

Figure 5-56. ES and Push-Pull ES Converter, Efficiency Versus Power Output

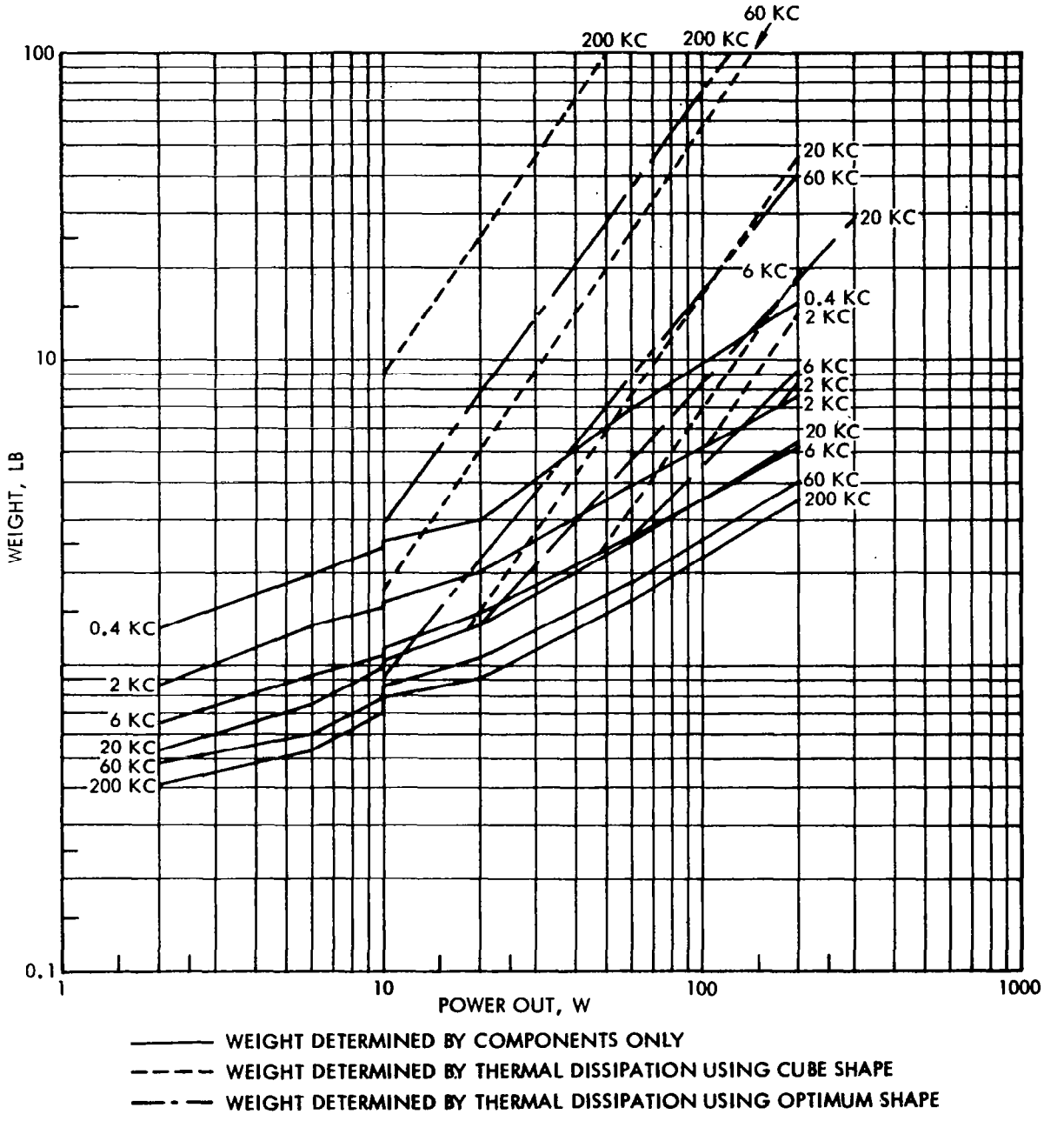

Figure 5-57. RSWI Converter Weight

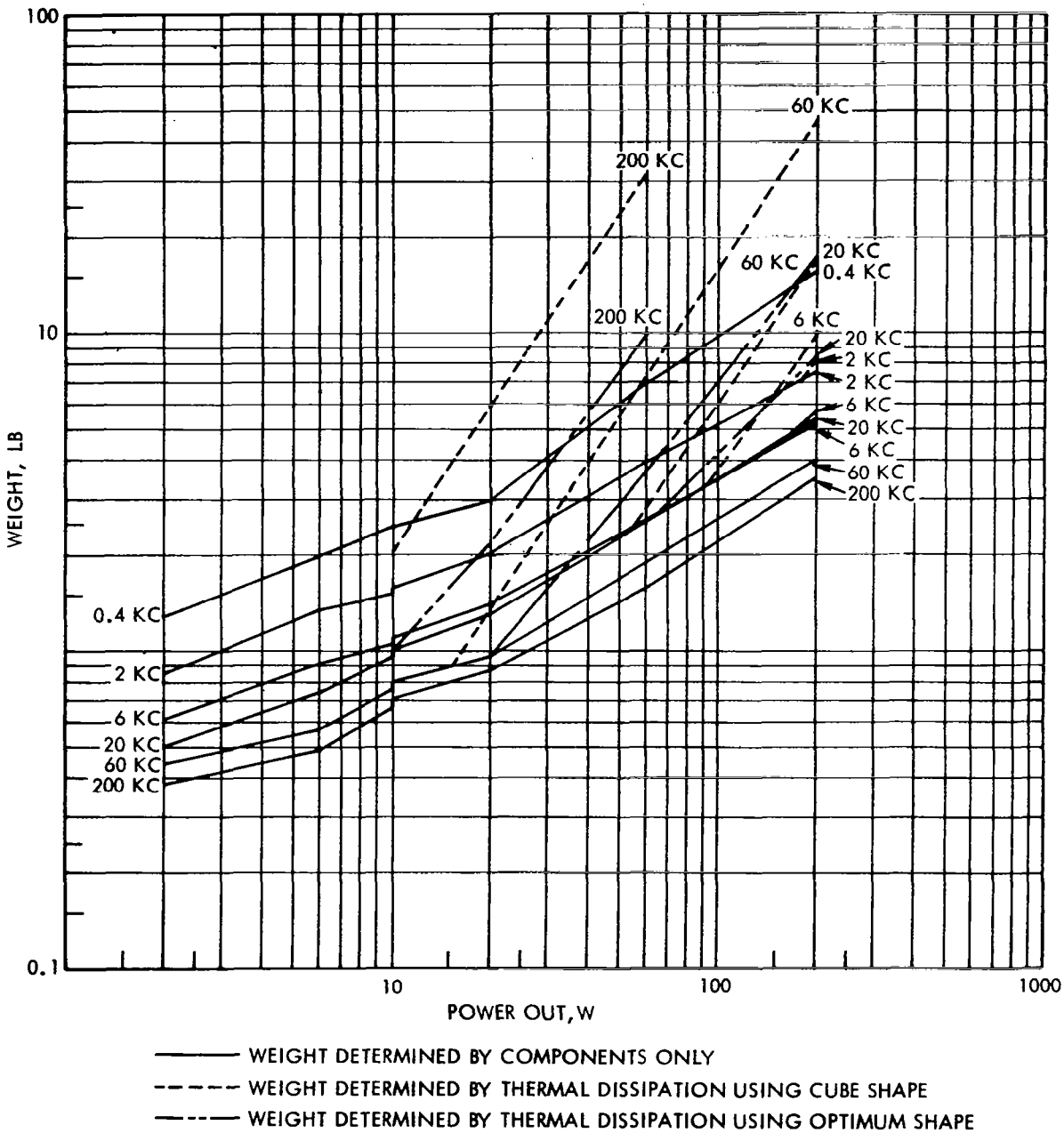

Figure 5-58. PWI Converter Weight

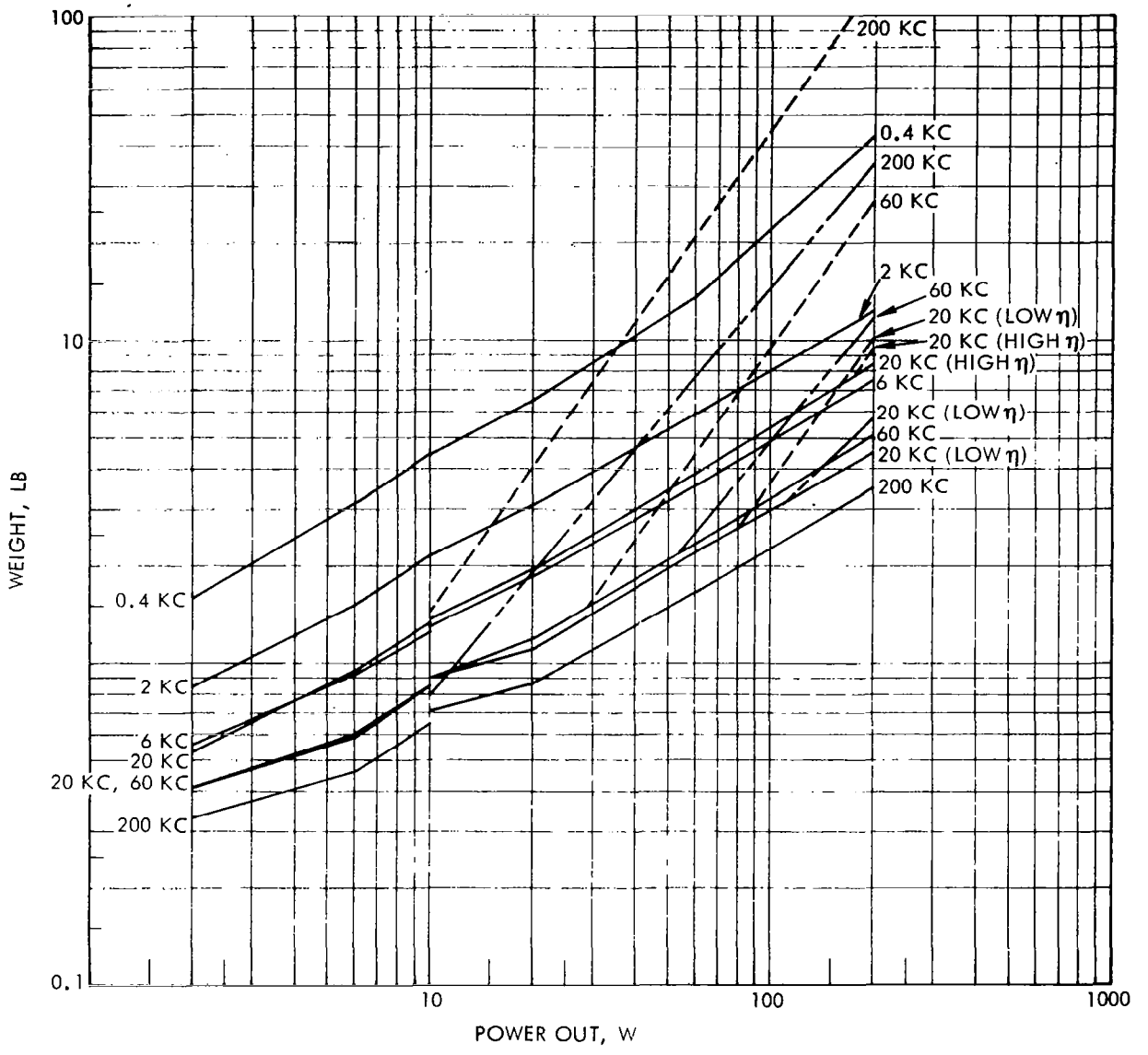

——— WEIGHT DETERMINED BY COMPONENTS ONLY

– – – – – WEIGHT DETERMINED BY THERMAL DISSIPATION USING CUBE SHAPE

———– – – WEIGHT DETERMINED BY THERMAL DISSIPATION USING OPTIMUM SHAPE

Figure 5-59. ES Converter Weight

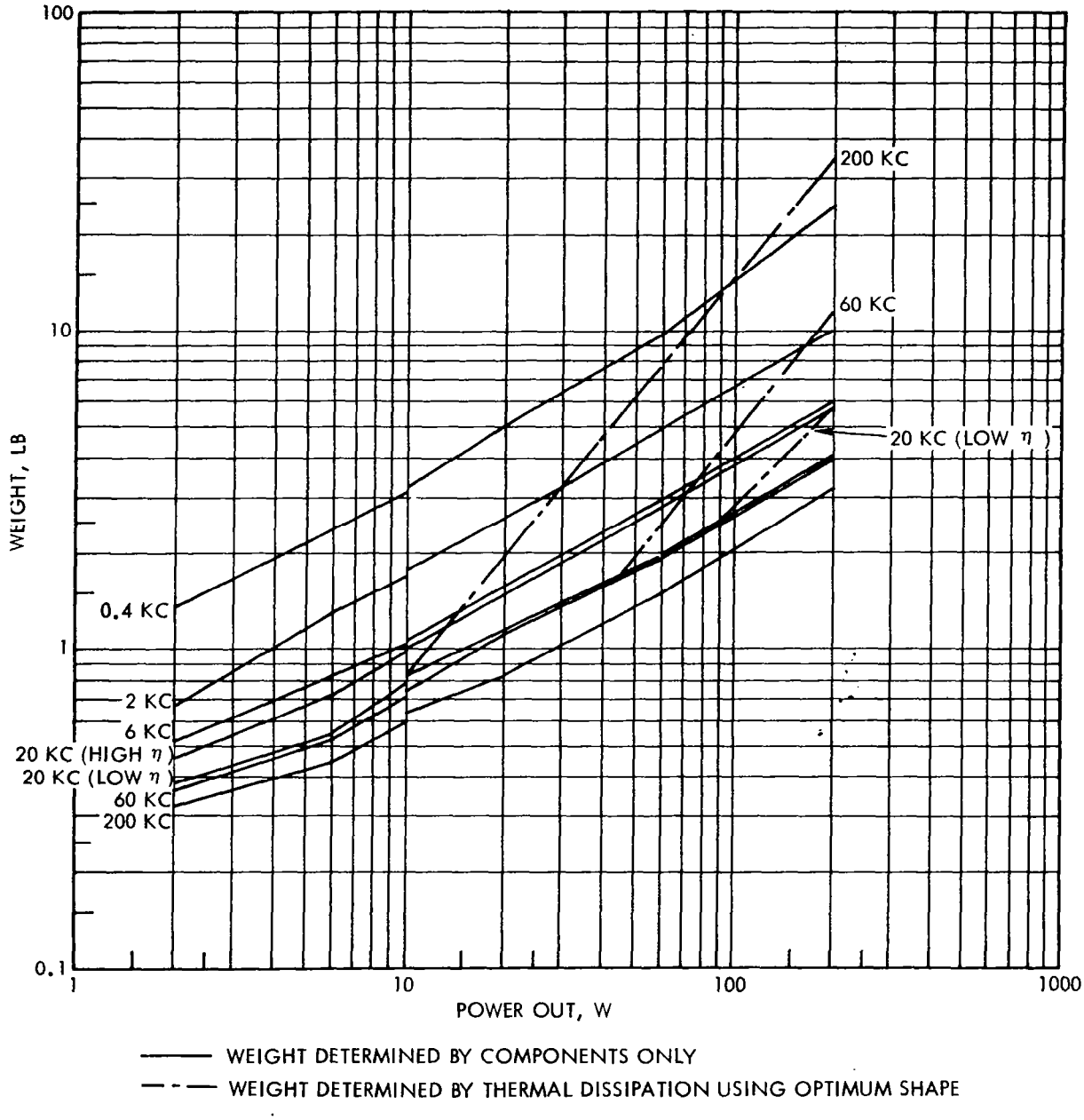

Figure 5-60. ES Push-Pull Converter Weight

6. ELECTRICAL POWER SYSTEM OPTIMIZATION METHOD (EPSOM)

6.1 GENERAL

Since 1957 the United States has launched over 350 unmanned spacecraft consisting of many types with a large variety of mission objectives. Relatively few of these spacecraft have been of identical design although a great number of the missions have had similar overall requirements. Each spacecraft has contained its own custom-designed electrical power system. These have ranged from simple battery packs to relatively complex combinations of solar array, battery, and nuclear power source. The large assortment of power system designs can be attributed to the following major factors.

- Diversified mission requirements
- Different orbits
- Variety of vehicle designs
- Various methods of attitude control
- Changing state-of-the-art in power system components
- Different power system designers with varied experience and convictions
- Lack of standardization

After nine years of accumulated satellite design experience, these questions arise:

- Is the power system design of today better than yesterday's?
- Is today's power system design the best that the state-of-the-art will allow?
- Is today's power system design being used to its maximum capability?
- How can these questions be answered objectively?

This study program - Satellite Power Systems Configurations for Maximum Utilization of Power - is an attempt to answer these questions and establish an objective method for continuously evaluating power system designs.

EPSOM is one technique of directly comparing two or more power system designs on the basis of any one optimization criterion. Proper use of state-of-the-art parametric data permits an ordered objective comparison among those designs evaluated. The technique is based upon the logical step-by-step process which a power system designer normally uses for analysis and optimization. This process has been reduced to mathematical equations which can be evaluated to determine the relative maximum utilization of power for those power system designs under consideration. As a preliminary part of the comparative analysis optimization, the design parametric data for each type of equipment is analysed to determine its own optimization interactions (Parametric Sub-optimization Data). This information is then reduced to rules of thumb called Design Optimization Guidelines. The second preparatory part of EPSOM - Power Requirement Organization - is the establishment of a systematic method of analyzing spacecraft power requirements so that various power system designs can be synthesized. The synthesized power designs will tend to be close to the optimum because the aggregate Design Optimization Guidelines form the basis for organizing the power requirements into groups that should provide the better performance for the chosen criteria.

Figure 6-1 is an information flow diagram showing the total optimization process and how the various steps relate to each other. Starting from the left, the input information required for designing the power system is represented by the three boxes - Mission Definition and Constraints, Power Profile and Requirements, and the Optimization Criteria. From this information a broad concept of the power system can be formulated, i.e. the general type of energy source, the need for energy storage, and the degree of regulation and power conditioning. Knowing the possible constituents for the power system, idealized or limiting performance designs for each type of equipment are formulated. These idealized designs are defined within the constraints established by the mission. The applicable parametric data for each of these equipments are then independently analyzed to determine the best operating conditions which would enhance the optimization. These conditions constitute the

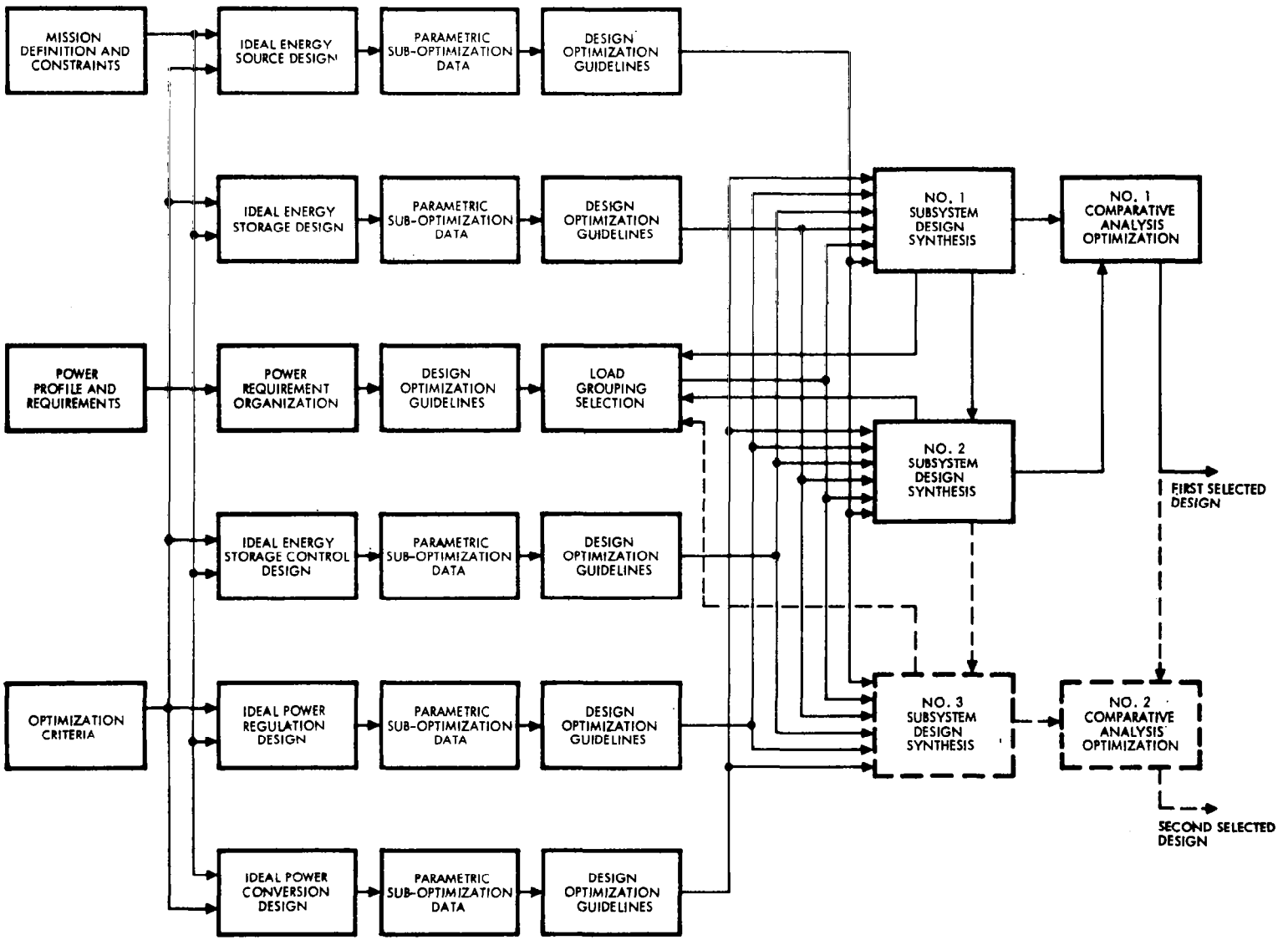

Figure 6-1. Optimization Flow Diagram

Parametric Suboptimization Data from which the Design Optimization Guidelines can be generated for each type of equipment.

The satellite electrical power requirements and profile are next analysed to determine the organization or grouping which takes advantage of the equipment suboptimization information. Sometimes the Design Optimization Guidelines for two or more equipments are in conflict. A compromise in the Design Optimization Guidelines is then necessary for the conceptual power system design taking into consideration the information provided by the power profile and requirements. These guidelines permit an orderly organization of the power requirements and provide the logic for modifying the idealized equipment designs to minimize the loss in performance.

The organization of power requirements provides one or more groupings of the loads such that the required types of power system equipment can be selected and synthesized into one or more power system configuration. The performance values, enhancing the primary optimization criterion, are determined from the parametric data for each of the selected equipments.

- The performance values are then mathematically combined into a system performance number, such as percent efficiency, for each of the synthesized configurations. Direct comparison of these system performance numbers provides a relative evaluation of the proposed configurations.

- Additional system configurations may be suggested during this Comparative Analysis Optimization and introduced into the evaluation process. Continuing iterations for candidate configurations can be made, evaluated, and compared until the maximum performance system is identified.

- The numerical value obtained for this optimum configuration is directly related to the accuracy of the equipment parametric data used. However, the relative comparison of these numbers among the candidate configurations is objectively correct since the same set of parametric data is used for all configurations.

When all configurations have been evaluated and ranked for the primary optimization criterion, such as efficiency, the complementary performance values for the secondary criteria (for example, weight) can be determined from the same parametric data at the previously established

operating points. Thus, a complete performance picture related to both primary and secondary criteria (e.g., efficiency and weight) is available.

6.2 INPUTS TO ELECTRICAL POWER SYSTEM DESIGN

Design of a satellite electrical power system is strongly influenced by the defined mission and the specified electrical load requirements. The important parameters specified by the mission definition which directly affect the electrical power system design are:

- Orbit ephemerides
- Type of payload
- Operating life
- Reliability
- Maximum spacecraft weight and envelope

Indirectly, these same parameters may further restrict the power system design by the limitations they pose upon other major subsystems. For example, the type of payload and orbit ephemerides may limit the choice of vehicle attitude control, which in turn could restrict the use of one or more solar array configurations. The following factors are typical of these intermediate mission constraints bearing upon the power system design:

- Type of attitude control
- Shape of the vehicle structure
- Antenna size, shape, and directionality
- Vehicle orientation
- Payload location and orientation requirements

The electrical load requirements usually control the choice of power conditioning equipment. The following load characteristics limit the choice of power conditioning equipment and the suitable configurations:

- Voltages
- Voltage regulation
- Average and peak power
- Orbital duty cycle
- Frequency
- Frequency regulation

- Ripple and noise
- EMC (electromagnetic compatibility)
- Over-load protection
- Over - and/under - voltage susceptibility

Within these bounds the system designer is free to choose the state-of-the-art designs and configurations which best satisfy the stated optimization criteria. The optimization criteria are usually established at the mission and/or spacecraft system level. Performance may be optimized for a specified mission to one or more of the following criteria:

- Efficiency
- Weight
- Reliability
- Volume
- Cost

Often the optimization of one performance parameter requires the compromise of one or more of the others. At other times, optimization of one parameter contributes to the optimization of another. Maximization of equipment efficiency usually approaches the minimum weight and volume design for the power system.

6.3 PERFORMANCE LIMITS OF IDEALIZED EQUIPMENT DESIGNS*

Although the technological state-of-the-art is improving each year, there have been no significant break throughs which would alter the performance boundaries for idealized designs. The following performance factors provide upper limits for some of the more common electrical power system equipments.

6.3.1 Energy Sources

Photovoltaic energy sources operating in near-earth space have the idealized performance limits which normally can not be exceeded with state-of-the-art hardware, as shown in Table 6-I.

*Do not use the performance values from this section for design purposes.

Table 6-I. Solar Array Idealized Performance Factors

	W/lb	W/sqft
Oriented panels	15	13
Fixed paddles	5	5
Body mounted	6	4

In practice, each of these array types will have performance values less than those listed because of the orbital requirements and/or thermal designs.

6.3.2 Energy Source or Storage Controls

Performance values for energy source controls are a function of several power system variables: power, load changes, voltage, switching, frequency, temperature, and type of circuit. The maximum efficiency that can be expected under ideal operating conditions is approximately 98 percent. The maximum average efficiency over all operating conditions is in the neighborhood of 94 to 96 percent. Equipment weights for source and storage controls vary over a very large range, depending upon the component and circuit selection. The values presented in Table 6-II indicate the performance spread in w/lb for the more optimistic designs as a function of output power.

6.3.3 Energy Storage

The three common satellite battery types have the following idealized performance factors shown in Table 6-III.

Amp-hr and watt-hr efficiencies for each of these battery types are strongly affected by the specific application and operating conditions as shown by the parametric data of Section 5.4.

Table 6-II. Energy Source or Storage Control Idealized Weight Factors

	Power Output (w)						
	1	5	10	20	50	100	200
w/lb	3	10	17	18	20	25	30

Table 6-III. Packaged Battery Idealized Performance Factors

Type	Energy Density (w-hrs/lb)	Amp-hr Efficiency (percent)	W-hr Efficiency (percent)
Silver zinc, primary	100	-	-
Silver cadmium, secondary	35	98	77
Nickel cadmium, secondary	20	98	88

6.3.4 Power Conditioning Equipment

Parametric data presented in Subsection 5.6 for the power conditioning equipment indicates a broad range of performance factors. Table 6-IV summarizes the more idealistic values for each type of equipment.

6.3.5 Power Distribution Equipment

Typical harness weight as a function of power system output power ranges between 2 and 7 w/lb. An idealistic value of 10 w output per lb of harness weight would apply to most satellite designs.

Performance factors for power switching, under- and over-voltage protection, telemetry sensors, etc. are very difficult to generalize, since mission requirements usually control the need for this equipment rather than any one power system characteristic. The estimated weight per lb of power system weight for existing satellites ranges between 4 and 10 percent. Therefore, an idealistic value might be in the neighborhood of 2 percent.

Table 6-IV. Power Conditioning Equipment Idealized Performance Factors

Type	Power Density (w/lb)	Efficiency (percent)
TR-Unit	2000	98
Regulator	250	98
Inverter	150	96
Converter	50	92

6.4 PARAMETRIC SUBOPTIMIZATION DATA

Parametric suboptimization data is parametric data such as presented in Section 5 after all of the parameter interactions have been considered and properly weighed for each optimization criterion. For example, Table 5-V presents converter suboptimization data which provide the minimum equipment weight. As in this example, the suboptimization data are usually defined for discrete bands of power, frequency, and for a specific circuit or configuration.

Processing all of the parametric data provided in Section 5 into parametric suboptimization data represents an enormous quantity of combinations and permutations. Experience has shown that the necessary data can best be derived from the broad parametric data when the scope of interest has been narrowed by specific mission constraints and power requirements and when the optimization criteria have been stated. Several examples of parametric suboptimization data have been included in Section 5 where the parameter interactions were not obvious.

6.5 DESIGN OPTIMIZATION GUIDELINES

Design optimization guidelines follow directly from the parametric suboptimization data. Hence, the compilation would be large and appear contradictory in its totality unless clearly catalogued for each specific design situation.

The following are generalized optimization guidelines some of which apply to the equipment design level, and others to the power system level. Guidelines for power requirements organization are included in Paragraph 6.6.

6.5.1 Power Conditioning Equipment

- Efficiency usually improves as the following parameters change:

  Increased – output power, input voltage, output voltage

  Decreased – switching frequency, operating temperature range, EMI requirements, ripple requirements, input voltage range, output voltage regulation requirements, dynamic loads, ambient temperature, number of outputs

Input to output voltage ratio approaches unity for transformerless circuits

Dissipative circuits are replaced with nondissipative circuits

- Weight usually decreases as the following parameters change:

  Increased – switching frequency, input voltage output voltage

  Decreased – output power, output voltage regulation requirements, operating temperature range, EMI requirements, ripple requirements, dynamic loads, ambient temperature, input voltage range, number of outputs

  Input to output voltage ratio approaches unity for transformerless circuits

  Dissipative circuits are replaced with nondissipative circuits

- Reliability usually increases as the following parameters change:

  Increased – efficiency, redundancy

  Decreased – operating temperature range, EMI requirements, ambient temperature, number of outputs, parts count, power dissipation.

6.5.2 Batteries

- Efficiency usually improves as the following parameters change:

  Increased – depth of discharge (AgCd, NiCd), charge or discharge operating temperature (AgCd), operating temperature during discharge (NiCd), charge rate(NiCd)

  Decreased – cycle life (AgCd, NiCd), discharge rate (AgCd, NiCd), charge rate (AgCd), operating temperature during charge (NiCd)

- Weight usually decreases as the following parameters change:

  Increased – depth of discharge (AgCd, NiCd), charge or discharge operating temperature (AgCd), operating temperature during discharge (NiCd), charge rate (NiCd)

Decreased – cycle life (AgCd, NiCd), energy storage requirements (AgCd, NiCd), discharge rate (AgCd, NiCd), charge rate (AgCd), operating temperature during charge (NiCd)

- Reliability usually improves as the following parameters change:

  Increased – temperature control (AgCd, NiCd), cell voltage control (NiCd)

  Decreased – depth of discharge (AgCd, NiCd), cycle life (AgCd, NiCd), temperature extremes (AgCd, NiCd)

  Positive limiting of maximum charge voltage (NiCd)

  Positive limiting of maximum charge current (AgCd)

6.5.3 Solar Cell Array

- Efficiency usually improves as the following parameters change, assuming loads can accept available array power:

  Increased – array absorptivity, solar cell AMO basic efficiency, sun-solar cell spectral match

  Decreased – angle of incidence, temperature, temperature range, radiation degradation, temperature gradient across array, insolation gradient across array

  Match loads to solar array maximum power point

- Weight usually decreases as the following parameters change:

  Increased—efficiency, effective cell area

  Decreased – array structural weight, cover glass thickness, cell thickness

- Reliability usually improves as the following parameters change:

  Increased – radiation protection

  Decreased – temperature extremes

  Positive sun orientation

  Optimum series-parallel cell interconnections

  Open-cell circuit protection

6.5.4 Power System

- Efficiency usually improves as the following factors change:

  Increased – equipment efficiency, battery efficiency, solar array efficiency, output power, bus voltage

  Decreased – load variations, quantity of equipment parallel redundancy, dark to light ratio

- Weight usually decreases as the following factors change:

  Increased – solar array efficiency, equipment efficiency

  Decreased – battery weight, solar array weight, output power, quantity of equipment, standby redundancy

- Reliability usually improves as the following factors change:

  Increased – redundancy

  Decreased – parts count, temperature extremes radiation environment, mission life requirement, quantity of eclipse cycles

6.6 POWER REQUIREMENTS ORGANIZATION

6.6.1 General

Satellite electrical load requirements are characteristic of a given mission and vehicle design. For example, the electrical loads and duty cycles of a communications type satellite are predominantly functions of the transmitter and receiver requirements. The power requirements accumulated for communications equipment (Section 3.1) show the need for a wide range of dc voltages (3 to 1500 v), with relatively close regulation. Significant amounts of power are required for each rf output stage depending upon the range, data rate, antenna gain, and output frequency. Multiples of this power can result if redundant equipment is used or if more transmitters are required for broader coverage of the frequency spectrum. Thus, it is possible to make some general observations about the characteristics of the electrical power system required to satisfy a given type of satellite mission. Specific power system requirements can only be defined when the vehicle design, mission constraints, subsystem inventory, ephemerides, and mission philosophy are enumerated.

6.6.2 Generalized System Block Diagram

The acumen for organizing a given set of power requirements to enhance the resultant power system optimization can be obtained by analyzing a generalized satellite power system block diagram such as Figure 6-2. A power system can be reduced to an energy source, source control, energy storage, storage control, and power conditioning equipment. The energy source may be made up of a combination of series and parallel elements. The symbol P_A represents one of these elements and, for a solar array, it constitutes the maximum power received by the element P_A from normal incident sun under optimum mission conditions. The sum of all P_A elements on the satellite represents the maximum power received if all elements were illuminated. Associated with each power element P_A is an efficienty η_A. The efficiency η_A represents all of the steady state and transient conditions affecting the conversion of sunlight to electrical power. It may include, but is not limited to the following factors:

- Basic AMO cell efficiency
- Solar array aspect ratio, i.e., ratio of the illuminated solar cell projected area to the total cell area
- Angle of incidence for the illuminated projected area
- Solar cell temperature coefficient
- Solar cell cover slide transmittance
- Solar cell cover slide angle of incidence correction factor
- Solar cell radiation degradation factor
- Solar array impedance match to power system

Thus, η_A is the efficiency of the elemental energy source for a given design and set of operating conditions, and represents the utilization of the design as well as the conventional energy conversion efficiencies.

The energy source control may be implemented in many configurations. Each power element may have a series or parallel control represented by η_{SN} and η_{PN}, respectively; or the total source may have a single series or parallel control represented by η_{S3} and η_{P3}.

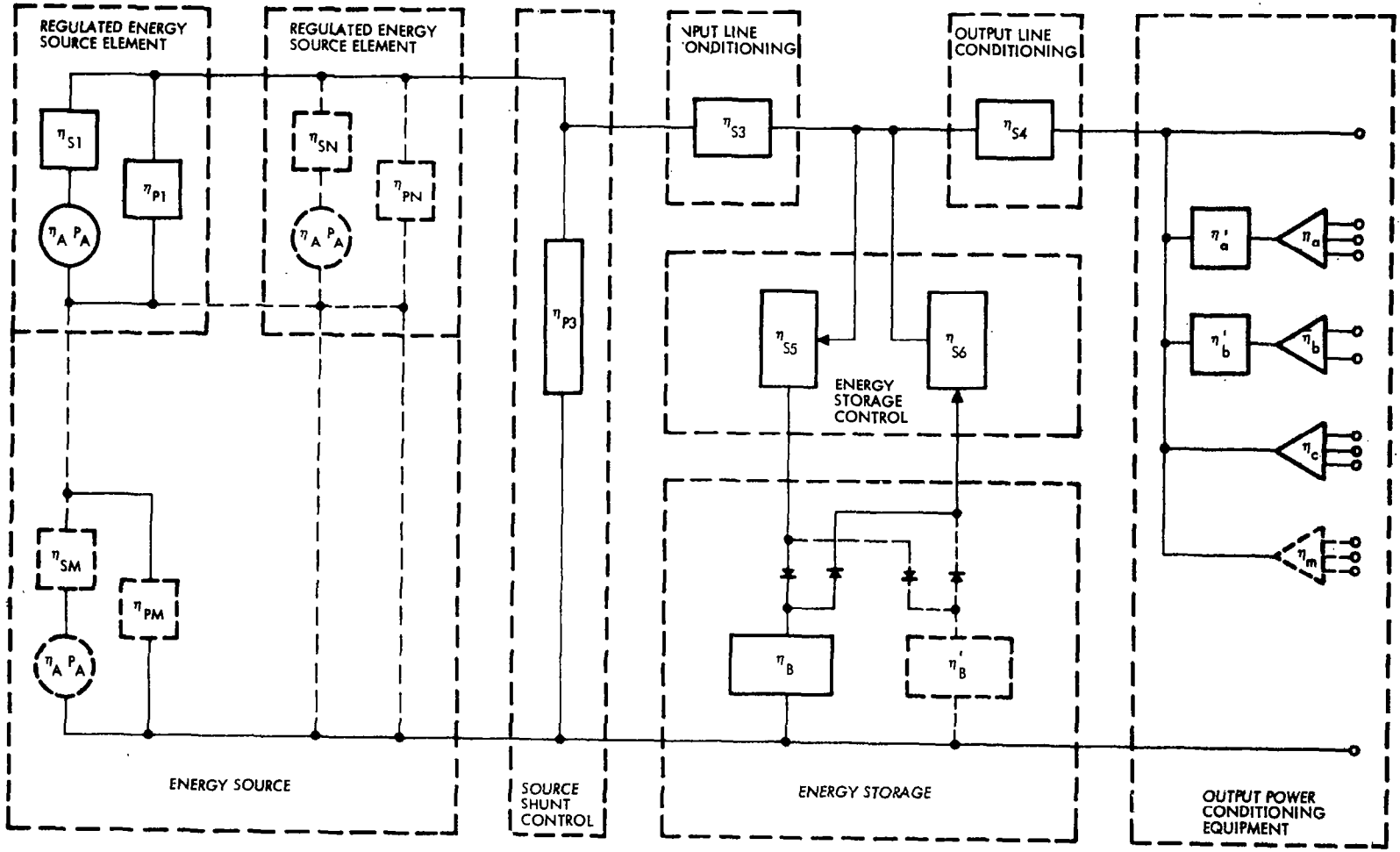

Figure 6-2. Generalized Power System Block Diagram

Energy storage, when required, can be considered a parallel load on the energized energy source, or a parallel source of energy if used for peak overloads. When the energy source is not energized, the storage elements become the source of power. Every type of energy storage has an associated efficiency factor η_B, which represents the ratio of output energy to input energy. For the battery case, η_B is the battery watt-hr efficiency. This efficiency factor only applies to the amount of energy supplied to the system load by the energy storage elements. The energy storage efficiency factor is related to the system load by the dark to sunlight ratio for a solar-array battery system. The overall system efficiency is directly affected by the energy storage usage and efficiency.

Energy storage control has an input and/or an output efficiency represented by η_{S5} and η_{S6}, respectively. These are both multipliers of the energy storage efficiency and degrade the system efficiency proportionately.

Power conditioning equipment — regulators, inverters, converters, and TR units — may be arranged in many configurations depending upon the individual load requirements and the type of power system configuration preceding them. It is here that the analysis and organization of the power requirements have the strongest influence. The block diagram represents centralized power conditioning efficiency by η_{S4}, and distributed power conditioning efficiencies by $\eta_{a,b,c,\ldots m}$. Centralized equipment efficiencies affect the power system efficiency directly, since all or a large portion of the output power must pass through this equipment. Distributed equipment efficiencies affect the system efficiency in proportion to the percentage of the total output power handled by each. The efficiency of one output (distributed) power conditioning equipment is independent of all others, except other equipments following it in series. For example, the equipment represented by η'_a in Figure 6-2 will change its efficiency to some degree as the value of η_a varies, but η_b, η_c, $\ldots . \eta_m$ values are unaffected.

The block diagram of Figure 6-2 is generalized because it can represent any power system by assignment of individual or composite

efficiency values to each representative block. Wherever the block represents a nonexistent function, a value of 100 percent is assigned. Analysis of this block diagram will show that:

- Low efficiencies for the output power conditioning equipments are accentuated by each efficiency value between it and the energy source
- Efficiencies of parallel equipments are independent
- Efficiencies of series equipments are dependent according to the magnitude of power change
- Low efficiencies are more tolerable for small amounts of power than for large amounts
- System efficiency is directly proportional to the energy storage and control efficiencies, and the percentage of output energy required to go through the storage branch
- The efficiency of a series or parallel control equipment such as ηS_3 and ηP_3, can de defined to be an equivalent multiplier of the input power controlled.

6.6.3 Analysis of Loads

Selection of loads for assignment to the output power conditioning equipments is dependent upon the specified optimization criterion and load requirements. Previously (Section 3), specific loads were related to major subsystems. Now, they will be considered in terms of voltage magnitude, regulation percentage, power level, frequency, etc. in order to apply the design optimization guidelines derived from the parametric data. A review of the parametric design data shows that system efficiency has the following functional relationship with output power:

$$\eta = f\left[b\left(1 - e^{-k\Delta_i}\right)^a\right] \qquad (1)$$

where

η = total efficiency of power system less prime energy generator and storage

Δ_i = percentage of total output power per output circuit

a, b, k = constants for the particular type of conditioning equipment and operating voltages

The relationship of system efficiency to output voltage is also exponential, but shallower than for power output. Percent regulation and the number of voltage outputs affect efficiency, but are noticeable only when the output power and voltages are held constant.

Equipment weights are similarly related to output power and voltage for conventional designs. Extremely low weight designs are possible in special cases where efficiency, lifetime, and reliability can be sacrificed. These special cases are not included in this study. The proportional increase of weight with output power is offset by the simultaneous increase in efficiency. Thus, it is possible to trade off weight and efficiency at any given power level.

Certain generalizations can be made about maximizing system efficiency as applied to the selection of loads. The following is a list of the more important guidelines bearing on load selection and grouping:

- Power requirements should be grouped in large amounts for processing by regulators, inverters, converters and/or transformer-rectifiers.
- Power conditioning and control equipment should be used only when necessary.
- Efficiencies of power conditioning and control equipment generally decrease in the following order for constant power outputs: TR units, inverters, regulators, and converters.
- Efficiencies of power conditioning and control equipment generally increase as power output increases, output voltage increases, voltage regulation percentage increases, number of output voltages decreases, the ratio of input/output voltage for regulators approaches unity, and as the input voltage regulation percentage decreases.
- Efficiency of the battery is dependent upon state of charge, charge rate, discharge rate, charge temperature, and discharge temperature.
- Operating efficiency of the solar array is dependent upon initial solar cell efficiency, illumination intensity, radiation history, temperature, and matched load impedance.
- The power required from the battery, especially that requiring conditioning, should be minimized.

6.6.4 Load Grouping and Power System Configuration Selection

Application of these guidelines can best be explained by an example. Table 6-V presents the Mission III Load Power Requirements which are used in Section 7 for illustrating optimization of the scientific satellite mission. Optimization of system efficiency is the chosen criterion. The two right hand columns of Table 6-V were generated to obtain some insight into the relative magnitudes of power and voltage for each output requirement.

Each power system designer may wish to analyze and organize the power requirements in his own way. The following procedure is suggested as one way to apply the guidelines to arrive at a logical organization of requirements for selecting groups of voltages when the optimization criterion is maximization of power system efficiency. Table 6-VI is the result of applying this procedure to the requirements of Table 6-V.

The process bv which Table 6-VI was developed is as follows:

1) All output voltages were listed in descending order and numbered sequentially starting with 1. The sequential column is labeled A.

2) Column B was formed by assigning numbers according to the output power for that voltage in descending order, starting with 1.

3) The output power at each voltage (taken from Table 6-V) was multiplied by that voltage. According to the descending order of magnitude of the product (P x V), numbers were assigned sequentially and listed in Column C.

4) The assigned numbers from Column A, B, and C were summed for each voltage and listed in the column labeled (Σ A, B, C). Column D was formed by assigning numbers sequentially, starting with 1, according to the magnitude of the above sum (Σ A, B, C) in ascending order (i.e., 1 represents the lowest sum).

5) Column E was formed by calculating in sequence the cumulative percentage of the total system power for each voltage listed. The sequence should parallel the order given in Column A.

6) Column F was formed by calculating in sequence the cumulative percentage of the total system power for each power output. The sequence for calculating should parallel the numerical order given by Column B, and should be recorded opposite the correct voltage.

7) Column G was formed by calculating in sequence the cumulative percentage of the total system power for each output. The sequence for calculating should be in the numerical order given by Column C and should be recorded opposite the correct voltage.

8) Column H was formed by again calculating the cumulative percentage of total system power but following the numerical sequence given by Column D.

9) All output voltages were arranged in descending order of their percentage regulation. Within each group having the same regulation percentage the output voltages should be arranged in descending order of voltage. This list was numbered sequentially starting with 1 for the highest percentage regulation. Column I, adjacent to Column H, was formed by listing the sequential number determined above opposite the correct voltage.

The numerical sequence of Column A reflects the preference for selecting the outputs according to voltage. Equipments assigned the higher voltages will tend to be of higher efficiency. The numerical sequence provided by Column B shows the selection preference according to the magnitude of power required at each voltage. Equipments assigned voltages having the larger amounts of power will also tend toward higher efficiencies. Clearly, equipments assigned high voltages with large amounts of power will provide the higher efficiencies. The numerical sequence of Column C provides a relative preference according to the product of voltage and power. The very large products (low sequence numbers) represent high efficiency capability, and the very small products (high sequence numbers) represent poor efficiency capability. The products falling in between are not indicative by themselves, because their position could be caused by any one of the following combinations: low power and moderate voltage, low voltage and moderate power, medium-low power and voltage. Therefore, reference to Coumns A and B is necessary to properly assess their efficiency capability. This is most

Table 6-V. Mission III Load Power Requirements

Item No.	Voltage	Volt Amps/W	% Regulation	Frequency	Remarks	Voltage x Power	Percent of Total Power
1.	135 ac	302/100.7	+20, -15	400 cps	Ø A	13,594.5	36.17
2.	125 ac	139/46.3	+20, -15	400 cps	Ø B	5,787.5	16.63
3.	115 ac	15/8.0	±2.0	400 cps		920.0	2.87
4.	+ 70 dc	42.3	±2.0			2,961.0	15.19
5.	+ 28 dc	9.0	+20, -15			252.0	3.23
6.	28 ac	12/10.8	+20, -15	400 cps		302.4	3.88
7.	26 ac	6/2.0	+20, -15	400 cps		52.0	0.72
8.	+ 23 dc	5.8	±2.0			133.4	2.08
9.	+ 20 dc	7.0	±1.5		C.T. GRD	140.0	2.51
10.	- 20 dc	7.0	±1.5		C.T. GRD	140.0	2.51
11.	18 ac	3/1.6	±2.0	400 cps		28.8	0.57
12.	+ 16 dc	11.3	±1.0		C.T. GRD	186.2	4.06
13.	- 16 dc	0.4	±1.0		C.T. GRD	6.4	0.14
14.	+ 10 dc	0.5	±3.0			5.0	0.18
15.	+ 9 dc	21.1	±1.0			190.3	7.58
16.	- 6 dc	4.1	±1.0			24.7	1.47
17.	+ 5 dc	0.5	±1.0			2.5	0.18
		477/278.4					100

Table 6-VI. Mission III Load Power Requirements Organization

Item No.	Output Voltage	Voltage Rank	Power Rank	VxP Rank	$\sum$A, B, C	$\sum$A, B, C Rank	Cumulative Percent of Total Power For A	Cumulative Percent of Total Power For B	Cumulative Percent of Total Power For C	Cumulative Percent of Total Power For D	Volt Reg Rank	Cumulative Percent of Total Power For Vac	Cumulative Percent of Total Power For Vdc
		A	B	C	—	D	E	F	G	H	I	J	K
1.	135 ac	1	1	1	3	1	36.17	36.17	36.17	36.17	1	36.17	—
2.	125 ac	2	2	2	6	2	52.80	52.80	52.80	52.80	2	52.80	—
3.	115 ac	3	8	4	15	4	55.67	89.61	70.86	70.86	7	55.67	—
4.	+70 dc	4	3	3	10	3	70.86	67.99	67.99	67.99	8	—	15.19
5.	+28 dc	5	7	6	18	6	74.09	86.74	77.97	77.97	3	—	18.42
6.	28 ac	6	6	5	17	5	77.97	83.51	74.74	74.74	4	59.55	—
7.	26 ac	7	13	12	32	12	78.69	98.90	97.43	97.43	5	60.27	—
8.	+23 dc	8	11	11	30	11	80.77	96.71	96.71	96.71	9	—	20.50
9.	+20 dc	9	10	9	28	9	83.28	94.63	92.12	92.12	11	—	23.01
10.	-20 dc	10	9	10	29	10	85.79	92.12	94.63	94.63	12	—	25.52
11.	18 ac	11	14	13	38	13	86.36	99.47	98.00	98.00	10	60.84	—
12.	+16 dc	12	5	8	25	7	90.42	79.63	89.61	82.03	13	—	29.58
13.	-16 dc	13	17	15	45	15	90.56	99.97	99.61	99.61	14	—	29.72
14.	+10 dc	14	15	16	45	16	90.74	99.65	99.79	99.79	6	—	29.90
15.	+ 9 dc	15	4	7	26	8	98.32	75.57	85.55	89.61	15	—	37.48
16.	- 6 dc	16	12	14	42	14	99.79	98.18	99.47	99.47	16	—	38.95
17.	+ 5 dc	17	16	17	50	17	99.97	99.83	99.97	99.97	17	—	39.13

easily accomplished by summing the numerical values in Columns A, B and C for each voltage. The resulting values can again be reduced to a numerical sequence starting with 1 for the lowest sum as shown in Column D. The sequence for very large and very small products are not normally affected by this summing. The mid-range product (PxV) sequence is now weighted by the relative magnitude of voltage and power.

The voltages having the larger output power should be given the preference if Column D sequence differs from Column C. Generally, Column D will reflect the desired order of preference.

The next step is to determine the number of groups (or power conditioning equipments), and voltage assignments for each group. The auxiliary information provided by Columns E, F, G, H, I, J and K assists in this determination. For example, Columns J and K reveal that approximately 61 percent of the total power is ac, and 52.8 percent of the total power is represented by the first two ac voltages indicated by Column D. Only two ac voltages Items 7 and 11 do not fall within the first five preferred voltages (Column D), and they represent a very small amount of power. Therefore, it would seem reasonable to select an inverter as one of the equipments to supply all of the ac voltages. Two of the six ac voltages require close regulation. The regulation requirements of the other four are typical of an unregulated bus, and should not require a regulator. The remaining voltages to be considered are dc. Assuming a solar-array battery power system, the main dc bus voltage can be selected from the list of dc voltage requirements. Item 5, the +28-v requirement is the best choice on this mission for two reasons. Its regulation requirements are loose enough so that a regulator is not required, and it is the highest dc voltage requirement which does not exceed 50 vdc, the upper limit for a reasonable solar-array and battery design. The remaining dc voltages require close regulation, and can be derived in several ways as follows:

1) A TR unit operating from the above inverter, and having regulators as required on the outputs.

2) An ac regulator(s) operating, from the above inverter and then a TR unit or units as required.

3) A regulated converter or converters operating from the dc solar-array battery bus.

4) A regulated inverter supplying all ac loads and TR units for the dc loads.

Using the previously established guidlines, an estimate of the above configurations would select (4) the regulated inverter as the most efficient system. The optimum choice can be made by evaluating each of the above system configurations, using the Comparative Analysis Optimization technique. This technique is explained in the following paragraphs, and three mission examples are numerically evaluated in Section 7.

6.7 COMPARATIVE ANALYSIS OPTIMIZATION

The total input electrical power from the basic energy source to the system for a given satellite design and set of operating conditions (see Figure 6-2) can be defined as

$$\left(P_{in}\right)_1 = \eta_A \sum P_A \tag{2}$$

where

P_A = maximum available power from the energy source element under optimum mission conditions

η_A = efficiency associated with the energy source for a given set of operation conditions

Energy source controls can be either series or parallel in nature. The efficiency associated with these controls is designed by (η_s) or (η_p). From the regulated or controlled source the total input power (P_{in}) to the system is

$$\begin{aligned} P_{in} &= \eta_A \eta_s \sum P_A \quad , \text{ or} \\ &= \eta_A \eta_p \sum P_A \end{aligned} \tag{3}$$

Similarly, the efficiencies associated with each piece of control or power conditioning equipment can be multiplied by its input power. The total power to the loads is then equal to the sum of the input power elements

decreased by the system efficiency factors. For the solar array - battery type system, the division of energy proportioned by the discharge - charge (dark to light) ratio must be considered. The total power to the loads can also be expressed as follows

$$P_{out} = \sum_{i=1}^{m} P_i = P_{out} \sum_{i=1}^{m} \Delta_i \tag{4}$$

where

P_i = the output power associated with each equipment directly supplying the loads

Δ_i = percent of the total system output power associated with the equipment carrying each P_i amount of power

The element of regulated source power associated with a P_i is:

During sunlight

$$P_{in} = \left[\sum_{i=1}^{m} \frac{P_i}{(\eta_{p3}\eta_{s3}\eta_{s4}\eta_i)} \right] + \left(P_{in}\right)_{dark} \tag{5}$$

where η_{p3}, η_{s3}, η_{s4} are the efficiencies related to the equipments conditioning the P_i power.

During dark

$$\left(P_{in}\right)_{dark} = \sum_{i=1}^{m} \frac{P_i \left(\frac{\tau}{t} - 1\right)}{(\eta_{p3}\eta_{s3}\eta_{s4}\eta_{s5}\eta_B\eta_{s6}\eta_i)} \tag{6}$$

During sunlight (Substitute Equation 6 into Equation 5)

$$P_{in} = \frac{1}{\eta_{p3}\eta_{s3}\eta_{s4}} \sum_{i=1}^{m} \left(\frac{P_i}{\eta_i}\right) \left[\frac{\left(\frac{\tau}{t} - 1\right)}{\eta_{s5}\eta_{s6}\eta_B} + 1 \right] \tag{7}$$

where (τ) is the total orbit time and (t) is the sunlight time of the orbit.

The total maximum available power from the energy source under optimum mission condition is

$$\sum P_A = \frac{1}{\eta_A \eta_p^* \eta_{p3} \eta_{s3} \eta_{s4}} \sum_{i=1}^{m} \left(\frac{P_i}{\eta_i} \right) \left[\frac{\left(\frac{\tau}{t}\right) - 1}{\eta_{s5} \eta_{s6} \eta_B} + 1 \right] \tag{8}$$

This equation can be separated into two parts, one related to the energy through the battery circuit and the other directly to the load.

Let

$$(\eta_A \eta_p \eta_{p3} \eta_{s3} \eta_{s4}) = \eta_c$$

and

$$(\eta_{s5} \eta_{s6} \eta_B) = \eta_d$$

then

$$\sum P_A = \left(\frac{1}{\eta_c} \sum_{i=1}^{m} \frac{P_i}{\eta_i} \right) + \left[\frac{1}{\eta_c \eta_d} \sum_{i=1}^{m} \frac{P_i \left(\frac{\tau}{t} - 1 \right)}{\eta_i} \right] \tag{9}$$

Since $P_i = \Delta_i P_{out}$,

$$\sum P_A = \left(\frac{P_{out}}{\eta_c} \right) \left\{ \left(\sum_{i=1}^{m} \frac{\Delta_i}{\eta_i} \right) + \left[\frac{\left(\frac{\tau}{t} - 1 \right)}{\eta_d} \sum_{i=1}^{m} \frac{\Delta_i}{\eta_i} \right] \right\} \tag{10}$$

The total power system efficiency (H) can be expressed as follows

$$H = \frac{P_{out}}{\sum P_A} = \frac{\eta_c}{\left(\sum_{i=1}^{m} \frac{\Delta_i}{\eta_i} \right) + \left[\frac{\left(\frac{\tau}{t} - 1 \right)}{\eta_d} \sum_{i=1}^{m} \frac{\Delta_i}{\eta_i} \right]} \tag{11}$$

*η_s may be substituted for η_p depending on type of energy source control

The total power system efficiency (H) can be maximized by

1) Increasing η_c, the power conditioning efficiency

2) Increasing η_d, the battery charge-discharge efficiency

3) Decreasing $\left[(\tau/t) - 1\right]$, the dark-to-light ratio

4) Increasing

$$\sum_{i=1}^{m} \eta_i$$

the output stage efficiency of the power conditioning equipment

Therefore, for each proposed power system configuration, equipment efficiencies can be substituted into Equation (11). The resulting (H) for each configuration can then be compared in magnitude. The highest resulting number (closest to unity) will indicate the most efficient configuration.

The equipment weights for each of these configurations, corresponding to the established operating points, can be determined. Thus the total system weight for each configuration is obtained for comparison.

In contrast, the minimum weight power system typically contains power conditioning equipment whose design is a compromise between maximum efficiency and minimum weight equipment. For most designs of the power conditioning equipment, maximum equipment efficiency is not synonymous with minimum equipment weight. Because of the usual efficiency-weight tradeoff for the power conditioning equipment, the minimum weight power system would not utilize the maximum efficiency equipment. This is true unless the weight reduction in the battery and solar array, due to the power conditioning equipment efficiency improvement, completely offsets the accompanying increase in equipment weight necessary to obtain the maximum equipment efficiency. The most favorable compromise, starting from the minimum weight power conditioning equipment, is reached by incrementally increasing the power conditioning equipment weight until the resultant power saving, (due to the high efficiency) translated into battery and solar array weight reduction is just equal to the added incremental equipment weight. Thus the minimum weight power system design can also be ascertained for each configuration.

7. OPTIMIZATION OF MISSION EXAMPLES

7.1 MISSION DEFINITION AND ANALYSIS

The three missions specified by NASA/GSFC are typical for existing and future earth orbiting vehicles. Their primary requirements and constraints are summarized in Table 7-I.

Table 7-I. Selected Missions

	Mission I	Mission II	Mission III
Orbit	Synchronous equatorial	Sun-synchronous	Elliptical, 31 deg inclined
Mission	Communications	Mapping, navigation	Scientific experiements
Altitude	19,323 nmi	600 nmi	200 to 180,000 nmi
Life	5 yr	1 to 3 yr	1 yr
Control system	Active 3- or 2-axis	As necessary	3 axis
Load power	150 to 500 w	150 to 500 w	300 w
Subsystem power inventory	Assigned by TRW	Assigned by TRW	Assigned by TRW

7.1.1 Mission I

The communications satellite specified for Mission I has some stringent operational requirements. Because its primary purpose is to handle communications with earth stations, earth pointing of its transmitting and receiving antennas from an earth-synchronous position is a major design constraint on the vehicle configuration and attitude control subsystem. Several design concepts which can satisfy these requirements are discussed below.

Of the attitude control methods considered for active communications satellites, the most commonly selected method employs a spin-

stabilized, cylindrically shaped vehicle having its spin axis normal to the orbital plane. This method is considered the more reliable, and requires the least amount of energy for controlling the vehicle. The solar array should be body mounted whenever possible, providing a relatively lightweight, high performance design. This design was chosen for the Mission I satellite.

7.1.1.1 Spherical or Cylindrically Shaped Body, Spin-Stabilized (Two-Axis Control)

When the vehicle spin axis is oriented normal to the orbital plane, earth pointing of the antennas can be accomplished by mechanically or electrically despinning the antennas. Electrical power is required for antenna despinning and vehicle spin axis correction control. The solar array can be either body mounted or fixed paddles. Both of these array configurations have similar performance. A choice based upon performance would depend entirely upon the vehicle design limitations. However, the fixed paddle configuration usually presents an interference pattern for the antennas and may cause vehicle stability problems. Therefore, the body mounted array is preferred.

When the vehicle spin axis is oriented in the orbital plane, continuous earth pointing of the antennas can be accomplished by precessing the vehicle attitude once per orbit. Electrical power is required for the flywheel and/or gas jet attitude control. The reliability of this continuous attitude correction is low for the required life of five years. Again, the solar array can either be paddles or body mounted. The spherical configuration is usually preferred by power system designers for this body mounted array because the cylindrical shape with solar cells mounted on its ends requires a larger number of solar cells.

7.1.1.2 Nonspinning, Two-Axis Control

Active attitude control of a nonspinning earth-oriented body usually employs gas jets and flywheels. Motion about the third axis, which is parallel to the local vertical, is uncontrolled or at most damped. The primary function of the attitude control system is to maintain earth pointing of the third axis (antenna axis). The solar array for this type of

vehicle control can also be body mounted or fixed paddles. Fully oriented paddles require the additional control of the third axis of the vehicle and are discussed in Paragraph 7.1.1.3.

Because the motion about the third axis is uncontrolled, either solar array configuration would be subject to varying thermal excursions. The upper and lower temperature limits of these excursions are more extreme than for the spin-stabilized vehicle. Thus, the solar array performance is less predictable as a function of time, and in general less efficient. The two-axis nonspinning vehicle control system is probably the least desirable for maximizing power system performance.

7.1.1.3 Three-Axis Control

Three-axis attitude control can be either active or semi-active. The active three-axis control is the same as the two-axis nonspinning system with the addition of stabilization about the third axis. Third axis stabilization either maintains a zero angular rate about the third axis, usually by inertial sensors, or maintains a varying attitude about the third axis so that some pointing reference is maintained. The latter method is normally found when a fully oriented solar array is used and the pointing reference is the sun. Active three-axis control permits the use of body mounted solar arrays, fixed paddles, or fully oriented paddles. Fully oriented paddles usually are used to take advantage of the full stabilization.

Semi-active three-axis control is exemplified by the gravity gradient stabilized vehicle. The gravity gradient technique maintains earth pointing of the vehicle, and active control is only required for the third axis. Because the control forces of the gravity gradient system are very small, disturbances caused by stationkeeping or paddle orientation must be minimized. Body mounted or fixed paddle solar arrays are most common for this method of vehicle control. Varying thermal excursions are again present. However, the temperature extremes may be less than for the nonspinning two-axis controlled vehicle and more predictable.

7.1.2 Mission II

Greatest earth coverage for the mapping or navigational functions of Mission II is provided when a polar orbit is used. This mission was specified to be sun synchronous which is a special polar orbit case. Sun-synchronous orbits possess unusual properties because of the unique characteristics which define them. These orbits have a nodal regression rate equal in magnitude and sense to the mean rate of revolution of the earth about the sun (about 0.985 deg per day). The sun-synchronous orbits maintain their initial orientation relative to the sun. These orbits are retrograde and lie between inclination angles of 95.7 deg and 180 deg at altitudes up to 3225 nmi. For certain mission requirements, a noon-midnight sun-synchronous orbit can be selected which provides good photography for about one-half of every revolution. Conversely, twilight sun-synchronous orbits can be established in which the space vehicle is never in the shadow of the earth, eliminating the need for energy storage (batteries, etc.) if solar power is used. Orbits having any ratio of dark to light between these two extremes can be achieved by using the proper launch time. For the purposes of this study, only the two extreme cases for an altitude of 600 nmi will be considered. All vehicles in sun-synchronous orbits having a lifetime of 9 months or longer require station-keeping. This is a result of earth anomalies and drift rates established by launch errors.

Several vehicle and solar array configurations are available for these specialized orbits. However, the operational function of earth pointing the payload equipment and/or antenna presents restrictions very similar to those of Mission I. The following paragraphs discuss noon-midnight and twilight orbits.

7.1.2.1 Noon-Midnight Orbits

All vehicle and solar array configurations used for this orbit experience full shadow and full sunlight once per orbit. The ratio of dark to light is dependent solely upon the orbital altitude and eccentricity.

1) Spin-Stabilized Control

The spin-stabilized vehicle with its spin axis normal to the orbital plane has the same type of problems and possible solutions as outlined for Mission I. Synchronizing the

antennas and/or payload with the earth view is usually the overriding factor in configuration selection. Similarly, the configurations for the spin axis lying within the orbital plane have been covered for Mission I. However, one new condition for this orientation is made possible because of the sun-synchronous characteristic. If the vehicle is not precessed, it will maintain a fixed orientation in inertial space. Thus, one surface of the vehicle will always be perpendicular to the earth-sun line. This is advantageous for the solar array and electrical power system, but presents earth tracking problems for the payload/antenna equipment.

2) Nonspinning Two-Axis Control

Active two-axis control for sun-synchronous orbits presents the same advantages and disadvantages as stated for Mission I. A slight improvement in solar array performance is obtained for polar orbits because the approximate change of ±23 deg in earth-sun line from the equatorial plane has no effect. Again this mode of control is less desirable.

3) Three-Axis Control

Active control of the three axes of the vehicle for this orbit presents the same considerations as given for Mission I. The effect of ecliptic angle, again, is of no concern.

The method of control normally chosen for noon-midnight orbits is the spin-stabilized vehicle whose spin axis is parallel to the orbital plane. The vehicle would be precessed one revolution per orbit to permit payload/antenna earth tracking. This mode of control is preferred because the earth tracking accuracy for mapping and navigation payloads is usually greater than for communications. Also, electronic and/or mechanical despinning of the optical payload sensors has not been fully developed for the accuracies required.

7.1.2.2 Twilight Orbits

The significant advantage of twilight orbits is the availability of continuous full sunlight. Battery power or energy storage would only be required for the launch-acquisition phase and subsequent reacquisitions that become necessary. All previous attitude control and solar array considerations presented for the noon-midnight orbits apply. Due to the full sunlight condition, the solar array used on a spin-stabilized vehicle is simplified and smaller. Because solar cells would not be required

on the ends of the vehicle defined by the spin axis, a cylindrical body would be preferred.

7.1.3 Mission III

The attitude control system for this mission has been specified as being three axis. Because of the variety of experiments normally carried by this type of vehicle and their diverse performance requirements, active three-axis stabilization is the only practical method. Therefore, full three-axis active attitude control was assumed for analysis of this mission. It should be noted that some specialized scientific satellites flown in this orbit could use other three-axis attitude control methods. In general, the electrical power requirements would be less for these special cases.

7.1.4 Summary of Mission Analysis

The vehicle shape, solar array, and attitude control selections for each mission are summarized in Table 7-II.

Table 7-II. Vehicle Shape, Solar Array, and Attitude Control Selections

	MISSION I	MISSION II		MISSION III
		Noon-Midnight	Twilight	
Vehicle Shape	Cylindrical	Spherical	Cylindrical	(Not critical)
Attitude Control	Spin axis stabilized normal to orbital plane	Spin axis stabilized in the orbital plane and precessed once per orbit	Spin axis stabilized in the orbital plane and precessed once per orbit	Active three - axis control
Solar Array	Body mounted	Body mounted	Body mounted	Paddle mounted, fully oriented

7.2 DESIGN OPTIMIZATION GUIDELINES

Satellite electrical power systems are discussed here according to their functional elements. These functional elements may or may not be

physically located within the same piece of hardware. In general, ac or dc voltages exceeding 150 to 200 v would not be distributed outside of the equipment in which they were generated. Thus, user equipment requiring high voltages would contain the high voltage portion of the power conditioning function. Equipment parametric data derived throughout this study indicate that high bus voltages (50 to 100 v) are desirable for best efficiency, provided the using equipment requirements are reasonably close to the chosen bus voltage. A lower bus voltage should be chosen if it would eliminate a stage of power conditioning by direct connection to the bus.

The functional elements of a power system can be identified as follows:

1) Energy source
2) Energy source control or regulator
3) Energy storage
4) Energy storage control or regulation
5) Power Conditioning Equipment
    a) Regulators (ac or dc)
    b) Inverters (dc to ac)
    c) Converters (dc to dc)
    d) Transformer-rectifiers (ac to dc)

For each of these functional elements many configurations, combinations, and circuit designs exist. The equipment design choice is primarily the responsibility of the design engineer and is a function of his knowledge of the state-of-the-art. However, the parametric data presented by this study does indicate to the design engineer the importance of certain parameters and their interactions, such that the total power systems performance can be maximized. General guidelines for the design of each type of functional equipment are discussed in the following paragraphs. Implementing these guidelines may not necessarily result in optimized individual pieces of equipment but should provide the best overall electrical power system.

7.2.1 Energy Source

The energy sources considered in this study have been limited to two types, solar cell arrays and radioisotope thermoelectric generators (RTGs), with the largest emphasis on the solar cell arrays. Solar arrays can be divided into three basic categories: body mounted, fixed paddles, and movable oriented paddles.

Body mounted solar arrays are usually spherical, cylindrical, or multi-faceted approximations of either. The geometric configurations for body mounted cells allow a maximum of 35 percent utilization of the total array. Practical values for body mounted configurations are 20 to 23 percent. The choice of optimum geometric configuration is controlled by the specified orbit and type of control system selected to satisfy the mission objectives. Body mounted arrays are usually preferred on spinning satellites for the following reasons:

- Lower average operating temperature
- Higher energy density (w/lb)
- No deployment equipment required
- No complex attitude control functions required
- Short and direct electrical connections into the satellite
- Less temperature extremes.

The major disadvantages of their use are:

- Maximum design power is limited by the available and usable vehicle surface area
- Any protrusion from the satellite (such as an antenna) can cause decreased power due to shadowing
- Mismatching of solar cell strings when subjected to varying temperatures and illumination decreases output power.

Fixed solar array paddles are designed to accommodate the satellite shape (including the launch fairing) and method of attitude control. In general, a paddle array performs in a manner very similar to a body mounted array except its size is not limited by available satellite surface area. Operating temperatures are comparable to the body mounted array.

Oriented solar array paddles are the least desirable from the vehicle system standpoint. They are the most efficient user of active solar cell area, but the average conversion efficiency is lower due to the higher average operating temperature. Penalties for deployment and orienting equipments result in lower reliability, and lower power densities (w/lb). Normally, oriented solar arrays are used when large amounts of power are required and/or vehicle configuration and attitude control modes prevent acceptable performance from fixed arrays. The orbit and mission requirements will establish the choice criteria.

7.2.2 Energy Source Control or Regulator

An energy source control or regulator can be of the shunt or series type. Each of these two types have many design variations such as dissipative, nondissipative, switching, proportional, etc. Most applications requiring continuous control use regulators. Those not requiring active control in the normal operating mode use limiters or limit controls. Limit controls are commonly associated with protecting other equipment connected to the energy source, whereas regulators perform a continuous function of adjusting the energy source output characteristic. Limit type controls are more efficient than regulators during normal operation. Switching type regulators or controls most often have the highest efficiencies. Therefore, they are preferred whenever power system efficiency is important. The more efficient types of regulators and controls are:

- Full (or partial) switching type shunt
- Pulsewidth modulated (PWM) buck, boost, or buck-boost regulator
- Sequential shunt (or series) regulator
- Shunt voltage (or current) limiting control
- Series voltage (or current) limiting control.

The choice of the most efficient type depends upon the specific load requirements and subsystem configuration.

7.2.3 Energy Storage

Energy storage for a satellite power system is required because of solar array dark periods or peak power requirements on a transient basis. Except for very special cases when a capacitor will suffice, chemical storage batteries are commonly used. Primary type batteries may be used for missions where only the launch period requires stored power or when nonrecurring peak loads exist. The majority of applications utilize secondary batteries of the nickel-cadmium or silver-cadmium type. The charge and discharge efficiencies of the silver-cadmium type are slightly better than the nickel-cadmium. Nickel-cadmium batteries have more application because of their greater cycle life and capability of meeting mission times in excess of one year.

The charge and discharge current densities, as well as operating temperature control the battery performance, cycle life, and efficiency. Maximum performance is obtained from a nickel-cadmium battery 1) during discharge, when the battery temperature is high (80 to 90°F) and the current density is relatively low ($i_d \approx 0.1$), and 2) during charge, when the battery temperature is low (30 to 40°F), and the current density is high ($i_c \approx 1$). The silver-cadmium battery requires the same discharge but different charge conditions for maximum performance. Maximum ampere-hour capacity and efficiency are obtained when low charge rates ($I_c \approx c/4$) at high temperatures (80 to 90°F) are possible. Because low charge rates are highly desirable, silver-cadmium batteries should only be considered for missions having a dark-to-light ratio (S) less than 33 percent. Missions having an (S) value greater than 33 percent are possible if the penalties of shorter life and lower battery efficiency can be tolerated.

The choice of battery and its operating conditions is probably the most important phase of electrical power system design affecting system efficiency, weight, and reliability. Rarely will a solar array battery system allow battery watt hour efficiencies greater than 85 percent. Most often the efficiencies are in the 70 to 75 percent range. Whenever the mission includes eclipses, 100 percent of the output power during eclipse is handled by the battery and thus subjected to this low efficiency factor.

Further degradation of the efficiency factors occur for large values of the mission dark-to-light ratio (S). Because of this critical efficiency condition, it is necessary to minimize the output loads supplied by the battery and especially those loads having low efficiency power conditioning equipment. Intelligent thermal design of the battery environment can prevent additional efficiency losses. The proper choice of battery charge-discharge controls plays an important role in determining the battery thermal environment as well as directly affecting the system efficiency, battery life and reliability.

7.2.4 Energy Storage Control or Regulation

Control of the energy storage (battery) charge and discharge functions is a very complex requirement. As previously stated, the battery charge and discharge rates directly affect battery efficiency and operating environment. The addition of regulation or control into the system incorporates more equipment inefficiencies and reliability considerations. The ideal approach is to use only the bare essentials, such as nonpower-dissipating switches, to make maximum charging current available to the battery. This design approach is practical because the solar array is power limited and, when the battery is directly connected to the bus for charging, the bus potential will be set by the battery voltage. Additionally, the battery normally requires recharging immediately after an eclipse period when the cold solar array has excess power capability. Thus, the efficiency of this simple battery charge control approaches 100 percent. During the final charge period, the battery requires a reduced charge rate to prevent excessive temperatures and thermal problems. Simultaneously, the array is heated and returns to its normal sunlight temperature and power level. A simple voltage dropping resistor is usually sufficient to limit the trickle charge rate and maintain a highly efficient and reliable control circuit. A similar direct connection to the bus can be made for discharge, provided the power conditioning or user equipment is designed to accept the voltage extremes set by the battery charge-discharge voltage characteristic. Infrequently, the orbital and load requirements are such that a highly efficient pulse-modulated regulator is required for charge or discharge control.

Whenever energy storage is required for RTG systems, a similar direct control is desirable. The function of a battery in an RTG system is to supply peak or transient loads which seldom require closely regulated voltage. Usually, the RTG has a source regulator which decreases the need for further battery charge control. Therefore, direct coupling to the peak loads is common.

7.2.5 Power Conditioning Equipment

Power conditioning equipment consists of converters, inverters, transformer-rectifier (TR) units, and line regulators. The parametric data presented in Section 5 of this report indicate many characteristic similarities for these equipments. Efficiency and weight are nonlinear functions of power output level. Operating frequency has a significant and direct effect upon both parameters because of the magnetic and semiconductor circuit characteristics. Changing operating frequency creates an exchange between efficiency and weight of the equipment. The best compromise is determined at the electrical power system level, since a change in equipment efficiency is translated into new weights for the energy source, energy storage, and storage control equipments. The change in power conditioning equipment weight is balanced against the net system weight change.

The maximum efficiency curves on Figure 7-1 show the relative efficiencies for the four types of power conditioning equipments. For a given power requirement, various combinations of these four equipments can be used. The optimum efficiency combination may be determined by the EPSOM method, described in Section 6 of this report. Use of this method for the three specified satellite missions (See Table 7-I) are found in Paragraph 7-3.

7.3 POWER SYSTEM CONFIGURATION SYNTHESIS

7.3.1 Mission I Configurations

The payload for Mission I is the communications equipment necessary to relay the radio, television, telephone, and facsimile intelligence between two or more ground stations. Over 85 percent of the load power for the 150-w system is required for the payload. These

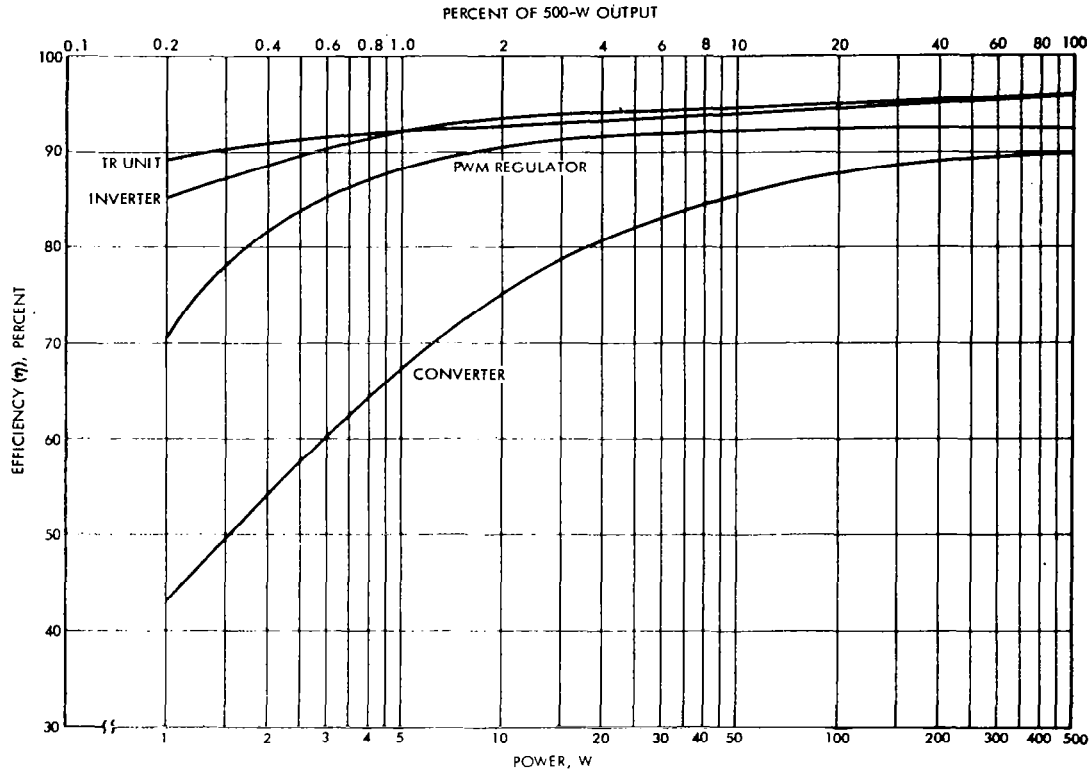

Figure 7-1. Maximum Efficiency as a Function of Power Output

load power requirements are given in Table 7-III. The requirements for a 500-w communications satellite would be over 95 percent for the payload. The Mission I payload represents four sets of communications equipment consisting of: 10-w traveling wave tubes (TWT), transmitters, driver stages, and receivers. Only a small amount of power is required for antenna despinning, attitude control, and stationkeeping. Several observations can be made about the load power requirements (Table 7-III).

- All output voltages are dc.
- All voltages except Item No. 8 require regulation tighter than an unregulated solar array or battery can provide.
- Only two additional levels of regulation are required.
- The voltage and power requirement for the four TWTs are identical.

Table 7-IV restates the load voltages, and presents the load requirements organization for Mission I. A review of the organization analysis given in Table 7-IV shows that the first seven voltages are predominately ranked within the first eight positions by four criteria: voltage, power, voltage x power, and the summation of the rank positions of the first three criteria. These seven voltages represent more than 75 percent of the total load power. Because the major portion of the loads are high voltage (>200 v) and associated with the TWTs, variations in the load organization are limited. TWT transmitters are very sensitive to voltage regulation tolerances and relative voltage magnitudes. Since the requirements for TWTs are for high voltage, it is recommended that the TWTs be supplied from power conditioning equipment located within the TWT equipment.

The suggested load requirements organization agrees with the technical need for conditioning these high voltages in one equipment. Four synthesized power system configurations which could satisfy the suggested organization are presented in Figures 7-2 through 7-5. The load voltage assignments are summarized in Table 7-V.

Table 7-III. Mission I Load Power Requirements

Item No.	Voltage (dc)	V-Amp/w	Regulation Percent	Frequency	Voltage x Power	Percent of Total Power
1.	+1440	1.60*	±1/2		2304.0	1.03
2.	+1340	4.80*	±1/2		6432.0	3.10
3.	+ 650	37.60*	±1/2		24440.0	24.26
4.	+ 620	0.04*	±1/2		24.8	0.03
5.	+ 570	0.40*	±1/2		228.0	0.26
6.	+ 550	71.60*	±1/2		39380.0	46.19
7.	+ 355	3.60*	±1/2		1278.0	2.32
8.	+ 28	3.50**	±15		98.0	2.26
9.	+ 28	2.40	±3		67.2	1.55
10.	- 15	2.50	±3		37.5	1.61
11.	+ 15	2.90	±3		43.5	1.87
12.	+ 10	2.60	±3		26.0	1.68
13.	- 6	1.40	±3		8.4	0.90
14.	+ 6	3.30	±3		19.8	2.13
15.	+ 3	16.80*	±1/2		50.4	10.84
		155.04				100.03

*TWT power is required from same converter.

**Peak power is 36.3 w.

Table 7-IV. Mission I Load Requirements Organization

Item No.	Output Voltage (dc)	Voltage Rank	Power Rank	VxP Rank	ΣA, B, C	ΣA, B, C Rank	Volt Reg. Rank	Cumulative Percent of Total Power For A	Cumulative Percent of Total Power For B	Cumulative Percent of Total Power For C	Cumulative Percent of Total Power For D
---	---	A	B	C	-	D	E	F	G	H	I
1.*	+1440	1	12	4	17	4	8	1.03	98.84	74.58	74.58
2.*	+1340	2	4	3	9	3	9	4.13	84.39	73.55	73.55
3.*	+ 650	3	2	2	7	1	10	28.39	70.45	70.45	24.26
4.*	+ 620	4	15	13	32	12	11	28.42	100.03	97.00	95.32
5.*	+ 570	5	14	6	25	7	12	28.68	100.00	77.16	79.42
6.*	+ 550	6	1	1	8	2	13	74.87	46.19	46.19	70.45
7.*	+ 355	7	5	5	17	5	14	77.19	86.71	76.90	76.90
8.	+ 28	8	6	7	21	6	1	79.45	88.97	79.42	76.16
9.	+ 28	9	11	8	28	9	2	81.00	97.81	80.97	91.81
10.	+ 15	10	8	11	29	10	3	82.61	92.97	95.29	93.68
11.	- 15	11	10	10	31	11	4	84.48	96.26	93.42	95.29
12.	+ 10	12	9	12	33	13	5	86.16	94.65	96.97	97.00
13.	- 6	13	7	15	35	14	6	87.06	91.10	100.03	99.13
14.	- 6	14	13	14	41	15	7	89.19	99.74	97.90	100.03
15.*	+ 3	15	3	9	27	8	15	100.03	81.29	91.81	90.26

*TWTs require their own converters. Total power required is dc power. Eighty-eight percent of the total power is for TWTs.

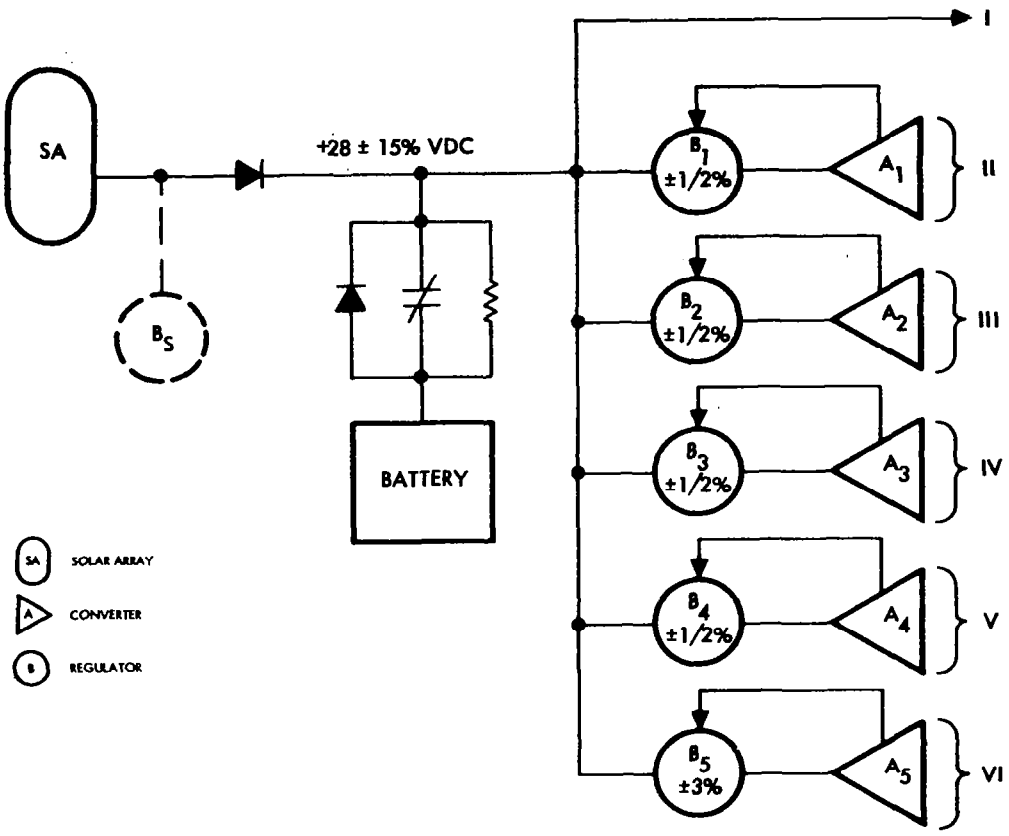

Figure 7-2. Mission I, Configuration 1

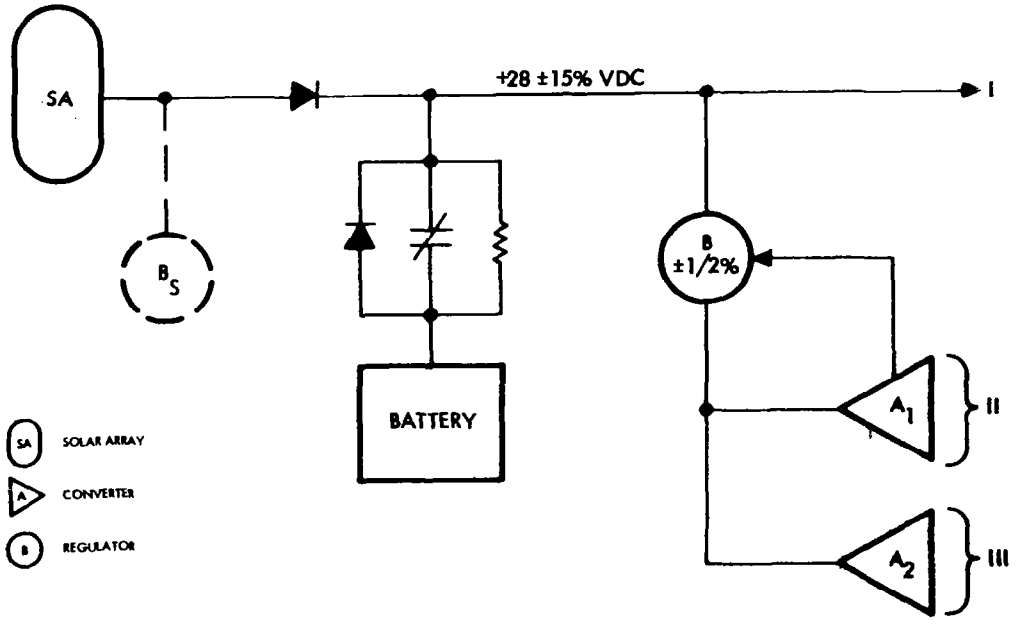

Figure 7-3. Mission I, Configuration 2

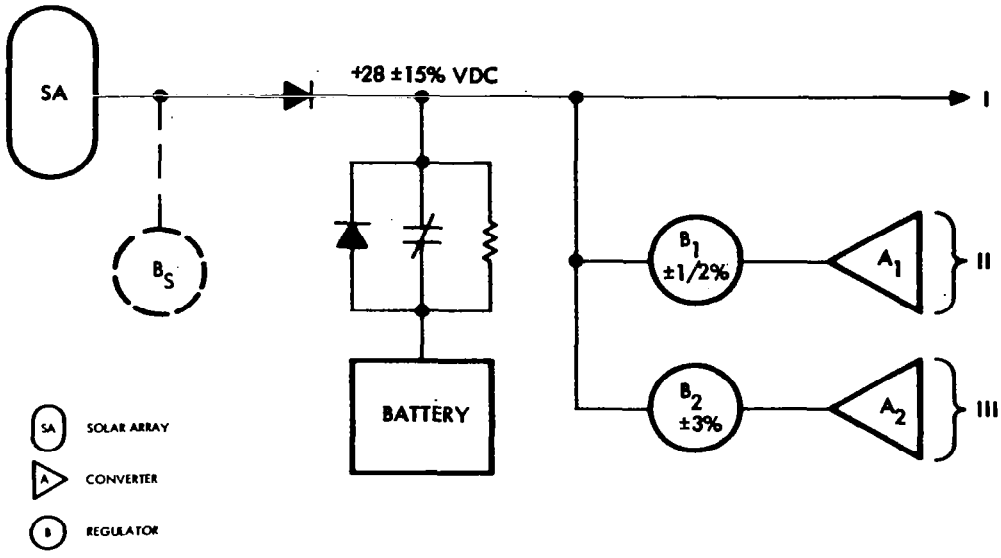

Figure 7-4. Mission I, Configuration 3

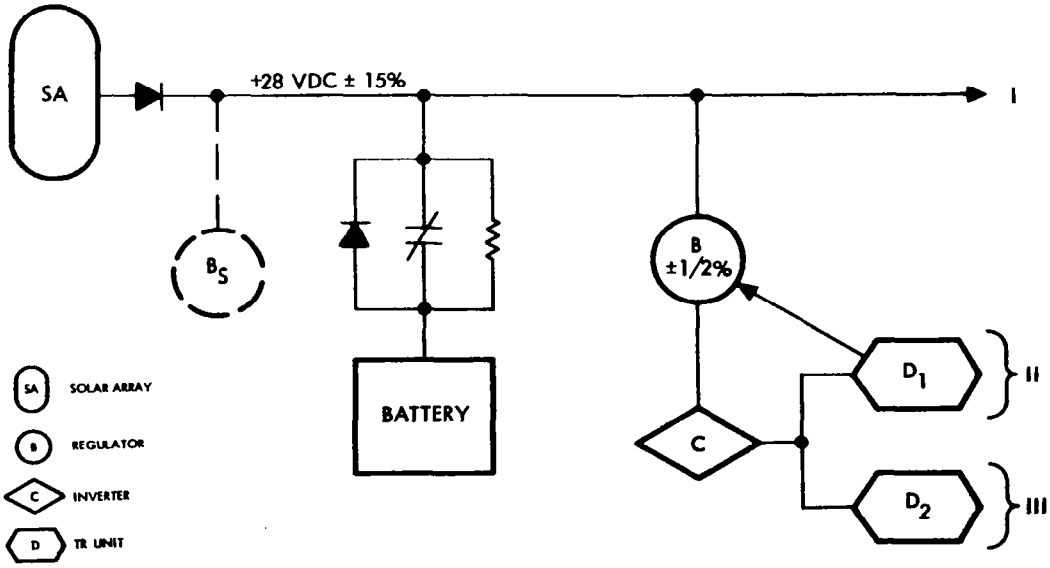

Figure 7-5. Mission I, Configuration 4

Table 7-V Mission I Load Voltage Assignments

Load	Voltage (dc)	Percent (±)	(w)	Total Power (w)
		Configuration 1		
I	+ 28	15	3.50*	3.5*
II	+1440	1/2	0.40	
	+1340	1/2	1.20	
	+ 650	1/2	9.40	
	+ 620	1/2	0.01	34.1
	+ 570	1/2	0.01	
	+ 550	1/2	17.90	
	+ 355	1/2	0.90	
	+ 3	1/2	4.30	
III	(Same as II)			34.1
IV	(Same as II)			34.1
V	(Same as II)			34.1
VI	+ 28	3	2.40	
	- 15	3	2.50	
	+ 15	3	2.90	15.1
	+ 10	3	2.60	
	- 6	3	1.40	
	+ 6	3	3.30	
				155.0
		- - - - - - - - - - - - - - -		
		Configurations 2, 3, and 4		
I	+ 28	15	3.50*	3.5*
II	+1440	1/2	1.60	
	+1340	1/2	4.80	
	+ 650	1/2	37.60	
	+ 620	1/2	0.04	
	+ 570	1/2	0.04	136.4
	+ 550	1/2	71.60	
	+ 355	1/2	3.60	
	+ 3	1/2	17.20	
III	+ 28	3	2.40	
	- 15	3	2.50	
	+ 15	3	2.90	15.1
	+ 10	3	2.60	
	- 6	3	1.40	
	+ 6	3	3.30	
				155.0

*Peak Power 36.3 w

Communications equipment loads are essentially constant, and it can be assumed that the voltage variation of the solar array battery bus will be due primarily to the illumination/temperature characteristics of the solar array and the charge/discharge characteristics of the battery. These variations would be within the ±15 percent required bus regulation at constant load. The addition of a solar array shunt regulator (voltage limiter) is shown (dotted) for each configuration, and would be needed to protect the battery from overvoltage if the system payload was turned off. The presence or absence of the shunt regulator (at full load) alters the system efficiencies for each configuration by a few tenths of one percent since its efficiency is 98 percent or better. Additional loss of system efficiency by the shunt regulator occurs only when light loads exist and excess solar array power is available.

The EPSOM method was applied to the four synthesized configurations. The dark-to-light ratio (S = 0.0526) for this mission was obtained from Figure 7-6, a plot of earth satellite orbital mission parameters. The values of efficiency (η) as a function of output power for each of the four types of power conditioning equipment were read from Figure 7-1. The maximum efficiency values were chosen for these mission examples only to demonstrate the application of EPSOM. Other values could be used from the parametric curves for an actual hardware design when more detailed load requirements are specified. For example, a frequency of 400 cps for all equipment may be specified by the satellite system requirements. Then a plot of 400-cps data points would be used.

The EPSOM equation derived in Section 6 for the total electrical power system efficiency (H) is:

$$H = \frac{\eta_c}{\left(\sum_{i=1}^{m} \frac{\Delta_i}{\eta_i} \right) \left[\frac{\frac{T}{t} - 1}{\eta_d} + 1 \right]}$$

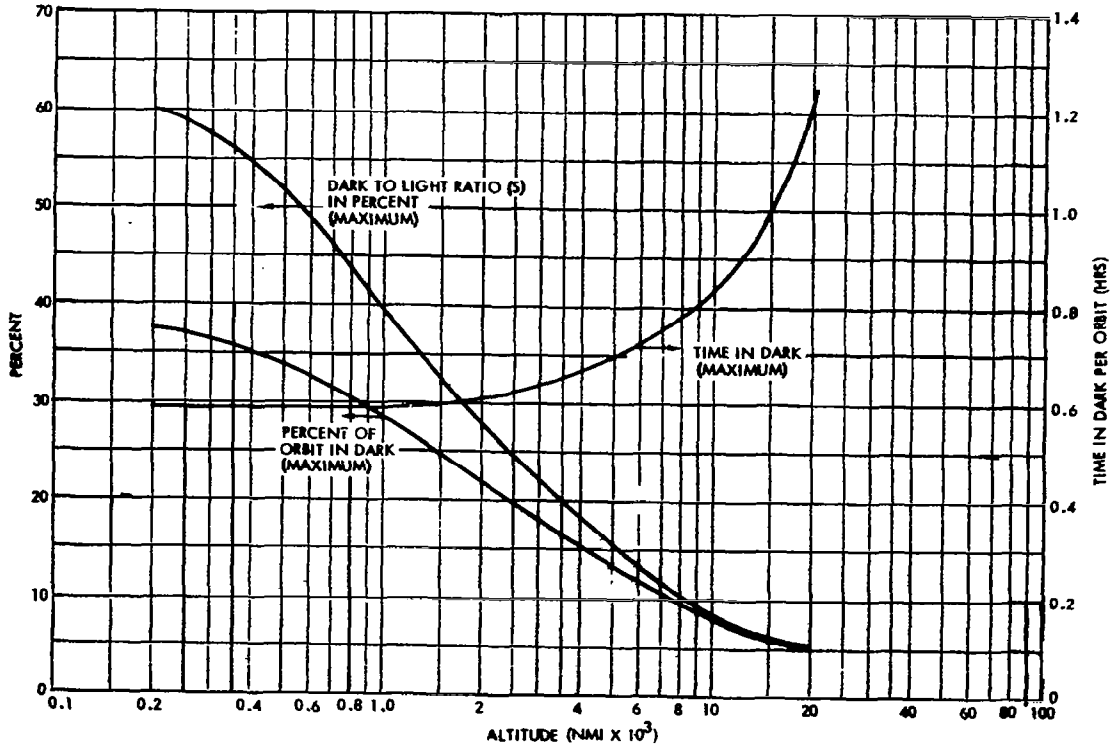

Figure 7-6. Mission Orbital Parameters

The evaluation of this equation for Mission I, Configuration 1, is as follows, with the values for intermediate steps summarized in Table 7-VI. The output power for each load equipment is assigned, and its percentage (Δ_i) of total output power is calculated. The efficiency (η_α) for each terminating equipment is determined from the curves of Figure 7-1. For the case of Load I, which is not power conditioned, it is considered at 100 percent efficiency. Loads II, III, IV and V each draw 34.1 w of power from converter A_1, A_2, A_3, and A_4, respectively. The converter curve, Figure 7-1, shows 83.7 percent efficiency at 34.1 w. Load VI is similarly calculated. The next step is to determine the output power (P_α) for each regulator (B_1 through B_5) by dividing each converter output power by its respective converter efficiency. Using these power values, the efficiencies (η_β) are determined from the regulator curve in Figure 7-1. By dividing each regulator output power by its respective efficiency, their input power (P_β) is determined. Since there are no more power conditioning equipments between the regulator inputs and the system power bus, the regulator inputs plus Load I can be summed to determine the total load bus power required from solar array or battery.

The battery (nickel-cadmium because of the mission life) amp-hr rating is determined from the load amp-hr and the cycle life derating factor as demonstrated in Appendix A. Next the watt hour efficiency is determined based upon charge and discharge rates and the respective battery temperatures. Because the battery is charged and discharged through relay contacts, the value of (η_d) in the (H) equation is equal to the battery watt hour efficiency. All configurations considered for Mission I require a nominal 14 amp-hr battery operating at 63 percent depth of discharge, and a watt hour efficiency of 70 percent. The watt hour efficiency is relatively low because of the low average charge rate.

The value of η_i in the (H) equation for each load (See Table 7-VI) is obtained by multiplying the efficiency values for each piece of power conditioning equipment in series, i.e., $\eta_{II} = \eta_{A1}\,\eta_{B1}$. The values of Δ_i/η_i are calculated for each load, i.e.,

$$\frac{\Delta_{II}}{\eta_{II}} = \frac{\Delta_{II}}{\eta_{A1}\,\eta_{B1}} = \frac{0.2200}{(0.837)\,(0.920)} = \frac{0.2200}{0.7700} = 0.2857$$

Table 7-VI. Mission I Configuration Evaluations

LOAD	OUTPUT W	Δ_i	η_α	P_α	η_β	P_β	η_γ	P_γ	η_i	Δ_i/η_i
Configuration 1										
I	3.5	0.0226	-	-	1.000	3.50			1.0000	0.0226
II	34.1	0.2200	0.837	40.74	0.920	44.28			0.7700	0.2857
III	34.1	0.2200	0.837	40.74	0.920	44.28			0.7700	0.2857
IV	34.1	0.2200	0.837	40.74	0.920	44.28			0.7700	0.2857
V	34.1	0.2200	0.837	40.74	0.920	44.28			0.7700	0.2857
VI	15.1	0.0974	0.786	19.21	0.913	21.04			0.7180	0.1357
Total	155.0	1.0000	-	-	-	201.66			-	1.3011
Total Bus						201.66				-
$\Sigma\Delta_i/\eta_i$										1.3011
$1/\Sigma$										0.7686
Configuration 2										
I	3.5	0.0226	-	-	1.000	3.50			1.0000	0.0226
II	136.4	0.8800	0.885	154.12	0.925	166.62			0.8186	1.0750
III	15.1	0.0974	0.786	19.21	0.925	20.77			0.7271	0.1340
Total	155.0	1.0000	-	173.33	0.925	190.89				1.2316
Total Bus						190.89				-
$\Sigma\Delta_i/\eta_i$										1.2316
$1/\Sigma$										0.8120
Configuration 3										
I	3.5	0.0226	-	-	1.000	3.50			1.0000	0.0226
II	136.4	0.8800	0.885	154.12	0.925	166.62			0.8186	1.0750
III	15.1	0.0974	0.786	19.21	0.913	21.04			0.7176	0.1357
Total	155.0	1.0000	-	-	-	191.16				1.2333
Total Bus						191.16				-
$\Sigma\Delta_i/\eta_i$										1.2337
$1/\Sigma$										0.8108
Configuration 4										
I	3.5	0.0226	-	-	-	-	1.000	3.50	1.0000	0.0226
II	136.4	0.8800	0.949	143.73	0.952	150.98	0.925	163.22	0.8357	1.0530
III	15.1	0.0974	0.930	16.24	0.952	17.06	0.925	18.44	0.8190	0.1189
Total	155.0	1.0000	-	159.97	0.952	168.04	0.925	185.16	-	1.1945
Total Bus								185.16	-	-
$\Sigma\Delta_i/\eta_i$								-	-	1.1945
$1/\Sigma$								-	-	0.8372

Then the value of

$$\sum \frac{\Delta_i}{\eta_i}$$

and its reciprocal are calculated (See Table 7-VI). The values of:

$$\left(\frac{\tau}{t} - 1\right) = S = 0.0526$$

$$\eta_d = 0.70$$

$$\eta_A = 0.10 \quad \text{(assumed constant for all configurations)}$$

$$\eta_c = \eta_A$$

are substituted into the (H) equation. η_c equals η_A since there are no more power conditioning equipments to consider. If the solar array shunt regulator is included, then $\eta_c = \eta_{B_s}\,\eta_A$. The value of H for Configuration 1 is:

$$H = \frac{0.10}{(1.3011)\left(\frac{0.0526}{0.70} + 1\right)} = 0.0715 = 7.15 \text{ percent}$$

The total average power required from the solar array can be determined by dividing the total output power (155 w) to the loads by the value of H/η_A (0.715). For Configuration 1 this is 216.8 w. The differences between the total average solar array power and the total load bus power is the power delivered to the battery for charging (15.2 w). Table 7-VII summarizes the power system performance values for each of the four configurations.

Applying the EPSOM evaluation method to the four proposed system configurations resulted in an improvement of power system efficiency for Configuration 4 approximately 9 percent over Configuration 1. The solar array of Configuration 4 is 17.74 w smaller than the array for Configuration 1.

Table 7-VII. Mission I Summary

Configuration	Power Out (w)	Bus Power (w)	Array Power (w)	Array Power Differential (w)	*System Efficiency (H) Percent
1	155.0	201.66	216.82	17.74	7.15
2	155.0	190.89	205.25	6.17	7.55
3	155.0	191.16	205.57	6.49	7.54
4	155.0	185.16	199.08	0	7.79

*Assumes solar cell array efficiency to be 10 percent AMO.

This system improvement is attributable to the 16.5 w reduction in bus power because of the improved net efficiency of the power conditioning equipment, and the additional 1.24 w saved by not requiring the battery to deliver this 16.5 w during the dark period. The EPSOM method of evaluating all proposed configurations provides a positive configuration selection. Additionally, the method permits identification of those equipments and/or equipment groupings contributing the most to the system power losses. Knowing where and how the losses are generated permits the design engineer to improve individual equipment designs as well as suggesting better system configurations.

7.3.2 Mission II Configurations

The payload for Mission II could be of several varieties such as weather mapping; geodetic surveys; geotectonic surveys; and land, air, and sea navigational aids. The payload power requirements defined by Table 7-VIII were chosen for a representative weather mapping satellite. A TWT transmitter was selected for data transmittal to earth stations. Similar to the TWTs of Mission I, it requires high voltages that are closely regulated and magnitude related. Other high voltages are required for optical sensors which scan the atmosphere of the earth for weather data. As previously discussed in Paragraph 7.1.2, a sun-synchronous orbit can be of two types. The attitude control system for either type requires a significant amount of electrical power. That

Table 7-VIII. Mission II Load Power Requirements

Item No.	Voltage	V-Amps/w	Percent Regulation	Phase	Voltage x Power	Percent of Total Power
1.	+5000 dc	0.6*	±10		3000.0	0.36
2.	+1000 dc	0.1	± 1		100.0	0.06
3.	- 940 dc	9.4**	± 1/2		8836.0	5.63
4.	- 545 dc	15.0**	± 1		8175.0	8.98
5.	+ 450 dc	0.1	± 3		45.0	0.06
6.	+ 300 dc	5.0*	± 3		1500.0	2.99
7.	+ 150 dc	0.1	± 3		15.0	0.06
8.	115 ac	40/20.0***	+20, -15	ϕA	2300.0	11.98
9.	115 ac	20/10.0***	+20, -15	ϕB	1150.0	5.99
10.	+ 80 dc	0.4**	± 1		32.0	0.24
11.	+ 50 dc	0.3	± 3		15.0	0.18
12.	28 ac	30/15.0***	± 2	ϕB	420.0	8.98
13.	+ 28 dc	10.0	+20, -15		280.0	5.99
14.	+ 28 dc	12.0	± 2		336.0	7.19
15.	+ 20 dc	3.0	± 3		60.0	1.80
16.	- 20 dc	3.0	± 3		60.0	1.80
17.	+ 16 dc	20.0	± 3		320.0	11.98
18.	- 16 dc	8.0	± 3		128.0	4.79
19.	+ 12 dc	5.0	± 3		60.0	2.99
20.	+ 6 dc	7.0	± 3		42.0	4.19
21.	- 6 dc	5.0	± 3		30.0	2.99
22.	6 ac	5.0	± 3	ϕA	30.0	2.99
23.	+ 4.2 dc	13.0	± 3		54.6	7.78
		212.0/167.0				100.0

*Must be from same converter.
**TWT, must be from same converter.
***Same subsystem.

portion of the power required for the power gyros (flywheels) is usually two-phase ac, and thus should be generated in the same equipment to maintain proper synchronization and phasing. The total satellite power requirements (167 w) can be divided into three major categories — payload (62 w), attitude control subsystem (65 w), and communication and data handling (40 w).

If the satellite power were to increase to 500 w, the growth would occur in the payload and communications and data handling equipment. The following allocation of power is estimated for a 500-w system.

Payload	-	270 w
Attitude control	-	90 w
Communication and data handling	-	140 w

Table 7-IX provides the load voltages and the Load Requirements Organization. The following observations can be made about the load power requirements for the 167-w system:

- The ac loads constitute 30 percent of the total load, and 60 percent of the ac loads require loose regulation.
- Only three outputs, amounting to less than 10 w, require regulation better than 2 percent.
- The lower (<100 v) dc voltages making up 46 percent of the total power require only moderate regulation.

A review of the organization analysis given in Table 7-IX shows that the first six preferred voltages are ranked within the first nine positions. Considering this result and the need for grouping the ac requirements and the high voltage requirements, Table 7-X summarizes the load assignments used for Mission II, Configurations 1 through 5. These five configurations are shown in Figures 7-7 through 7-11.

The system bus voltage was chosen to be 28 vdc in order to minimize the voltage conversion for unregulated type loads. The solar array battery regulation should provide better than the required +20, -15 percent. A possible solar array shunt regulator (voltage limiter) is also included for this mission and has the same considerations enumerated for Mission I.

Table 7-IX. Mission II Load Requirements Organization

Item No.	Output Voltage	Voltage Rank	Power Rank	VxP Rank	$\Sigma_{A,B,C}$	$\Sigma_{A,B,C}$ Rank	V Reg. Rank	Cumulative Percent of Total Power for A	Cumulative Percent of Total Power for B	Cumulative Percent of Total Power for C	Cumulative Percent of Total Power for D	Cumulative Percent of Total Power for Vac	Cumulative Percent of Total Power for Vdc
-	-	A	B	C	-	D	E	F	G	H	I	J	K
1. **	+5000 dc	1	18	1	20	4	4	0.36	99.39	0.36	26.95	-	0.36
2.	+1000 dc	2	21	12	35	11	20	0.42	99.87	74.91	70.12	-	0.42
3. *	- 940 dc	3	9	5	17	3	23	6.00	74.49	26.95	26.59	-	6.00
4. *	- 545 dc	4	3	6	13	2	21	15.00	32.93	35.93	20.96	-	15.00
5.	+ 450 dc	5	22	17	44	13	5	15.10	99.93	89.34	74.97	-	15.10
6. **	+ 300 dc	6	12	3	21	6	6	18.10	86.46	15.33	35.93	-	18.10
7.	+ 150 dc	7	23	22	52	20	7	18.14	99.99	99.81	93.83	-	18.14
8. ***	115 ac	8	1	2	11	1	1	30.12	11.98	12.34	11.98	11.98	-
9. ***	115 ac	9	7	4	20	5	2	36.11	62.87	21.32	32.93	17.96	-
10. *	+ 80 dc	10	19	19	48	18	22	36.35	99.63	93.77	89.58	-	18.38
11.	+ 50 dc	11	20	23	54	21	8	36.53	99.81	99.99	94.01	-	18.56
12. ***	28 ac	12	4	7	23	7	18	45.51	41.92	44.91	44.91	26.95	-
13.	+ 28 dc	13	8	10	31	10	3	51.50	68.86	70.06	70.06	-	24.55
14.	+ 28 dc	14	6	8	28	8	19	58.68	56.89	52.10	52.10	-	31.74
15.	+ 20 dc	15	16	13	44	14	9	60.48	97.23	76.71	76.77	-	33.53
16.	- 20 dc	16	17	14	47	16	10	62.28	99.03	78.50	86.35	-	35.33
17.	+ 16 dc	17	2	9	28	9	11	74.25	23.95	64.07	64.07	-	47.31
18.	- 16 dc	18	10	11	39	12	12	79.04	79.28	74.85	74.91	-	52.10
19.	+ 12 dc	19	13	15	47	17	13	82.03	89.45	81.50	89.34	-	55.09
20.	+ 6 dc	20	11	18	49	19	14	86.22	83.47	93.53	93.77	-	59.28
21.	- 6 dc	21	14	20	55	22	15	89.21	92.44	96.76	97.00	-	62.28
22.	6 ac	22	15	21	58	23	16	92.20	95.43	99.75	99.99	29.94	-
23.	+ 4.2 dc	23	5	16	44	15	17	99.99	49.70	89.28	84.55	-	70.06

*TWT, require own converters.
**Equipment require voltages together.
***Same equipment, two-phase power.

Table 7-X. Mission II Load Voltage Assignments

LOAD	VOLTAGE	PERCENT	w	w
I	+28 dc	+20, -15	10.0	10.0
II	+50 dc	±3	0.3	
	+28	±2	12.0	
	+20	±3	3.0	
	-20	±3	3.0	
	+16	±3	20.0	76.3
	-16	±3	8.0	
	+12	±3	5.0	
	+ 6	±3	7.0	
	- 6	±3	5.0	
	+ 4.2	±3	13.0	
III	+5,000 dc	±10	0.6	
	+1,000	± 1	0.1	
	+ 450	± 3	0.1	5.9
	+ 300	± 3	5.0	
	+ 150	± 3	0.1	
IV	- 940 dc	±0.5	9.4	
	- 545	±1	15.0	24.8
	+ 80	±1	0.4	
V	115 ac ØA	+20, -15	20.0	
	115 ac ØB	+20, -15	10.0	
	28 ac ØB	± 2	15.0	50.0
	6 ac ØA	± 3	5.0	
		Total		167.0

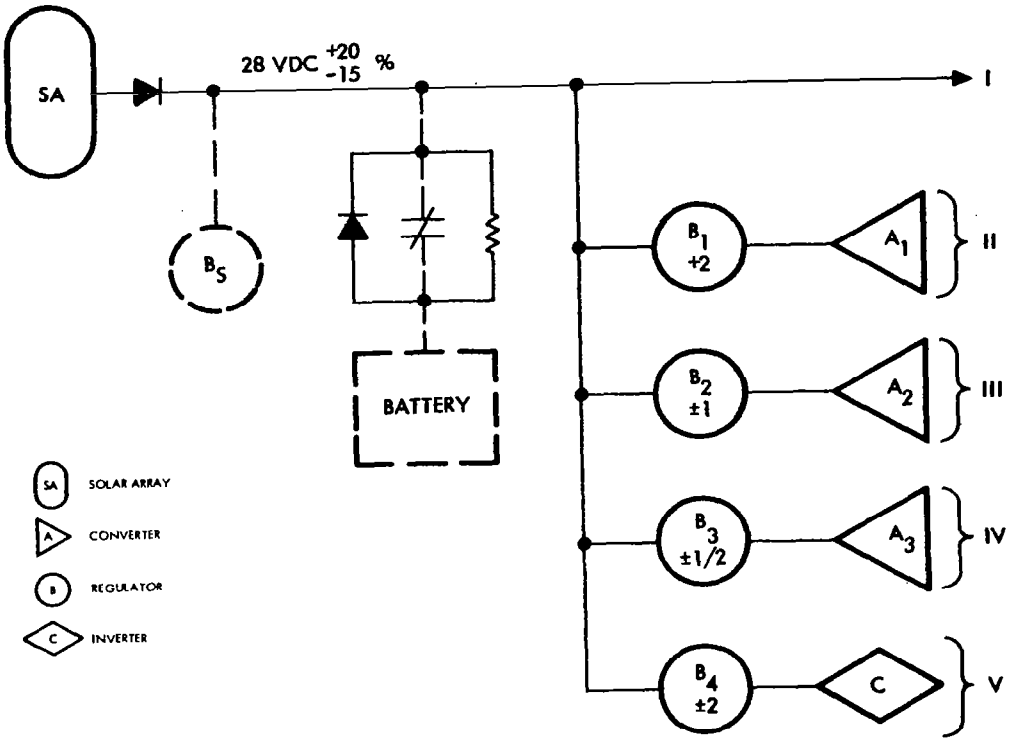

Figure 7-7. Mission II, Configuration 1

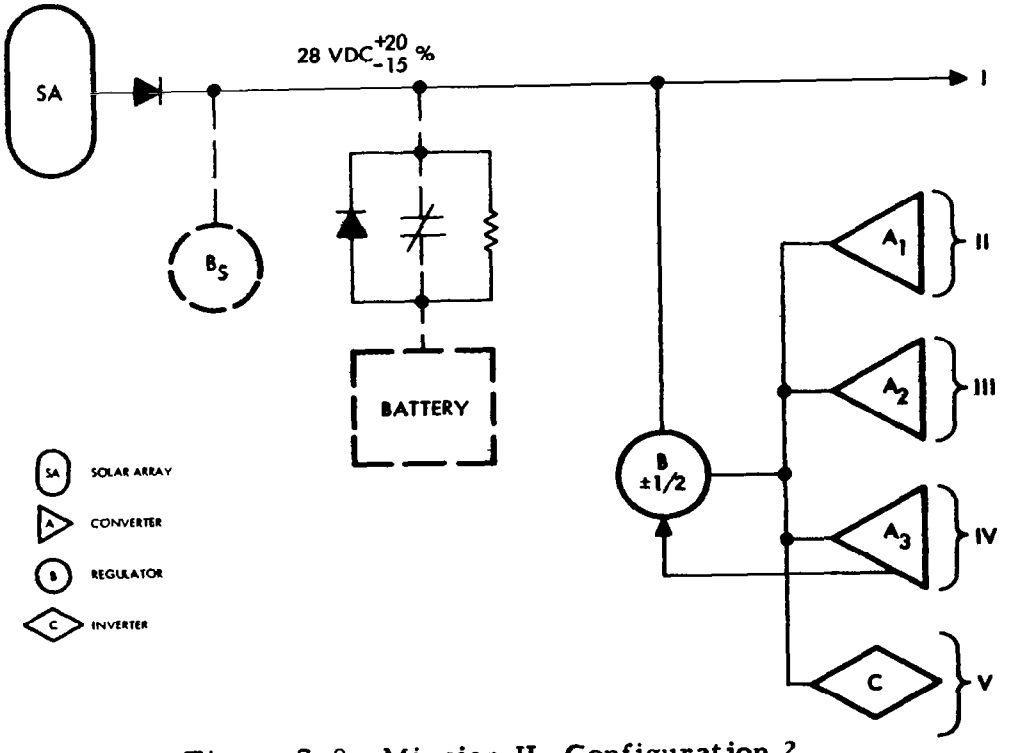

Figure 7-8. Mission II, Configuration 2

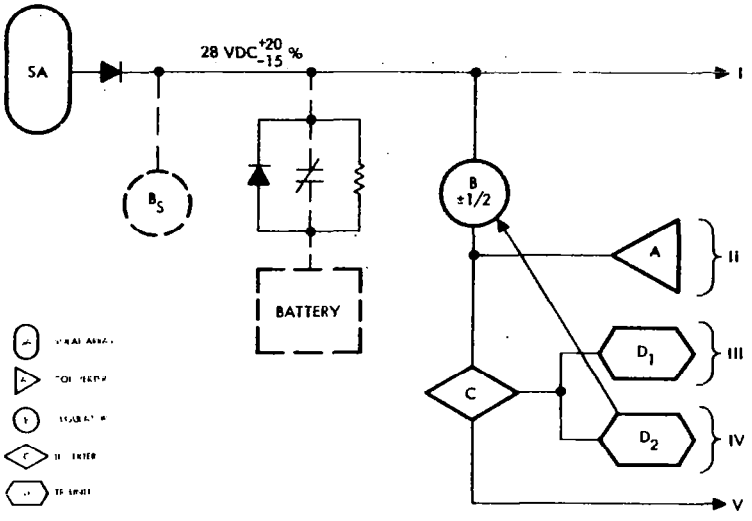

Figure 7-9. Mission II. Configuration 3

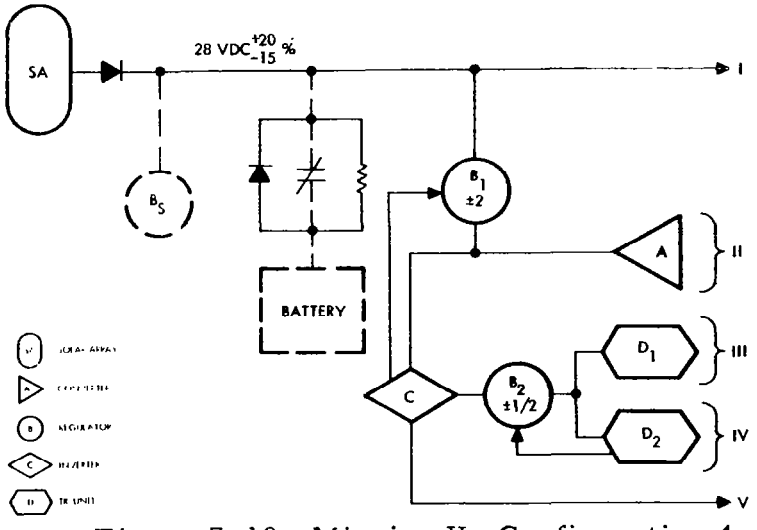

Figure 7-10. Mission II, Configuration 4

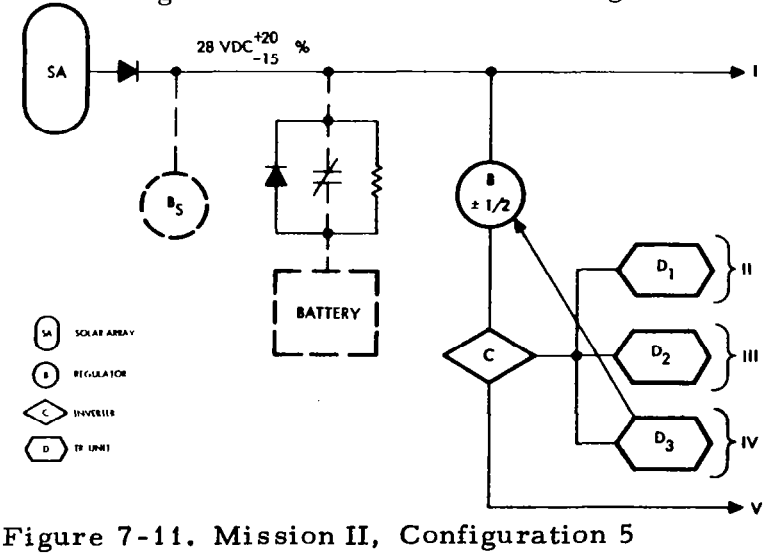

Figure 7-11. Mission II, Configuration 5

The EPSOM technique was used to compare the five synthesized configurations. The dark-to-light ratio (S) was determined to be 0.487 (Figure 7-6) for the noon-midnight orbit. The same step-by-step process, as used for Mission I, was used to determine numerical values for substitution into the (H) equation. Table 7-XI summarizes each configuration evaluation. The specified three-year life requires a minimum of 14,460 battery cycles for the noon-midnight orbit. Therefore, a nickel-cadmium battery operating at 20 percent depth of discharge is required (see Section 5.4.2). The battery should have a 25 amp-hr capacity operating at 76.5 percent w-hr efficiency. It should be noted that the twilight orbit does not require a battery except for launch and initial attitude acquisition. The major effect on the power system of no battery is the higher system efficiency and smaller solar array required. The solar array efficiency (η_A) was again assumed to be 10 percent so that relative comparisons would be easy. Table 7-XII summarizes the results of the configuration evaluations for both extremes of a sun-synchronous orbital launch. A significant improvement in system performance is shown for the twilight orbit.

Although there is only 0.22 percent difference in system efficiency between the best configuration (No. 5) and the lowest efficiency configuration (No. 1), it represents a 14.43 w smaller solar array for the noon-midnight orbit. Sixty-one percent of this 14.43 w is attributed to the power conditioning equipment efficiencies and the remaining 5.6 w to the processing of that power by the battery.

The value of the EPSOM method is shown by this mission example. Not only can one evaluate all proposed configurations in a simple, positive manner, but the equipments responsible for the system inefficiencies can be readily identified. The same mission launched into the twilight sun-synchronous orbit and using the same best configuration (No. 5), would reduce the required solar array by 124.87 w which is 63.7 percent of the bus power. Additionally, the weight of the battery and charge controls could be eliminated with the attendant improvement in reliability. The total weight savings as a result of the smaller solar array, elimination of the secondary battery, and the charge controls, as well as a significant reliability improvement, indicate the advantage of the twilight orbit selection.

Table 7-XI. Mission II Configuration Evaluations

LOAD	OUTPUT W	Δ_i	η_α	P_α	η_β	P_β	η_γ	P_γ	η_δ	P_δ	η_i	Δ_i/η_i
Configuration 1												
I	10.0	0.0599	-	-	1.000	10.00					1.0000	0.0599
II	76.3	0.4569	0.869	87.80	0.923	95.12					0.8021	0.5696
III	5.9	0.0353	0.695	8.49	0.900	9.43					0.6255	0.0564
IV	24.8	0.1485	0.820	30.24	0.918	32.94					0.7528	0.1973
V	50.0	0.2994	0.945	52.91	0.921	57.45					0.8703	0.3440
Total	167.0	1.0000	-	179.44	-	204.94					-	1.2272
Total Bus						204.94						-
$\Sigma\Delta_i/\eta_i$												1.2272
$1/\Sigma$												0.8149
Configuration 2												
I	10.0	0.0599	-	-	1.000	10.00					1.0000	0.0599
II	76.3	0.4569	0.869	87.80	0.925	94.92					0.8038	0.5684
III	5.9	0.0353	0.695	8.49	0.925	9.18					0.6429	0.0549
IV	24.8	0.1485	0.820	30.24	0.925	32.69					0.7585	0.1958
V	50.0	0.2994	0.945	52.91	0.925	57.20					0.8741	0.1425
Total	167.0	1.0000	-	179.44	0.925	203.99					-	1.2215
Total Bus						203.99						-
$\Sigma\Delta_i/\eta_i$												1.2215
$1/\Sigma$												0.8187
Configuration 3												
I	10.0	0.0599	-	-	-	-	1.000	10.00			1.0000	0.0599
II	76.3	0.4569	-	-	0.869	87.80	0.925	94.93			0.8038	0.5684
III	5.9	0.0353	0.921	6.41	0.949	6.75	0.925	7.30			0.8085	0.0437
IV	24.8	0.1485	0.933	26.58	0.949	28.00	0.925	30.27			0.8190	0.1813
V	50.0	0.2994	-	50.00	0.949	52.69	0.925	56.96			0.8778	0.3411
Total	167.0	1.0000	-	82.99	0.949	175.24	0.925	199.46			-	1.1944
Total Bus								199.46				-
$\Sigma\Delta_i/\eta_i$												1.1944
$1/\Sigma$												0.8372
Configuration 4												
I	10.0	0.0599	-	-	-	-	-	-	1.000	10.00	1.0000	0.0599
II	76.3	0.4569	-	-	-	-	0.869	87.80	0.925	94.92	0.8038	0.5684
III	5.9	0.0353	0.921	6.41	0.919	6.97	0.949	7.35	0.925	7.95	0.7430	0.0475
IV	24.8	0.1485	0.933	26.58	0.919	28.92	0.949	30.47	0.925	32.94	0.7527	0.1973
V	50.0	0.2994	-	-	-	50.00	0.949	52.69	0.925	56.96	0.8778	0.3411
Total	167.0	1.0000	-	32.99	0.919	85.89	0.949	178.31	0.925	202.77	-	1.2142
Total Bus										202.77	-	-
$\Sigma\Delta_i/\eta_i$												1.2142
$1/\Sigma$												0.8236
Configuration 5												
I	10.0	0.0599	-	-	-	-	1.000	10.00			1.0000	0.0599
II	76.3	0.4569	0.943	80.91	0.952	84.99	0.925	91.88			0.8304	0.5502
III	5.9	0.0353	0.921	6.41	0.952	6.73	0.925	7.28			0.8110	0.0435
IV	24.8	0.1485	0.933	26.58	0.952	27.92	0.925	30.18			0.8216	0.1807
V	50.0	0.2994	-	50.00	0.952	52.52	0.925	56.78			0.8806	0.3400
Total	167.0	1.0000	-	163.90	0.952	172.16	0.925	196.12			-	1.1743
Total Bus								196.12				-
$\Sigma\Delta_i/\eta_i$												1.1743
$1/\Sigma$												0.8516

Table 7-XII. Mission II Summary

Noon-Midnight Orbit					
Configuration	Power Out (w)	Bus Power (w)	Array Power (w)	Array Power Differential (w)	*System Efficiency (H) Percent
1	167.0	204.93	335.40	14.43	4.98
2	167.0	203.98	333.82	12.90	5.00
3	167.0	199.47	326.49	5.52	5.12
4	167.0	202.77	331.88	10.91	5.03
5	167.0	196.10	320.97	0	5.20
Twilight Orbit					
Configuration	Power Out (w)	Bus Power (w)	Array Power (w)	Array Power Differential (w)	*System Efficiency (H) Percent
1	167.0	204.93	204.93	8.83	8.15
2	167.0	203.98	203.98	7.88	8.19
3	167.0	199.47	199.47	3.37	8.37
4	167.0	202.77	202.77	6.67	8.24
5	167.0	196.10	196.10	0	8.52

*Assumes Solar Cell Array efficiency to be 10 percent AMO.

7.3.3 Mission III Configurations

The payload for Mission III is scientific experiments. Section 3.4 presented a summary of the power requirements for many types of satellite experiment packages. In general, each experiment consumes relatively little power, but most scientific satellites carry many experiments which account for 30 to 50 percent of the total system load. A large variety of voltages are usually specified and many of them have regulations of one percent or better. Most satellites designed to carry scientific experiments are required to be adaptable to a variety of experiment groups. This diversity of experiments establishes a need for a very stable, well-oriented satellite having the flexibility of providing a near optimum environment for each experiment. Similarly, the power system must be flexible in its capabilities and still provide a stable energy source for the experiments, attitude control system, data handling, and communication equipment. Tables 7-XIII and 7-XIV present the system load power requirements and power requirement organization for Mission III.

Four power system configurations were synthesized which satisfy these load requirements. They are presented in Figures 7-12 through 7-15. The ac loads constitute over 60 percent of the total system power and require very little regulation, if any. These facts suggest a centralized inverter with some of its outputs regulated and rectified as needed for the dc requirements. The combinations of power conditioning equipment used in synthesizing the four configurations required the regrouping of the voltages. Table 7-XV presents the voltage assignments for each of the four configurations.

The EPSOM technique was again used to compare and evaluate the relative system efficiencies. The orbit requirements for this mission as stated in Table 7-I allow some variation in orbit period and eclipse time depending upon the exact orbit eccentricity and launch time. An orbital period (τ) of 180 hr with a 2.5 hr eclipse was chosen for this mission example. The dark-to-light ratio (S) is therefore 0.01408. This long orbit period results in 48 to 49 eclipses per year, allowing a 90 percent depth of discharge for the battery. The low number of discharge cycles, the long sunlight periods for charging, and continuously warm vehicle temperatures suggest the use of a silver-cadmium battery. The discharge

Table 7-XIII. Mission III Load Power Requirements

Item No.	Voltage	V Amps/w	Percent Regulation	Frequency	Remarks	Voltage x Power	Percent of Total Power
1.	135 ac	302/100.7	+20, -15	400 cps	ϕA	13,594.5	36.17
2.	125 ac	139/46.3	+20, -15	400 cps	ϕB	5,787.5	16.63
3.	115 ac	15/8.0	±2.0	400 cps		920.0	2.87
4.	+ 70 dc	42.3	±2.0			2,961.0	15.19
5.	+ 28 dc	9.0	+20, -15			252.0	3.23
6.	28 ac	12/10.8	+20, -15	400 cps		302.4	3.88
7.	26 ac	6/2.0	+20, -15	400 cps		52.0	0.72
8.	+ 23 dc	5.8	±2.0			133.4	2.08
9.	+ 20 dc	7.0	±1.5		C.T. GRD	140.0	2.51
10.	- 20 dc	7.0	±1.5		C.T. GRD	140.0	2.51
11.	18 ac	3/1.6	±2.0	400 cps		28.8	0.57
12.	+ 16 dc	11.3	±1.0		C.T. GRD	186.2	4.06
13.	- 16 dc	0.4	±1.0		C.T. GRD	6.4	0.14
14.	+ 10 dc	0.5	±3.0			5.0	0.18
15.	+ 9 dc	21.1	±1.0			190.3	7.58
16.	- 6 dc	4.1	±1.0			24.7	1.47
17.	+ 5 dc	0.5	±1.0			2.5	0.18
		477/278.4					99.97

Table 7-XIV. Mission III Load Requirements Organization

Item No.	Output Voltage	Voltage Rank	Power Rank	VxP Rank	∑A, B, C	∑A, B, C Rank	Cumulative Percent of Total Power For A	Cumulative Percent of Total Power For B	Cumulative Percent of Total Power For C	Cumulative Percent of Total Power For D	Volt Reg Rank	Cumulative Percent of Total Power For Vac	Cumulative Percent of Total Power For Vdc
		A	B	C	–	D	E	F	G	H	I	J	K
1.	135 ac	1	1	1	3	1	36.17	36.17	36.17	36.17	1	36.17	–
2.	125 ac	2	2	2	6	2	52.80	52.80	52.80	52.80	2	52.80	–
3.	115 ac	3	8	4	15	4	55.67	89.61	70.86	70.86	7	55.67	–
4.	+70 dc	4	3	3	10	3	70.86	67.99	67.99	67.99	8	–	15.19
5.	+28 dc	5	7	6	18	6	74.09	86.74	77.97	77.97	3	–	18.42
6.	28 ac	6	6	5	17	5	77.97	83.51	74.74	74.74	4	59.55	–
7.	26 ac	7	13	12	32	12	78.69	98.90	97.43	97.43	5	60.27	–
8.	+23 dc	8	11	11	30	11	80.77	96.71	96.71	96.71	9	–	20.50
9.	+20 dc	9	10	9	28	9	83.28	94.63	92.12	92.12	11	–	23.01
10.	-20 dc	10	9	10	29	10	85.79	92.12	94.63	94.63	12	–	25.52
11.	18 ac	11	14	13	38	13	86.36	99.47	98.00	98.00	10	60.84	–
12.	+16 dc	12	5	8	25	7	90.42	79.63	89.61	82.03	13	–	29.58
13.	-16 dc	13	17	15	45	15	90.56	99.97	99.61	99.61	14	–	29.72
14.	+10 dc	14	15	16	45	16	90.74	99.65	99.79	99.79	6	–	29.90
15.	+ 9 dc	15	4	7	26	8	98.32	75.57	85.55	89.61	15	–	37.48
16.	- 6 dc	16	12	14	42	14	99.79	98.18	99.47	99.47	16	–	38.95
17.	+ 5 dc	17	16	17	50	17	99.97	99.83	99.97	99.97	17	–	39.13

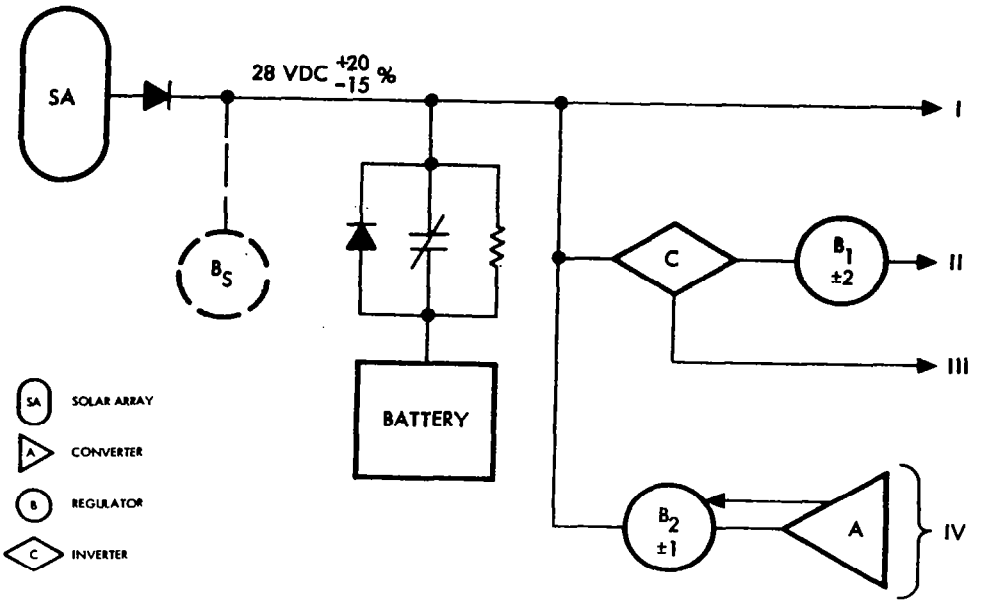

Figure 7-12. Mission III, Configuration 1

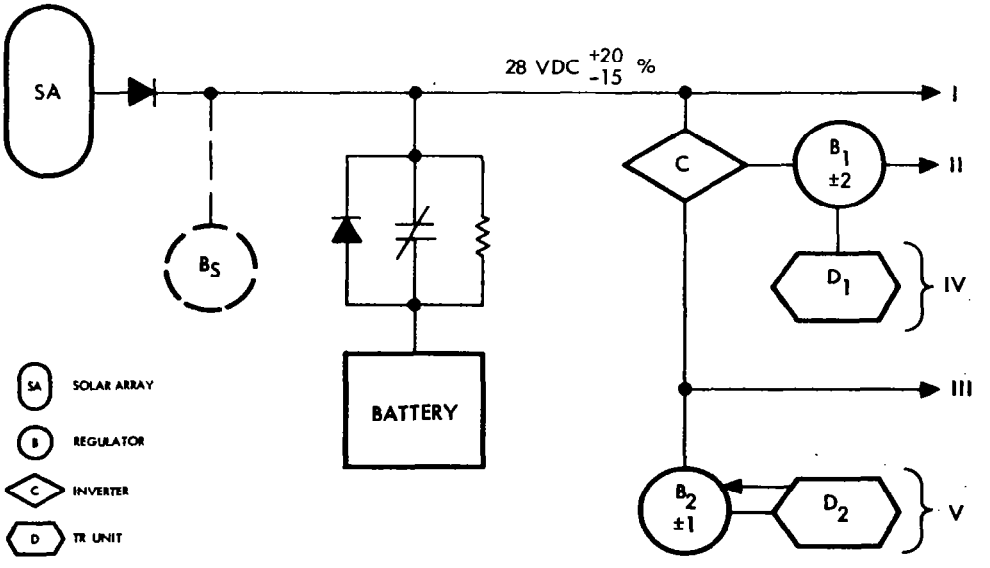

Figure 7-13. Mission III, Configuration 2

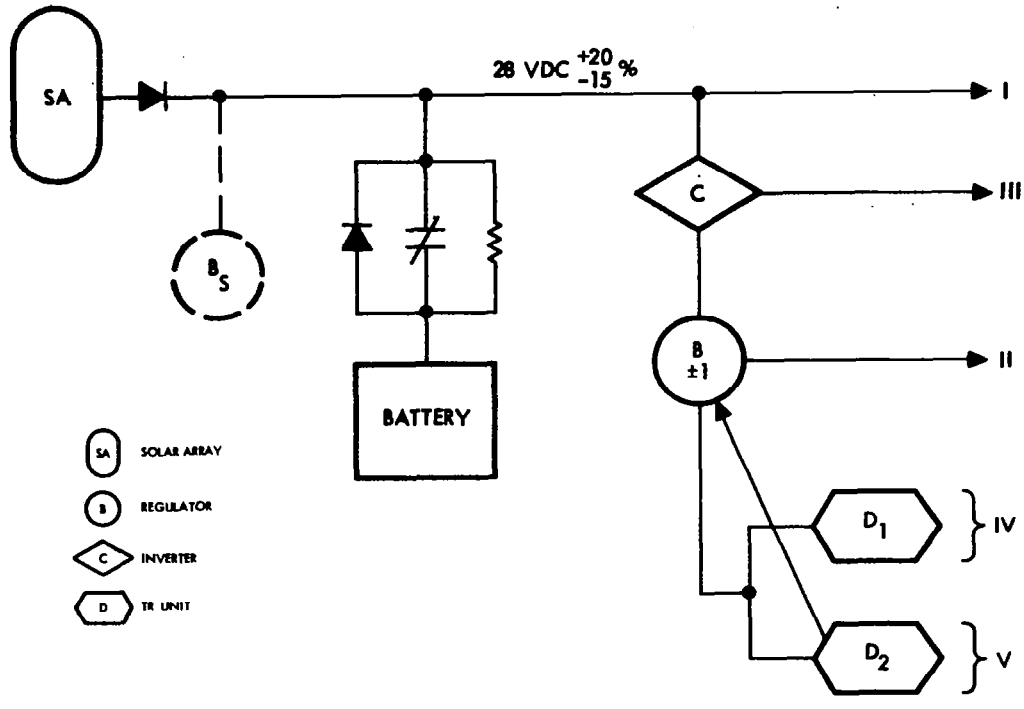

Figure 7-14. Mission III, Configuration 3

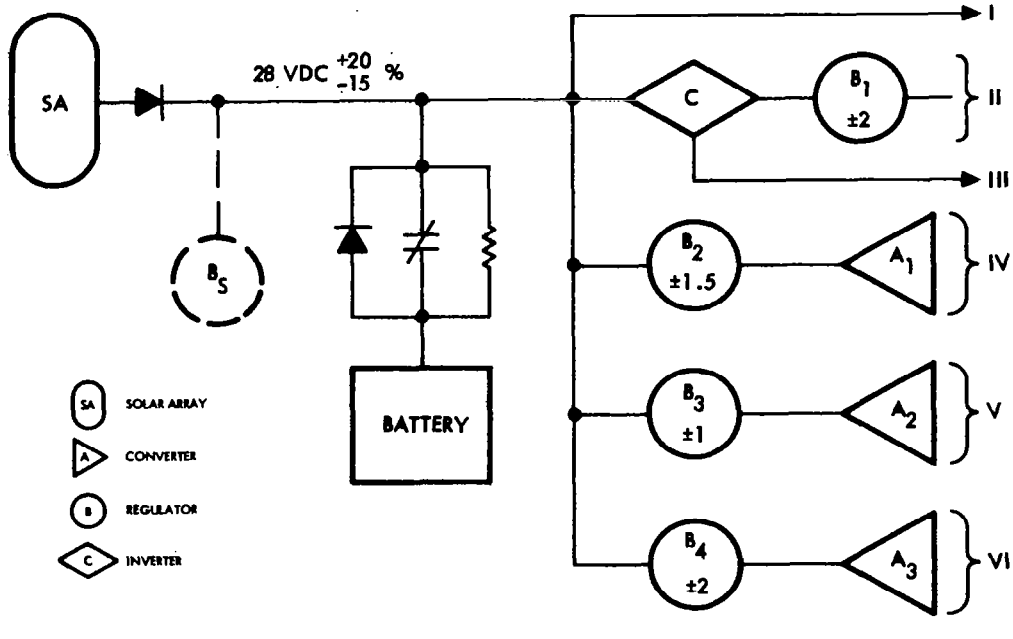

Figure 7-15. Mission III, Configuration 4

Table 7-XV. Mission III Load Voltage Assignments

Load	Configuration 1			Load	Configuration 2 or 3			Load	Configuration 4		
	(V)	(Percent)	(W)		(V)	(Percent)	(W)		(V)	(Percent)	(W)
I	28 dc	+20, -15	9.0	I	+28 dc	+20, -15	9.0	I	+28 dc	+20, -15	9.0
II	115 ac	±2	9.6	II	115 ac	±2	9.6	II	115 dc	±2	9.6
	18 ac	±2			18 ac	±2			18 dc	±2	
III	135 ac	+20, -15	159.8	III	135 ac	+20, -15	159.8	III	135 dc	+20, -15	149.0
	125 ac	+20, -15			125 ac	+20, -15			125 dc	+20, -15	
	28 ac	+20, -15			28 ac	+20, -15			26 ac	+20, -15	
	26 ac	+20, -15			26 ac	+20, -15					
IV	+70 dc	±2	100.0	IV	+70 dc	±2	48.6	IV	+20 dc	±1.5	25.3
	+23 dc	±2			+23 dc	±2			+10 dc	±3.0	
	+20 dc	±1.5			+10 dc	±3			-20 dc	±1.5	
	-20 dc	±1.5							28 ac	+20, -15	
	+16 dc	±1.0		V	+20 dc	±1.5	51.4	V	+16 dc	±1.0	37.4
	-16 dc	±1.0			-20 dc	±1.5			+9 dc	±1.0	
	+10 dc	±3.0			+16 dc	±1.0			+5 dc	±1.0	
	+9 dc	±1.0			-16 dc	±1.0			-6 dc	±1.0	
	-6 dc	±1.0			+9 dc	±1.0			-16 dc	±1.0	
	+5 dc	±1.0			-6 dc	±1.0					
					+5 dc	±1.0		VI	+70 dc	±2	48.1
									+23 dc	±2	
		Total	278.4			Total	278.4			Total	278.4

would be approximately C/2.5 which is acceptable for good performance from the silver-cadmium.

Table 7-XVI presents the calculation values for evaluating the system efficiency equation (H). The battery capacity required is 30 amp-hr, and can be operated at a w-hr efficiency of 70.2 percent. This relatively low efficiency is due to the extremely long charge period causing the battery to reach full charge and then standby on trickle charge.

Although the total load power for this mission is approximately twice the power specified for Missions I and II, the system efficiency for all configurations is the highest. Usually the higher power delivered from batteries causes low system efficiencies. Mission III is an exception, due to the highly eccentric orbit which provides an excellent value for (S). The configuration comparative analysis for Mission III is summarized in Table 7-XVII.

The power system efficiency varied from 8.52 percent to 8.87 percent, a difference of 0.35 percent representing a solar array size differential of 12.79 w. This variation in array size (4 percent) is relatively small and the major portion is attributable to the power conditioning equipment efficiencies. It is significant that both Configurations 2 and 3 have the higher system efficiencies and differ only by 0.01 percent. Both of these configurations use essentially an ac distribution system, i.e., the major portion of the load power is processed by a central inverter. The basic difference between these two systems is the choice of regulator configuration. One provides a central regulator with tight requirements, while the other uses two regulators. Because these two systems are essentially equal in efficiency, the configuration choice between them can be made on the basis of other criteria.

Table 7-XVI. Mission III Configuration Evaluation

LOAD	OUTPUT w	Δ_i	η_α	P_α	η_β	P_β	η_γ	P_γ	η_i	Δ_i/η_i
Configuration 1										
I	9.0	0.0323	-	-	1.000	9.00			1.0000	0.0323
II	9.6	0.0345	0.902	{10.64}	0.952	11.18			0.8587	0.0402
III	159.8	0.5740	-	{159.80}	0.952	167.86			0.9520	0.6029
IV	100.0	0.3592	0.878	113.90	0.923	123.40			0.8104	0.4432
Total	278.4	1.0000	-	(170.44)	(0.952)	311.44			-	1.1186
Total Bus						311.44				-
$\Sigma\Delta_i/\eta_i$										1.1186
$1/\Sigma$										0.8940
Configuration 2										
I	9.0	0.0323	-	-	-	-	1.000	9.00	1.0000	0.0323
II	9.6	0.0345	-	{9.60}	0.922	10.41	0.955	10.90	0.8805	0.0392
III	159.8	0.5740	-	{-}	-	159.80	0.955	167.33	0.9550	0.6010
IV	48.6	0.1746	0.940	{51.70}	0.922	56.07	0.955	58.71	0.8277	0.2109
V	51.4	0.1846	0.941	54.62	0.921	59.31	0.955	62.10	0.8277	0.2230
Total	278.4	1.0000	-	(61.30)	(0.922)	285.59	0.955	308.04	-	1.1064
Total Bus								308.04		-
$\Sigma\Delta_i/\eta_i$										1.1064
$1/\Sigma$										0.9038
Configuration 3										
I	9.0	0.0323	-	-	-	-	1.000	9.00	1.0000	0.0323
II	9.6	0.0345	-	9.60	0.924	10.39	0.955	10.88	0.8824	0.0391
III	159.8	0.5740	-	-	0.924	159.80	0.955	167.33	0.9550	0.6010
IV	48.6	0.1746	0.940	51.70	0.924	55.95	0.955	58.59	0.8295	0.2105
V	51.4	0.1846	0.941	54.62	0.924	59.11	0.955	61.90	0.8304	0.2223
Total	278.4	1.0000	-	115.92	0.924	285.25	0.955	307.70	-	1.1052
Total Bus								307.70		-
$\Sigma\Delta_i/\eta_i$										1.1052
$1/\Sigma$										0.9048
Configuration 4										
I	9.0	0.0323	-	-	1.000	9.00			1.0000	0.0323
II	9.6	0.0345	0.902	{10.64}	0.951	11.19			0.8578	0.0402
III	149.0	0.5352	-	{149.00}	0.951	156.68			0.9510	0.5628
IV	25.3	0.0909	0.820	30.85	0.919	33.57			0.7536	0.1206
V	37.4	0.1343	0.840	44.52	0.920	48.39			0.7728	0.1738
VI	48.1	0.1728	0.851	56.52	0.921	61.37			0.7838	0.2205
Total	278.4	1.0000	-	159.64	0.951	320.20			-	1.1502
Total Bus						320.20				-
$\Sigma\Delta_i/\eta_i$										1.1502
$1/\Sigma$										0.8694

Table 7-XVII. Mission III Summary

Configuration	Power Out (w)	Bus Power (w)	Array Power (w)	Array Power Differential (w)	*System Efficiency (H) Percent
1	278.4	311.41	317.77	3.80	8.76
2	278.4	308.03	314.22	0.36	8.86
3	278.4	307.69	313.87	0	8.87
4	278.4	320.22	326.76	12.79	8.52

*Assumes solar cell array efficiency to be 10 percent AMO.

8. RTG POWER SOURCE

8.1 INTRODUCTION

Part of the effort during this study was devoted to consideration of the use of radioisotope thermoelectric generators (RTGs) as primary spacecraft power sources. This section covers RTG characteristics as they relate to power system design optimization in the following areas:

- Thermoelectric conversion efficiency
- Alternate methods of RTG control
- Estimated weight versus power level for Pu-238 RTGs
- Power systems for three earth-orbital missions.

The major difference between an RTG and a solar photovoltaic array is that the RTG is a self-contained power plant while the solar array is dependent on the sun as an energy source. In an RTG, heat produced from the radioactive decay of a suitably encapsulated isotope fuel is converted directly into electricity by thermocouples. As in all heat engines, conversion efficiency is dependent upon the temperature difference maintained across the conversion device, in this case the hot and cold junctions of the thermocouples. Because the waste heat has to be rejected by radiation to space, the size and weight of an RTG are also dependent upon the junction temperatures chosen.

The use of RTGs in space has been extremely limited because of certain undesirable characteristics:

- High cost and limited availability of isotope fuels
- Radiation and magnetic interference with experiments
- Potential hazards
- Relatively low power-to-weight ratio.

As these disadvantages are gradually overcome by improved technology, the use of RTGs will probably increase, for applications which can benefit from RTGs desirable features:

- Continuous power output
- No sun orientation required
- Relatively insensitive to external environment
- Compact configuration.

8.2 THERMOELECTRIC CONVERSION EFFICIENCY

The efficiency with which heat is converted into unregulated electrical power in an RTG is primarily a function of the thermoelectric properties of the thermocouple materials and the junction temperatures. Lead telluride (PbTe) and silicon germanium (SiGe) are the two types of thermocouples which have been developed for use in RTGs. PbTe couples have been used exclusively in all existing RTGs, because of the more advanced state of development, while the newer SiGe couples are planned for future units.

The conversion efficiencies of these two thermocouples are shown in Figure 8-1 as a function of hot junction temperature (T_h) at two cold junction temperatures (T_c), of 500 and 600°F. The dashed curves represent 10 and 15 percent of the theoretical Carnot efficiencies at the temperatures indicated. The efficiencies of both materials are seen to be bracketed by these two limits within the ranges shown. Carnot efficiency is defined by the ratio $\frac{T_h - T_c}{T_h}$, where T_h and T_c are in absolute temperature units.

It is evident from Figure 8-1 that for the same cold junction temperatures, PbTe is superior in efficiency at hot junction temperatures up to approximately 1200°F, which is its maximum safe operating point. The use of SiGe, without sacrificing efficiency, requires higher hot junction temperatures, preferably 1500°F or higher. The upper limit for SiGe is approximately 1800°F.

While high conversion efficiency is desirable in minimizing the amount of isotope fuel required for a given electrical output, it is necessary in practice to compromise efficiency for other reasons. The hot

junction temperature is limited by available materials for heat source capsules as well as degradation of the thermocouple performance with time. The cold junction temperature is limited by its effect on the size and weight of the heat rejection system in space applications, where the fourth power law governs thermal radiation. These conflicting factors tend to result in designs with conversion efficiencies within the narrow range of 4 to 6 percent. Typical hot and cold junction temperatures are 1000°F and 500°F, respectively, for PbTe, and 1500°F and 600°F for SiGe. Except for minor effects of heat leaks through insulation, efficiency is not sensitive to the power level of the RTG because of the modular nature of the thermocouples.

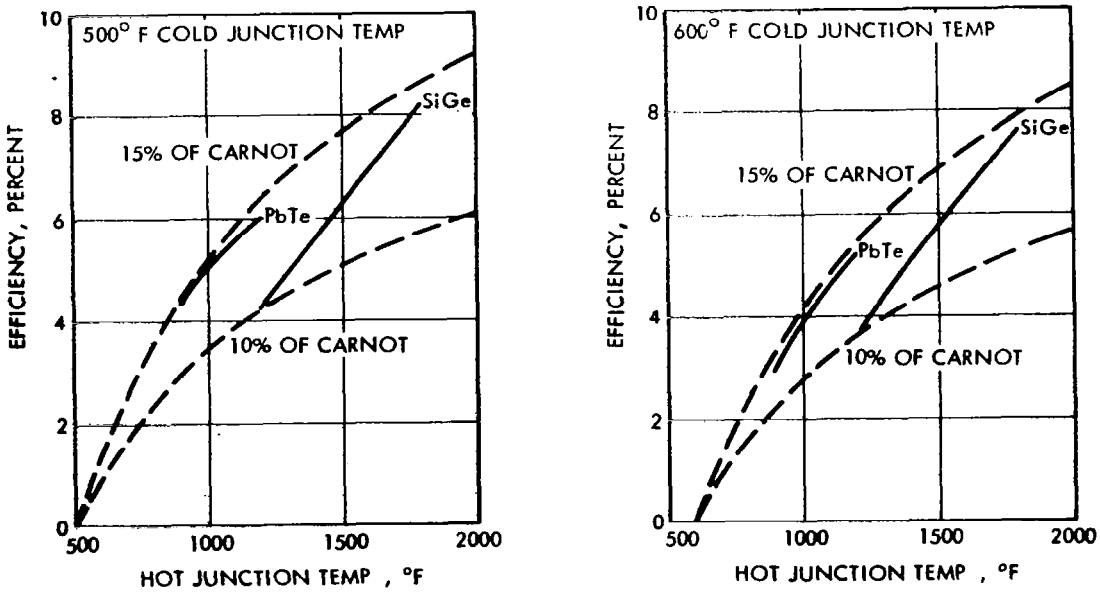

Figure 8-1. Thermoelectric Conversion Efficiency of Typical PbTe and SiGe Couples

8.3 RTG WEIGHT

The weight of an RTG is primarily a function of its output power level. Existing units, such as the 30-w SNAP-19, are in the 1-w/lb class. Future units are being designed for 2 w/lb. Figure 8-2 shows weight as a function of power for RTGs in the 25- to 350-w range, using Pu-238 fuel and designed for random intact reentry. The approximate equation for this curve is also shown in Figure 8-2. The higher power-to-weight ratio at the higher power levels is based on (1) projected advancements in fuel capsule technology, (2) the use of SiGe thermocouples at higher hot and cold junction temperatures than those presently used for PbTe, and (3) more efficient utilization of structural materials in larger units.

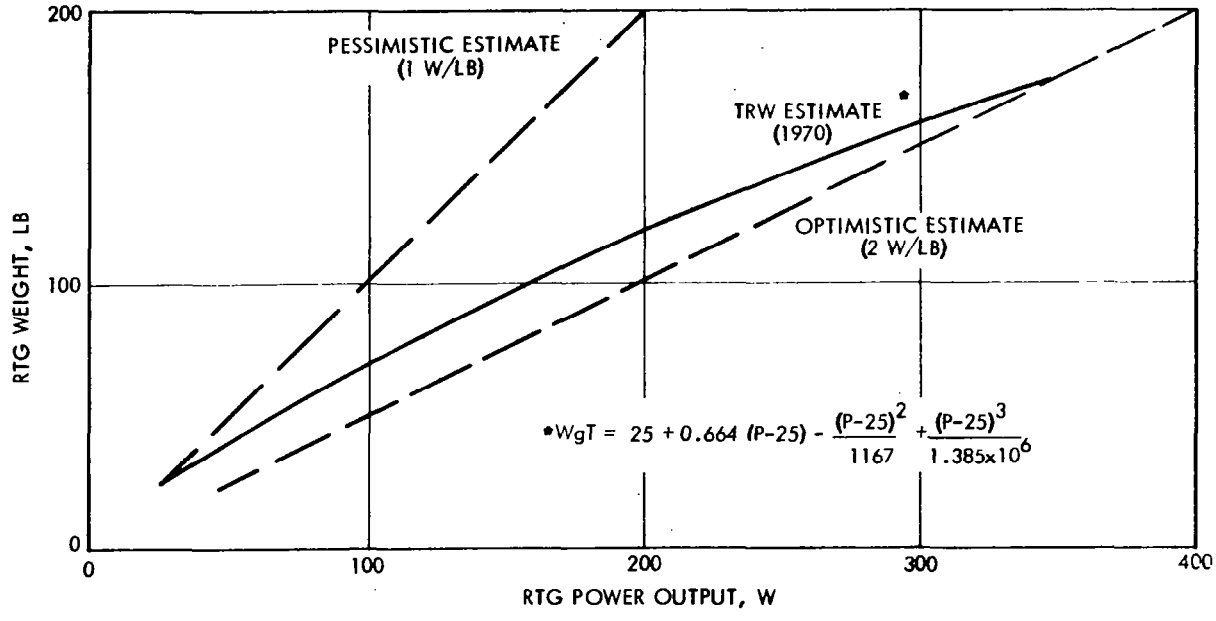

Figure 8-2. Estimated RTG Weight as a Function of Power Output

8.4 RTG CONTROL METHODS

The typical characteristics of a thermoelectric generator with a constant heat input are illustrated in Figure 8-3. The design point is normally chosen at the maximum output power (and efficiency) condition corresponding to V_o and I_o. The cold junction temperature, T_c, is at its minimum value at this point, and the hot junction temperature, T_h, is about midway between its extreme values. T_h varies with output current I, because the Peltier cooling effect at the hot junctions is a function of this current. T_h rises toward its maximum value as I is reduced to zero (open circuit). Figure 8-4 shows a performance map obtained at TRW on an advanced SiGe thermoelectric generator module with an electrical heat source. The I-V characteristics are shown for both constant T_h (solid lines) and constant heat input (dashed lines).

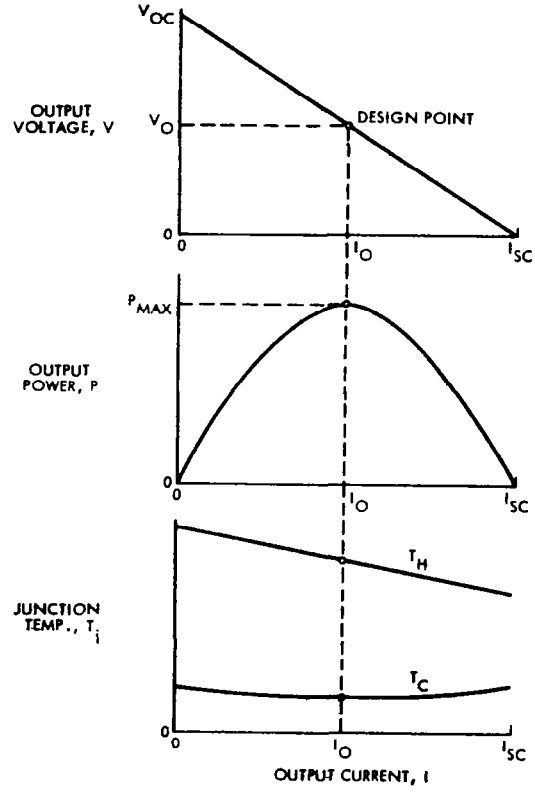

Figure 8-3. Typical Characteristics of Thermoelectric Generator With Constant Heat Input

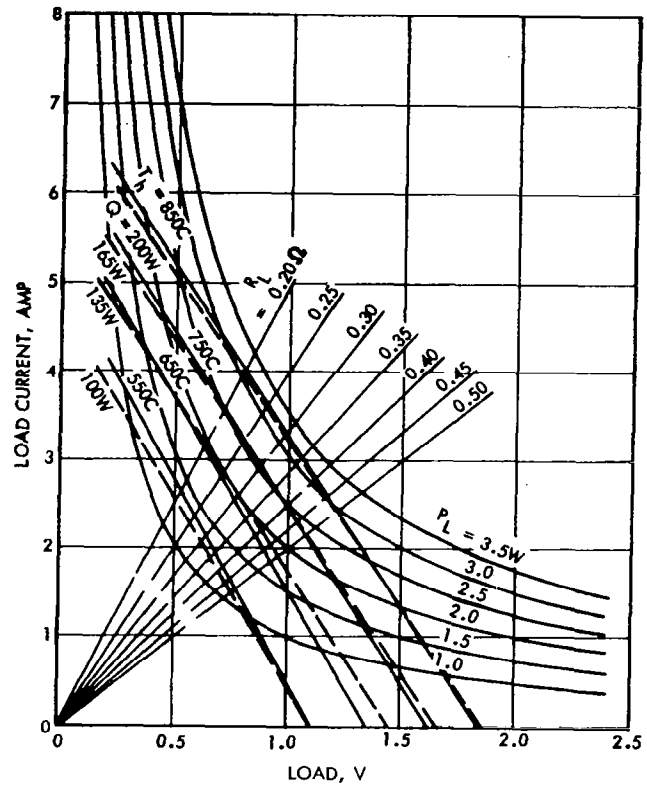

Figure 8-4. Performance Map of SiGe Module

It is highly desirable to keep T_h from exceeding its design point value in order to prevent increased degradation of the thermocouple materials. Hence, a source control device is needed to operate the generator at its design point regardless of the actual load. The magnitude of the excursion in T_h in the absence of such a control depends primarily upon the value of the load current at design point (I_o) and may be as high as 200 to 300°F in some cases.

While it is possible to design the generator so that T_h is at the maximum safe value at open circuit conditions, a penalty is then paid in reduced performance at the maximum power point due to the reduction in T_h. Thus, it is necessary that the RTG be operated at its design point voltage from no load to full load to provide maximum utilization of an RTG power source without penalizing its performance at the maximum power point.

Methods for maintaining a constant output voltage include:

(1) Controlling the loads to maintain a constant total load on the RTG. This may not be practical in most cases.

(2) Shunting the RTG with zener diodes or transistors. This has been used successfully with solar arrays in many applications. Shunt dissipation may sometimes cause thermal problems, particularly if it leads to widely varying power dissipation within the spacecraft. Externally located shunt elements may result in low temperature problems during eclipses.

(3) Shunting the RTG periodically via a dumping resistor whose resistance is approximately equal to the source resistance. The resistor can be mounted externally to minimize thermal problems within the spacecraft.

(4) Short circuiting the RTG periodically to maintain a constant average voltage. By using a switching speed which is high relative to the RTG's thermal time constant, the equivalent load appears constant to the RTG, which results in a slight increase in cold junction temperature under low load conditions.

The type of control to be used depends upon the application. For those spacecraft designs where it is desirable to maintain a constant dissipation within the equipment compartment in the presence of varying loads, the use of dissipative shunt elements distributed with the compartment is a good solution. The shunt dissipation tends to counterbalance the effect of load variations. On the other hand, the switching short circuit approach may be preferred as a means of reducing the thermal energy dissipated outside the RTG to a minimum, where such dissipation would create difficulties in thermal control. For the earth-orbiting missions covered in this study, the dissipative shunt control is considered the best approach.

8.5 RTG POWER SYSTEMS

The following paragraphs discuss the use of RTG's in place of solar arrays for the three earth orbital missions previously listed.

In the case of Mission I (synchronous communications satellite), the load profile is essentially constant with time except for short duration peaks required by solenoid valves in the attitude control system. These peak loads are estimated to be 10 w per valve, lasting from 0.05 sec to 6.5 min in duration. Only one valve is actuated at a time. Power for these peak loads could be supplied either by a larger RTG or by energy

storage devices, i.e., batteries or capacitors which are charged by the RTG. The larger RTG requires an increase of approximately 5 percent in RTG power level, and an increase in RTG weight of 4 lb. The use of capacitors would not be satisfactory for the relatively long-duty cycles involved. In view of the 5-yr mission life desired, the larger RTG approach appears to offer a more reliable system than that of a secondary battery, with a minor weight penalty of about 1 or 2 lb. Figure 8-5 is a simplified block diagram of an RTG power system for Mission I.

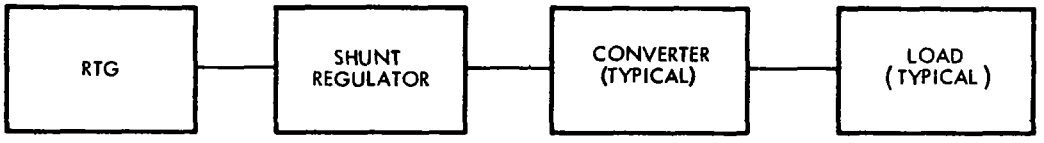

Figure 8-5. RTG Power System (Mission I)

In the case of Mission II (mapping, navigation), the load profile is characterized by relatively long periods of constant power, followed by shorter periods of peak power demand for interrogation. In this case, oversizing the RTG by about 50 percent to satisfy these peak loads is unsatisfactory, and the shorter mission life involved (1 to 3 yr) results in the choice of secondary batteries for energy storage. Note that the batteries are sized for peak loads only and not for eclipse operation as in a photovoltaic system. As a result, the RTG power system requires a smaller battery than the solar power system (for earth-orbital missions).

The application of an RTG to Mission III requires careful consideration of interactions between the RTG and the scientific experiments. Certain instruments, such as magnetometers, ionization chambers, and particle detectors, are sensitive to the magnetic and radiation properties of RTGs. Various methods are available for minimizing such interference. Such methods include the use of local shielding, increased distance between the RTG and sensitive instruments, and the use of nonmagnetic materials in the RTG. Aside from this disadvantage, however, an RTG power system could be used for this mission. The power profile is relatively constant and is similar to Mission I. Small peak loads, about 10 min long for reaction wheels and gas valves, can be satisfied with secondary batteries.

The estimated weights of RTG power sources for the three missions are found in Table 8-I. Estimated weights for secondary batteries (Missions II and III only) required for peak loads are also given. The RTG weights are based on the curve of Figure 8-2, assuming that a single RTG is employed for each mission. It should be noted that these estimates would be higher if several smaller units were used in combination to provide the required outputs.

Table 8-I. Weight Summary of RTG Power Sources

	Mission		
	I	II	III
RTG power output (w)	190	160	270
Estimated RTG weight (lb)	114	100	150
Energy storage method	None	Battery	Battery
Usable battery capacity (w-hr)	None	20	33
Estimated battery weight (lb)	None	7	10
Total power source weight (RTG and battery) (lb)	114	107	160

A simplified RTG power system block diagram is shown in Figure 8-6 (Missions II and III).

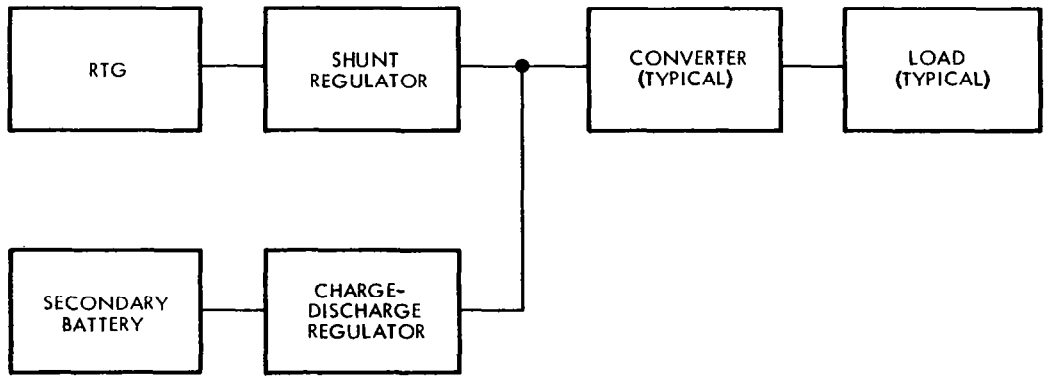

Figure 8-6. RTG Power System (Missions II and III)

9. STANDARDIZATION RECOMMENDATIONS

Standards in industry and government have come into being for one of two reasons:

1) When a sufficiently large portion of the practicing scientific community have informally adopted the usage because it was inherently the best design or method for accomplishing the task. Formal standards are then prepared which in fact document that which is already in existence.

2) When a large variety of designs or methods, not significantly different, are in use throughout the scientific community which fundamentally accomplish the same task, a need for standardization is created. Standards then come into existence because somebody having authority so directs.

The scientific field of satellite electrical power system design appears to fall within the boundaries of the second reason. The only identifiable repetitive usage is that of solar cells and batteries as satellite energy sources. However, within these disciplines, very little evidence of standardization exists.

The need for standardization in satellite electrical power system designs was recognized at the beginning of this study. Hence, one task was to search out and identify those areas where standards could be initiated. A review of the existing user equipment characteristics, power system designs, power system equipment characteristics, and power requirements, suggests three possible areas where the establishment of standards could improve power system designs and their utilization. These areas are:

1) Standard dc voltages

2) Standard ac voltages and frequency

3) Standard circuits and modularization of power conditioning equipment

9.1 STANDARD DC VOLTAGES

A compilation of the dc voltages required by the load equipments reported in Section 3 shows a total of 48. These do not include the

variations introduced by the degrees of regulation for any one voltage, nor the plus and minus requirements. Table 9-I lists the 48 voltages.

Table 9-I. Load Equipment DC Voltages

2.5	12.2	25.0	355
3.0	12.4	26.0	545
3.1	12.8	26.5	570
5.0	13.0	27.0	620
5.1	15.0	28.0	650
6.0	16.0	30.0	940
7.0	16.7	45.0	1200
8.0	18.0	70.0	1250
9.0	18.5	75.0	1340
9.9	20.0	150.0	1350
10.0	22.0	165.0	1440
12.0	23.0	210.0	3000

The division of these voltages among the using subsystems is:

Transmitters	19
Receivers	9
Decoders	5
Data Handling	6
Attitude Control	16
Experiments	22

No more than 12 of the 48 voltages are common in two or more subsystems. Table 9-II lists the number of subsystems which use these 12 voltages.

An analysis was performed on the dc voltage requirements lower than 50 vdc, used in the mission analyses of Section 7. Table 9-III presents these results, showing the percent of total system power required at each voltage. This listing essentially spans the same range of requirements compiled from Section 3, except those high voltages which are normally derived within the users equipment.

Table 9-II. Twelve Voltages Common to More than One Subsystem

DC Volts	No. of Subsystems
3.0	2
5.0	3
6.0	4
8.0	3
9.0	2
10.0	4
12.0	4
16.0	5
18.0	3
20.0	4
26.0	2
28.0	3

Table 9-III. Voltage Analysis from Mission Examples

	Voltage (≤50 vdc)	Mission Category			Average for Three Missions	Average Total Per Group
		I	II	III		
		Percent Low Voltage Power	Percent Low Voltage Power	Percent Low Voltage Power	Percent Low Voltage Power	Percent Low Voltage Power
Group I	±50	-	0.3	-	0.1	30.9
	+28	16.7	25.5	13.5	18.6	
	-23	-	-	8.7	2.9	
	±20	-	7.0	21.0	9.3	
Group II	±16	-	32.4	17.5	16.6	36.9
	±15	15.2	-	-	5.1	
	+12	-	5.8	-	1.9	
	-10	7.4	-	0.7	2.7	
	+ 9	-	-	31.7(b)	10.6	
Group III	± 6	13.3	13.9	6.1	11.1	32.2
	- 5	-	-	0.8	0.3	
	- 4.2	-	15.1	-	5.0	
	- 3	47.4(a)			15.8	
		100.0	100.0	100.0	100.0	100.0

(a) TWT heater power can be designed for any voltage up to 20 vdc or ac.

(b) Digital circuit power can be at a lower voltage.

The voltages presented in Table 9-III were divided into three groups so that each group represented approximately one third of the total system power. Within Groups I and II, the 28-v and 16-v loads are, respectively, the largest percentage. In Group III, the 3-v load is largest with the 6-v requirement being a close second. Because the 3-v load is predominately for the TWT heaters, that portion of the power could be combined with the 6-v loads, making it the largest and most representative for the group.

Equipments using the voltages in Group I are primarily heaters, motors, solenoids, etc., which require very little regulation. Group II covers the range of voltages normally used by analog circuits and other electronic devices. The third group encompasses voltages used in digital circuits, filament heaters, and telemetry signals. Although this study did not develop a conclusive justification for selecting specific standard voltages, it appears that a reduction to a single voltage for each of the three groups of Table 9-III would be economical for new equipment designs without compromising performance. The power system performance could be improved because of this standardization, by increasing efficiency, reducing weight, and permitting better utilization of the power.

The following voltages are recommended as low voltage dc standards, +50, ±28, ±15, ±10, and ±5 at this time. Although the summary given in Table 9-III would suggest +28 vdc rather than +50 vdc, an estimate of future requirements suggests a change to a higher value. Future systems will require larger amounts of power, such as 500 w or more. The main bus current for the higher power systems could be reduced approximately 50 percent by using the higher bus voltage. The result will be lower weight hardware and distribution equipment as well as lower power losses. In general, the efficiencies of power conditioning equipment will also improve at the higher voltage. The 5-v recommendation for the third group is based on the fact that telemetry equipment has standardized 5-vdc signals and future satellite designs will utilize more integrated circuits. Integrated circuits are usually limited to 5-to 6-vdc maximum.

9.2 STANDARD AC VOLTAGES

A similar analysis of the ac load voltage requirements revealed the following seven voltages:

5.0, 6.3, 18.0, 26.0, 115, 125, 135

By and large, the attitude control type of equipment and heaters utilize the ac power. These equipments generally require 400 cps, one or two phase power at 115 to 135 and/or 28v.

The parametric data of Section 5 show that excellent equipment efficiencies can be attained at the lower frequencies, but with some power system weight penalty. Satellite designs using a relatively large amount of ac power require further investigation in order to optimize the choice of frequency for best utilization of satellite weight and maximum power system efficiency. Where the using equipment requires large amount of 400 cps, it is recommended that 115 vac, 400 cps, 2 phase; and 28 vac, 400 cps, single phase be established as standard. Satellite systems which do not have a definite 400 cps requirement, should use a higher frequency, in the area of 2 kc, for best over-all performance.

9.3 STANDARD CIRCUITS

The results of the parametric data analysis, Section 5, suggest the use of the ES-type of power conditioning circuit for best efficiency, low weight, and good reliability designs. Power systems requiring the use of a converter, in contrast to an inverter and separate TR-unit, should always be able to use the ES-type of equipment. The mission analysis and power system optimization performed in Section 7 indicates that maximum utilization of power, high efficiency and low weight result when centralized conversion equipment is used. The results further suggest that a central inverter, with or without regulation as required, provides a more optimum power system. If the three mission examples truly are representative of most earth orbiting, unmanned satellites, then it can be concluded that a centralized inverter utilizing an ac bus provides the optimum system design.

Once standard voltages are established in practice, power system equipments can be optimized for efficiency, weight, and reliability. These optimum circuit designs will then lend themselves to modularization, providing additional savings in production costs, and increased reliability.

10. DECLARATION OF NEW TECHNOLOGY

There has been no new technology (NASA Form 1162 - September 1964- New Technology) developed during the course of work under this contract, NAS5-9178.

APPENDIX A

ENERGY STORAGE – NICKEL CADMIUM BATTERY EXAMPLE

1. INTRODUCTION

Energy storage equipment characteristics and parametric data are presented in Section 5.4 of this report. Use of nickel-cadmium battery curves and, thus, a better understanding of the parametric interactions is demonstrated by the following battery design example. Figure numbers refer to Section 5.4.2, Figures 5-28 through 5-40.

2. NICKEL CADMIUM BATTERY DESIGN EXAMPLE

From the spacecraft mission and orbital considerations the following requirements are given:

Life	1000 cycles
Load capacity at end of life (C_d)	3 amp-hr
Discharge current (I_d)	3.0 amps
Discharge temperature (T_d)	50°F
Charge current (I_c)	1.5 amps
Charge temperature (T_c)	96°F

Step (a):

Assume $i_d = 0.5 \frac{\text{amps}}{\text{amp-hr}} = 0.5$ 1/hr

Define: $i_d = \frac{I_d}{C_e}$, and $i_c = \frac{I_c}{C_e}$

C_d = Discharge capacity at end of life for a given charge current density (i_c) and amp-hr efficiency (η)

C_e = Maximum available capacity at end of life for a given charge current density (i_c) and discharge current density (i_d)

C'_e = Maximum available capacity at end of life for a given optimum charge and discharge current

C_r = Manufacturers amp-hr rated capacity

Step (b):

From Figure 5-28, at $i_d = 0.5$ and $T_d = 50^{\circ}F$.

$C_e/C'_e = 0.825$

(Before any derating occurs, $C_e = C_d \pm 3$ amp-hr)

$$C'_e = \frac{C_d}{0.825} = 3.636 \text{ amp-hr}$$

$$i_c = \frac{I_c}{C'_e} = \frac{1.5 \text{ amps}}{3.636 \text{ amp-hr}} = 0.4125$$

Figures 5-29 through 5-33 are a set of efficiency curves for various charge temperatures.

Step (c):

Assume a charge efficiency of 90 percent.

Step (d):

From Figure 5-32 having a charge temperature of $96^{\circ}F$, read $C_d/C_e = 0.835$ for $\eta = 90$ percent, $i_c = 0.4125$.

Step (e):

Let a new C_d = 3.636 amp-hr from the previous C'_e calculation.

The new $C_e = \frac{C_d}{0.835} = \frac{3.636}{0.855} = 4.354$ amp-hr

This should be the derated amp-hr capacity required for these specific charge and discharge conditions. However $i_d = 0.5$ was assumed.

Step (f):

Examine the assumption: $i_d = 0.5$

$$i_d = \frac{I_d}{C_e} = \frac{3 \text{ amps}}{4.354 \text{ amp-hr}} = 0.689$$

Thus, $i_d \neq 0.5$ as assumed and a further iteration is required.

Step (g):

Return to Figure 5-28 for $i_d = 0.689$ and $T_d = 50^{\circ}F$.

New $C_e/C'_e = 0.800$

$$C'_e = \frac{C_e}{0.8} = \frac{3 \text{ amp-hr}}{0.80} = 3.750 \text{ amp-hr}$$

Step (h):

Calculate new i_c

$$i_c = \frac{I_c}{C'_e} = \frac{1.5 \text{ amps}}{3.750 \text{ amp-hr}} = 0.400$$

Step (i):

From Figure 5-32 again obtain a new C_d/C_e where

$i_c = 0.400$, $\eta = 90$ percent

$C_d/C_e = 0.830$

$$C_e = \frac{3.750}{0.830} = 4.518 \text{ amp-hr}$$

Step (j):

Reexamine last value of i_d used

$$i_d = \frac{I_d}{C_e} = \frac{3 \text{ amps}}{4.518 \text{ amp-hr}} = 0.664$$

This $i_d \neq 0.689$ last assumed. A further iteration is required.

Step (k):

Return to Figure 5-28 for $i_d = 0.664$, $T_d = 50^{\circ}F$

New $C_e/C_e' = 0.805$

$$C_e' = \frac{3 \text{ amp-hr}}{0.805} = 3.726$$

Step (l):

Calculate new i_c

$$i_c = \frac{1.5 \text{ amps}}{3.726 \text{ amp-hr}} = 0.4025$$

Step (m):

From Figure 5-32, new $C_d/C_e = 0.832$

$$C_e = \frac{3.726}{0.832} = 4.478 \text{ amp-hr}$$

Step (n):

Reexamining i_d assumption

$$i_d = \frac{3 \text{ amps}}{4.478 \text{ amp-hr}} = 0.6699$$

This is close enough to assumed

$$i_d = 0.664$$

Therefore:

C_e = 4.478 amp-hr

I_d = 3 amps, i_d = 0.67

I_c = 1.5 amps, i_c = 0.335

Step (o):

From Figure 5-34, the depth of discharge C_e/C_r for 1000 cycles is 55 percent. Therefore the rated capacity required to be installed for minimum weight and maximum reliability is

$$C_r = \frac{4.478 \text{ amp-hr}}{0.55} = 8.4 \text{ amp-hr or } 8 \text{ amp-hr}$$

Step (p):

From Figure 5-35, the weight of packaged battery is 0.95 lb per cell. The battery total weight is determined by multiplying this number by the number of cells required to meet the system bus voltage.

APPENDIX B

DERIVATION OF PARAMETRIC DATA FOR FIGURES 5-45, 5-48, AND 5-49

1. INTRODUCTION

The converter parametric data presented in Paragraph 5.6.2 on page 5-16 have been expanded so that the efficiency and weight performance of the individual sections, i.e., the preregulator, inverter, and transformer-rectifier (TR), can be identified separately. This will allow tradeoffs to be made between a single converter which provides the functions of a regulator, inverter, and TR units, and discrete equipment, such as a regulator, inverter, and TR units. The derivation of the parametric data presented in Paragraphs 5.6.2, 5.6.3, and 5.6.4 follow. Table B-I lists the design criteria from which the curves in Figure 5-45 were derived.

Table B-I. Design Criteria

Converter Type:	Preregulator dc-to-dc
Input Voltage:	28 ± 15% vdc
Single Output Voltage:	28 ± 2% vdc
Ripple and Noise:	± 1%
Overload Protection:	Current limiting
Temperature:	0 to 50°C
Redundancy:	None

To clarify the usefulness and applicability of these data, the power, frequency, weight, and efficiency of existing dc-to-dc converter hardware were compared with the data presented in Figure 5-45. The existing hardware designs were adjusted to the same criteria by using the efficiency correction factor presented in Figure 5-47 of Section 5.6.2.

The information presented in Figure 5-45 was intended to show the change in direction and relative magnitude of the various parameters. It is expected that these parameters will deviate somewhat because of the many variables affecting the designs. The data compare favorably at the lower power levels. Because high power level hardware (200 to 500 w) is practically nonexistent, a comparison of the data extrapolation cannot readily be verified at this time. Table B-II presents a comparison of the hardware data points with the curves in Figure 5-45.

Table B-II. Comparison of Parametric Data and Hardware Designs

CONVERTER DESIGN	OUTPUT VOLTAGE	POWER (W)		EFFICIENCY (%)		FREQUENCY (KC)		WEIGHT (lb)	
		ACTUAL	GRAPH	ACTUAL	GRAPH	ACTUAL	GRAPH	ACTUAL	GRAPH
1	+28, +15, -28 vdc	34.64	35	.78	79.5	10	10	3.0	2.8
2	+4.2 vdc	15	15	77.5* 68	76	10	10	1.45	1.50
3	+4.2 vdc	5	5	71* 63	62	10	10	1.10	0.93
4	+12.6, +6.6, -3.6, -6.0, +15, -15 vdc	2.75	2.75	57.2* 55	55	10	10	1.45	0.8
5	+12.8, +16.7, +16.0, +10.0, +15, -12.4, -16.0, +10 vdc; 15 va	9.00	9.0	68.5* 66.4	72	6.5	6.5	3.2	1.3
6	-940, -545, +80 vdc; 4.875 vac	26	26	78.5* 80	78.5	6.5	6.5	2.35	2.5
7	+6.5, -6.65 vdc	13.99	14	71 * 66	76	3.3	3.3	3.0	1.7
8	+23, +70 vdc	21.60	21.6	75.5* 74	77	3.3	3.3	2.8	2.2
9	+16, +10, -6.2, -16.1 vdc	1.91	1.91	36 * 34	52	3.3	3.3	0.6	0.84
10	+28, +12.2, +10, -6.2 vdc	3.69	3.69	42* 40	57	3.3	3.3	1.1	1.0
11	+23, +70 vdc	26	26	70	79	2.4	2.4	2.2	2.8
12	+23, +70 vdc	22.1	22.1	69	78	2.4	2.4	2.2	2.5

NOTE: *-Actual Efficiency corrected for +28 vdc single output

2. DERIVATION OF CONVERTER PARAMETRIC DATA

The general equation for the converter efficiency parameter shown in Figure 5-45 is:

$$\eta_o = \frac{P_o}{P_o + (P_f)_o + (P_s)_o + (P_m)_o} \quad (1)$$

$$\eta_1 = \frac{P_o}{P_o + (P_f)_o + (P_s)_1 + (P_m)_1} \quad (2)$$

where

P_o = Power output

η_o = Converter efficiency at given (P_o) and (f_o)

$(P_f)_o$ = Fixed losses at a given power output

$(P_s)_o$ = Semiconductor component losses

$(P_m)_o$ = Magnetic component losses

Converter efficiency (η_1) at a given (P_o) and a new (f_1) is:

$$\eta_1 = \frac{1}{1 + \frac{(P_f)_o}{P_o} + \left[\frac{1}{\eta_o} - \frac{(P_f)_o}{P_o} - 1\right]\left[0.6 + 0.15\left(\frac{f_1}{f_o}\right) + 0.25\left(\frac{f_1}{f_o}\right)^{0.1}\right]} \quad (3)$$

$$W_o = X_o + Y_o + Z_o \quad (4)$$

where

W_o = converter weight for output of (P_o) at (f_o)

X_o = $W_o/3$ = weight of electronic components

Y_o = $W_o/3$ = weight of magnetic components

Z_o = $(X_o + Y_o)/2$ = weight of chassis and miscellaneous hardware

The new converter weight (W_1) for output of (P_o) at (f_1) is:

$$W_1 = X_o + Y_o\left(\frac{f_o}{f_1}\right)^{0.4} + 1/2\left[X_o + Y_o\left(\frac{f_o}{f_1}\right)^{0.4}\right]$$

$$W_1 = \frac{W_o}{2}\left[1 + \left(\frac{f_o}{f_1}\right)^{0.4}\right] \quad (5)$$

The equation relating weight to output power at a constant frequency is

$$W_i = W_o \left[\frac{P_i}{P_o} \right]^K \qquad (6)$$

The factor (K) varies with frequency and the W_o used. Table B-III provides the approximate values for K in the area of interest.

The cross plots of weight-vs-power output and frequency-vs-power output are shown in Figure B-1 for the same design centers used in Figure 5-45. The curves of Figure B-2 relate the variation of the fixed losses $(P_f)_o$ with output power and the resulting efficiency (η_o) given by Equation (1).

The complete curves of Figure 5-45 were generated by taking the performance data of an existing converter as a design center. From this design center, the variation of efficiency (η_o) and weight (W_o) at a constant power were extrapolated using the relationships given by Figures B-1 and B-2. Other design centers were similarly used for different power outputs.

Table B-III. K Factors Versus Switching Frequency for Converters

FREQUENCY (KC)	$P_1 > 10W$; $P_o = 10W$		$P_1 < 10W$; $P_o = 1W$	
	K	W_o (lb)	K_1	$(W_o)_1$ (lb)
0.06	0.645	5.2	0.46	1.8
0.3	0.666	3.0	0.40	1.2
1.0	0.676	2.1	0.40	0.82
3.0	0.670	1.5	0.35	0.67
10.0	0.700	1.2	0.30	0.6
20.0	0.715	1.0	0.26	0.55
30.0	0.745	0.9	0.255	0.5
200.0	0 ----	----	0.270	0.35

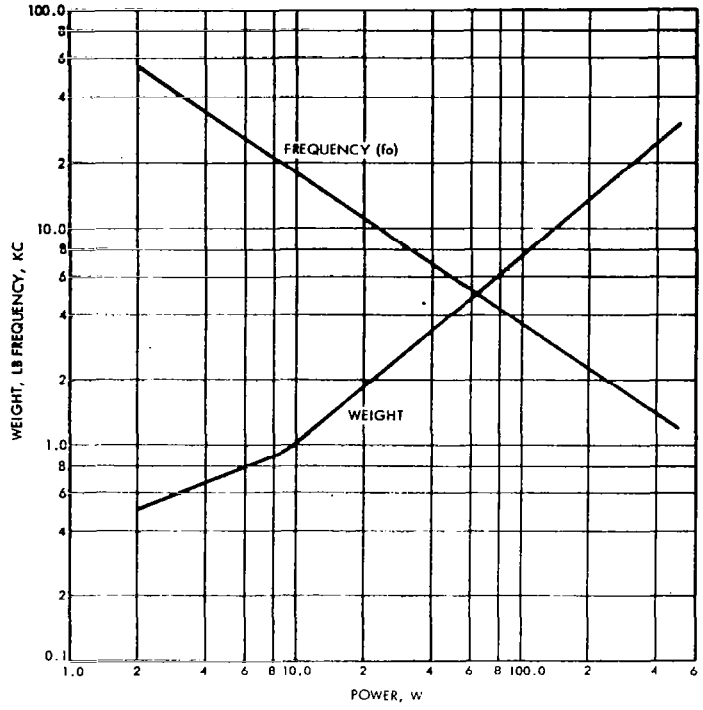

Figure B-1. Design Center Parameters for Converters

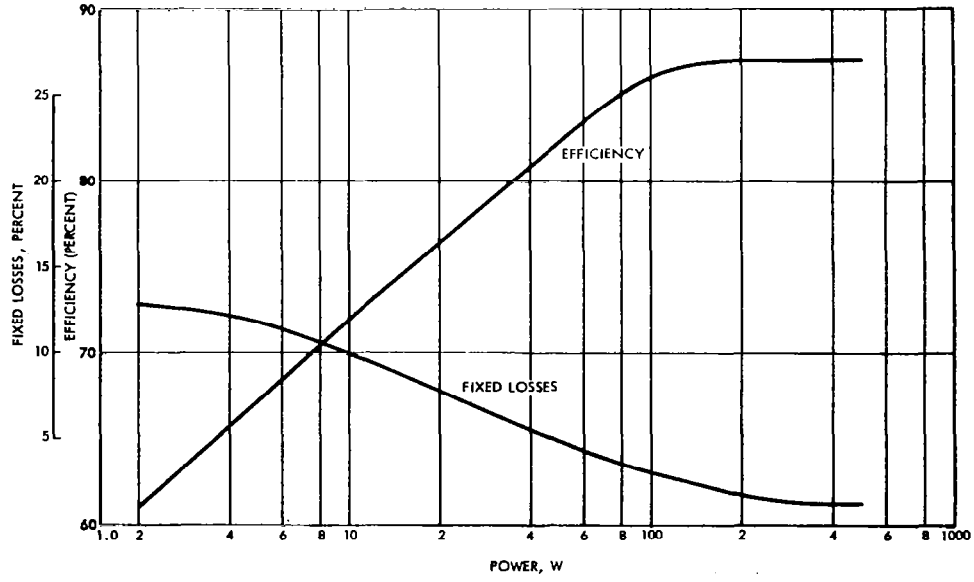

Figure B-2. Design Center Efficiencies for Converters

3. INVERTERS

When the inverter function provided by a converter is considered as a separate piece of equipment, equations such as the following result:

$$W_j = \frac{W_m}{3}\left[1 + 2\left(\frac{f_m}{f_j}\right)^{0.4}\right] \tag{7}$$

$$\eta_j = \frac{1}{1 + \left[\frac{1}{\eta_m} - 1\right]\left[0.6 + 0.15\left(\frac{f_j}{f_m}\right) + 0.25\left(\frac{f_j}{f_m}\right)^{0.1}\right]} \tag{8}$$

The composite parametric curves for inverter designs, shown in Figure 5-48, were generated from design centers as were the converter data. Figure B-3 provides the design center parameters used in conjunction with Equations (7) and (8) to generate Figure 5-48.

4. TR-UNITS

The transformer-rectifier (TR) function of the converter can also be considered as a separate entity. The following equations relate efficiency (η_h), weight (W_h) and operating frequency (f_h).

$$W_h = \frac{W_n}{16}\left[1 + 15\left(\frac{f_n}{f_h}\right)^{0.4}\right] \tag{9}$$

$$\eta_h = \frac{1}{1 + \left[\frac{1}{\eta_n} - 1\right]\left[0.6 + 0.0667\left(\frac{f_h}{f_n}\right) + 0.333\left(\frac{f_h}{f_n}\right)^{0.1}\right]} \tag{10}$$

Figures 5-49 and B-4, respectively, present the parametric design curves and design center parameters for the TR designs.

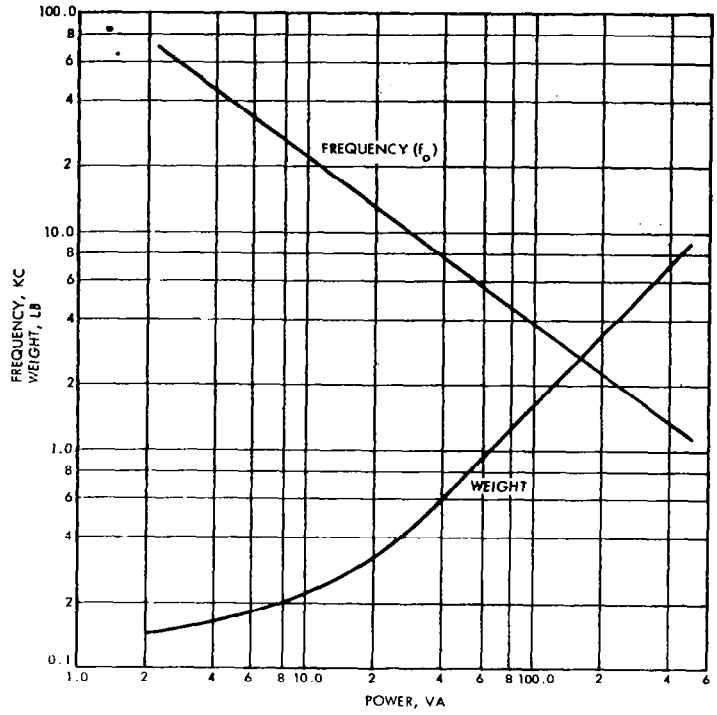

Figure B-3. Design Center Parameters for Inverters

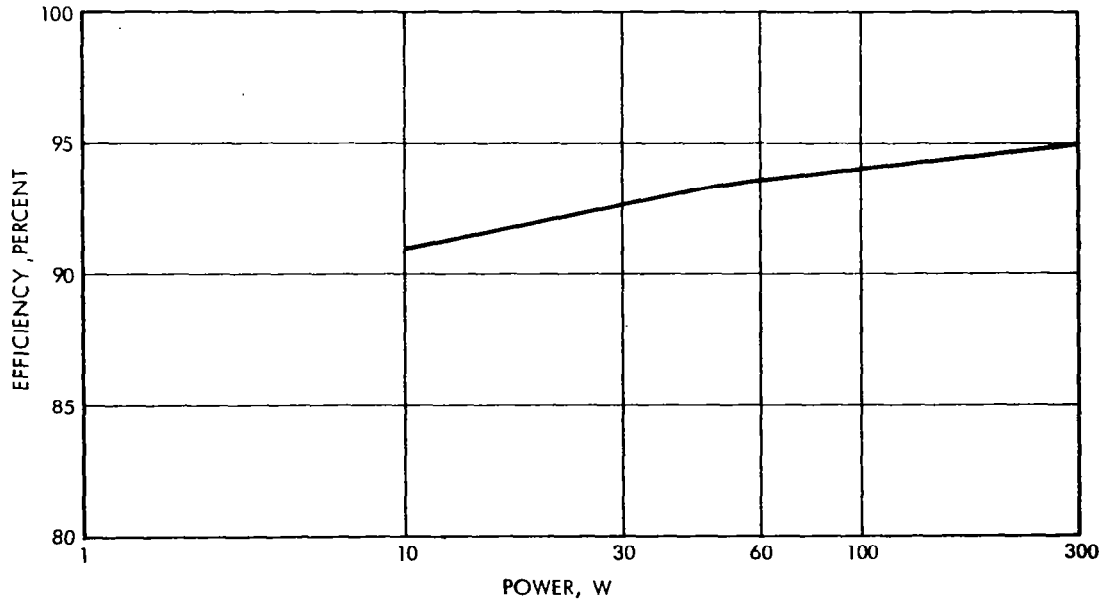

Figure B-4. Design Center Efficiencies for TR Units

APPENDIX C

DERIVATION OF REGULATED CONVERTER PARAMETRIC DATA

1. INTRODUCTION

The regulated dc-to-dc converter was chosen as the investigation model because it is representative of and contains all of the power conditioning functions — regulating, inverting, transforming, and rectifying — found in a satellite electrical power system. A common converter requirement specification was selected to meet typical power conditioning requirements. Four basic regulated converter circuits were analyzed: (1) regulated squarewave converter (RSWI) Figure C-1; (2) pulsewidth converter (PWI) Figure C-2; (3) energy storage converter (ES) Figure C-3; and the push-pull energy storage converter (Push-Pull ES) Figure C-4. Weight and efficiency as functions of output power and switching frequency were derived for each functional section of the circuits.

Circuit efficiency and weights were reduced to frequency-dependent and independent components for convenient identification of frequency limitations resulting from circuit design and component selection. Baseline designs were established for each section of the circuit for a selected number of applicable power outputs. Expansion of the design data about each baseline design established crossover points. Data synthesis for the complete circuit resulted from selecting the more optimum values between the crossover points for each circuit section. The final converter parametric data is the result of synthesizing the applicable groups of data derived for each functional section of the converter circuit.

2. MODEL CONVERTER SPECIFICATION

The following model converter specification was established as typical for the primary and secondary requirements. Design techniques, component selection, and circuit configurations that will meet this specification are investigated to determine interactions and tradeoffs.

2.1 Primary Requirements

• Output power	1 to 200 w, parametrically variable
• Input voltage range	28 vdc ±15 percent
• Output voltage	28 vdc
• Thermal	-20 to +50°C, mounting base temperature

2.2 Secondary Requirements

2.2.1 Reliability

• Redundancy	None
• Fault isolation	None

2.2.2 Performance

• Output regulation	±3 percent
• Load variation	50 to 100 percent of rated load
• Audio susceptibility	3 volts p-p from 30 cps to 150 kc
• Regulation against dynamic load variation	Not required
• Close tolerance regulation	Not required
• Output ripple	±2 percent

2.2.3 Number of Outputs: 1

2.2.4 Conducted Interference: MIL-I-6181

2.2.5 Special Requirements: None

3. CONVERTER CIRCUITS

3.1 Regulated Square Wave Converter (RSWI)

The block diagram of the RSWI converter is shown in Figure C-1, in a configuration convenient for weight and efficiency analysis. Simplified schematics are indicated in each block. All operating frequencies as noted in each block are referenced to the squarewave switching frequency (f) of this circuit. A pulsewidth preregulator is included in the RSWI design in order to meet the ±3 percent regulation requirement. Inversion is

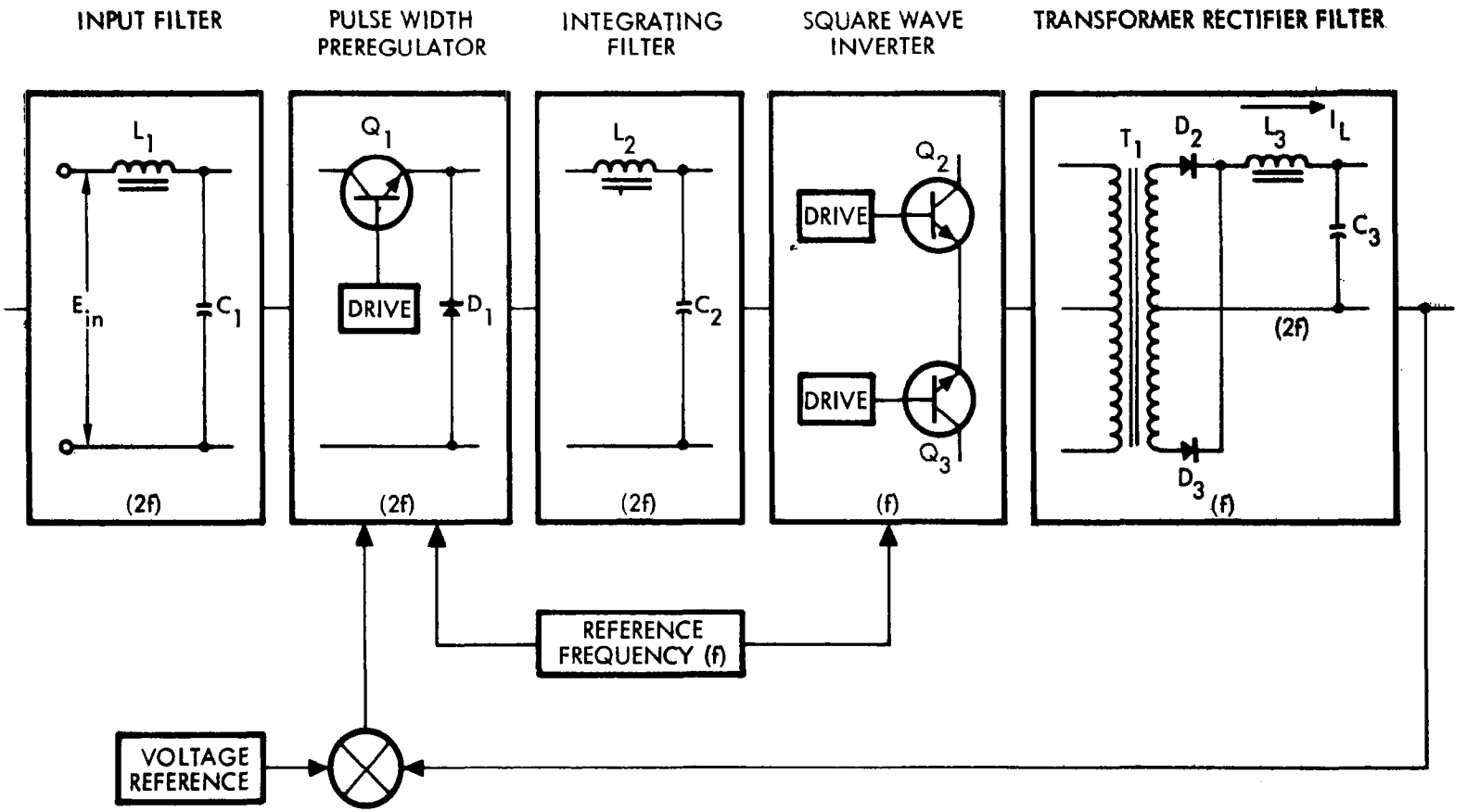

Figure C-1. Block Diagram, RSWI Converter

performed by a switch consisting of two transistors operating in push-pull into a nonsaturating power transformer. A saturating drive core provides the drive and also determines the reference switching frequency (f). The squarewave output of the transformer is rectified and filtered to provide the necessary regulated dc voltage.

3.2 Pulsewidth Converter (PWI)

The block diagram of the PWI converter is shown in Figure C-2. The PWI circuit combines inversion and regulation functions in the pulsewidth inverter stage. Switching reference frequency (f) is determined by a separate oscillator transistor. Duty cycle of the inverter switch is controlled by an error amplifier to maintain a constant average rectified output voltage, independent of input voltage and load variations. The pulsewidth modulated waveform out of the transformer is rectified and then smoothed in the output integrating filter.

3.3 Energy Storage Converter (ES)

The block diagram of the ES converter is shown in Figure C-3. When the transistor is ON, energy is stored in the transformer/inductor (air-gapped transformer) through its primary winding, while load power is supplied from the integrating capacitor. The induced emf in the transformer/inductor secondary is blocked from producing an output current by the diode. When the transistor is switched OFF, the secondary emf reverses and the stored energy is discharged through the secondary winding, to supply load power and to recharge the output integrating capacitor. If the transistor ON time is set equal to T/2 at nominal input voltage and load, then the ON-OFF periods may be varied with input voltage and load variations to maintain constant output voltage.

3.4 Push-Pull Energy Storage Converter (Push-Pull ES)

The block diagram of the (Push-Pull ES) converter is shown in Figure C-4. The basic operation is the same as for the (ES) circuit except that Q_1 and Q_2 transistors alternate ON and OFF, providing power to the load on each half cycle. Assuming the same size components and switching frequency, the (Push-Pull ES) circuit can provide twice the power output of the (ES) circuit. The efficiency remains essentially the

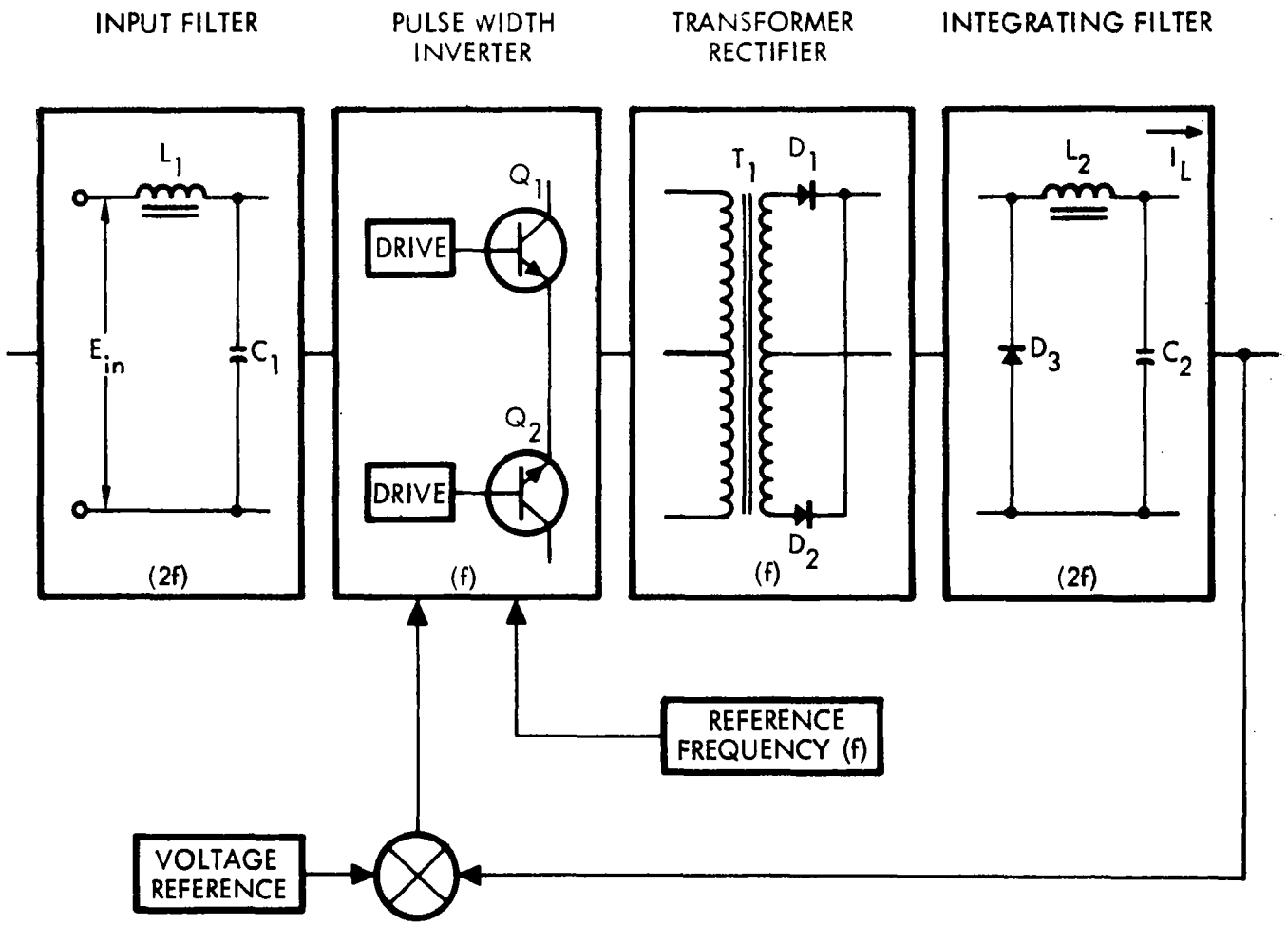

Figure C-2. Block Diagram, PWI Converter

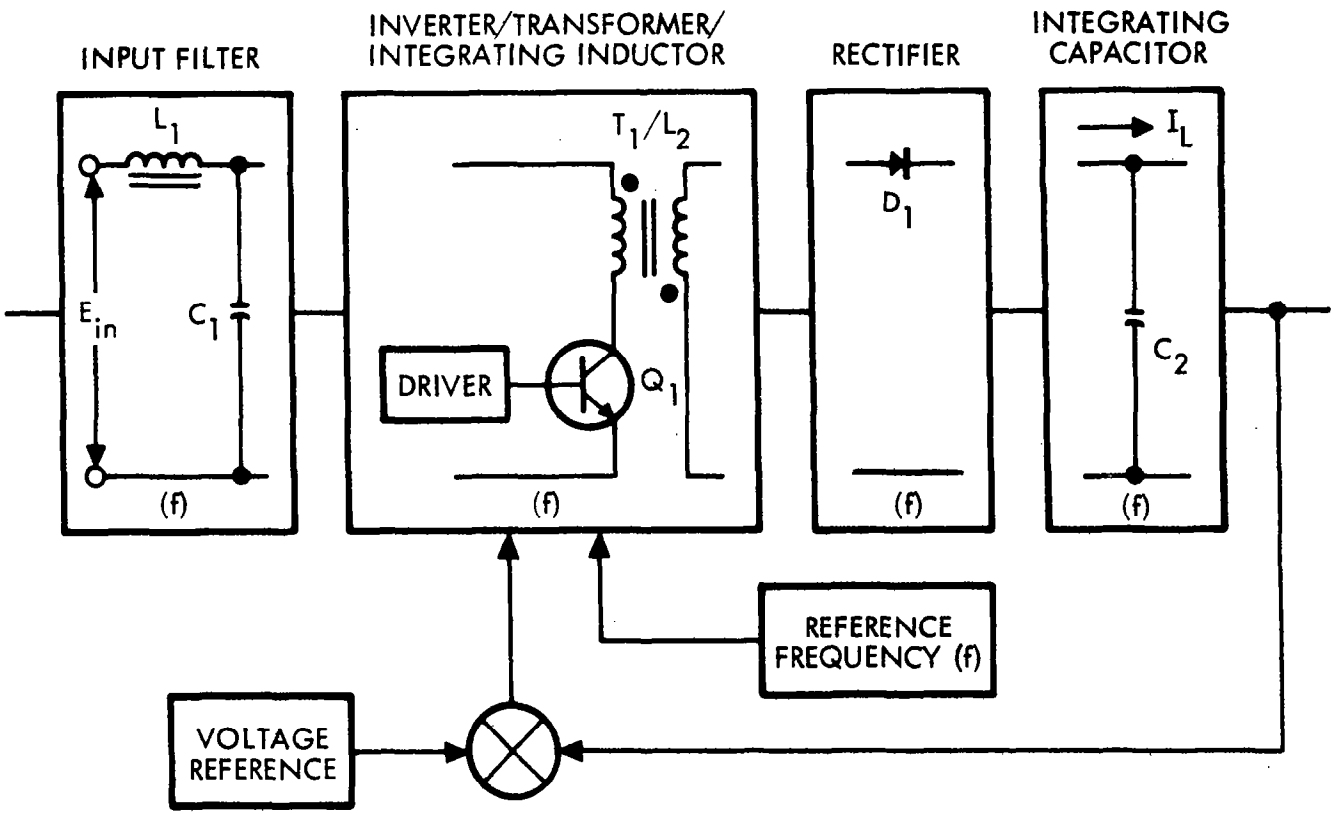

Figure C-3. Block Diagram, ES Converter

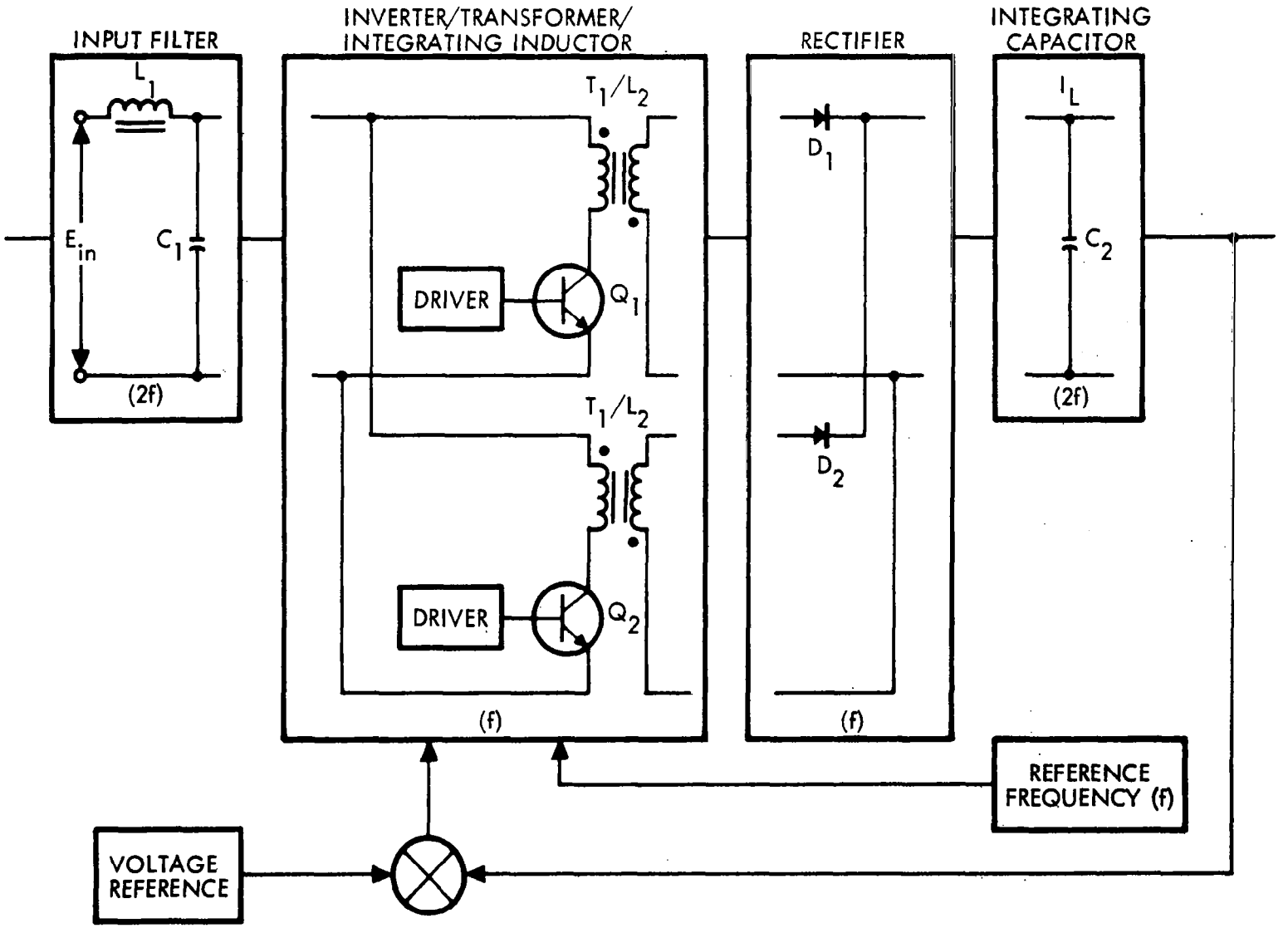

Figure C-4. Block Diagram, ES Push-Pull Converter

same for both circuits and the weight increase is approximately equal to the weight of the added (ES) circuit inverter/transformer/integrating inductor and rectifier. The input filter and integrating capacitor remain the same size because their operating frequency has now doubled. Thus, a significant improvement in weight per watt output is obtained.

4. PARAMETRIC DATA CALCULATIONS

Design centers for the converter circuits are selected at typical frequency and power ratings according to the design criteria discussed below for each individual type circuit. Design centers are selected for each frequency or power range where component characteristics (i. e., power dissipation or weight) become limiting and a change in component type is required. These design centers are then expanded over the power and frequency spectrum according to the mathematical model noted.

Weights and efficiencies are calculated from these performance equations for each circuit section using component specifications from manufacturers' data sheets.

The accuracy of this method is periodically checked by comparing selected test data with the parametric data calculated. For example, measured semiconductor loss data allows a straightforward comparison with the calculated data.

The following paragraphs provide the design considerations for each component and combinations of components making up the functional circuit sections.

4. 1 Input Filter Design

LC input filter is used for all four converter circuit designs, based on the following common requirements:

- The capacitor must supply I load for a period of 1/2f, where (f) is the switching frequency
- Capacitor ripple voltage is less than 1 volt p-p nominal, or less than 10 percent of regulator range
- LC resonant frequency is less than f/5 (f = switching frequency), so that resonant peaks occur before regulator corner frequency.

The filter operating frequency for each of the circuits is related to the reference switching frequency (f) as noted on each circuit block diagram.

4.1.1 Capacitor Design

Tantalum-foil capacitors are applicable for operating frequencies up to 20 kc. Because input filter capacitance requirements are relatively large, tantalum-foil units provide a low specific weight for best weight optimization. However, a large dissipation factor must be accepted. Ceramic capacitors are applicable for operating frequencies of 20 kc and higher when the capacitive requirements are smaller. The higher specific weight for ceramic units is less important than the gains attainable by their lower dissipation factor. Figure C-5 presents the input-filter power loss-frequency data.

The following equations relate the weight and dissipation factor (efficiency) for each of the two types of capacitors as a function of output power and operating frequency as defined on the block diagrams.

- Weight (M_c)

$$M_c = K_1 f^{-1} P_{out} \text{ (lb)} \qquad (1)$$

where

$$K_1 = 7.10 \times 10^{-3} \frac{\text{lb kc}}{\text{watt}} \qquad (f \leq 20 \text{ kc})$$

$$K_1 = 5.50 \times 10^{-2} \frac{\text{lb kc}}{\text{watt}} \qquad (f > 20 \text{ kc})$$

- Efficiency (N_c)

$$N_c = 100 - K_2 f \text{ (percent)} \qquad (2)$$

where

$$K_2 = 6 \times 10^{-2} \text{ kc}^{-1} \qquad (f \leq 20 \text{ kc})$$

and

$$K_2 = 6 \times 10^{-3} \text{ kc}^{-1} \qquad (f > 20 \text{ kc})$$

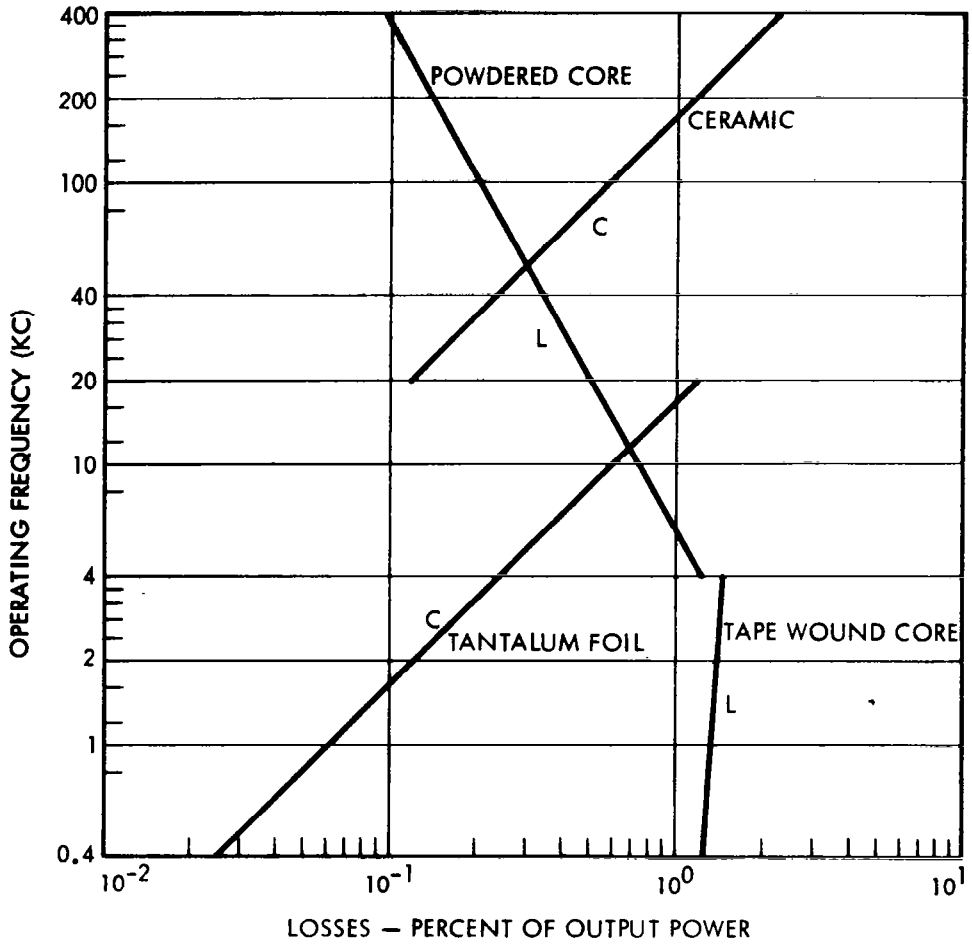

Figure C-5. Input Filter Losses for all Four Converter Circuits

4.1.2 Inductor Design

Laminated core materials are applicable for operating frequencies up to 4 kc. Above 4 kc, powdered cores are necessary to obtain adequate high-frequency permeability. When inductance requirements are large, such as for the input filter, it is desirable to use the laminated core materials to minimize weight by storing energy in an air gap. The core losses associated with the resulting ac flux density are acceptable when they are approximately equal to the copper losses.

The following equations relate the weights and power losses (efficiency) for each of the two types of core materials (Figure C-5) as a function of output power and operating frequency:

- Weight (M_L)

$$M_L = K_3 f^{-0.75} \left(P_{out}\right)^{0.75} \text{ (lb)} \qquad (3)$$

where

$$K_3 = 9.1 \times 10^{-3} \frac{\text{lb kc}}{\text{watt}} \qquad (f \leq 4 \text{ kc})$$

$$K_3 = 1.80 \times 10^{-2} \frac{\text{lb kc}}{\text{watt}} \qquad (f > 4 \text{ kc})$$

- Efficiency (N_L)

$$N_L = 100 - \left(K_4 f^{0.68} + K_5 f^{-0.75}\right) \text{(percent)} \qquad (4)$$

where

$$K_4 = 0.5 \text{ kc}^{-1} \qquad (f \leq 4 \text{ kc})$$

$$K_4 = 0.02 \text{ kc}^{-1} \qquad (f > 4 \text{ kc})$$

$$K_5 = 0.05 \text{ kc} \qquad (f < 4 \text{ kc})$$

$$K_5 = 3.5 \text{ kc} \qquad (f > 4 \text{ kc})$$

4.1.3 Input Filter Summary

All four of the baseline circuits being considered have an input LC-type filter. The function and operating modes of the filter for each circuit

are very similar, although the operating frequencies differ. The following summary equations combine the capacitor and inductor equations from the previous paragraphs.

- Weight (M)

$$M_1 = M_{C1} + M_{L1} \text{ (lb)}$$

$$M_1 = K_1 f^{-1} P_{out} + K_3 f^{-0.75} \left(P_{out}\right)^{0.75} \text{ (lb)} \qquad (5)$$

- Efficiency (N)

$$N_1 = N_{C1} N_{L1} \text{ (percent)}$$

$$N_1 = (100 - K_2 f) \left[100 - \left(K_4 f^{0.68} + K_5 f^{-0.75}\right)\right] \text{ (percent)}$$

4.2 Integrating Filter Design

An LC-type integrating filter is used in the output of the pulsewidth preregulator in the RSWI circuit, and in the outputs of the PWI and push-pull ES converter circuits. The integrating filter for the ES circuit performs differently and is discussed in Subsection 4.3. The (L_2) inductor for the push-pull ES circuit is integral with the transformer. The specification requirement that regulation be maintained to 50-percent minimum load requires that the inductor (L_2) limit the change in current (ΔI) to 100 percent of the load current (I_L) during the period 0.3/f, where (f) is the switching frequency. In order to maintain closed-loop stability, the resonant frequency of the inductor and capacitor must be greater than f/25 (f = switching frequency).

The weight-power loss tradeoff for the inductor design, Figure C-6, suggests the use of Hypersil core material for operating frequencies below 4 kc. Above 4 kc, Permalloy core material would be selected.

The capacitor design is similar to that of Paragraph 4.1.1, for the input filter design, with tantalum-foil capacitors used up to 20 kc and ceramic capacitors above 20 kc.

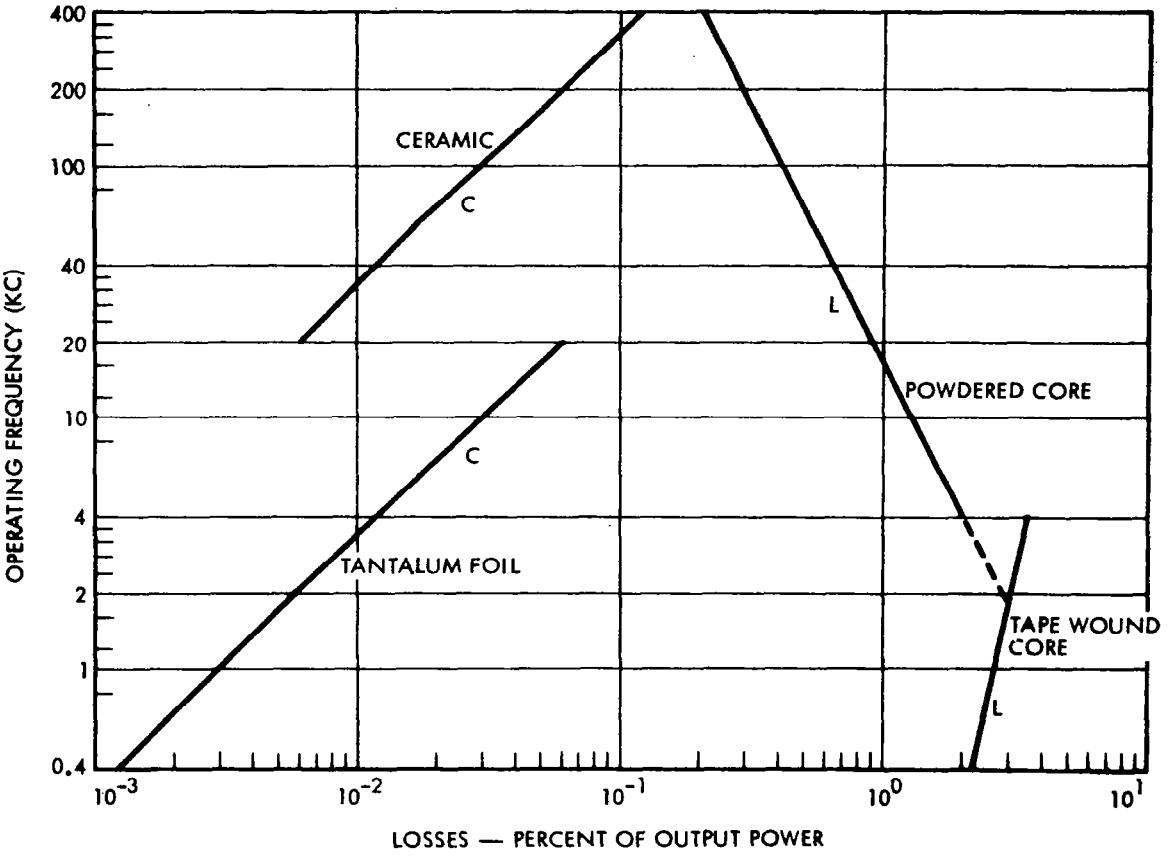

Figure C-6. Integrating Filter Losses for RSWI, PWI, and Push-Pull ES Converter Circuits

The following expressions provide the weight and efficiency relationships for the integrating filter design as functions of output power and operating frequency as defined on the block diagrams.

- Weight (M)

$$M_2 = M_{L2} + M_{C2} \text{ (lb)} \tag{7}$$

$$M_2 = K_6 f^{-0.75} \left(P_{out}\right)^{0.75} + K_7 f^{-1} P_{out} \text{ (lb)}$$

where

$$K_6 = 3.5 \times 10^{-2} \frac{\text{lb kc}}{\text{watt}} \qquad (f < 4 \text{ kc})$$

$$K_6 = 7.3 \times 10^{-2} \frac{\text{lb kc}}{\text{watt}} \qquad (f \geq 4 \text{ kc})$$

$$K_7 = 2.2 \times 10^{-2} \frac{\text{lb kc}}{\text{watt}} \qquad (f < 20 \text{ kc})$$

$$K_7 = 1.8 \times 10^{-1} \frac{\text{lb kc}}{\text{watt}} \qquad (f \geq 20 \text{ kc})$$

- Efficiency (N)

$$N_2 = N_{L2} N_{C2} \text{ (percent)} \tag{8}$$

$$N_2 = \left[100 - \left(K_8 f^{0.68} + K_9 f^{-0.75}\right)\right]\left(100 - K_{10} f\right) \text{ (percent)}$$

where

$$K_8 = 1.2 \text{ kc}^{-1} \qquad (f < 4 \text{ kc})$$

$$K_8 = 0.05 \text{ kc}^{-1} \qquad (f \geq 4 \text{ kc})$$

$$K_9 = 0.8 \text{ kc} \qquad (f < 4 \text{ kc})$$

$$K_9 = 5.6 \text{ kc} \qquad (f \geq 4 \text{ kc})$$

$$K_{10} = 3 \times 10^{-3} \text{ kc}^{-1} \qquad (f \leq 20 \text{ kc})$$

$$K_{10} = 3 \times 10^{-4} \text{ kc}^{-1} \qquad (f > 20 \text{ kc})$$

4.3 Energy Storage Filter Design

The energy-storage filter is also an integrating filter, but utilizes the large inductance of the inverter transformer. Thus, only an output capacitor need be added.

The specification requirement for regulation to 50-percent minimum load requires the inductor to limit the current change (ΔI) to 100 percent of the load current (I_L) during the period 0.5/f, where (f) is the switching frequency. The closed-loop stability requires the resonant frequency of the inductor and capacitor to be greater than f/25 (f = switching frequency). This requirement, rather than the output ripple specification, controls the capacitance value.

Selection of the core material and type of capacitor as a function of the operating frequency, Figure C-7, for the (ES) circuit, and Figure C-6 for the (push-pull ES) circuits, is similar to the integrating filter design, for the RSWI and PWI converters namely Hypersol for frequencies below 4 kc and Permalloy above 4 kc.

The following equations represent the weight and efficiency design relationships for the ES converter circuit.

- Weight (M)

$$M_3 = M_{L2} + M_{C2} \text{ (lb)}$$

$$M_3 = K_{11} f^{-0.75} \left(P_{out}\right)^{0.75} + K_{12} f^{-1} P_{out} \text{ (lb)} \qquad (9)$$

where

$$K_{11} = 5.1 \times 10^{-2} \frac{\text{lb kc}}{\text{watt}} \qquad (f < 4 \text{ kc})$$

$$K_{11} = 1.02 \times 10^{-1} \frac{\text{lb kc}}{\text{watt}} \qquad (f \geq 4 \text{ kc})$$

$$K_{12} = 4.9 \times 10^{-2} \frac{\text{lb kc}}{\text{watt}} \qquad (f < 20 \text{ kc})$$

$$K_{12} = 3.6 \times 10^{-1} \frac{\text{lb kc}}{\text{watt}} \qquad (f \geq 20 \text{ kc})$$

- Efficiency (N)

$$N_3 = N_{L2} N_{C2} \text{ (percent)}$$

$$N_3 = \left[100 - \left(K_{13} f^{0.68} + K_{14} f^{-0.75}\right)\right] \left(100 - K_{15} f\right) \qquad (10)$$

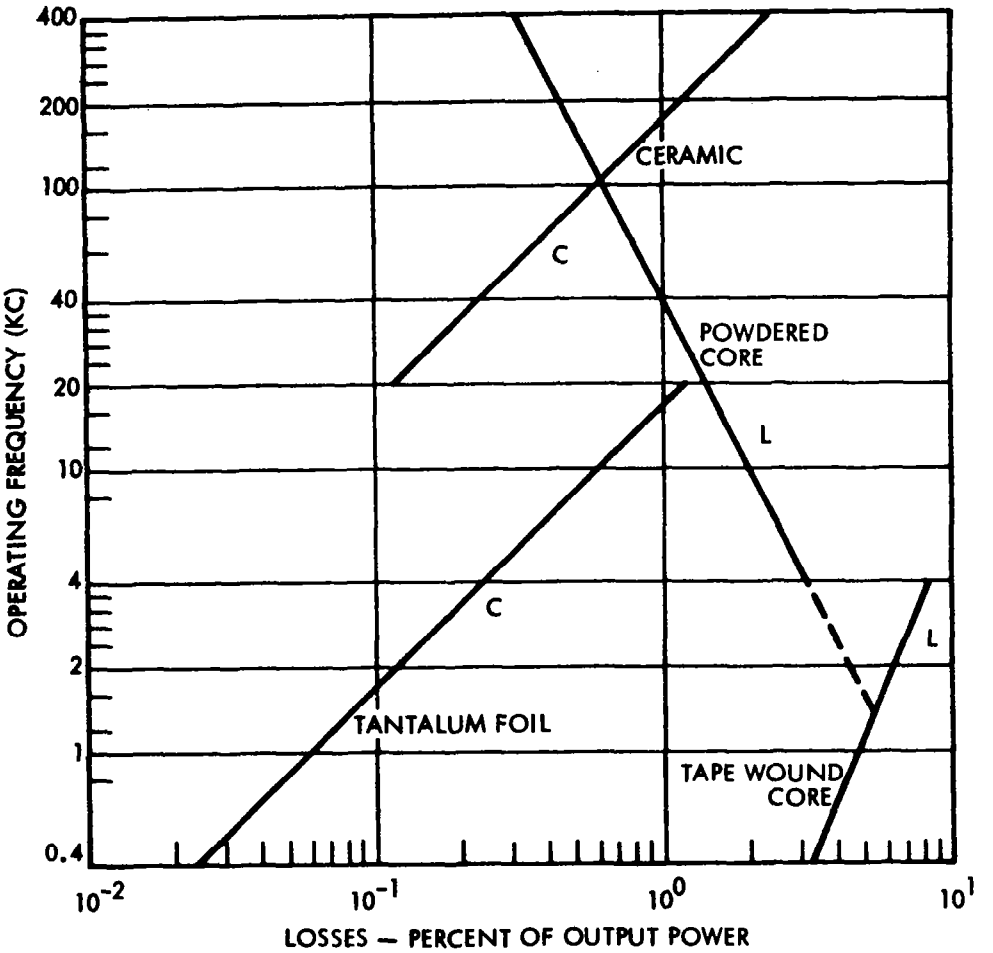

Figure C-7. ES Converter, Integrating Filter Losses

where

$K_{13} = 1.6\ kc^{-1}$ $(f < 4\ kc)$

$K_{13} = 0.075\ kc^{-1}$ $(f \geq 4\ kc)$

$K_{14} = 1.2\ kc$ $(f < 4\ kc)$

$K_{14} = 8.4\ kc$ $(f \geq 4\ kc)$

$K_{15} = 6 \times 10^{-2}\ kc^{-1}$ $(f < 20\ kc)$

$K_{15} = 6 \times 10^{-3}\ kc^{-1}$ $(f \geq 20\ kc)$

4.4 Transformer Rectifier

The transformer-rectifier elements of the RSWI and PWI circuits are similar to the TR units reported in Paragraph 5.6.4, Page 5-23. The same parametric equations and curves are used to determine the weight and efficiencies for these circuits. Application of the TR data to the ES and push-pull ES converter circuits is not required since the transformer function is performed by the filter inductor, which is the controlling design requirement. The rectifier data for the ES and push-pull ES converter circuits is included with the semiconductor data.

4.5 Semiconductor Circuit Design

Each of the circuits considered contain both transistors and diodes whose weight and efficiencies depend strongly upon the output power and switching frequency. The semiconductor weights considered here include only the component weight. The hardware weight required for structural and thermal reasons is derived in Subsection 4.7.

Semiconductor losses are divided into a steady-state (frequency independent) component, and a switching (frequency dependent) component. Steady-state losses consist of drive circuit power and saturation dissipation. Switching losses result during transition between the minimum voltage, full current ON state; and the full voltage, zero current OFF state. At the higher operating frequencies, the efficiency of the equipment is reduced because of the higher average switching losses.

A theoretical model analysis was performed on the circuits to establish the semiconductor currents, voltage, instantaneous power losses, average power losses, and I-V curves. The items investigated were the transistor's turn-on time, turn-off time, and storage time, and the power diode's turn-on and turn-off or recovery time. Ideal transformers and chokes were used in the model and therefore magnetic capacitance and leakage inductance did not show up in the characteristic waveforms. The following is a list of parameters for typical fast switching semiconductors used in the circuits. Semiconductors with intermediate ratings are available but they do not have the necessary fast switching characteristics.

Transistors			
Transistor Type	Turn-on Time t_1	Turn-off Time t_4	Storage Time t_5
1 amp 10 amp	100 nsec 1 μsec	100 nsec 1 μsec	200 nsec 2 μsec

Diodes			
Diode Type	Recovery Time t_2	Recovery Current I_R	Turn-on Time t_3
1 amp	150 nsec	Equals forward current	10 nsec
10 amp	500 nsec	Equals forward current	10 nsec

4.5.1 Regulated Square Wave Converter (RSWI)

The remaining portions of this circuit consist primarily of semiconductor components such as transistors and diodes. The functional sections of the circuit containing semiconductors, as shown in Figure C-1 are a switching dc pulsewidth preregulator and a conventional squarewave inverter.

The weights of the semiconductors – one transistor and one diode – in the pulsewidth preregulator are related to the two listed current ratings. A 10-watt (or less) converter would use the 1-amp transistor and diode weighing a total of 0.01 lb. Larger power converters, up to 200 w, would use the 10-amp devices weighing a total of 0.025 lb.

The power losses associated with the semiconductors are divided into steady-state and switching losses. The transistor steady-state losses consist of the base drive power and the saturated voltage drop power loss. The base drive power was calculated to be 2.7 percent of the output power, and 1.8 percent of the output power for the saturated voltage drop power loss.

The transistor switching losses in watts for the pulsewidth preregulator are related to the device switching times as given by the following equation

$$P_{loss} = \frac{1}{T}\left[t_1 \frac{E_{in} I_L}{2} + t_2 \frac{E_{in}}{2}(I_R + I_L) + t_3 \frac{E_{in} I_L}{2} + t_4 \frac{E_{in} I_L}{2}\right] (w) \qquad (11)$$

where T is period of one complete cycle and is equal to 1/f defined by the reference drive frequency

t_1 = transistor turn-on time

t_2 = diode recovery time

t_3 = diode turn-on time

t_4 = transistor turn-off time

t_5 = transistor storage time

E_{in} = input supply voltage

I_L = load current

I_R = diode recovery current

Note that t_5, the transistor storage time, does not appear in the above equation and does not contribute to the transistor losses. However, its effect is to decrease the total controllable range of the preregulator. The maximum percentage ratio for the control range is given by Equation (12).

$$\frac{(t_{on})_{max} - (t_{on})_{min}}{T} \times 100 = \frac{T - (t_1 + t_2 + t_3 + t_4 + t_5)}{T} \times 100 \text{ (percent)} \qquad (12)$$

Typical values of P_{loss} in Equation (11) for the two device ratings are:

$$\text{For 1-amp transistor: } 80 \times 10^{-8} f\, P_{out} \text{ (w)}$$

$$\text{For 10-amp transistor: } 470 \times 10^{-8} f\, P_{out} \text{ (w)}$$

The diode steady-state power loss was calculated to be 3.5 percent of the output power. The diode switching loss is given by Equation (13).

$$P_{loss} = \frac{t_2 E_{in} I_R}{2T} \text{ (w)} \tag{13}$$

This switching loss occurs during the turn-off time only, because very little energy is required to turn the diode on. The maximum losses occur at maximum input voltage. The evaluation of Equation (13) provides the following values of P_{loss} for each diode rating:

$$\text{For 1 amp: } 23 \times 10^{-8} f\, P_{out} \text{ (w)}$$

$$\text{For 10 amp: } 120 \times 10^{-8} f\, P_{out} \text{ (w)}$$

The weight of the two transistors in the squarewave inverter section is 0.01 lb for 1-amp devices (less than 10 w), and 0.025 lb for the 10-amp devices (10 to 200 w).

As before, the power losses associated with the transistors are divided into steady-state and switching losses. The steady-state losses are calculated to be 2.7 percent of the output power for the base drive power and 1.8 percent of output power for the saturated voltage drop power loss.

The transistor switching losses for the squarewave inverter section are given by Equation (14).

$$P_{loss} = \frac{I_\beta \beta E_{in}}{T} \left[\frac{3(t_5 - t_1)}{2} + t_4 + \frac{t_1}{2} \right] \text{ (w)} \tag{14}$$

where

I_β is the transistor base current

β is the transistor current gain

The above equation gives the loss of only one transistor of the inverter; therefore the total switching losses are double that given by Equation (14). Note that t_5, the storage time, has a predominant effect on the power loss and that the transistor collector current can reach a value many times the load current depending on the actual beta of the transistor at the operating current level. Proper circuit design can minimize the losses due to t_5. The values of P_{loss} in Equation (14) for two transistors at each selected current rating are:

$$\text{For 1 amp: } 120 \times 10^{-8} f\, P_{out} \text{ (w)}$$

$$\text{For 10 amp: } 1200 \times 10^{-8} f\, P_{out} \text{ (w)}$$

4.5.2 Pulsewidth Converter (PWI)

The semiconductor sections of this circuit as shown in Figure C-2 are the pulsewidth converter transistors and the diode in the integrating filter. The weight of these semiconductors is 0.015 lb for the 1-amp rating (less than 10 w), and 0.045 for the 10-amp rating (10 to 200 w).

The total transistor and diode losses are identical to the inverter transistors and diode losses provided for the (RSWI) design described in Paragraph 4.5.1.

4.5.3 Energy Storage Converter (ES)

One transistor and driver stage in the inverter/transformer/integrating inductor section and one diode in the rectifier section, as shown in Figure C-3, constitute all of the semiconductors in this circuit. The weights of the semiconductors are the same as given for the pulsewidth regulator, i.e., 0.01 lb and 0.025 lb.

The steady-state power losses in the transistor due to driver power is 2.7 percent of the output power. The saturated voltage drop power losses are 1.8 percent of the output power. The steady-state diode loss is 2.5 percent of the output power.

Switching losses in the power transistor are given by Equation (15)

$$P_{loss} = \frac{E_{in} I_L}{T} (2t_1 + t_2 + 2t_3 + 2t_4) \text{ (w)} \qquad (15)$$

Again maximum power loss occurs at maximum input voltage. The values of P_{loss} in Equation (15) for the two transistor ratings are:

$$\text{For 1 amp: } 63 \times 10^{-8} f P_{out} \text{ (w)}$$

$$\text{For 10 amp: } 480 \times 10^{-8} f P_{out} \text{ (w)}$$

The diode switching losses are

$$P_{loss} = \frac{t_2 E_{in} I_R}{2T} \text{ (w)} \qquad (16)$$

The values of P_{loss} in Equation (16) for the two ratings are

$$\text{For 1 amp: } 1.2 \times 10^{-8} f P_{out} \text{ (w)}$$

$$\text{For 10 amp: } 40 \times 10^{-8} f P_{out} \text{ (w)}$$

4.5.4 Push-Pull Energy Storage Converter (Push-Pull ES)

The quantity of semiconductors for this circuit is twice that required for the (ES) converter circuit. Thus, the semiconductor weights are doubled, i.e., 0.02 lb and 0.05 lb.

The power losses in the second half of the inverter/transformer/integrating inductor and rectifier sections are identical to those reported in the previous paragraph. Because these losses are given as a percentage of output power, and the output power for the (push-pull ES) converter circuit is double that of the (ES) converter circuit, the percentage values remain the same. Thus, the percent efficiency is unchanged.

4.6 Error Amplifier Circuit

The error amplifiers for each of the circuits are similar in design and consist of the voltage reference circuit, two stages of amplifier gain and conversion circuit providing the transistor(s) drive power.

The power losses can be defined as a constant value and a variable value which is a function of the drive power. The constant power losses for the voltage reference and the two stages of gain are 200 mw for output powers greater than one watt, and 120 mw for output powers less than one watt. The variable power losses for the low-level conversion circuit of the drive power is 30 percent of the total circuit drive power.

The weights of the error amplifiers have a fixed component and a variable component which is a function of the drive power. The fixed component of weight for the voltage reference circuit and two stages of amplification is 0.022 lb. The variable weight component associated with the conversion circuit for the drive is given by the following equation

$$M = 0.03 + 0.2\, P_{drive} \text{ (lb)} \qquad (17)$$

4.7 Structural Weight

The converter structural weights are subject to two design requirements.

- The structure must support the components, meet vibration and shock specifications, and allow convenient assembly, test, and maintenance.
- The structure must transfer waste heat to the external environment.

One of these two requirements will establish the larger but necessary equipment weight for each output power level and frequency. When the equipment weight is established by the first requirement, the curve of Figure C-8 was used to determine equipment weight from the calculated components weight. The ratio of equipment weight to components weight (Figure C-8) increases below a 10-lb components weight because component sizes approach a minimum limit independent of power. This

determination of equipment weight also establishes the minimum volume in which the components could be packaged. An average value of 0.05 lb/in.^{3} was used to calculate the minimum volume.

In order to make a quick determination if the equipment weight would be established by the heat transfer requirement rather than the mechanical requirements, the curve of Figure C-9 was used to determine the equipment weight from the power losses calculated using the equations of the previous sections. Figure C-9 was based upon the following assumptions:

- Heat is transferred away from the converter by conduction and radiation only, due to the vacuum environment.
- The ambient temperature is 50°C.
- The equipment temperature rise is limited to 20°C with an emissivity of 0.9.
- The average heat conduction rate to the mounting base is 0.5 w/in.^{2} of base area.
- The average heat radiation rate is 0.1 w/in.^{2} of surface area.
- The average equipment density is 0.035 lb/in.^{3}
- The equipment structure is cube shaped.

The cube shape was chosen because it has the largest volume-to-surface area ratio for the most common packaging shapes. If the height of a rectangular shaped box is assumed equal to or less than the length or width, then a cube is also the limiting shape for the stated heat-transfer conditions. Whenever the equipment weight determined from Figure C-9 is less or equal to the equipment weight established by Figure C-8, the required weight is not established by the heat dissipation, since any other desirable shape would provide a greater heat transfer. Thus, the correct weight is determined from Figure C-8.

Figures C-10, C-11, C-12, and C-13 present the converter equipment weights as a function of power level, frequency, and packaging limitations for the four analyzed converter circuits. The solid lines represent the total packaged weight as determined from Figure C-8, when only

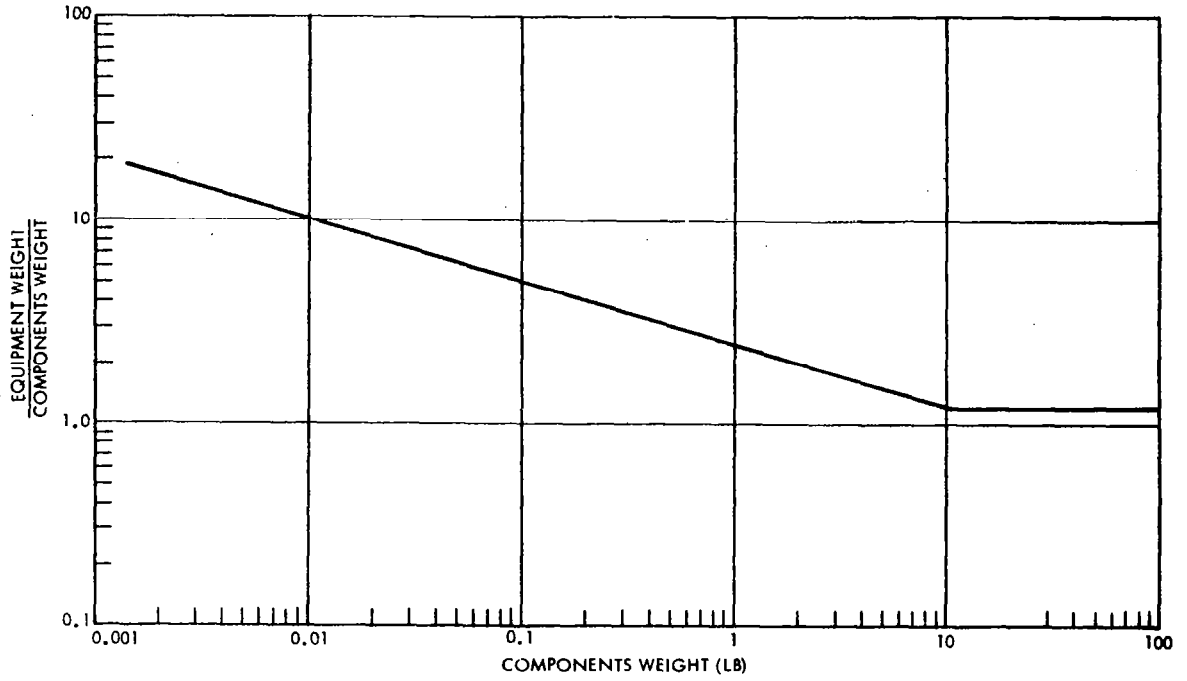

Figure C-8. Ratio of Equipment Weight to Components Weight

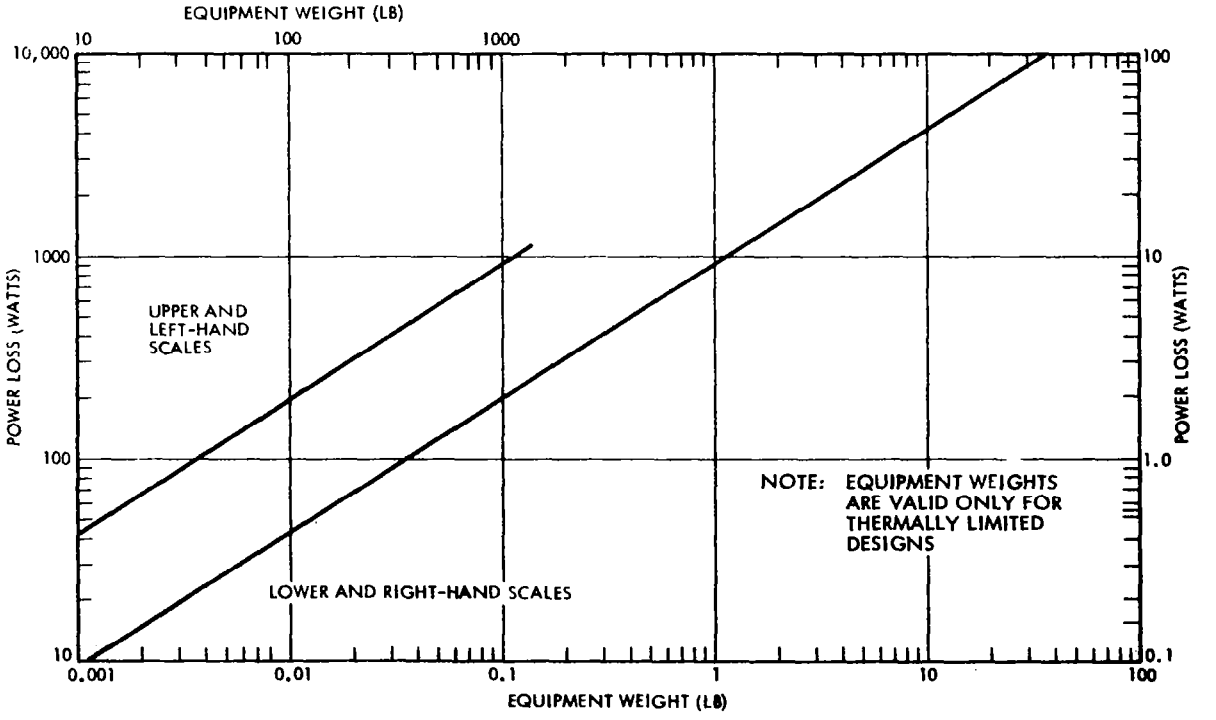

Figure C-9. Equipment Power Dissipation Versus Weight

component and minimum structural weights are considered. The uniformly dashed lines, starting from their respective intersection with the solid lines, represent the total packaged weight as determined from Figure C-9 when thermal dissipation requires an increase in surface area and, therefore, an increase in volume and weight. Because the cube is the least thermally desirable rectangular shape, the dashed lines represent maximum equipment weight when the equipment becomes thermally limited.

Analysis of the heat transfer parameters related to the package geometry disclosed a graphical method (Figures C-14 and C-15) for choosing the most optimum rectangular shape. The derivation and use of these curves is presented in Appendix D. The objective of the heat-transfer analysis was to increase the package thermal dissipation without unnecessary volume and weight increases. The assumed heat conduction and radiation rates, 0.5 and 0.1 $w/in.^2$, respectively, were found to be on-the-average, representative of most spacecraft designs. Therefore, the rates were not varied for this analysis. Starting with a cube having a constant minimum volume set by components to be packaged, the surface area can be increased by reducing the height until a minimum height, set by the largest component, is reached. A further increase in surface area and, therefore, heat dissipation is accomplished by holding constant the minimum height and volume, and changing the base shape from a square to a rectangle. Maximum heat transfer for this minimum volume is reached when the length to width ratio is increased to its maximum practical limit. Figure C-14 presents heat dissipation (watts) as a function of a square base area (length-to-width ratio K = 1), height and volume. Figure C-15 presents similar data when the length-to-width ratio (K) = 5. A maximum ratio of 5 was considered practical for most designs.

The converter weights represented by the uniformly dashed, maximum weight lines on Figures C-10, C-11, C-12, and C-13, were optimized, by using Figures C-14 and C-15, to provide a true minimum volume, minimum weight design consistent with the required heat dissipation. The irregularly dashed curves represent these optimum weights. The amount of heat dissipated for each converter design as a function of output power and frequency was obtained from the efficiency curves presented in Figures C-16, C-17, and C-18. The basic efficiency and weight data given by these parametric curves were assembled using the previous equations.

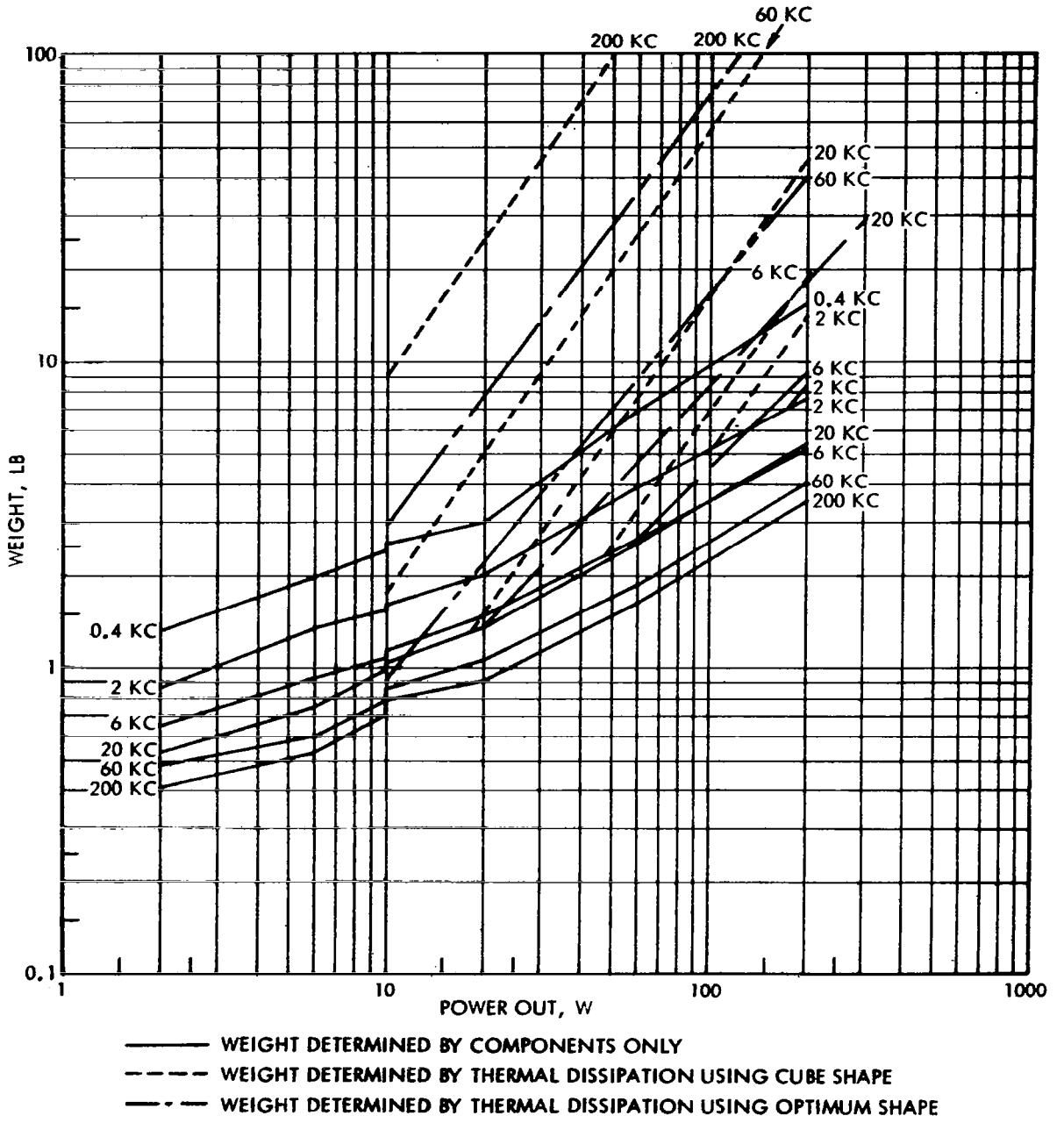

Figure C-10. RSWI Converter Weight

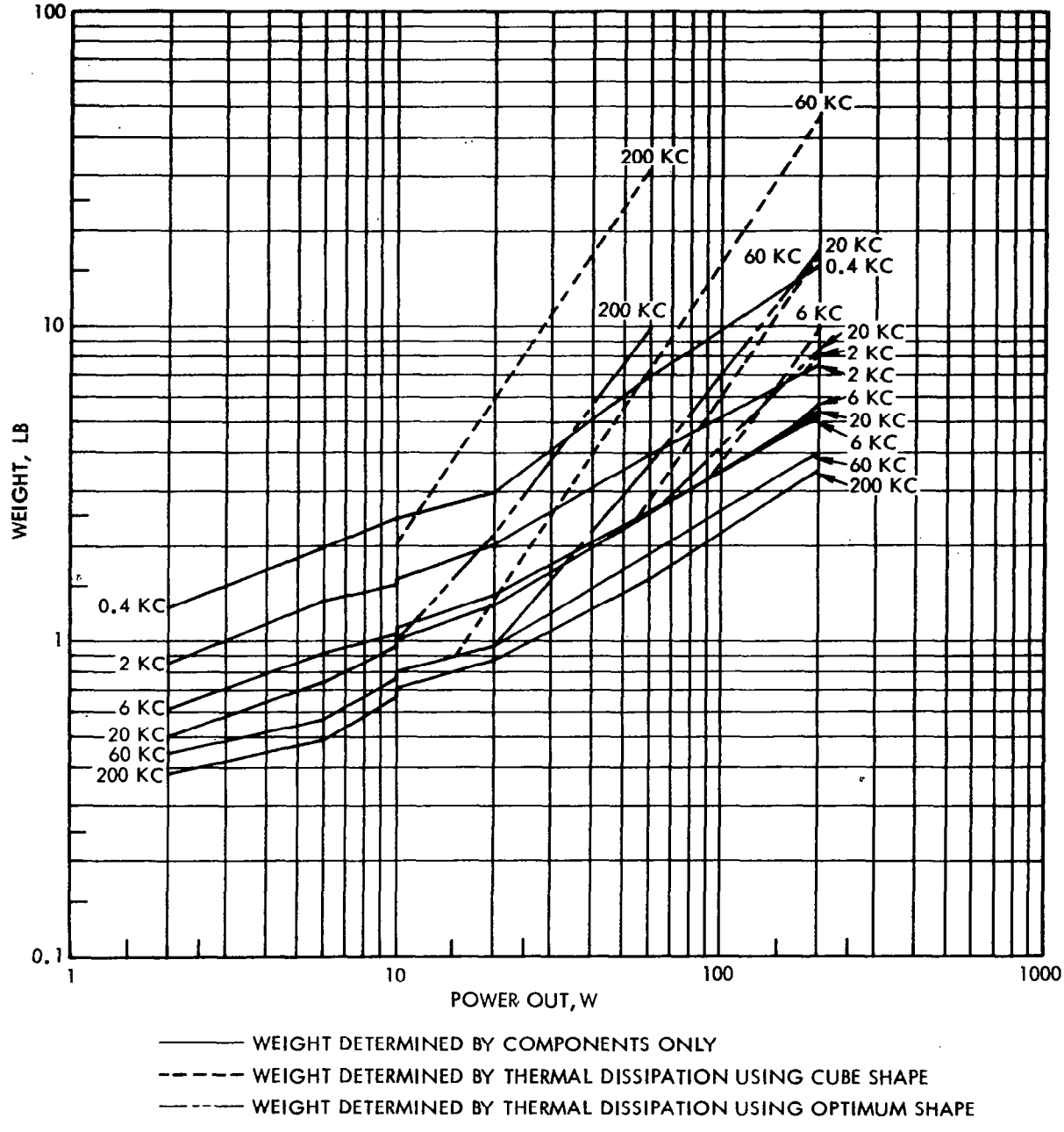

Figure C-11. PWI Converter Weight

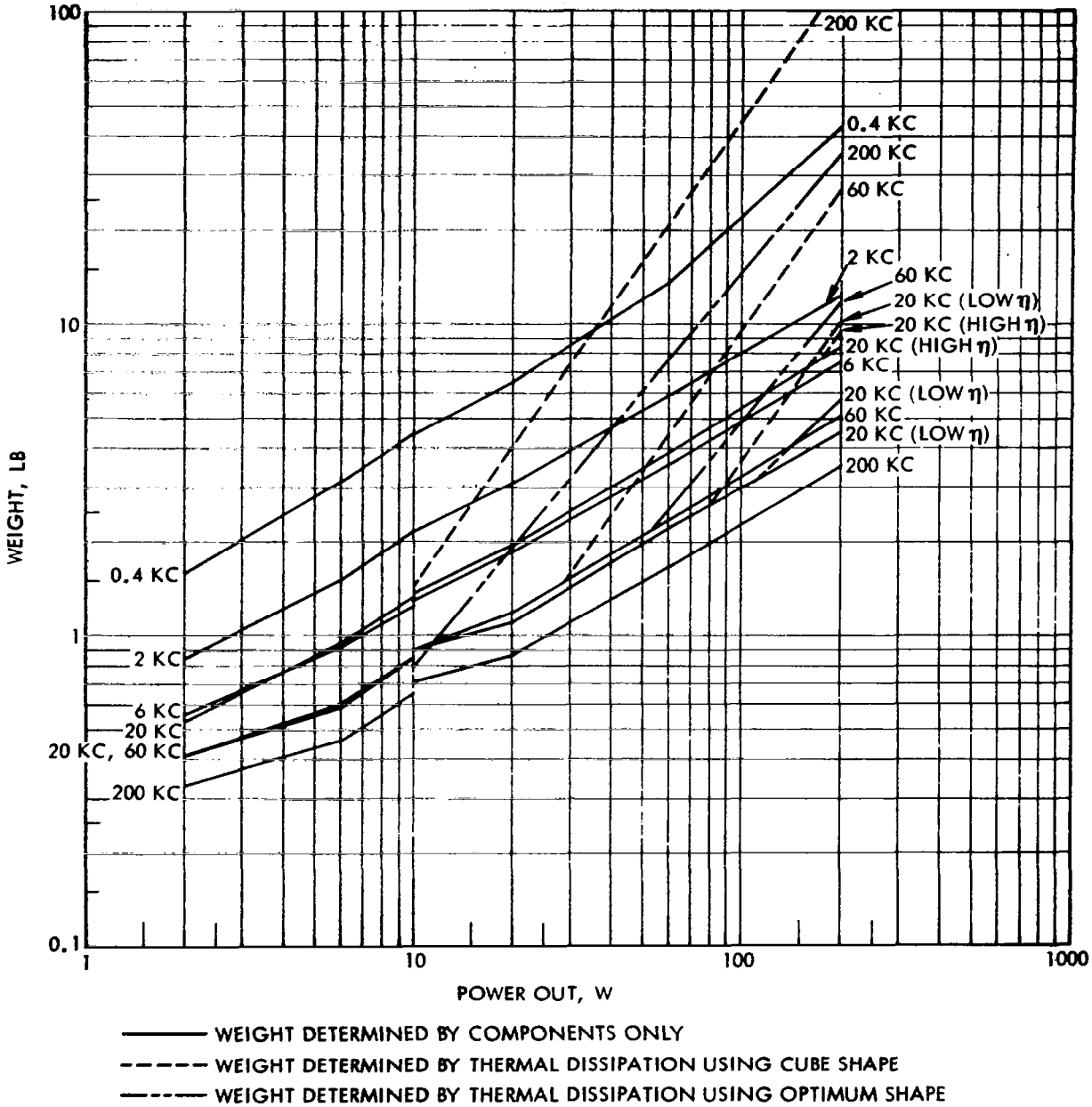

Figure C-12. ES Converter Weight

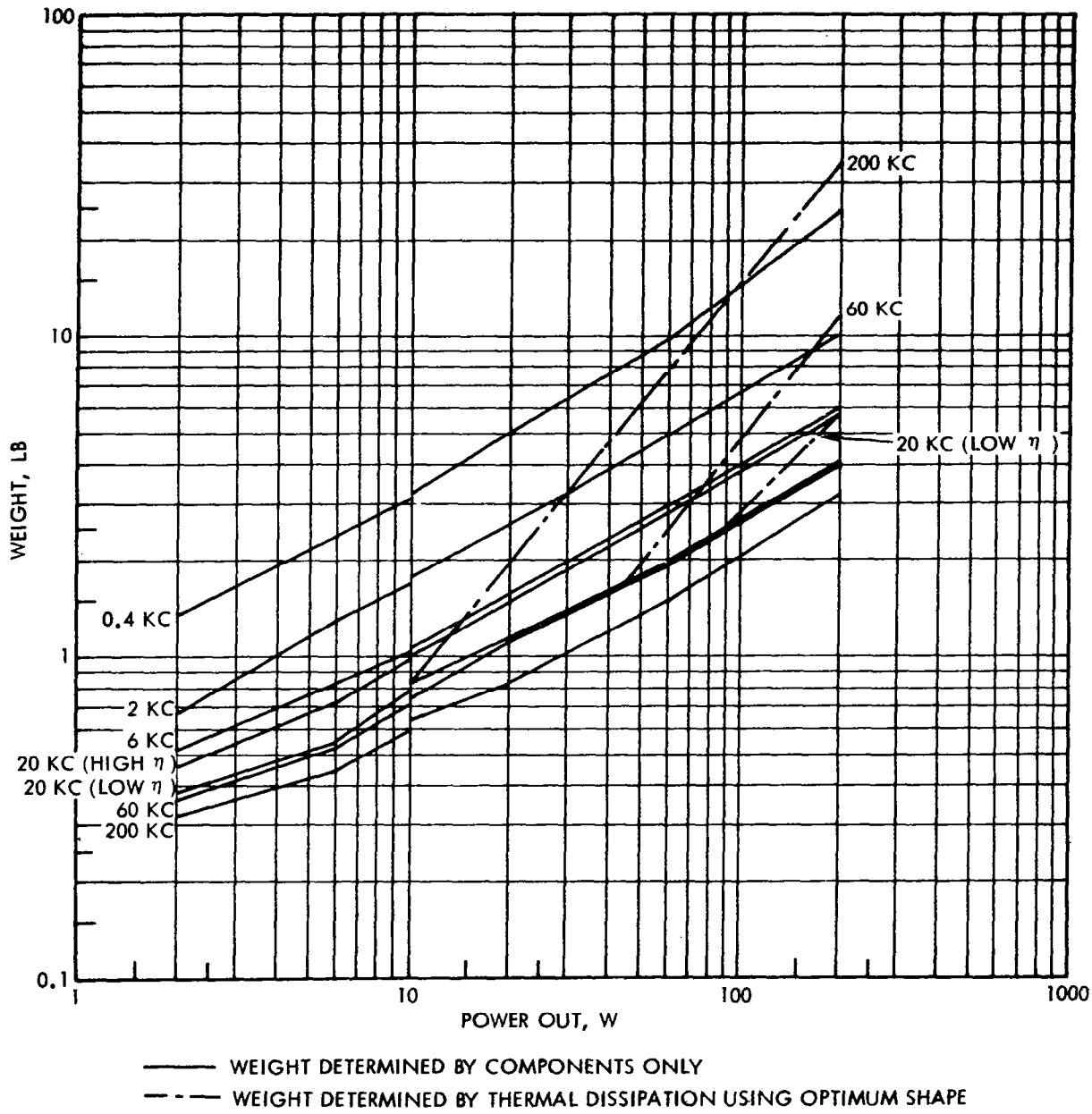

Figure C-13. ES Push-Pull Converter Weight

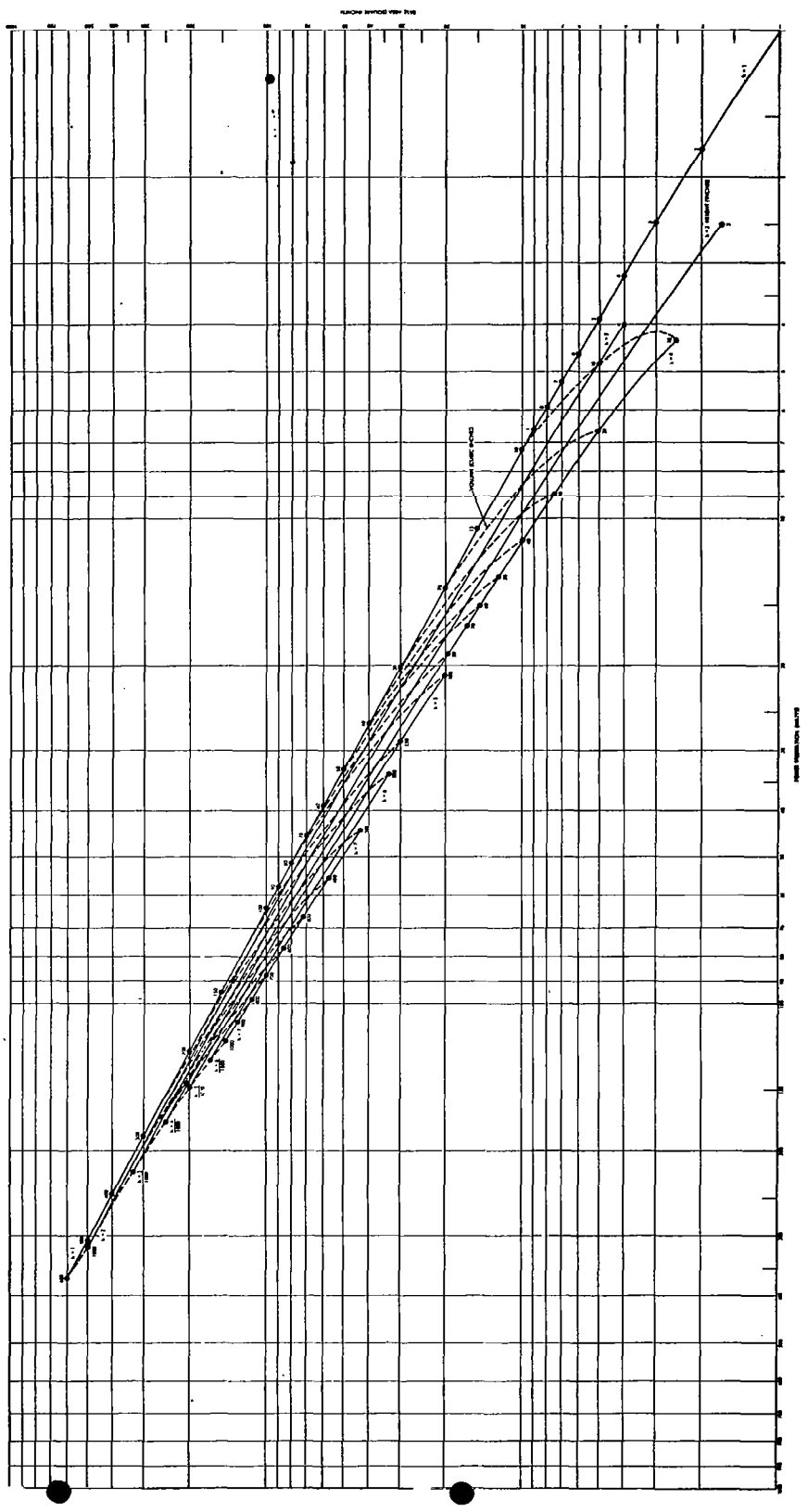

Figure C-14. Structure – Thermal Optimization – K = 1

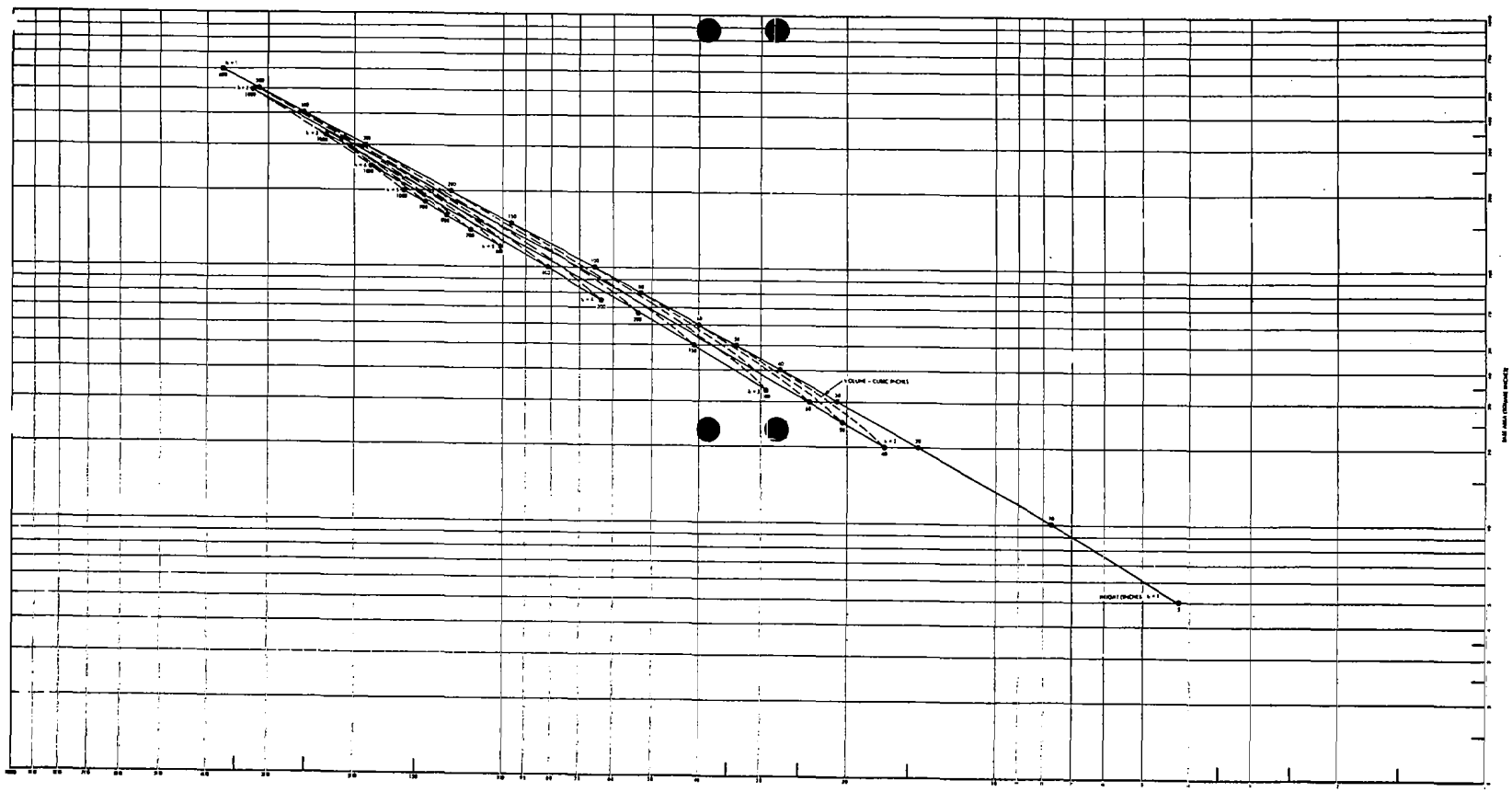

Figure C-15. Structure – Thermal Optimization – K = 5

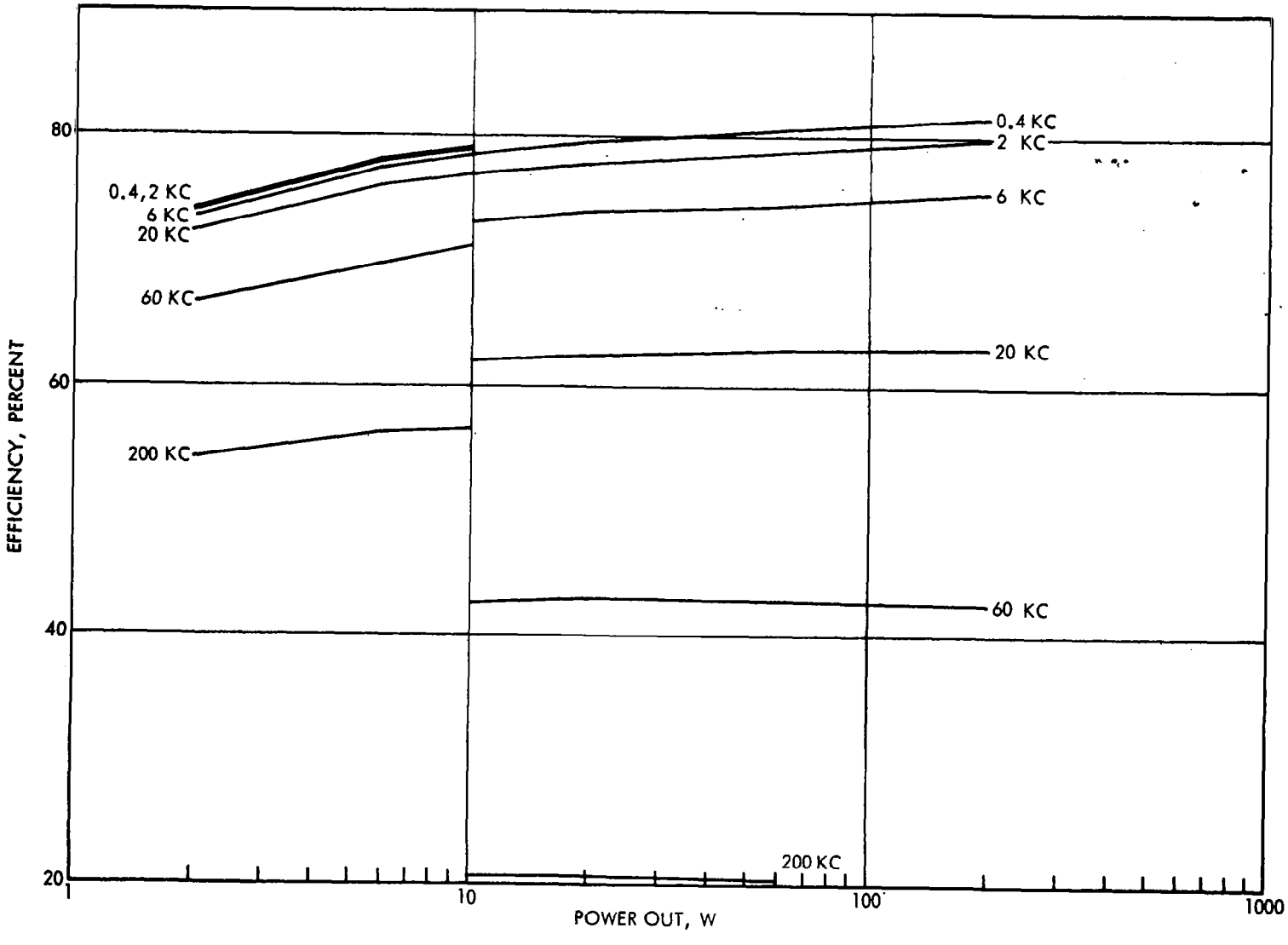

Figure C-16. RSWI Converter, Efficiency Versus Power Output

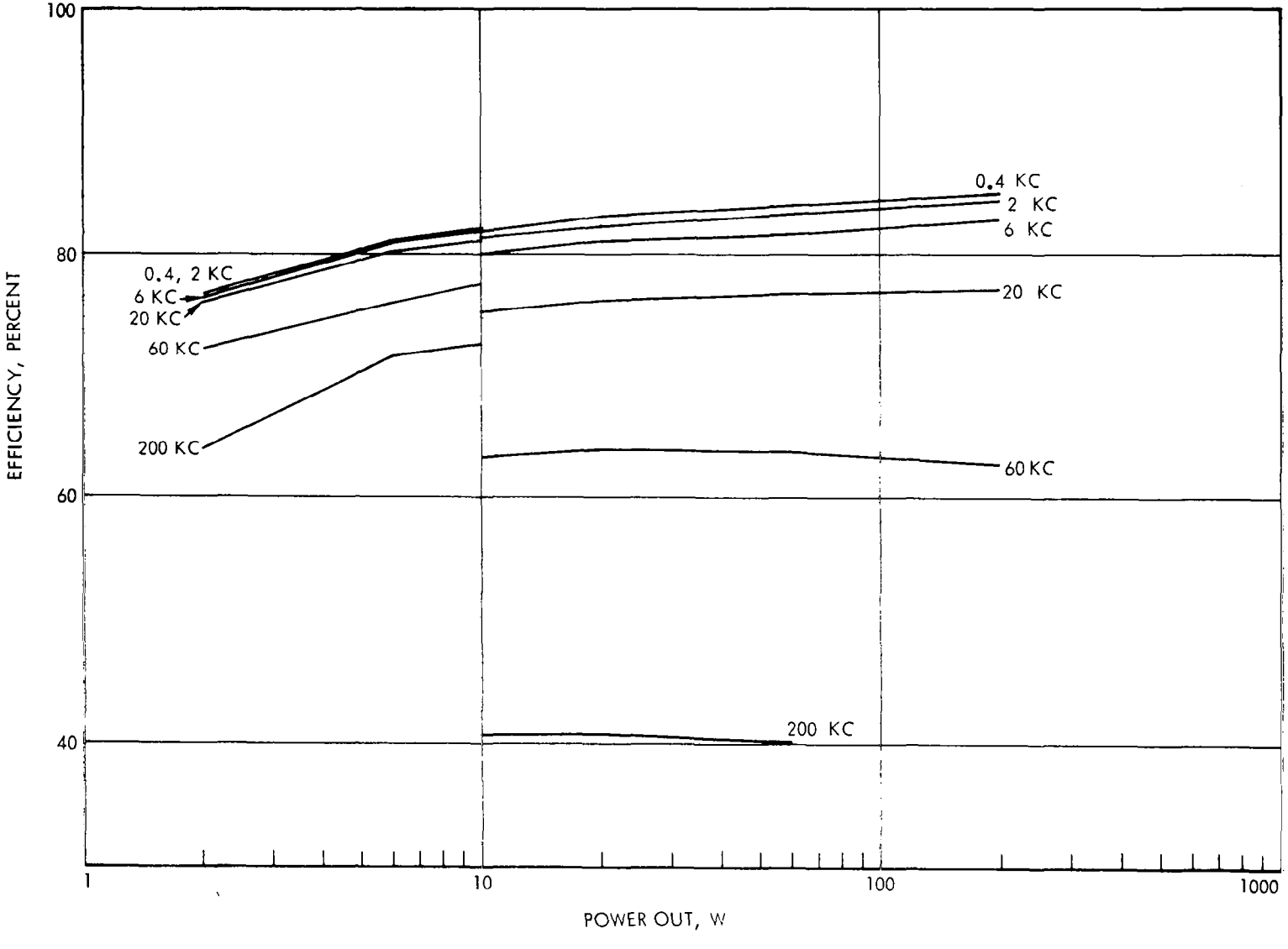

Figure C-17. PWI Converter, Efficiency Versus Power Output

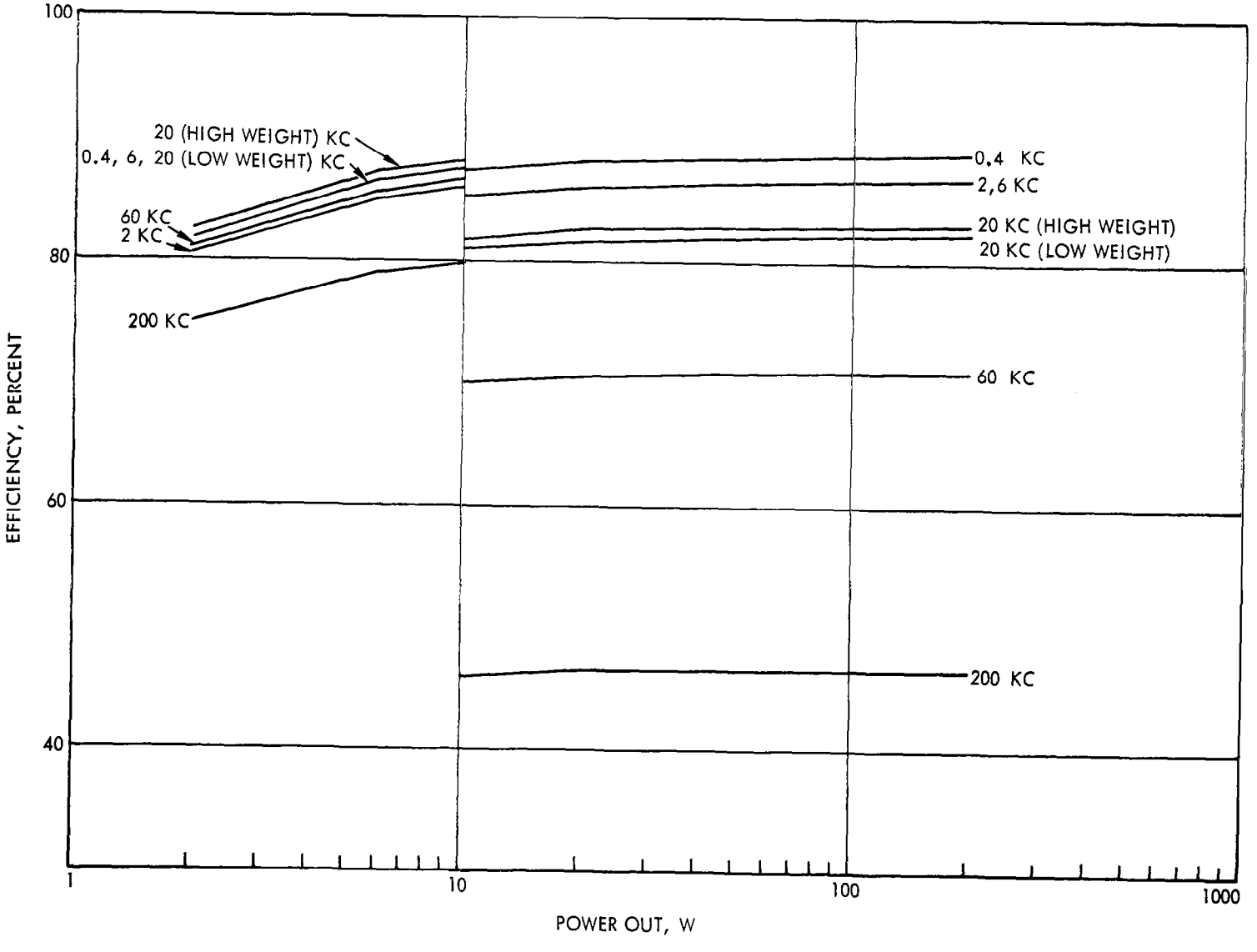

Figure C-18. ES and Push—Pull ES Converter, Efficiency Versus Power Output

APPENDIX D

ELECTRONIC EQUIPMENT THERMAL PACKAGING OPTIMIZATION

1. INTRODUCTION

Packaging of electronic equipment for use in spacecraft presents new challenges for the designer because of the many parameters requiring optimization. The following requirements are usually critical and thus provide a serious need for investigation, design analysis, and tradeoffs to determine the correct compromise which will provide the most optimum system design:

- Minimum weight
- Minimum volume
- Adequate heat transfer or insulation
- Adequate mechanical strength to meet environmental specifications
- Convenient shape.

The minimum volume is usually established by the type and quantity of components to be packaged. If the heat dissipation required is not excessive, this minimum volume will also set the minimum weight required to meet the mechanical requirements. When the heat dissipation is above normal, increases in weight and volume usually result. The following optimization procedure is one method of directly determining the minimum weight and volume design when excessive heat dissipation is present. Knowledge of component sizes and weights, minimum structural weight necessary to meet the mechanical environment, and required heat dissipation are prerequisites.

2. GEOMETRICAL SHAPES

The geometrical shape of an electronic equipment package is generally controlled by one or more of the following criteria:

- Quantity, size, and shape of components to be packaged
- Weight, maximum temperature, and heat dissipation of components to be packaged

- Size, shape, and configuration of spacecraft in which equipment package is to be mounted
- Heat transfer characteristics, ambient temperature, and thermal environment of the spacecraft.

The more common shapes in use are the sphere, right circular cylinder, the rectangular parallelepiped. Each of these are briefly considered, with the rectangular parallelepiped shape selected as the basis of the optimization procedure. A similar procedure would be applicable to other geometrical shapes.

The minimum surface area per unit volume for each of the above shapes is:

$$\text{Sphere } \frac{\text{area}}{\text{volume}} = \frac{3}{r_s} \qquad r_s = \text{radius}$$

$$\text{Cylinder } \frac{\text{area}}{\text{volume}} = \frac{4}{r_c} \qquad \text{height } h_c = \text{radius } r_c$$

$$\text{Rectangular } \frac{\text{area}}{\text{volume}} = \frac{6}{\ell_r}, \quad w_r = h_r = \ell_r \quad \text{(width, height, length)}$$

When these ratios are reduced to a common dimension, such as ℓ_r of the cube, their relative magnitudes are:

$$\text{Sphere } \frac{\text{area}}{\text{volume}} = \frac{4.8375}{\ell_r}$$

$$\text{Cylinder } \frac{\text{area}}{\text{volume}} = \frac{5.8584}{\ell_r}$$

$$\text{Rectangular } \frac{\text{area}}{\text{volume}} = \frac{6}{\ell_r}$$

The rectangular parallelepiped was chosen because it has the largest surface area per unit volume and is a convenient shape for packaging electronic components. The right circular cylinder may be more optimum for special cases since its base area is larger than the cube base area by a factor of 1.4646 for equal minimum volumes.

3. RECTANGULAR PARALLELEPIPED PACKAGING OPTIMIZATION

3.1 Design Considerations

An electronic equipment package operating in a spacecraft in space has two means of transferring its waste heat to the external environment. Radiation to the surrounding equipment, spacecraft, and space usually accounts for 50 percent or less of the total heat transfer. Conduction to the mounting base or spacecraft heat sink is the predominate mode of heat transfer and may account for 50 percent or more of the total. The rate of heat transfer by conduction generally exceeds the radiation rate by a factor of 5 or more. When this is true, maximizing the mounting base area per unit volume will maximize the total heat transfer. Since the cube has the minimum surface area per unit volume of any rectangular parallelepiped, and if it is assumed that the height should not exceed either the length or width of the base, then the base area can be increased per unit volume in two ways. First, the height, h, can be reduced and the square base area increased proportionately until the minimum allowable height, established by the largest component dimensions, is reached. Second, this minimum height can be held constant and the length, ℓ, to width, w, ratio ($K = \ell/w$) increased from 1, until a maximum allowable K factor is reached. This final shape, having minimum height and maximum K factor, provides the maximum heat transfer for a given volume whenever the base conduction rate is equal to or greater than the radiation rate. A reasonable maximum K factor is approximately 5.

An electronic equipment circuit design establishes the type, size, weight and quantity of components to be packaged. Also, the heat dissipation and temperature limit requirements can be calculated. The component information provides the minimum volume and weight, as well as limiting dimensions, such as the minimum height. Consideration of the mechanical environmental specifications further defines the minimum structure weight and packing factor. Data on this basic design can then be used to determine if sufficient surface area is available to transfer the required amount of heat. Determination of this fact is difficult because of the many variables involved. If it is determined that the surface area is insufficient, changing the basic package design to satisfy the thermal requirements and minimizing the associated penalties presents further problems.

The following assumptions and optimization method were derived to provide a rapid, simple, graphical method for solving these two problems.

3.2 Assumptions

The minimum volume and weight established by the mechanical design can easily be checked for thermal adequacy by considering the volume in the shape of a cube. If the surface area of the cube can transfer the required heat, then any other rectangular shape is more than adequate. The following heat transfer and configuration constraints were assumed:

- Heat is transferred away from the equipment package by conduction and radiation only, due to the vacuum environment
- The spacecraft average ambient temperature is 50°C
- The average equipment temperature rise is limited to 20°C with an emissivity of 0.9
- The average heat conduction rate to the mounting base is 0.5 w/sq. in. of base area
- The average heat radiation rate is 0.1 w/sq in. of surface area
- The average equipment density is between 0.035 and 0.05 lb/cu in.
- The K factor (ratio of base length to width) ranges from 1 to 5
- The height, h, is always equal to or less than the width.

3.3 Optimization Method Derivation

The mechanical and circuit designs provide the following parameter values:

- Minimum volume
- Minimum weight
- Minimum permissible dimensions
- Maximum heat dissipation.

Equation (1) relates three of these parameters for a rectangular parallelepiped within the constraints and assumptions previously listed.

$$P_T = C_1 A_B + C_2 \left[2h(w + \ell) + A_B\right]$$

$$P_T = 0.5\ A_B + 0.2\ h\ell\ \frac{(K + 1)}{K} + 0.1\ A_B \qquad (1)$$

$$P_T = 0.6\ A_B + 0.2\ h\ell\ \frac{(K + 1)}{K}$$

where

P_T = maximum heat dissipation, watt

C_1 = heat conduction coefficient, watt/sq in.

C_2 = heat radiation coefficient, watt/sq in.

h = height of rectangular parallelepiped, in.

w = width of rectangular parallelepiped, in.

ℓ = length of rectangular parallelepiped, in.

$A_B = w\ell$ = area of the base, sq in.

$K = \ell/w$ = length-to-width ratio

The minimum volume and minimum weight are related by equipment density coefficient as given by Equation (2).

$$V_{min} = \frac{W_{min}}{C_3} \qquad (2)$$

where

$V_{min} = w\ell h = \ell^2 h/K = A_B h$, cu in.

W_{min} = minimum equipment weight, lb

C_3 = average equipment density, lb/cu in.

Figures D-1 and D-2 present Fquation (1) as functions of P_T, A_B, h, and K. Figures D-1 and D-2 hold K = 1 and K = 5 constant, respectively. Constant volume lines are shown for selected values of A_B and h.

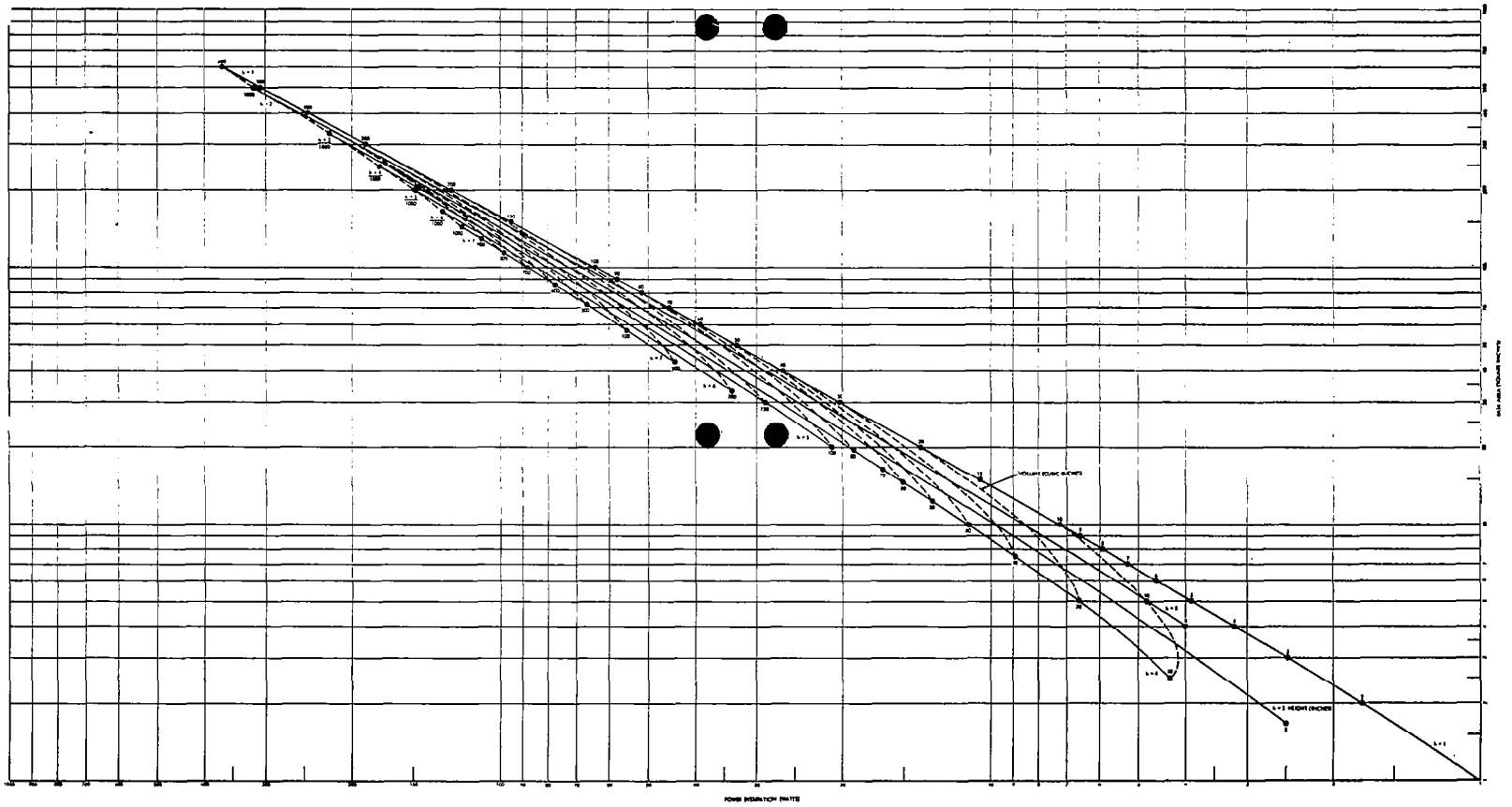

Figure D-1 Structure—Thermal Optimization—K = 1

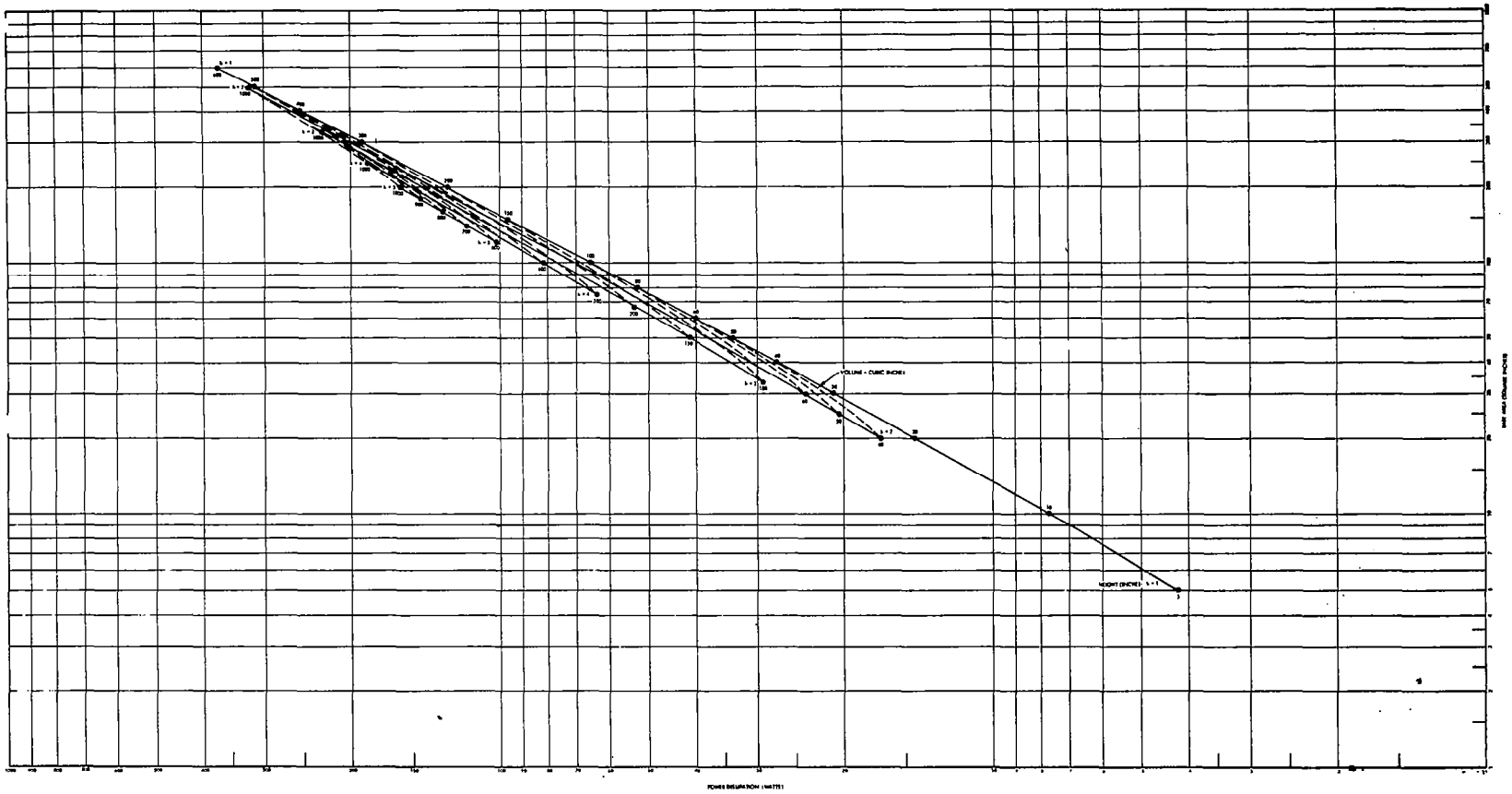

Figure D-2. Structure—Thermal Optimization—K = 5

3.4 Graphical Solutions

The mechanically limited minimum volume for a given electronic equipment is determined from Equation (2). Knowing the maximum heat dissipation, minimum volume, and limiting dimensions, the following steps can be used to determine the optimum minimum volume and shape for a thermally limited design.

Step 1.

Enter Figure D-1 at the intersection of the known values of P_T and V_{min}.

Read the value of h at this intersection point, i.e., $h = h_1$.

If h_1 is equal to or greater than h_{min}, the mechanically limited V_{min} is thermally acceptable. Any rectangular parallelpiped having a height equal to or less than h_1 and volume equal to V_{min} will meet or exceed the required thermal dissipation.

Step 2.

If h_1 is less than h_{min}, enter Figure D-2 (K = 5) for the same values of P_T and V_{min}. At this point of intersection read the value of h, i.e., $h = h_2$.

If h_2 is equal to h_{min}, read the corresponding value of A_B at that intersection point. The optimum mechanical and thermal design is a rectangular parallelepiped having a height equal to h_2, a base area equal to A_B, a length ℓ equal to

$$(K A_B)^{1/2}$$

with K = 5. This design has the same minimum volume and weight determined by the mechanical requirements.

Step 3.

If h_2 is greater than h_{min}, the minimum volume and weight determined by the mechanical requirements are adequate. The lowest acceptable value of K can be determined when h is set equal to h_{min}. K_{min} could be determined graphically if other figures similar to Figure D-2 were plotted for values of K between 1 and 5. K would equal K_{min} on that figure which contained an intersection for $V = V_{min}$, P_T, $h = h_{min}$, and $A_B = V_{min}/h_{min}$. An analytical solution is available by solving Equation (1) for K, knowing $h = h_{min}$, $A_B = V_{min}/h_{min}$.

Equation (3) provides the solution of Equation (1) for the correct value of K.

$$K = \frac{(y^2 - 2) + y(y^2 - 4)^{1/2}}{2} \tag{3}$$

where

$$y = \frac{K + 1}{K^{1/2}} = \frac{P_T - 0.6\, A_B}{0.2\, h\, A_B}$$

Step 4.

If h_2 is less than h_{min}, the mechanically established minimum volume and weight are not thermally acceptable, and the volume and weight must be increased. The optimum volume, weight, and shape meeting the thermal and mechanical requirements are established by the optimum value of A_B on Figure D-2 where the given value of P_T and $h = h_{min}$ intersect. The optimum length (ℓ) is equal to (K x optimum $A_B)^{1/2}$, i. e.,

$$\ell = \left[5\, (A_B)_{opt}\right]^{1/2}$$

The optimum weight is determined by Equation (4).

$$W_{opt} = \frac{h_{min}\, (A_B)_{opt}}{C_3} = \frac{V_{opt}}{C_3} \tag{4}$$

The above steps provide the exact solution for the required minimum weight and volume design of a rectangular parallelepiped meeting both the mechanical and thermal requirements. Similar curves can be plotted for other geometrical shapes and/or assumed thermal coefficients.

"The aeronautical and space activities of the United States shall be conducted so as to contribute . . . to the expansion of human knowledge of phenomena in the atmosphere and space. The Administration shall provide for the widest practicable and appropriate dissemination of information concerning its activities and the results thereof."

—NATIONAL AERONAUTICS AND SPACE ACT OF 1958

NASA SCIENTIFIC AND TECHNICAL PUBLICATIONS

TECHNICAL REPORTS: Scientific and technical information considered important, complete, and a lasting contribution to existing knowledge.

TECHNICAL NOTES: Information less broad in scope but nevertheless of importance as a contribution to existing knowledge.

TECHNICAL MEMORANDUMS: Information receiving limited distribution because of preliminary data, security classification, or other reasons.

CONTRACTOR REPORTS: Scientific and technical information generated under a NASA contract or grant and considered an important contribution to existing knowledge.

TECHNICAL TRANSLATIONS: Information published in a foreign language considered to merit NASA distribution in English.

SPECIAL PUBLICATIONS: Information derived from or of value to NASA activities. Publications include conference proceedings, monographs, data compilations, handbooks, sourcebooks, and special bibliographies.

TECHNOLOGY UTILIZATION PUBLICATIONS: Information on technology used by NASA that may be of particular interest in commercial and other non-aerospace applications. Publications include Tech Briefs, Technology Utilization Reports and Notes, and Technology Surveys.

Details on the availability of these publications may be obtained from:

SCIENTIFIC AND TECHNICAL INFORMATION DIVISION

NATIONAL AERONAUTICS AND SPACE ADMINISTRATION

Washington, D.C. 20546